Water Entrance Kinderdijk

Conceptual design for the multi-functional use of a discharge sluice

R. X. van der Vaart

TU Delft

Witteveen + Bos

Water Entrance Kinderdijk

Conceptual design for the multi-functional use of a discharge sluice

by

R. X. van der Vaart

to obtain the degree of Master of Science

at the Delft University of Technology

Student number:	4283058	
Thesis committee:	Prof. dr. ir. S. N. Jonkman,	TU Delft, main supervisor
	Dr. ing. M. Z. Voorendt,	TU Delft, daily supervisor
	Dr. ir. H. W. M. van der Ham,	TU Delft
	Ir. G. R. Spaargaren,	Witteveen+Bos

TU Delft

Witteveen + Bos

Preface

To obtain the degree of Master of Science at the Delft University of Technology a final thesis is written about my graduation project. My master is Civil Engineering with the track Structural Engineering and specialisation Hydraulic Structures. The topic of my graduation thesis is flood risk and structural safety of a primary flood defence with a modification of the existing hydraulic structure due to changes in the functionality.

First, I would like to thank my chairman Bas Jonkman and daily supervisor Mark Voorendt for guiding my graduation thesis from the master track Hydraulic Engineering even though my master track is Structural Engineering. They have helped me with the frequent reviewing of my report and feedback during my graduation.

Furthermore, I would like to thank Herbert van der Ham for the feedback and help on the structural part of my thesis.

In addition, I would like to express my thanks to Gerben Spaargaren, Menno Buckers and other colleagues from Witteveen + Bos who provided me with their knowledge, necessary information, many tips and enjoyable working environment during my graduation process.

Finally, I would like to thank my friends and family for their consistent support and confidence in me. A special thanks to my parents for enabling me to study at the TU Delft and providing me a pleasant working environment during the corona lock-down.

R. X. van der Vaart
Delft, June 2020

Summary

The World Heritage Site Kinderdijk consists of a landscape of preserved 18th-century windmills and is a popular touristic location. The number of visitors is continuously growing for the World Heritage Site at Kinderdijk. Visitors arriving via the water network have to cross a busy road to reach the heritage site. This is an unsafe and unfavourable situation. A new water entrance at Kinderdijk is the solution to this problem. The plan is to add the function of a pedestrian passage to the existing discharge sluice at Kinderdijk named the Elshoutsluice. The discharge sluice is part of a flood defence and must keep its original function.

Figure 1: Top view of the Elshoutsluice including marking of the culverts. River is at top side of figure (source: Google maps).

The objective of this thesis is to provide a conceptual structural design for the multi-functional use of the discharge sluice at Kinderdijk including the functions for water discharge, flood defence, passage for (motorised) vehicles and pedestrians, which fulfils standards for flood safety and buildings in the Netherlands. This thesis shows how to approach a design case for adjustments of an existing hydraulic structure as a part of a flood defence. A conceptual design was made for the adaptation of the Elshoutsluice. For this study a design method according to Roozenburg and Eekels (1995) and Voorendt (2020) was used.

The Elshoutsluice was divided into different subsystems and elements. The concepts for the location of the new pedestrian tunnel, the floor configuration, the roof and gates were developed. After the functional verification and evaluation, a selection was made from the best remaining alternatives for the elements and subsystems.

The selected alternative is a pedestrian tunnel above culvert number 2. As a result, the existing gates of culvert 2 will be replaced with new gates to provide flood protection in case of high water. A flap gate and a vertical unfolding gate are selected. The existing technical area expands above culvert number 3. A multi-functional space is included above culvert number 3. Culverts 1 and 4 remain unchanged. Additional soil will be placed on top of the structure to provide a slope for the connection of the heightened road on top of the sluice to the road at the adjacent levee.

The conceptual design and construction phase was checked for the flood safety based on the WBI 2017 and OI 2014 and fulfils the requirements. Stability checks were performed for governing load situations of the Elshoutsluice for the construction phase and use phase. The difference in loading on the structure for the initial design and the new situation was analysed. Additional checks are needed for the lateral walls in all the culverts and the top slab of culvert 1 and 4 due to the increase in shear force and bending moments.

The conclusion is the resulting conceptual design shown in Figure 2. Figure 3 gives a sketch of the resulting conceptual design of the Elshoutsluice for a cross-section at culvert 2.

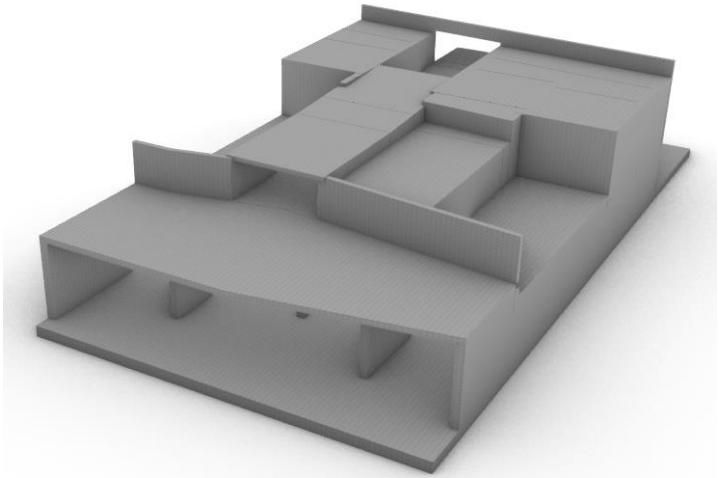

Figure 2: A 3D view of the resulting design for the Elshoutsluice. The river side is at the top of the figure. The culverts are numbered from left to right, see Figure 1.

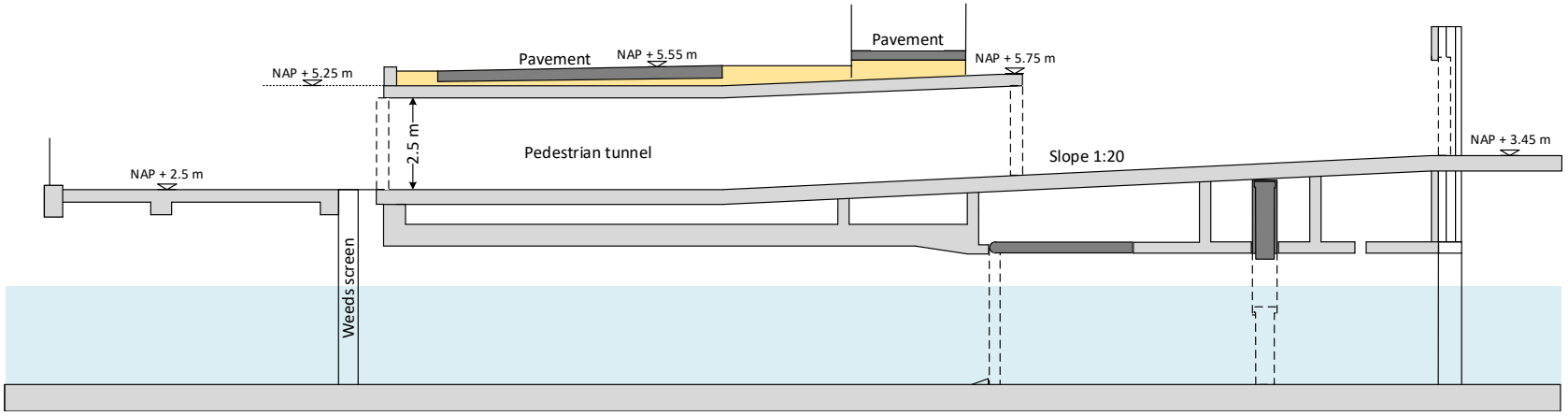

Figure 3: Side view of the resulting design for culvert number 2. The river side is at the right side of figure. New elements: pedestrian tunnel floor and rood, heightened pavement, opening wall at river side, the gates in the culvert and the 3 gates in the pedestrian tunnel.

Contents

1 Problem analysis

This chapter contains the problem analysis. At first, an introduction is given which explains the relevance of this study. Second, the situation in Kinderdijk is explained, which resulted in the adaptions for the Elshoutsluice. Third, the flood risks in the Netherlands are analysed.

1.1. Introduction

This study focuses on a discharge sluice in Kinderdijk, which is a village in the province of South Holland in the Netherlands. The discharge sluice is named the Elshoutsluice and discharges water into the river the Lek and is part of a primary flood defence. Its location is shown in Figure 1.1. A design concept was made for a pedestrian tunnel through the existing Elshoutsluice. This design was introduced as a solution to an infrastructure problem in Kinderdijk, mainly due to tourism. Structural elements and flood risk need more investigation for this design case regarding the additional function of the discharge sluice and the new flood safety standards. The questions regarding the new design of the Elshoutsluice resulted in this study.

Figure 1.1: The location of the Elshoutsluice in Kinderdijk (source: Google maps)

The result of this study is a conceptual design for the hydraulic structure in Kinderdijk. With this case study for a conceptual design of the Elshoutsluice a plan of action method is derived which can be applicable to similar situations of hydraulic structures as a part of a flood defence in the Netherlands.

Hydraulic structures in the Netherlands could be a part of the circa 3,500 kilometres of primary flood defences. Veiligheid Nederland in Kaart VNK (2014) screened around 1,000 hydraulic structures and marked approximately 400 structures as potentially high risk. Flood defences are needed since almost two-third of the Dutch population lives in areas prone to flooding. Protection against flooding has a high priority for the Dutch citizens and the Dutch economy. Ongoing investments and researches are needed to ensure flood risk reduction (VNK, 2014).

The Netherlands has many hydraulic structures in the form of weirs, pumping stations and locks.

Figure 1.2 shows the number of hydraulic structures constructed per decade. Many of these hydraulic structures will reach the expected design lifespan of 100 years in the coming decades. The last couple of years, there has been an increase in research of the possibilities to extend the lifespan of hydraulic structures. The details of the structural safety, repair techniques and the use of innovative ideas are needed to increase the lifespan. Preferably the remaining lifespan of the existing structure has to be used as efficiently as possible. It is necessary to anticipate to the future developments as stricter standards and multiple uses of a structure (Van der Vlist, Barneveld, Breedeveld, Van Doorn, & Luyten, 2019).

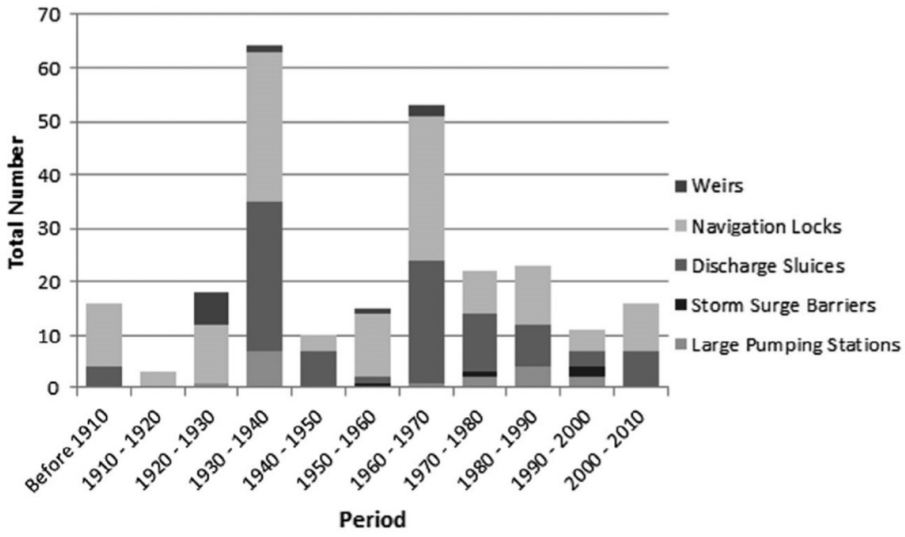

Figure 1.2: The construction year of various hydrualic structures in the Netherlands (source: Rijkswaterstaat) (Jonkman, Voortman, Klerk, & Van Vuren, 2018)

1.2. Kinderdijk

Kinderdijk is an icon of the Dutch water management throughout the centuries and it offers a view of the 18th-century landscape as a result of the preserved windmills. Since 1997, the area is an UNESCO world heritage site. A large part is a protected nature region since it is assigned as a Natura 2000 area. As a result of the scenery, the (international) tourism to Kinderdijk is a growing trend that has persisted for years (Gemeente Molenwaard, 2018).

1.2.1. History

Since the 11th-century reclamation took place in the area Alblasserwaard, this led to constant subsidence of the soil and the requirement of river levees. The water boards Overwaard and Nederwaard moved their drainage system with a canal to the lowest point at Elshout in the 14th century. Here the groundwater and rainwater could be discharged into the river the Lek. The water boards are divided by a middle quay. Nowadays Elshout is called Kinderdijk and both water boards merged with Alblasserwaard to one board, named Rivierenland. Figure 1.3 shows the locations of the Nederwaard and Overwaard in the current situation in Kinderdijk.

Figure 1.3: The distribution of the Overwaard and Nederwaard (source: google maps)

Drainage was getting harder since drained soil continued to

subside while the level of the river rose. With the introduction of windmills, it became possible to pump the water of the lower ground level to a higher level. In the 18th century both water boards built eight windmills each and water storage reservoirs at both sides of the canal, called the high storage basins. The canal itself is the low storage basin. The high storage basins both had three sluices each in connection with the river, called the Elshoutsluices.

In the 19th century, the steam pumps were introduced to replace the windmills. Not all windmills were demolished. These windmills still exist in Kinderdijk and they can even function, but they are not used anymore. The water boards Overwaard built a steam pumping station called Wisboom and Nederwaard built a station called Van Haaften. In the first half of the 20th century, the pumping station Van Haaften was electrified. A new electric pumping station was built south of station Wisboom to help this station.

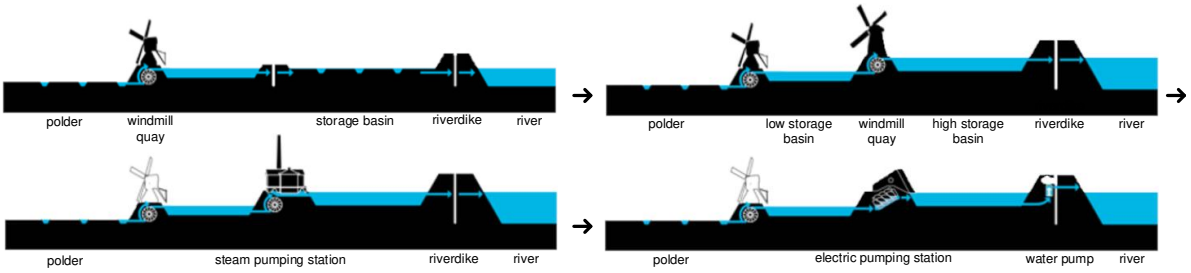

Figure 1.4: The history of the third drainage step (translated) (Land-ID & Cultuurhistory Projecten, 2016)

The station Van Haaften was demolished in the second half of the 20th century. In its place, a new pumping station was built named J.U. Smit. It pumps directly from the low storage basin into the discharge reservoir because of the high capacity of this pumping station. Due to the placement of a sheet pile wall between the discharge reservoir and the high storage basin of the Nederwaard, the storage basin has lost its regular function. Pumping station Wisboom has lost its purpose and the help station was demolished after the construction of the new pumping station, named Overwaard. Due to a new weir in the high storage basin, the water from the low basin can be pumped either to the high storage or to the river via the discharge reservoir. The station Overwaard changed its name to ir. G.N. Kok in 2010. Figure 1.5 shows the locations of the current pumping stations.

The sluices, Elshoutsluices, were replaced with a new sluice in the mid-80s. This is the sluice which still operative now. In 2002 an new pump system was added in the sluice, which is called the third drainage step (de Derde Trap) (H+N+S Landschapsarchitecten & Beek & Kooiman Cultuurhistory, 2013).

In September 2019 the new tourist visitor centre of the world heritage Kinderdijk had opened. A new bridge was realised to connect the visitor centre to the Wisboom pumping station.

1.2.2. Infrastructure

The infrastructure of Kinderdijk is described in two different categories. At first, tourism is discussed. Secondly, the water system is analysed. The map of Kinderdijk with marked locations is shown in the figure below.

Tourism

The number of visitors in Kinderdijk is estimated at around 600,000 in 2018 with an expected increase every year according to the institution Defacto Stedenbouw (2019). In the last years, measures were taken to manage the growing amount of tourist in Kinderdijk. The traffic pressure for the narrow road on the levee by touring cars is reduced by water entrance facilities such as the water

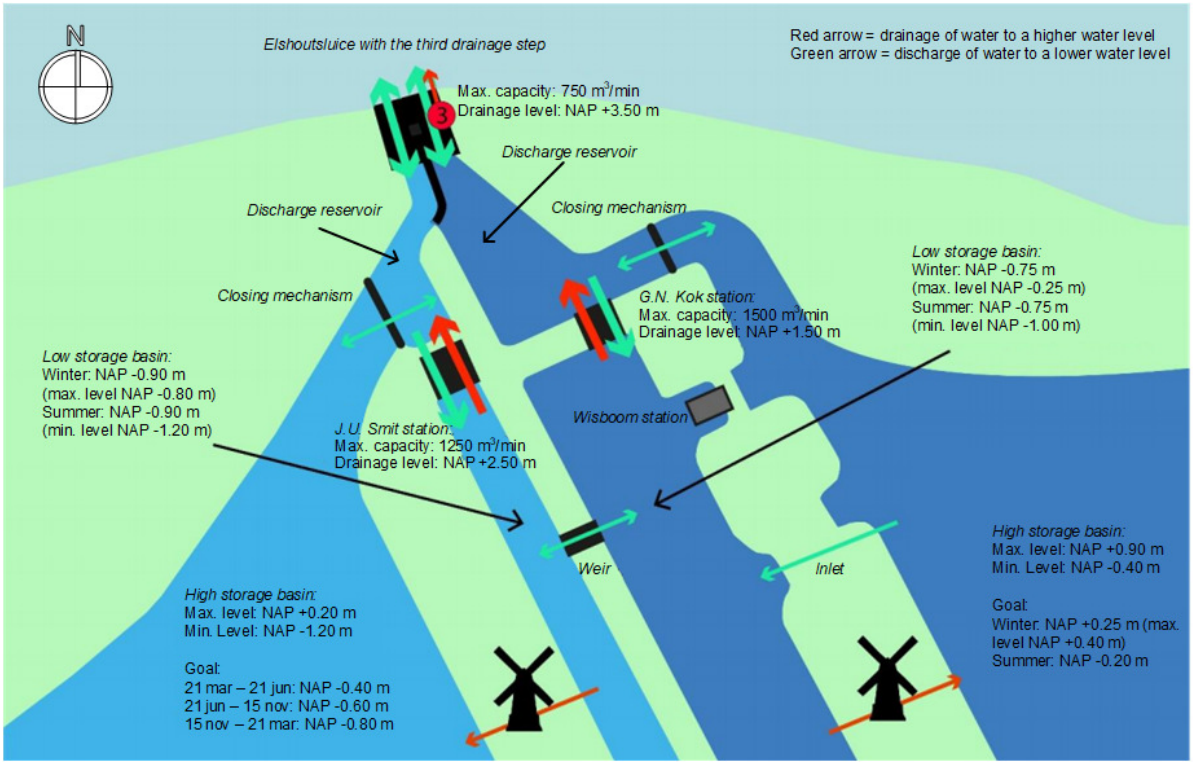

Figure 1.5: Watersystem with pump capacities and discharges (translated) (Gemeente Molenwaard, 2018)

Legend
1. Pier river cruise
2. Pier river cruise
3. Pier waterbus
4. Stop & Go
5. Entrance heritage site
6. Souvenir shop
7. Visitors centre
8. Bridge
9. Road crossing
10. Bridge
11. Entrance heritage site
12. Elshoutsluice
13. J.U. Smit station
14. G.N. Kok station
15. Monumental building

Figure 1.6: Map of Kinderdijk (source: Google Maps)

bus. Figure 1.6 shows the piers (1 & 2) for river cruise ships and the pier (3) for the water bus which connects with the public transport in Dordrecht and Rotterdam. Gemeente Molenwaard (2018) indicates that around 250,000 visitors arrived via water in 2017 and the number of visitors increases with circa 20,000 per year. Touring cars deliver tourist at the Stop and Go area for busses (4).

Visitors who arrive via the water bus cross the road and walk through the (main) entrance of the world heritage site (5) and walk past the souvenir shop (6) to the new visitor centre of World Heritage Kinderdijk (7). People have to cross the water by a bridge (8) which has not got a pedestrian lane yet. Many visitors by bicycle cycle past the (main) entrance since it is not marked very well.

The crowd who arrives by cruise ship crosses the road (9) and enters the area via a bridge (10) to the windmill quay. In agreement with the water board, the entrance by road (11) and bridge (10) will be closed off for visitors of the world heritage site.

A large number of visitors create a logistic problem and nuisance in Kinderdijk. Tourists who arrive mainly focus on the first view of the windmills which results in dangerous situations in traffic (Gemeente Molenwaard, 2018).

Watersystem

Kinderdijk is part of dike ring 16 Alblasserwaard en Vijfheerenland, see Figure 1.7. The water board is Waterschap Rivierenland. Dike ring 16 consists of 86.2 km length of flood defences and has 24 hydraulic structures according to VNK (2014). The levee surrounds an area of 39,200 ha with 212,800 inhabitants.

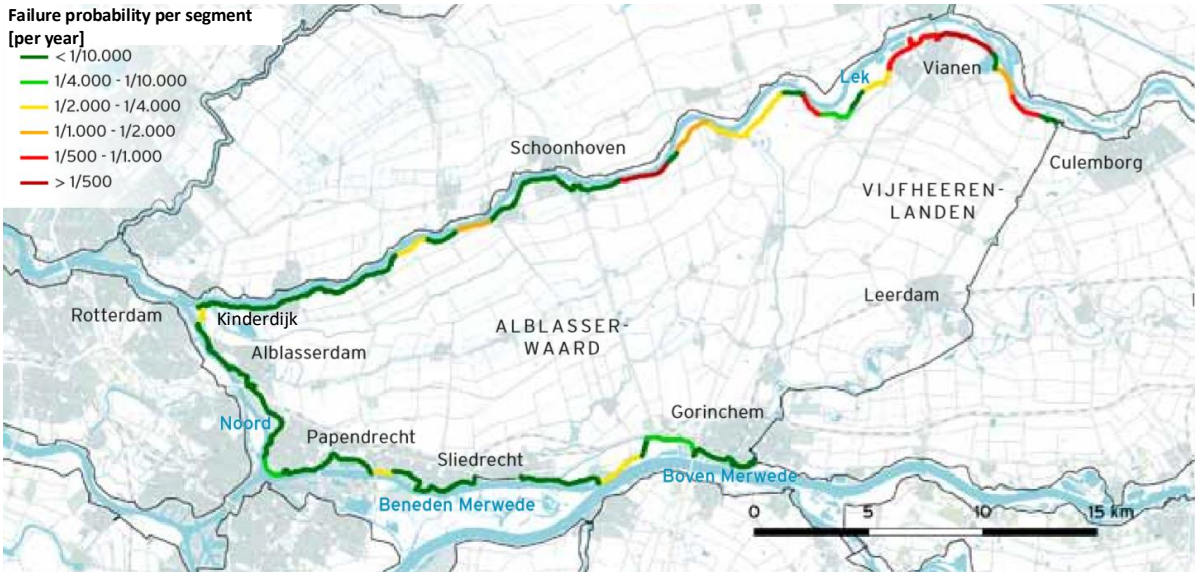

Figure 1.7: The dike ring area 16 (VNK, 2014)

The levee at Kinderdijk is part of dike segment 16-2 from Sliedrecht to Streefkerk and has the name Lekdike. The alert value [1] of the failure probability in a random year is 1/30,000 and the required lower threshold is 1/10,000 for this section according to Informatiehuis Water (IHW) (2017). An explanation of the alert value and the lower threshold is given in Appendix A. The latter value is referred to as the safety standard.

Figure 1.6 shows an operating discharge sluice (12), the J.U. Smit pumping station (13) and the sta-

[1] The alert value is named signal value in the lecture notes of the flood defences course. The name alert value is selected in this report.

tion ir. G.N. Kok (14).

The water board Rivierenland is the manager of the flood defences and water systems. The road on the levee is owned by the municipality. The levee eastward of Kinderdijk has recently been strengthened (Gemeente Molenwaard, 2018).

1.2.3. Elshoutsluice

The Elshoutsluice is a sluice for water management. The water is discharged through four culverts in the sluice. Figure 1.8 indicates the locations of these culverts, including the numbering used to reference each culvert. Above these tunnels are closing mechanisms for high water protection and technical areas. A pump system is placed in the fourth water culvert. In normal circumstances, the Elshoutsluice is closed. If it is necessary the sluice can be partially opened to let in the water of the river to the polders (Waterschap Rivierenland, 2018a).The sluice can be partially opened (25-30 cm) in dry periods.

Figure 1.8: Top view of the Elshoutsluice (source: Google maps)

The water board has decided that the maximum water level of the high water storage basin should be lowered from NAP + 0.90 m to NAP + 0.40 m because the stability of its quays is not sufficient. Strengthening of the quays is a significant and expensive solution due to the Natura2000-area and the world heritage site, which was the reason for the decision of changing the water level. This results in a decrease in the storage capacity of the high water basin. To compensate this capacity loss, a decision is made to increase the pump capacity of the pumping system in the Elshoutsluice. The capacity will be increased with 750 m^3/min and it was planned to realise this idea in 2019 (Waterschap Rivierenland, 2018a).

The following figures show the Elshoutsluice structure including the pumps, the closing mechanisms and the technical area. The roads on top of the structure are shown in the figures as well.

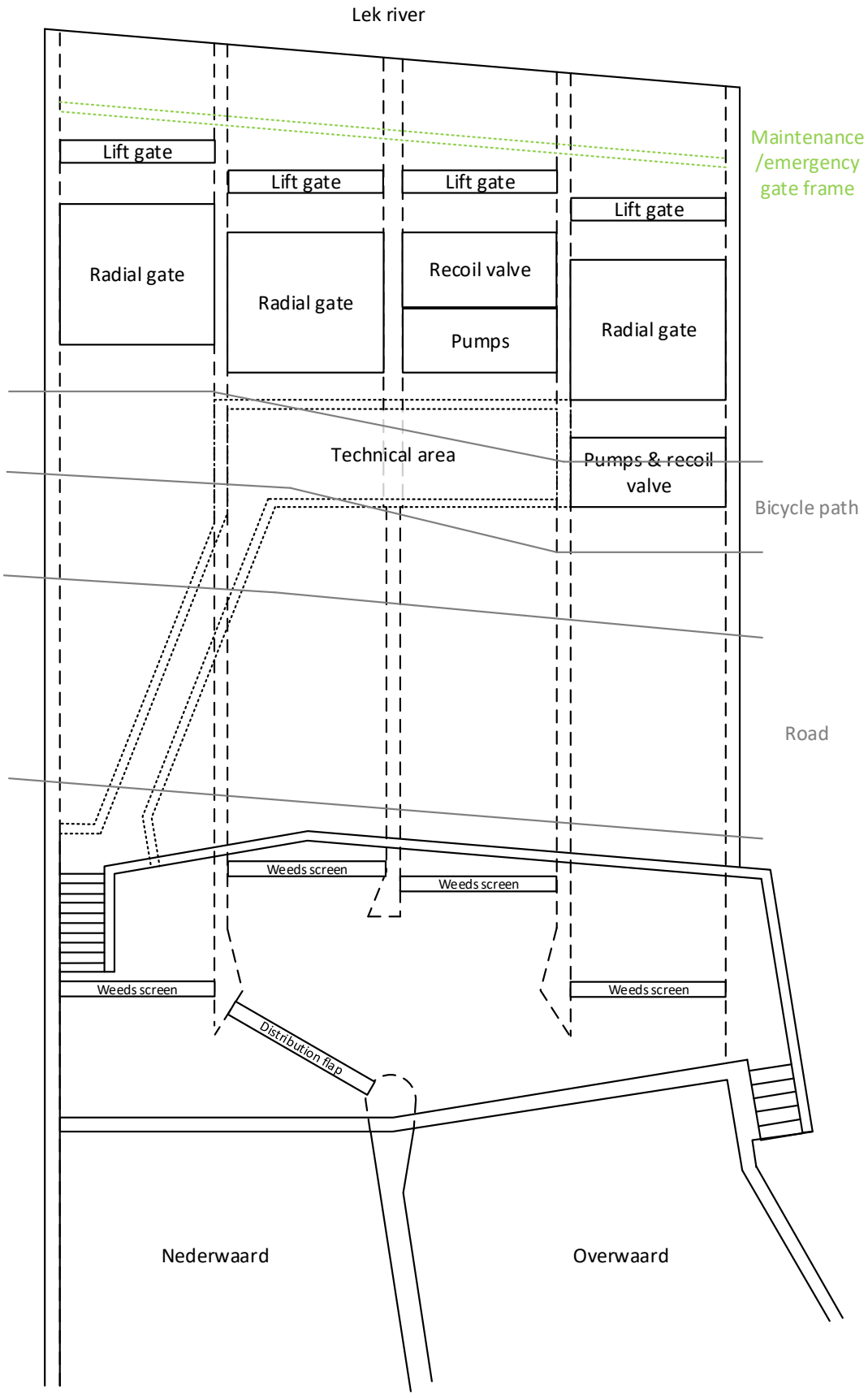

Figure 1.9: Top view ketch of the layout of the Elshoutsluice including the bicycle path and motorised vehicle road.

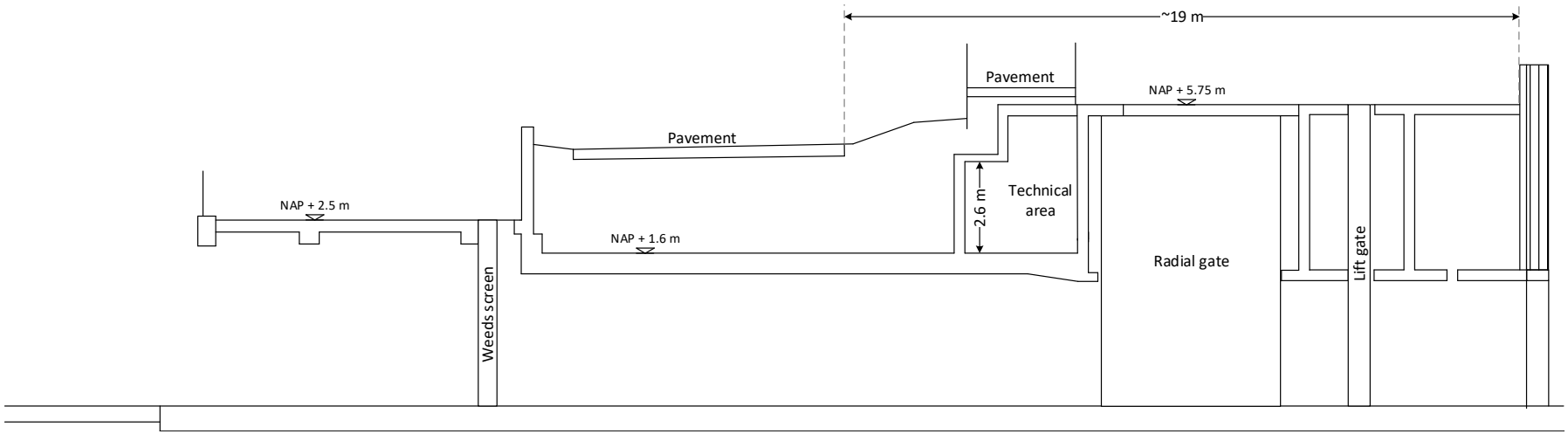

Figure 1.10: Side view sketch of culvert number 2. The river side is at the right side of figure.

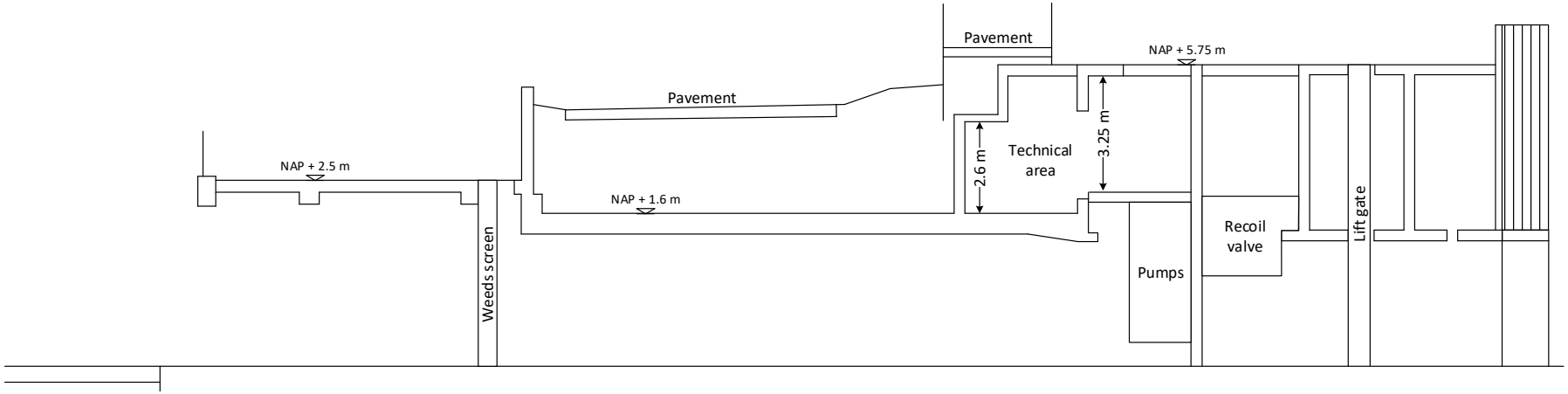

Figure 1.11: Side view sketch of culvert number 3. The river side is at the right side of figure.

1.2.4. Design competition

For the logistic problem of the tourists, a design competition was organised by the municipality Molenwaard. Of the five different design options, the design 'de derde trap' (literal translation: the third stairs) was chosen as the winner of the competition (Architectuur Lokaal, 2019). Visitors arriving by water can enter the world heritage area via a pedestrian tunnel going through the existing discharge sluice in this design. The visitors do not cross the levee road anymore. The current discharge sluice, the Elshoutsluice, has to be structurally modified to gain the additional pedestrian transportation function.

(a) Impression of the design viewed from the river

(b) Impression of the design viewed from the inland side

Figure 1.12: Design of the 3e trap (Tijhuis et al., 2019)

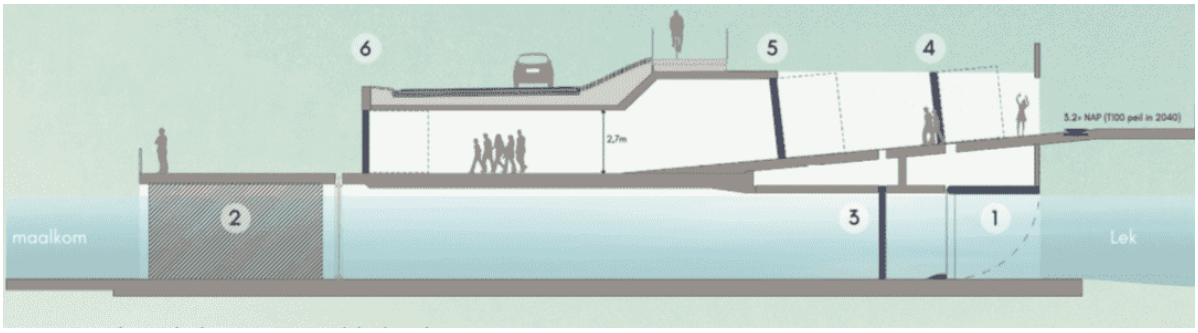

(a) The design for culvert number 2

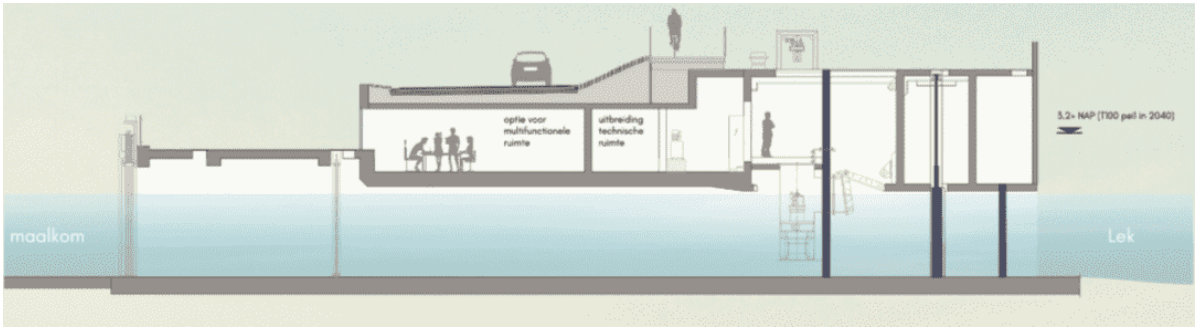

(b) The design for culvert number 3

Figure 1.13: Design of de derde trap (Tijhuis et al., 2019)

The water from the Nederwaard will be discharged through culvert number 1 and the water from the Overwaard will go through culverts 2, 3 and 4. This will be realised with the existing distribution flap in the Elshoutsluice. A straight pedestrian passage will be located above the second culvert of 27 meters long as can be seen in Figure 1.13a. The width of this tunnel will be 5.5 meters and the height 2.7 meters. The technical rooms at the place of the passage now shall be relocated above the third water discharge culvert. Above the water culvert 3 and 4 a new multi-functional space could be created. To make room for the pedestrian tunnel, the closing mechanism of the second culvert

must be replaced by another mechanism. From the passage, a view can be offered of the radial gate of water culvert number 1 (Tijhuis et al., 2019).

The visitors of the world heritage site arrive through the tunnel and continue to the path with a new pedestrian bridge over the lower water basin beside the now existing bridge for cars (8), see Figure 1.6. An impression of the bridge can be seen in Figure 1.12b. The tourist can follow their course to the new visitor centre of SWEK.

1.3. Flood risk reduction strategy

Most flood-prone areas in the Netherlands are protected by flood defences consisting of earthen dikes (levees), dams, dunes and storm surge barriers. For the purpose of water management and navigation, other types of hydraulic infrastructure are present such as sluices and gates. These structures are ageing and need to be upgraded or changed to maintain the safety standards regarding flood risk (Jonkman et al., 2018).

1.3.1. Flood risk analysis

The project Flood risk in the Netherlands (Veiligheid Nederland in Kaart, VNK) has performed a flood risk analysis for all primary flood defences in the Netherlands from 2006 to 2014 (VNK, 2014). In this research the probability of flooding was linked to the consequences of flooding to determine the risks, see Figure 1.14. With this information the government can take targeted and cost-effective measures to protect the Netherlands against flooding. The definition of the occurrence of a flood is when the average water depth in an area or neighbourhood with a single four-digit postcode exceeds 0.2 metres (TAW-ENW, 2016).

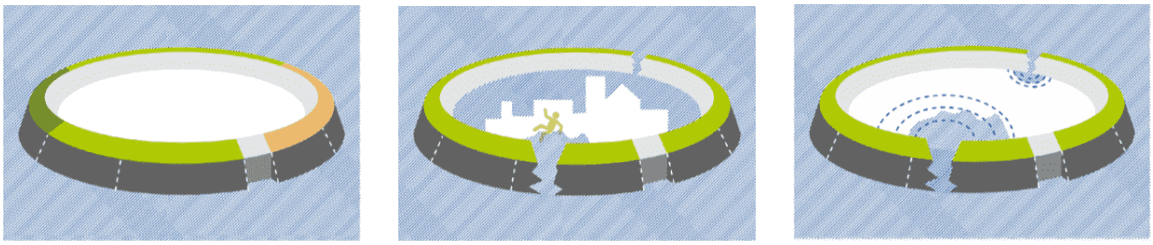

(a) **Probability of flooding:** The probability of a breach for each section of the levee system.

(b) **Impact of flooding:** The damage and casualties of any breach.

(c) **Flood risk:** For every section the probability of flooding is combined with the associated impact.

Figure 1.14: Probability of flooding x impact of flooding = flood risk (TAW-ENW, 2016)

Three risk criteria have been considered to determine the new flood risk safety standards VNK (2014):

- Economical risk: the economic damage expressed in euros per year. This criterion can be used in cost-benefit studies to determined where the sum of the costs and benefits is at its minimum.
- Local individual risk: the probability per year of the casualty of an individual person due to flooding of a dike ring area. Evacuation is included in this risk criterion. This risk criterion can be used for considerations about prevention, spatial planning and disaster management.
- Societal risk: the number of casualties as a direct result of flooding of an area. This risk is expressed in a graph which shows the probability of 1, 10, 1000, 1,000 or 10,000 casualties for an area.

The Netherlands was divided into dike ring areas as can be seen in Figure 1.15a. According to the

VNK (2014) the risk of flooding within a dike ring area can differ substantially while each part of the dike ring has the same safety standard. These differences originate from a variance in soil levels within a dike ring area and/or the compartments within an area.

1.3.2. New safety standards

New safety standards were introduced on 1 January 2017. The old standards were formulated in terms of a probability of exceeding of hydraulic load conditions which can consist of water levels and waves. A flood defence had to be able to withstand the load conditions safely. The Netherlands was split into dike ring areas. Figure 1.15a shows that per dike ring area the required safety standard could differ. This safety standard was based on the risk of a dike ring area. An example is the area of South Holland which is densely populated. The safety standard was 1/10,000 per year at South Holland, but for other dike ring areas around rivers the safety standard was 1/1,250 per year.

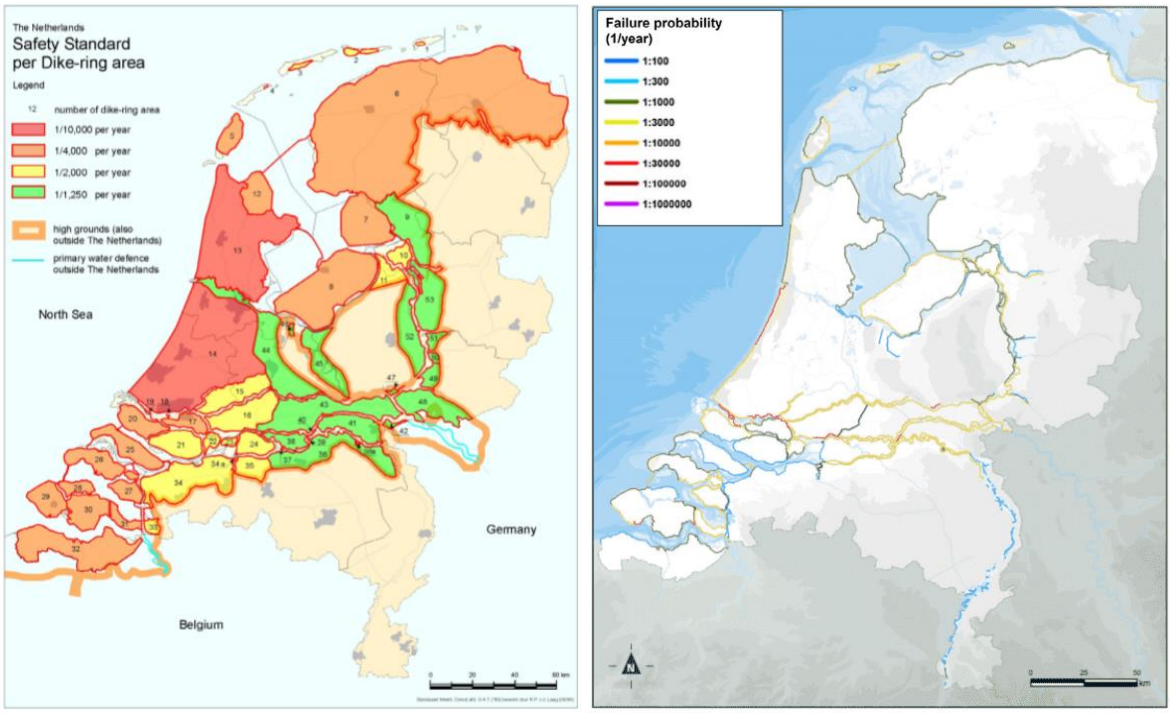

(a) Overview of dike rings with to the old safety standards used until 2016

(b) Overview of dike segments with the new safety standards used from 2017

Figure 1.15: Safety standards for flood defences in the Netherlands (Rijkswaterstaat) (Jonkman et al., 2018)

The Dutch government has proposed new safety standards since the size of the population in flood-prone areas has grown rapidly. Another reason for the new standards are the new insights into failure probabilities and failure mechanisms. These new standards have been derived from the project VNK (see subsection 1.3.1). The first significant change is that the new standards refer to maximal acceptable failure probability for segments of flood defences. The second change is in the distribution of protection levels in the Netherlands. High protection levels are not only assigned to the coastal side of the country but also to river areas (Jonkman et al., 2018).

The probability of flooding and the consequences are still included in the new safety standards. In addition extra investments are being made in areas with a risk of significant economic damage and many victims. Vulnerable and vital infrastructure, such as utilities and hospitals, receive extra attention. Another difference is the use of a dike segment approach instead of a dike ring approach which is shown in Figure 1.15b. Each segment has an unique code name and has a safety norm expressed

in the probability of flooding per year. All primary flood defences must meet the new safety standards in 2050 (Helpdesk Water, n.d.). As mentioned before in subsection 1.2.2, the required safety probability for the dike segment in Kinderdijk is 1/30,000 per year for the alert value and 1/10,000 per year for the lower threshold. The alert value is selected as the design value.

2

Problem statement and objective

In this chapter, the problem analysis is summarised in a problem statement. The objective of this report is explained. At last, the scope of this study is described in this part.

2.1. Problem statement

Due to the infrastructure problems at Kinderdijk, a design concept "De Derde Trap" has been made. Multiple problems and questions need to be solved with regards to maintaining the safety of the existing hydraulic structure, taking into account the new flood risk standard. One of the challenges is the new closing mechanism of the pedestrian tunnel. In addition, the current state of the sluice must be taken into account regarding the functional lifetime. Another challenge is how to connect the new structural elements to the remaining existing elements in the hydraulic structure. This results in the main problem statement:

The design concept "De Derde Trap" for the Elshoutsluice structure with the planned modifications and the changes in functionality is not yet verified for all the present requirements.

2.2. Objective

The goal of the design "De Derde Trap" is to provide a solution for the infrastructure problem for the tourists arriving via the river. This goal must be obtained without the loss of the current functions of the Elshoutsluice regarding the water-system and flood safety. In addition, it is necessary to include the planned modifications due to the new safety standards for flood risk reduction. Which concludes:

The objective of this thesis is to provide a conceptual structural design for the multi-functional use of the discharge sluice at Kinderdijk including the functions for water discharge, flood defence, passage for (motorised) vehicles and pedestrians, which fulfils standards for flood safety and buildings in the Netherlands.

With the use of this case study, a generic method will be derived for similar situations as the Elshoutsluice in Kinderdijk. Many hydraulic structures in the Netherlands will be analysed and possibly modified to meet the new requirements in 2050. Generic solutions can be given on how to solve encountered problems. Examples of problems that could be encountered are the availability of structural blueprints, the analysis of the rest lifespan and the (changing) environmental regulations.

2.3. Scope

The case water entree Kinderdijk has an infrastructure problem on a large scale, mainly due to tourism. This infrastructure problem is not further investigated since the focus is on the Elshoutsluice at Kinderdijk. However, not closing off the traffic in Kinderdijk during the construction phase is included in this report. The increasing number of tourists for the pedestrian tunnel is taken into account as well.

The connection of the pedestrian tunnel with the piers for the waterbus and the river cruise is not included in this report. The route from the pedestrian tunnel to the World Heritage Site Kinderdijk is not included as well.

The layout of the discharge sluice is rearranged with an additional pedestrian tunnel. This results in a different transfer of forces in the Elshoutsluice. This report focuses on the structural analysis of the discharge sluice when an pedestrian tunnel is added to the existing structure. With the structural analysis it is determined which existing elements need additional checks for the strength. The strength calculation itself is not included in this report.

This report focuses mainly on the failure mechanism non-closure of gates for the flood risk. Multiple existing closing mechanisms need to be replaced due to the additional pedestrian tunnel. The new tunnel itself needs to be closed with new gates as well. The effects of these changes are investigated.

Maintaining the flood protection during the use and construction phase is considered as well. The different failure mechanisms for hydraulic structures are included for this subject.

3

Methodology

In this chapter, a description of the used design method and the application of the method is given. At last, the report outline is explained.

3.1. Description of the civil engineering design method

This section gives the used method and an explanation of each step of the method.

3.1.1. Overview of the method

For this study a design method according to Roozenburg and Eekels (1995) and Voorendt (2020) is used. This method consists of seven design phases. Each phase is explained in the following subsections.

- Design phase 1: Problem analysis
- Design phase 2: Design definition
- Design phase 3: Development of concepts
- Design phase 4: Verification of concepts
- Design phase 5: Evaluation of alternatives
- Design phase 6: Integration of subsystems
- Design phase 7: Validation of the result

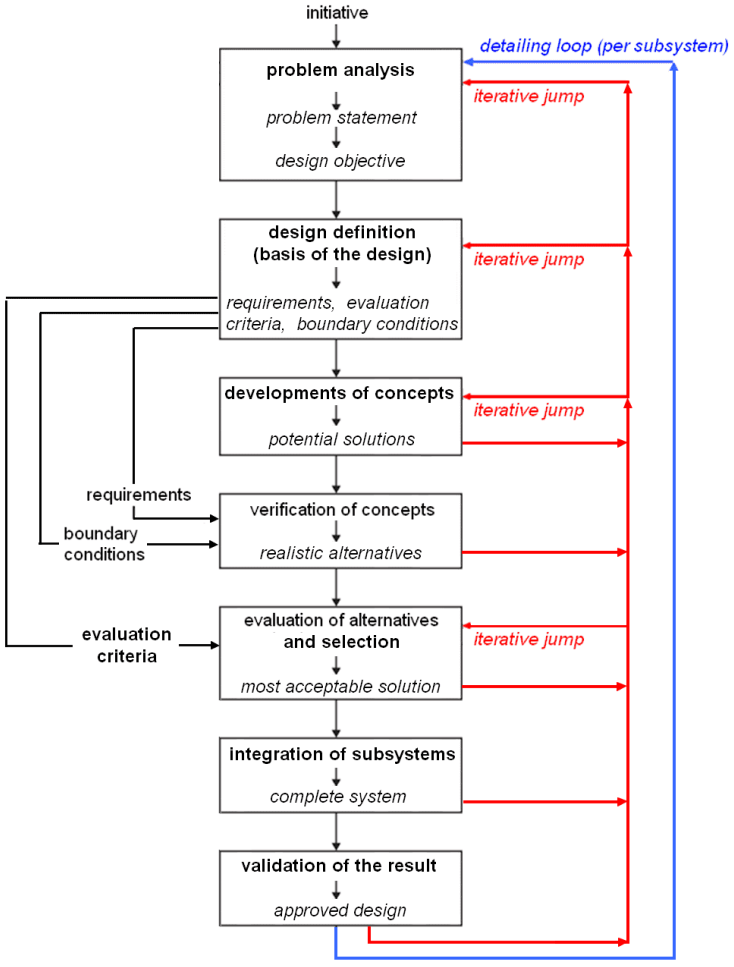

Figure 3.1: The design method according to Roozenburg and Eekels (1995) adjusted by Voorendt, M.Z.

3.1.2. Problem analysis

First, the problem and its environment need to be analysed. This design phase explains who, when and where a problem is experienced. With this analysis, the core problem can be summarised into a problem statement. From the analysis of the problem, the design objective can be formulated, which gives an idea of the problem. In the design objective, the expected performance of the future structure is described by formulation the desired functionality. The stated design objective is the basis of the programme of requirements (Voorendt, 2017).

3.1.3. Design definition

The purpose of the design that is described in the design objective has to be specified. This will be done in with a functional specification in the design definition phase. A clear overview of requirements for the desired functioning, circumstances and risk should be specified. These requirements can be grouped by type:

- Functional requirements, which describe the desired behaviour or performance of the (sub)system.
- Aspect requirements, which describe specific characteristics of the supporting system of the primary functioning system.
- External interface requirements, which result from adjacent elements in the surroundings which crosses or borders the system.
- Internal interface requirements, which result from the boundaries of system and subsystems.

A clear distinction needs to be made between the requirements and evaluation criteria. In addition boundary conditions need to be stated. These can be subdivided into at least five different categories: meteorological conditions, hydraulic conditions, nautical conditions, geotechnical conditions and geological conditions (Voorendt, 2017).

3.1.4. Development of concepts

In the third phase, the abstractly formulated design objective and the design definition should give a direction to generate initial concepts. This phase can be referred to as the basis of the design. Several sketches should be made to generate and explore different concepts. Reference projects can be looked at to provide additional ideas for concepts (Voorendt, 2017).

3.1.5. Verification of concepts

In this phase, the concepts of the development of concepts phase will be verified. With the functional verification, the concepts will be checked if it can fulfil its main functions. An important part of the aspect requirements is structural safety. Structural verification is needed to check whether a concept can be realised. This includes detailed strength, stability and constructability checks. The checks can be verified with the use of models (Voorendt, 2017).

3.1.6. Evaluation of alternatives and selection

In the evaluation of alternatives phase, a distinction is made between concepts and alternatives. The difference is that a concept is a not verified idea where an alternative is a verified concept. With a multi-criteria approach, the values of the design alternatives are determined. This could be done with relevant qualitative criteria. The best alternatives should be proposed in the selection phase. In addition, the consequences of the alternatives should be described. It could be useful to make a value-cost diagram to compare the best alternatives (Voorendt, 2017).

3.1.7. Integration of subsystems

The solutions for subsystems and components will be integrated into a complete functioning system in the sixth phase. An indication of the planning and structure has to be made. An optimal solution for the problem is made and the definition of 'optimal' is stated. The solution should be documented in a specific way that it can be constructed (Voorendt, 2017).

3.1.8. Validation of the result

Solutions for different components and elements must be integrated into a complete functioning system. The planning, total costs and spatial aspects have to be considered. A final check on the validity of the complete design is performed in this design phase. There is a difference between verification and validation. With validation, it is confirmed whether a system will perform its intended functions. Verification is the check whether the system design is correct (Voorendt, 2017).

3.2. Application of the civil engineering design method

The problem of the water entree of Kinderdijk is described, including the explanation of the surrounding area for the problem analysis phase. The problem statement, the objective and the scope are formulated.

An inventory of requirements, relevant laws, regulations and municipal plans is made for the design definition phase. It is described which functional aspects of the Elshoutsluice will change and which aspects will stay the same. The minimal dimension for a pedestrian passage are collected in this phase.

The development of concepts includes the location of the needed pedestrian tunnel and the floor configurations of the new tunnel. The options for possible new closing mechanisms are included in this phase as well. After the development of concepts, the concepts are verified based on the functional requirements. An evaluation, based on the evaluation criteria of the design definition, of the options and alternatives is made and the best alternatives are selected as a result. The evaluation in this thesis is performed per element instead of each total alternative which deviates from the method described in section 3.1. The reason for this are the many options for the elements which would result in even more total alternatives which is time consuming to evaluate. From the best alternatives, the preferred alternative for each element is selected. The alternatives are integrated into one preliminary design. The construction sequence is described for this design.

A design loop is made where the preliminary design is verified for the flood risk safety and the structural safety. The failure modes specific for hydraulic structures are checked. The flood risk is determined with the use of Riskeer and HydraNL. Stability checks are performed for the structural verification. For the structural safety a comparison is made of the loading on the Elshoutsluice for the initial design situation in 1985 and the new design with the current safety regulations. The load distribution in the structure is determined with the use of Matrixframe.

The validation of the result phase is not included in this report. The planning, total costs and consideration of the spatial aspects can be made as an extension of this thesis.

In obtaining a design solution for the Elshoutsluice, a generic method can be derived for other cases to cope with similar problems.

3.3. Report outline

In this section the report outline is given.

- Chapter 1 consists of the first part of the problem analysis phase, which is the problem statement.
- In Chapter 2 the second part of the problem analysis is given: the design objective.
- Chapter 3 describes the used methodology of this report. This is not part of a design phase, but the different phases are explained in this chapter.
- Chapter 4 consists of the design definition phase.
- In Chapter 5 the development of concepts, design phase 3, is described.
- In Chapter 6 the design phases verification of concepts, evaluation of alternatives and selection and the integration of subsystem are combined. The verification of concepts is performed based on the functional requirements.
- Chapter 7 describes the construction sequence for the preliminary design.
- Chapter 8 consists of a design loop to the phase of verification of concepts specific for flood risk safety.
- Chapter 9 consists of the verification of concepts phase for the structural safety.
- There is no design phase used in Chapter 10. This chapter consists of a general approach based on the performed design steps in the previous chapters.
- Chapter 11 gives the discussion, conclusion and recommendations.

4

Design definition

This chapter describes the functional specification of the Elshoutsluice in Kinderdijk. The desired functions, boundary conditions and evaluation criteria are specified.

4.1. Programme of functional requirements

The functional specification will be categorised in four different types of requirements according to the Guideline on Functional Specification of Rijkswaterstaat (2005). The first category is the functional requirements, which describes the desired behaviour or performance of the (sub)system. The second category is the aspect requirements, which describes specific characteristics of the supporting system of the primary functioning system. The third category is the interface requirements, which describes how the (sub)system fits in the environment and in itself (Voorendt, 2017).

4.1.1. Functional requirements

This subsection describes what the system should do. The current functional requirements of the Elshoutsluice in Kinderdijk are:

- Discharging rain- and groundwater into the river the Lek. Possible free-flow discharge up to 120 m^3/s according to (Waterschap Rivierenland, 2020).
- Letting in water from the Lek river in dry periods. The capacity of the old and new pumps together is 1500 m^3/min.
- Protecting the hinterland against floods at high water levels in the Lek river. The maximum required failure probability is 1/10,000 per year for the dike segment according to the water act. The alert value of 1/30,000 is selected as the design value for flood risk.
- Providing (motorised) vehicle transportation on top of the discharge sluice.

The additional functional requirement for the Elshoutsluice is:

- Providing a passage for pedestrians and wheelchair users as a solution to an infrastructure problem:
  - Circa 600,000 visitors in 2018 in Kinderdijk with an expected increase each year. The peak in an hour (based on two sample days in July) is approximately 750 arriving visitors (Defacto Stedenbouw, 2019).
  - Minimum passage height of 2.3 m according to Bouwbesluit 2012. Preferably a free height of at least 2.5 m is advised according to Haug and Schuurman (2019).
  - The pedestrian tunnel must be available for wheelchair users. A pedestrian path with

intensive use and/or regular used by people with walkers or wheelchairs must be at least 1.8 m wide. Preferably the path will have a minimum width of 2.4 m according to Haug and Schuurman (2019). The slope requirements are given in section F.1.
  - The minimum parapet height is 1 m for safety according to Bouwbesluit 2012.

4.1.2. Aspect requirements

Aspect requirements describe specific characteristics of how the system should support the primary functions. These requirements are divided into different standard categories according to Rijkswaterstaat (2005). The categories are safety, availability and reliability, appearance[1], sustainability, execution, maintenance, durability and demolition. Some categories are not applicable to this system. The aspect requirements of the Elshoutsluice per category are:

- Safety:
  - With fulfilment of the structural safety standards according to the Eurocodes.
  - With fulfilment of the flood risk safety standards according to the water act and WBI2017 for the end result and during the construction phase.
    - ◇ An alert value of 1/30,000 for the dike segment 16-2.
    - ◇ A lower threshold value of 1/10,000 for dike segment 16-2.
  - With no reduction of the flood risk safety of the end result compared with the current situation of the Elshoutsluice.
  - With inclusion of three gates for the new pedestrian tunnel according to Waterschap Rivierenland.
- Availability and reliability:
  - With extension of the functional lifespan.
  - With preservation of the surrounding monumental building(s).
- Appearance:
  - No requirements in this category.
- Sustainability:
  - Without pollution of the soil.
  - With minimum emission.
- Execution:
  - With minimal interruption of the traffic during the construction phase.
  - Without interruption of the navigation in the Lek river.
  - With modification of the existing structure.
- Maintenance:
  - Without hinder of maintenance due to the visitor infrastructure.
- Durability:
  - With anticipation to the expected increase of visitors in the future.
  - With anticipation to the expected future water levels.
- Demolition:
  - With demolition of existing concrete elements which blocks the new pedestrian tunnel.
  - With demolition of existing closing mechanism element which blocks the new tunnel.

[1] Rijkswaterstaat (2005) uses the category design instead of appearance. It is chosen to change this category to appearance for this thesis.

4.1.3. Interface requirements

The interface requirements are divided into external and internal requirements. External interface requirements result from adjacent elements in the surroundings which crosses or borders the system. The internal interface requirements result from the boundaries of system and subsystems (Voorendt, 2017).

The external interface requirement are:

- Preservation of the connection to the infrastructure for (motorised) vehicles.
- Anticipation to possible future strengthening of the adjacent levees as part of the flood defence segment 16-2.
- Integration of the new tunnel to the pedestrian infrastructure.

Internal interface requirements consists of:

- Connection of new concrete elements to the existing concrete structure.
- Integration of new closing mechanisms due to the pedestrian tunnel.

4.2. Boundary conditions

The boundary conditions describe the restriction of possibilities to what is possible in a given environment. According to Voorendt (2017) the boundary conditions can be arranged in distinct categories: geological, meteorological, hydraulic, nautical and geotechnical. The boundary conditions are determined in Appendix B. For each category, the relevant values are summarised below:

- Geological conditions:
  - A monumental building is located near the Elshoutsluice (number 15 in Figure 1.6).
  - The Elshoutsluice is located adjacent to the Lek river, which consists of fresh water.
  - The location is not prone to earthquakes.
- Meteorological conditions:
  - Wind: the governing wind direction is west for the waves.
- Hydraulic conditions:
  - Water levels Lek river: for the alert value NAP +3.66 m and for the lower threshold NAP +3.48 for reference year 2023. The water level for the reference year 2100 with climate scenario W^+ is NAP + 4.22 for the alert value and NAP + 4.05 m for the lower threshold.
  - Water levels discharge reservoirs: a maximum of NAP +2.50 m for Nederwaard and a maximum of NAP +1.50 m for Overwaard.
  - Waves: for the lower threshold a value of 1.42 m and for the alert value 1.32 m.
- Nautical conditions:
  - Shipping in the Lek: shipping must not be hindered during the construction phase. The probability of ship collision with the sluice is negligible because the shipping channel is not located nearby. The new connection of the pedestrian tunnel and the piers will prevent ship collision with the discharge sluice as well.
- Geotechnical conditions:
  - The soil layout: predominantly clay and peat. The sand layer starts at approximately NAP -14 m (Waterschap Rivierenland, 2020).

4.3. Evaluation criteria

The evaluation criteria are used to compare different concepts and alternatives. Some of the criteria can be derived from the stakeholders (Voorendt, 2017). The list of evaluation criteria used for the Elshoutsluice is:

- Adaptability to the increasing number of visitors in Kinderdijk
- Limitation of impact on the surroundings
- Connectivity pedestrian passage with hinterland
- Influence on the flood risk safety
- Influence on pedestrian flow
- Accessibility during high water
- User experience of the pedestrian tunnel
- Visual integration in the surrounding area

The evaluation criteria selected specifically for evaluation of the closing mechanisms in the culverts are:

- The number of movable parts of the gate type
- The option for manual closure of a gate type.
- Narrowing of the culvert in open situation.

5

Development of concepts

This chapter describes the development of concepts for the Elshoutsluice. First, the components are selected for which different concepts will be developed. Second, all the concepts per component are explained.

5.1. Selection of components for the concepts

A system can be divided into subsystems. In this case, the Elshoutsluice is chosen as the main system. The Elshoutsluice consists of different systems and elements shown in Figure 5.1. The layout of the Elshoutsluice is shown in Figure 6.3. An elaborate description of the current structure of the Elshoutsluice is given in section B.5. Concepts are developed for a selection of the subsystems in this chapter.

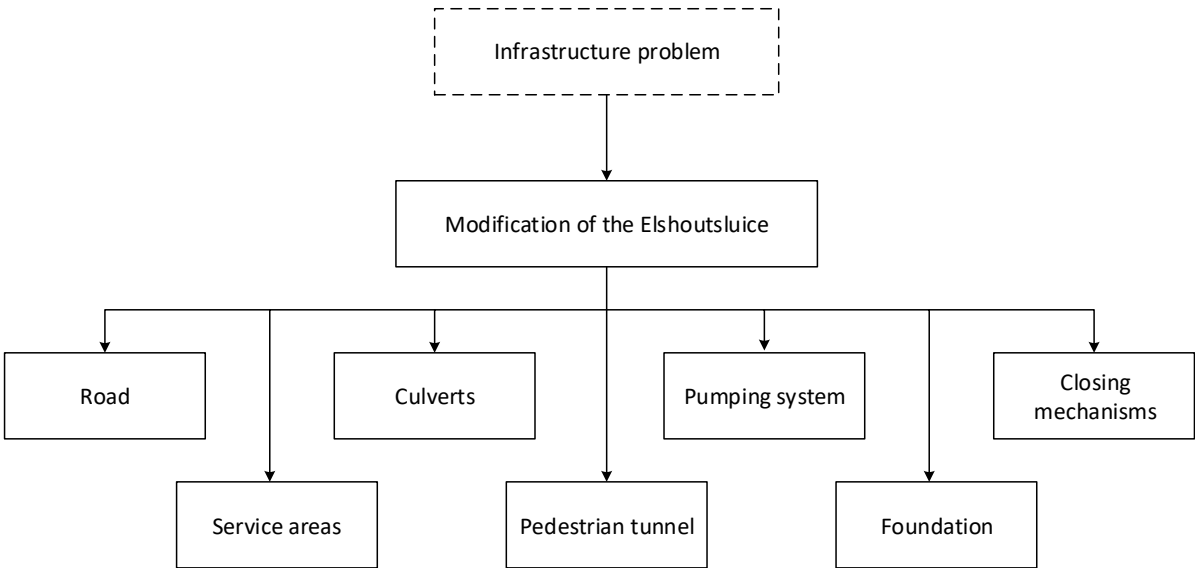

Figure 5.1: System decomposition

The Elshoutsluice structure has not reached the end of its designed lifespan of 100 years yet. It is preferred to keep as much of the existing structure as possible based on sustainability. Therefore, the culverts structure and the foundation will remain unchanged if possible. The pumping systems in culvert 4 and the pumps placed in culvert 3 recently are chosen to remain in place. As a result, there are no concepts given for the culverts structure, foundation and pumping systems.

A new pedestrian tunnel will be included as a subsystem. Various dimensions and locations are possible for this tunnel. Options for the width, placement, floor level and floor slope of the pedestrian tunnel are given in this chapter. Service areas such as the technical area are likely to be relocated due to the new tunnel. The current closing mechanisms in the Elshoutsluice can form an obstruction for the pedestrian tunnel. Substitution of different closing mechanisms can be needed. Therefore, concepts for various gate types are considered in this chapter as well.

The pavement on top of the levee will be removed and placed anew during the construction of the new pedestrian tunnel. This includes the bicycle path and the motorised vehicle road. The changes in the pavement highly depend on the chosen concepts and will be considered in a later stadium for this report.

5.2. The pedestrian tunnel

First, concepts are developed for the location of the new pedestrian tunnel. Drawing of the relocation of the technical area based on these concepts are given in Appendix D. Second, options are given for the floor of the new pedestrian tunnel.

Figure 5.2: Top view of the Elshoutsluice (source: Google maps)

5.2.1. Location of the pedestrian tunnel

A tunnel underneath the Elshoutsluice is not considered since the pile foundation is preferred to remain unchanged. The concepts are divided into two categories. The first is a pedestrian tunnel of 5.5 m width, which is the same as the culvert width. Pedestrian tunnels larger than 5.5 meters are in the second category. The concepts are shown in a sketch of the cross-section A-A from Figure 5.2.

Category 1: A pedestrian tunnel of 5.5 m wide

A pedestrian tunnel of 5.5 meter fits exactly above one of the existing culverts. There are four possible locations for the placement of this pedestrian tunnel inside the Elshoutsluice, shown in Figure 5.3. This results in the first four concepts, which are all shown in one figure below. Concept 1 is a pedestrian tunnel above culvert number 1. The second concept is a tunnel above culvert 2, the third above culvert 3 and the fourth above culvert 4. Excavation of the soil underneath the motorised vehicle road will be necessary for the placement of the new pedestrian tunnel.

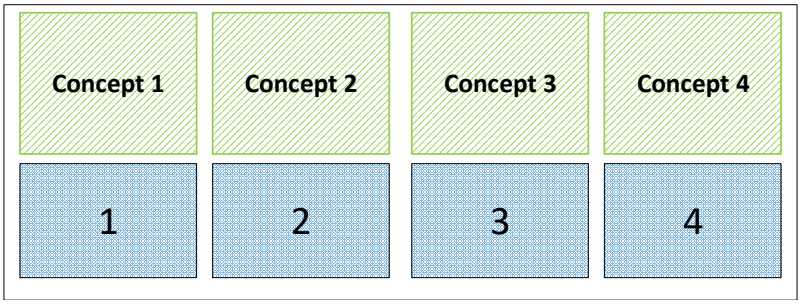

Figure 5.3: Sketch of concept 1, 2, 3 and 4 for the placement of the new pedestrian tunnel.

Concept number 5 and 6 are located outside of the Elshoutsluice. Figure 5.4 shows the locations of these concepts. The same height as the first four concepts is used for concept 5 and 6. The reason

for this is the connection with the ground level hinterlands.

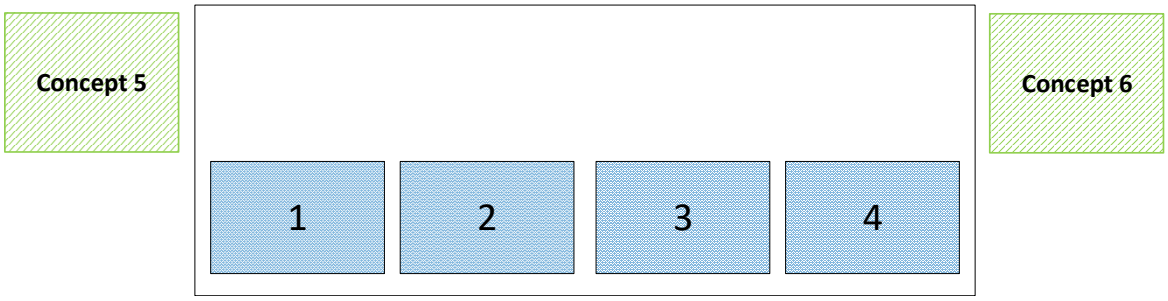

Figure 5.4: Sketch of concept 5 and 6 for the placement of the new pedestrian tunnel.

Category 2: A pedestrian tunnel wider than 5.5 m

It is possible that the capacity of a 5.5 meters wide pedestrian tunnel is not sufficient right now or in the future. In this case, a larger tunnel is needed. The second category of concepts includes options for pedestrian tunnels larger than 5.5 meters. Each concept represents a different tunnel width in this category. The possible locations are not given elaborately since this is already shown in the first category of concepts.

Concept 7 is an expansion of a pedestrian tunnel partly above another culvert, see Figure 5.5. This idea could be applicable for the locations of concepts 1, 2, 3, 4, 5 and 6.

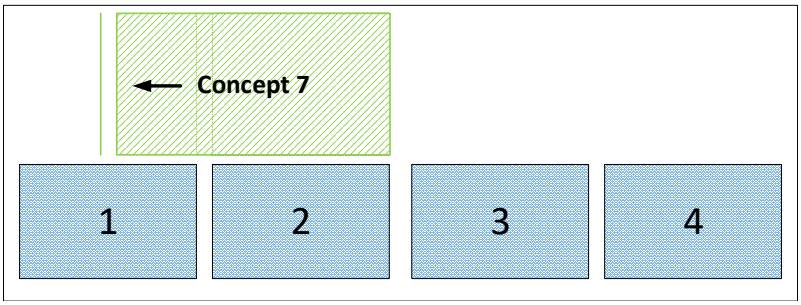

Figure 5.5: Sketch of concept 7 for an expansion of the pedestrian tunnel.

A pedestrian tunnel of approximately two times the culvert width is concept 8. Figure 5.6 shows a possible location for this tunnel width. This concept is possible above culvert 1 and 2, culvert 3 and 4 or outside of the Elshoutsluice as well.

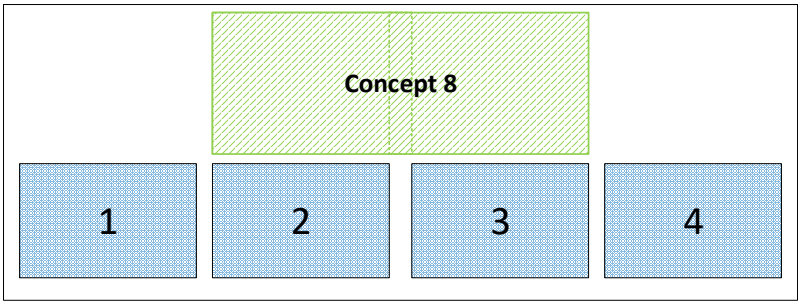

Figure 5.6: Sketch of concept 8 for an expansion of the pedestrian tunnel.

Concept 9 is a pedestrian tunnel with approximately three times the culvert width. This can be applied above culvert 1, 2 and 3 as can be seen in Figure 5.7 or above culvert 2, 3 and 4. The locations same as concept 5 and 6 are possibilities for this large pedestrian tunnel as well.

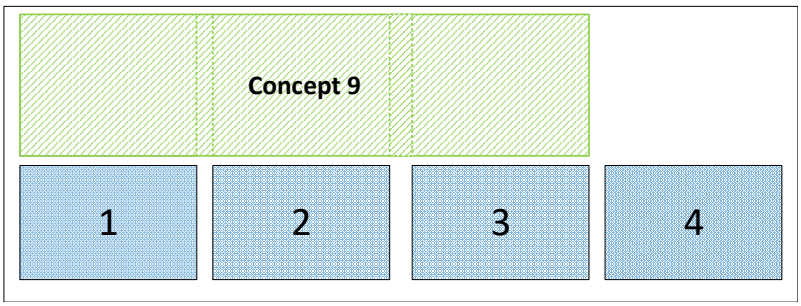

Figure 5.7: Sketch of concept 9 for an expansion of the pedestrian tunnel.

5.2.2. Floor of the pedestrian tunnel

The lowest point of the pedestrian tunnel could vary. The lower limit option is shown in Figure 5.8. In this case, the floor level at NAP +1.6 m will remain the same under the pavement. However, the platform outside of the tunnel needs to be lowered or a slope needs to be introduced to make a connection to the hinterland ground level at NAP + 2.5 m. The pavement for the motorised vehicles is currently at an average level of NAP + 4.6 m. There is just enough space for a pedestrian tunnel with a clearance of 2.5 m.

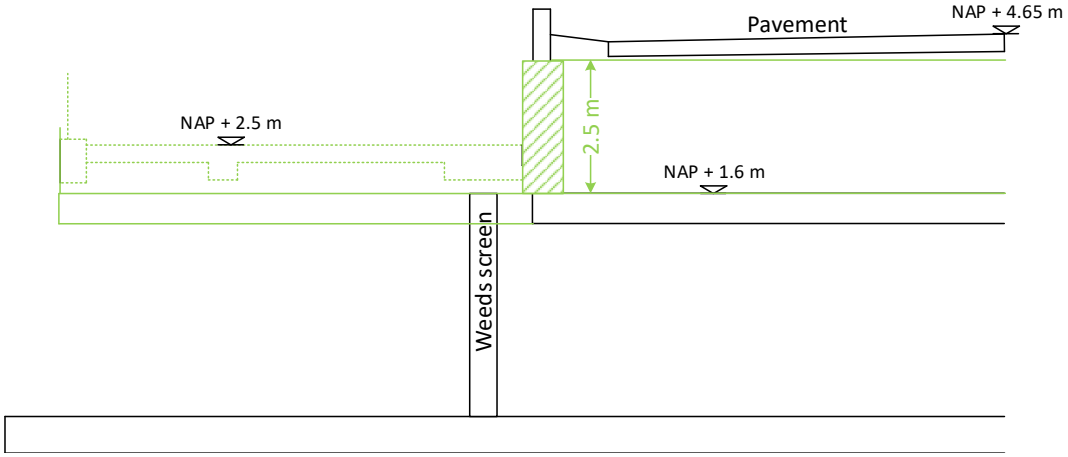

Figure 5.8: The option with the pedestrian floor at a level of NAP +1.6 m. The river side is at the right side of figure.

Figure 5.9 shows the upper limit option of the floor of the pedestrian tunnel. The level will be at NAP +2.5 m, which is the same as the platform outside of the tunnel. In this case, the pavement needs to be approximately 0.9 m higher than the current situation.

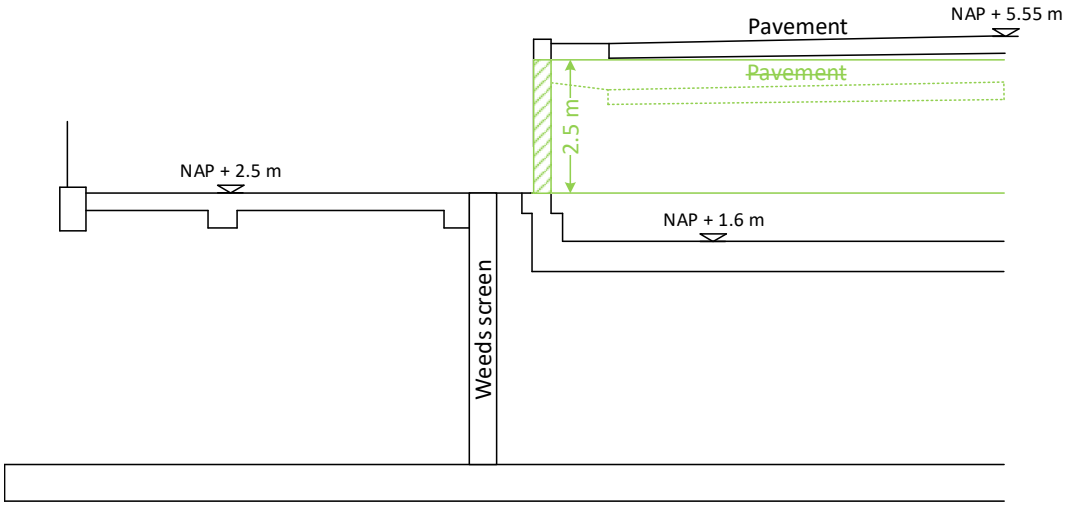

Figure 5.9: The option with the pedestrian floor at a level of NAP +2.5 m. The river side is at the right side of figure.

It is preferred to place the pedestrian tunnel entrance at the river side at a higher level than the hinterland level with regards to flood protection. The pedestrian tunnel will be used mainly by tourists for the world heritage site Kinderdijk. This includes the possibility of visitors with walking difficulties. The decision is made to make the entire tunnel available for wheelchair users with a slope and no stairs. The slope of the floor starts where the motorised vehicle road ends to reduce the possible increase of the road level. The distance between the road and the outer wall at the river side is approximately 19 m based on old drawings of the Elshoutsluice and google maps measurements. An analysis is made of the different options for the slope of the pedestrian tunnel in Appendix F based on the slope regulations for wheelchair users according to Bouwbesluit 2012. The number of mandatory platforms of 1.5 m increase with the steepness of the slope. This resulted in the slope options over 19 m shown in Figure 5.10. The maximum slope per option is:

- Option 1: a slope of 1:25.
- Option 2: a slope of 1:20.
- Option 3: a slope of 1:16 with mandatory platforms.
- Option 4: a slope of 1:12 with mandatory platforms.
- Option 5: a slope of 1:10 with mandatory platforms.

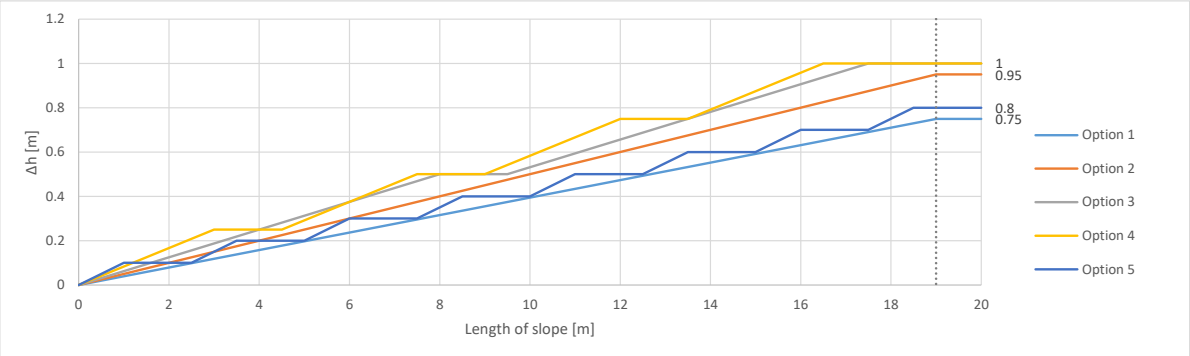

Figure 5.10: All the different slope configurations over a length of 19 meter

An elaborate explanation of the development of these options is given in Appendix F. These slope configurations are combined with the two possible floor levels shown in Figure 5.8 and Figure 5.9. All options are analysed in section F.2 and this resulted in the floor levels of the pedestrian tunnel at

the river side of the Elshoutsluice. These values are shown in Table 5.1.

Table 5.1: The pedestrian tunnel floor level at the river side of the Elshoutsluice for the slope configurations according to Figure 5.10 depending on the tunnel floor level under the road.

Alternative	Slope	Floor level at NAP + 1.6 m	Floor level at NAP + 2.5 m
Option 1	1:25	NAP + 2.35 m	NAP + 3.25 m
Option 2	1:20	NAP + 2.55 m	NAP + 3.45 m
Option 3	1:16	NAP + 2.60 m	NAP + 3.50 m
Option 4	1:12	NAP + 2.60 m	NAP + 3.50 m
Option 5	1:10	NAP + 2.40 m	NAP + 3.30 m

5.2.3. The roof

From Table 5.1 can be seen that the highest possible floor level is at NAP + 3.50 m. In this case the bottom of the roof slab will start at NAP + 6.00 m for a clearance of 2.5 m. This level is above the current roof top level of NAP + 5.75 m. As a result two concepts are developed. The first concept is to raise the roof top level above the pedestrian tunnel. The second concept is to remove a part of the roof above the pedestrian tunnel at the river side. This leads to a partly open tunnel.

5.3. Closing mechanisms

From the concepts of subsection 5.2.1 can be concluded that there is a possibility that a lift gate and/or a radial gate will obstruct the new pedestrian tunnel. A solution can be to close off one culvert and increase the capacity of the remaining culverts. Another solution is new gates at the location of the radial gate and lift gate. Besides the culverts, the new pedestrian tunnel will need closing mechanisms as well. In Appendix G an inventory of gate types is made. From this inventory a pre-selection is made for the gate types suitable for a discharge sluice, see section G.7. This results in the following gate types considered as options:

- Flap gate
- Radial gate
- Sector gate (horizontally/vertically hinged)
- Rotary segment gate
- Drum gate
- Single-leaf gate
- Vane gate
- Mitre gate
- Sliding gate
- Rolling gate
- Vertical lift gate
- Vertical sink gate
- Inflatable gate
- Unfolding gate (horizontally/vertically)

6

Functional verification and evaluation

The different concepts from Chapter 5 are verified based on the requirements of Chapter 4. In this chapter, a preferred alternative is chosen after a functional verification and evaluation of the different options given in Chapter 5.

6.1. Functional verification

The new design for the adaption of the Elshoutsluice must fulfil the required functions:

- Discharging rain- and groundwater to the Lek river.
- Letting in water from the river.
- Protecting hinterland against flooding.
- Providing (motorised) vehicle transportation passage.
- Providing passage for pedestrians.

All the concepts of Chapter 5 fulfil the requirements for discharging water to and from the Lek river, because the structure will not be closed off completely. New closing mechanisms will be included for the pedestrian tunnel and possibly the culvert(s) which results in fulfilment of hinterland protection. The bicycle road and motorised vehicle road on top of the Elshoutsluice could be relocated, but is not removed completely for all the concepts. Therefore, the function for vehicle transportation on top of the sluice is fulfilled. The verification of the function for providing a pedestrian passage is made based on the required pedestrian capacity.

An analysis of the level of service for a pedestrian tunnel with a width of 5.5 m is made in Appendix E. The levels of service of category A and B are considered acceptable, see section E.2. The expected number of visitors for two different growth scenarios are determined for 2030. A peak flow is estimated in persons per minute per meter effective width (W_E). Table 6.1 shows the results of the analysis of Appendix E. The conclusion is that a pedestrian tunnel of 5.5 m width is sufficient with the expected visitors growth in 2030.

Table 6.1: The conclusion of the determination of the level of service for a pedestrian tunnel of 5.5 m wide.

Year	**Average number of people**	**Estimated peak**	**People over W_E**	**LOS**
2018	25 p/min	38 p/min	10 p/min/m	A
2030 with 4% increase	39 p/min	59 p/min	15 p/min/m	A
2030 with 7% increase	55 p/min	83 p/min	21 p/min/m	B

Since the smallest concept width is 5.5 m, all the concepts of Chapter 5 meet the level of service

requirements. This results in fulfilment of all the functional requirements for all the concepts.

6.2. Evaluation

The evaluation is done per element of the Elshoutsluice. The elements are the width, location, floor level, floor slope and the roof of the pedestrian tunnel. The closing mechanisms will be evaluated separately for the culvert(s) and the pedestrian tunnel. After each evaluation a selection is made of the best alternative(s).

6.2.1. Width of the pedestrian tunnel

The width of the tunnel is evaluated on the criteria of adaptability to the increasing number of visitors in Kinderdijk. The first category of concepts are sufficient for the number of visitors up to at least 2030, therefore a tunnel wider than 5.5 m is for the current situation oversized. Wider tunnel concepts of category 2 could be possibilities for expansion in the further future if the increase of visitors continues. This result in a current selection of the concepts 1 up to and including 6 shown in Figure 6.1.

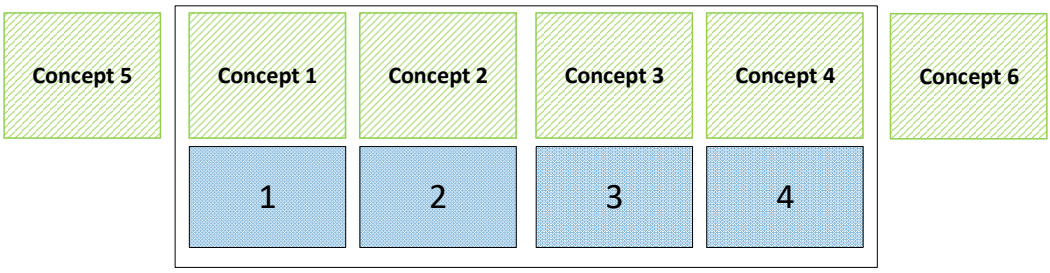

Figure 6.1: Sketch of concept 1, 2, 3, 4, 5 and 6 for the placement of the new pedestrian tunnel.

6.2.2. Location of the pedestrian tunnel

The location of the pedestrian tunnel is evaluated based on the limitation of impact on the surroundings criteria. Figure 6.3 shows a sketch of the current layout of the Elshoutsluice. It can be seen that the four culverts of the Elshoutsluice are not identical. There is a difference between pumps and gates. This results in different obstructions for a pedestrian tunnel above culvert 1 (concept 1) than for example a tunnel above culvert 4 (concept 4). The top view sketches of the four concepts are given in Appendix D.

(a) The road and bicycle path on top of the Elshoutsluice with the removable bicycle path above culvert number 4.

(b) The removable lifting frame above culvert number 3.

Figure 6.2: Photos of the Elshoutsluice in February 2020

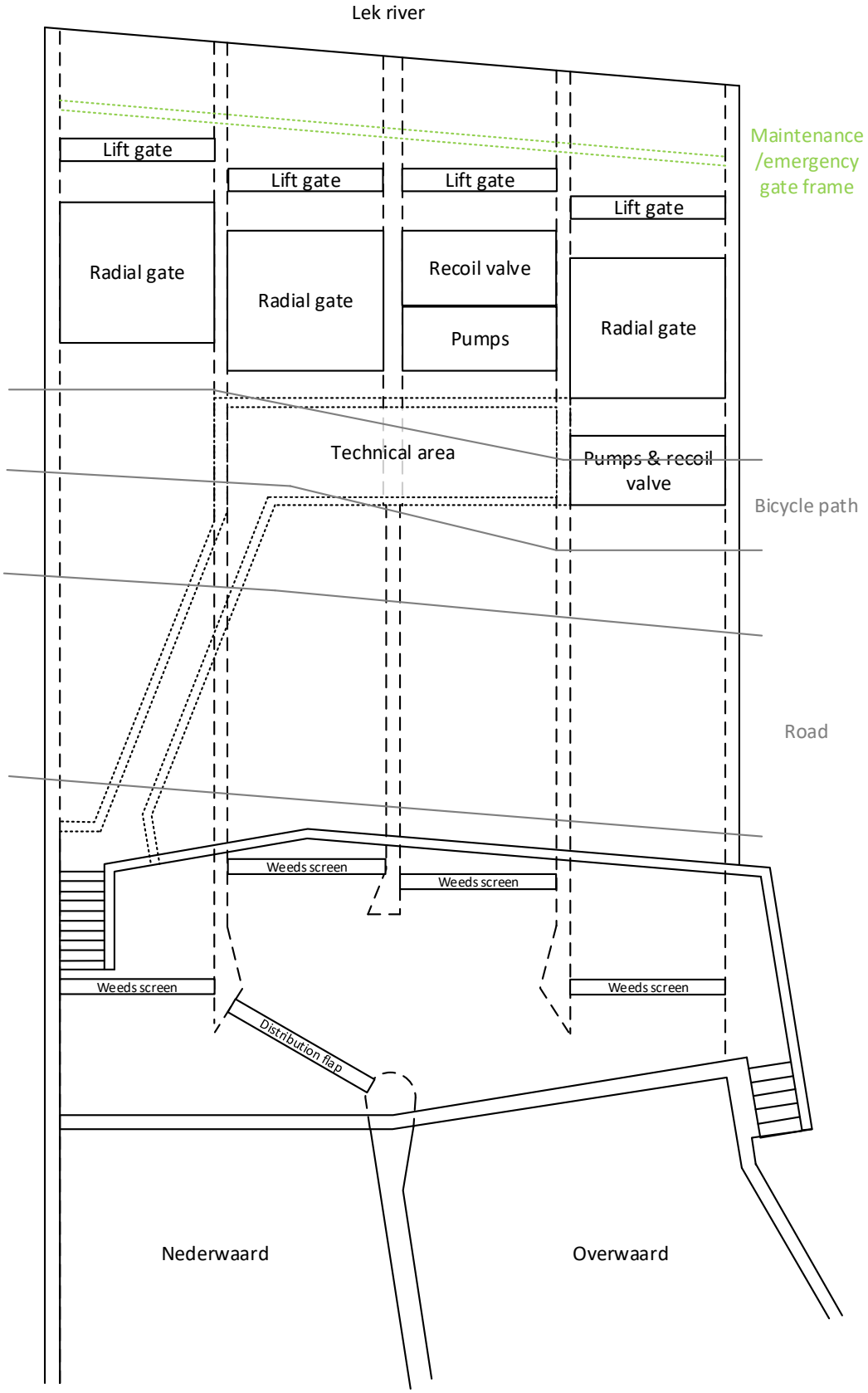

Figure 6.3: Top view sketch of the current layout of the Elshoutsluice including the bicycle path and motorised vehicle road.

The stairs hinterlands will obstruct concept 1, which can be seen in Figure 6.3. Above culvert number 4 there is a lifting frame for the pumps right above the pumps and under a removable bicycle path, which is shown in Figure 6.2a. This will form an obstruction for concept number 4. The lifting frame for the pumps in culvert number 3 is a removable frame on top of the Elshoutsluice structure. Figure 6.2b shows this lifting frame. This type of frame will form no obstruction for a tunnel above culvert 3. All the obstructions for the concepts 1, 2, 3 and 4 are collected and compared in Table 6.2.

Table 6.2: Comparison of obstructions for concepts 1, 2, 3 and 4.

Obstruction type	**Concept 1**	**Concept 2**	**Concept 3**	**Concept 4**
Radial gate	Yes	Yes	N.a.	Yes
Lift gate	Yes	Yes	Yes	Yes
Pumps	N.a.	N.a.	Possibly	Possibly
Recoil valve	N.a.	N.a.	Possibly	Yes
Maintenance gate frame	Yes	Yes	Yes	Yes
Technical area	The entrance tunnel	Yes	Yes	N.a.
Other	Stairs hinterlands	N.a.	Venting pipes	Lifting frame
Total obstructions	5	4	4/6	5/6

Culvert 1 and 2 are similar qua closing mechanisms. The main differences between concept 1 and concept 2 are the obstructions due to the technical area and the stairs connecting the platform hinterlands to the road on top of the sluice, see Table 6.2. Concept number 2 is preferred over concept number 1, since it does not include the demolishing of a concrete stairs. Therefore, concept 1 is not included as a best alternative.

Figure 6.4: The distance of 32.15 m road between the Elshoutsluice and the monumental building (source: Google Maps)

In the boundary conditions in section 4.2 is described that a monumental building is located near the Elshoutsluice. Figure 6.4 shows the location of the monumental building. This building must be unaffected during and after the construction of the new pedestrian tunnel. The new tunnel will be located nearby this building with concept number 6. To prevent possible damage to this monumental building due to a nearby construction site, concept 6 is excluded.

The concepts of a pedestrian tunnel above culvert 2 and 3 are compared. There is not much space available for the relocation of pipes needed for the pumps due to the floor of the new pedestrian tunnel. Many recently placed elements above culvert number 3 will be relocated. Culvert 2 has older elements than culvert 3. Therefore, the decision is made to exclude the option for a new pedestrian tunnel above culvert 3. The remaining best alternatives for the location are given in Figure 6.5

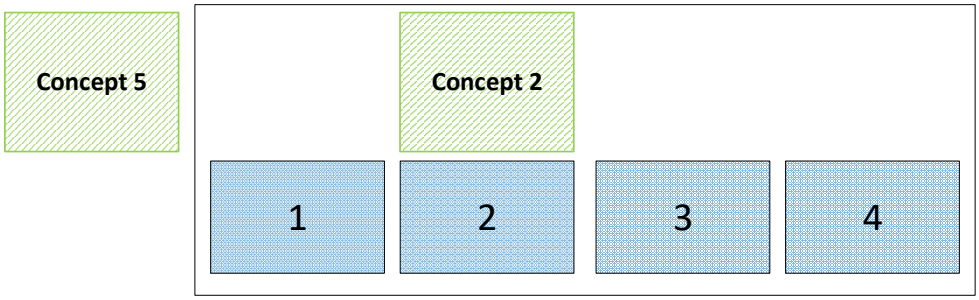

Figure 6.5: Sketch of the remaining concepts for the placement of the new pedestrian tunnel.

6.2.3. The floor of the pedestrian tunnel

The options for the floor of the pedestrian tunnel are evaluated on the criteria for limitation due to impact on the surroundings, connectivity of the hinterland, influence on the flood risk safety, influence on the pedestrian flow and accessibility during high water.

From subsection 5.2.2 is concluded that the road on top of the levee will rise 0.9 m in case of a pedestrian floor level at NAP + 2.5 m. The road level remains the same for a pedestrian tunnel floor level at NAP + 1.6 m. Slopes are needed with an increase of the road level. This could cause difficulties with the monumental building near the Elshoutsluice. The distance between the sluice and the monumental building is estimated with Google Maps and is approximately 32.15 m, see Figure 6.4.

In Appendix H a minimum length of the slope is determined for a height difference of 0.9 m. This resulted in a minimum length of 26.86 m which is below the 32.15 m available length. This proves that there is enough space between the monumental building and the sluice for the road slope. There could be an additional 5.5 m length available since a tunnel above culvert number 4 is excluded in subsection 6.2.2. This results in the slope starting right after culvert number three. However, this additional length is not available in the case of a multi-functional area above culvert 4.

A floor level at NAP + 2.5 m is verified and has a preference over a floor at NAP + 1.6 m due to connectivity with the hinterland ground level. With a floor at NAP + 1.6 m, multiple slopes are needed and/or the platform hinterlands need adjustments in level height. Therefore, the alternative of a floor level at NAP + 1.6 m is excluded. The floor level of NAP + 2.5 m is combined with the different slope configurations of subsection 5.2.2 and shown in Figure 6.6. The slopes are needed to provide a positive influence on the flood risk safety. For each slope configuration of Figure 6.6 the floor level at the outer wall of the Elshoutsluice is determined and given in Table 6.3.

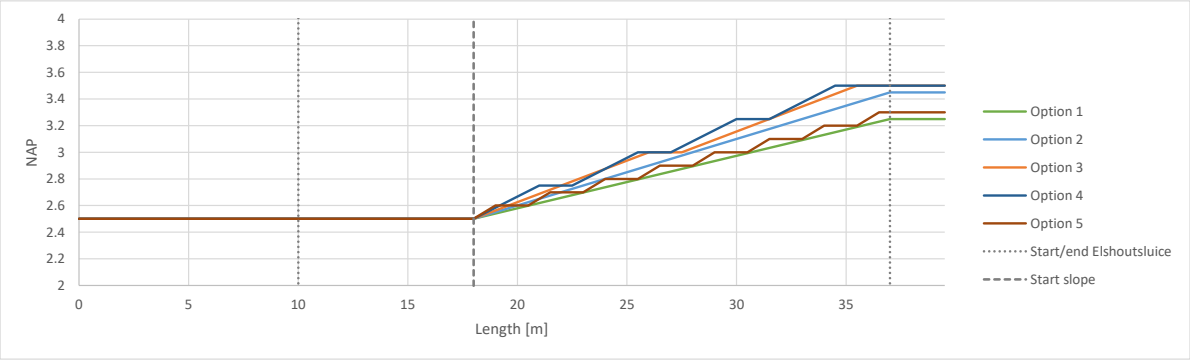

Figure 6.6: The slope configurations for a floor level at NAP + 2.5 m.

Table 6.3: The slope options from Figure 6.6 and the floor level at the outer wall of the Elshoutsluice.

Alternative	Slope	Floor level at river side
Option 1	1:25	NAP + 3.25 m
Option 2	1:20	NAP + 3.45 m
Option 3	1:16	NAP + 3.50 m
Option 4	1:12	NAP + 3.50 m
Option 5	1:10	NAP + 3.30 m

The results of the floor configuration in Table 6.3 are compared based on the influence on the pedestrian flow. The fifth option is excluded due to the combination of the many horizontal platforms and steep slopes. This only results in a slightly higher total height than option 1, which makes it an unprofitable option. Due to the steeper slopes, there is a higher chance that a wheelchair user needs more intermissions than the other options. This has a negative effect on the flow of visitors through the pedestrian tunnel. Option 4 is excluded as well, since it reaches the same level height as option 3 but with steeper slopes and more platforms.

The floor level at the river side needs to be high enough in case of high water levels at the Lek. If the water level is higher than the floor level, the pedestrian tunnel needs to be closed and can not be used. It is preferred for the pedestrian tunnel to be functional as much as possible. With HydraNL, the exceedance frequency of the water levels at the lek river are determined for climate scenario W+ for reference years 2050 an 2100. These frequencies are given in Figure 6.7 and Figure 6.8. Both reference year 2050 and 2100 are analysed, since the end of the design lifespan lies between these years. For each floor level height of the remaining alternatives, the exceedance frequency is calculated and compared in Table 6.4.

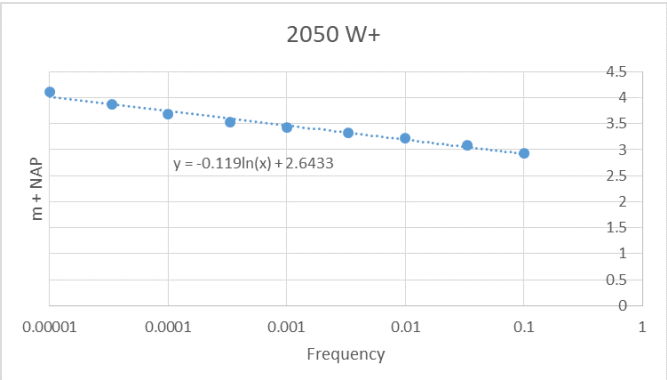

Figure 6.7: The exceedance frequency of the water level at the Lek for reference year 2050 with climate scenario W+.

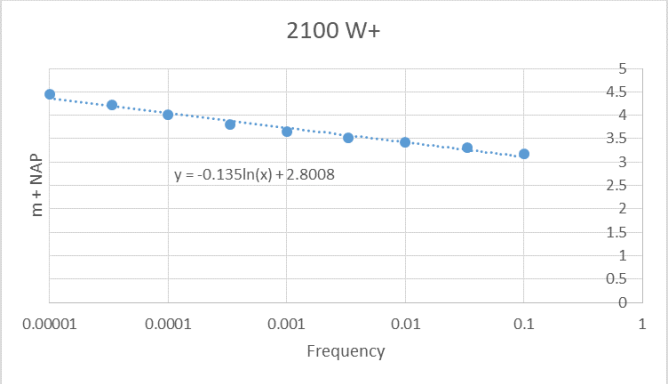

Figure 6.8: The exceedance frequency of the water level at the Lek for reference year 2100 with climate scenario W+.

Table 6.4: The exceedance frequency for the water levels equal to the selected options of Table 6.3.

Water level	**2050 W+** f [1/year]	**2100 W+** f [1/year]
NAP + 3.50 m	1/1338	1/175
NAP + 3.45 m	1/879	1/123
NAP + 3.25 m	1/164	1/28

It is preferred to extend the lifespan of the Elshoutsluice if possible. Therefore, the floor level height is checked if it will be sufficient for the highest climate scenario for 2100. From Table 6.4 can be concluded that frequency of occurrence for NAP + 3.25 m is much higher than the other alternatives. Therefore, the slope of 1:25 with a floor level of NAP + 3.25 m is not included as a best alternative.

6.2.4. The roof of the pedestrian tunnel

The roof of the pedestrian tunnel is evaluated based on user experience. The current roof of the Elshoutsluice will obstruct the pedestrian tunnel with the remaining slope alternatives. Sketches for a slope of 1:20 is given in Figure 6.9. Both options are considered as good alternatives. However, the user experience of a partly open tunnel can be more pleasant for pedestrians than a long closed tunnel. A partly open tunnel is selected as the best alternative.

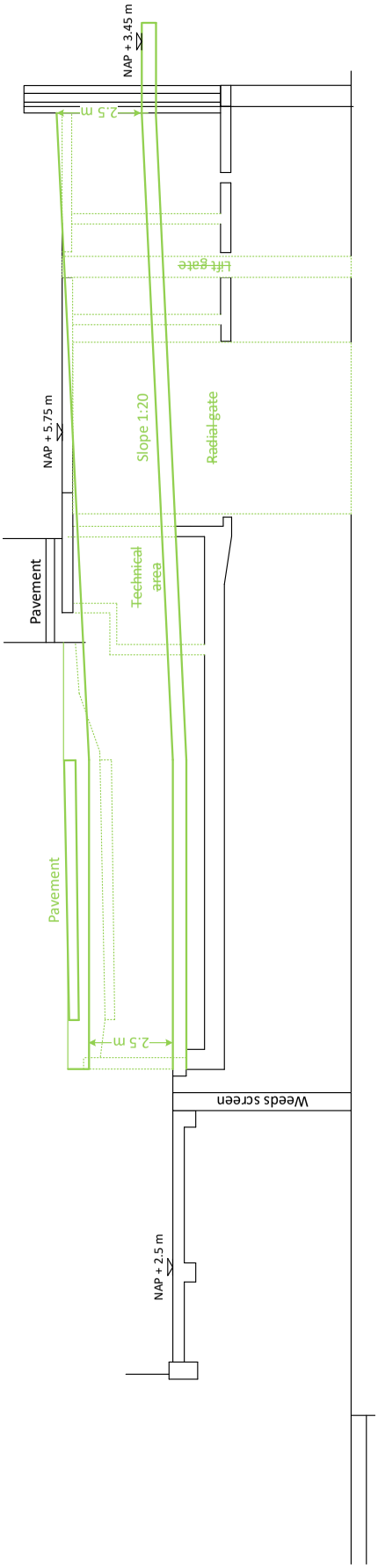

Figure 6.9: Sketch of a pedestrian tunnel with a slope of 1:20 above culvert number 2

6.2.5. The closing mechanisms

In section 5.3 a preliminary selection is made for closing mechanisms suitable for a discharge sluice in general. There are two concepts left for the placement of the pedestrian tunnel, given in subsection 6.2.2. This results in possible changes in culvert number 2 for the closing mechanisms. Besides the gates in the culverts, the pedestrian tunnel should be closed off as well in case of high water levels in the Lek river. New gates will be included in the tunnel. The closing mechanisms are evaluated on limitation due to the surroundings.

Culvert 2

Culvert 2 consists of a radial gate and lift gate. Both gates will block the new pedestrian tunnel and will be replaced by other gates. This subsection verifies the gate types from section 5.3. Since the current radial gate and lift gate do not fit in a culvert with a pedestrian tunnel, these gate types are excluded as an option. The lift-and-turn gate is only a possibility if the gate turns inside the culvert since there is no available space above the culvert to turn the gate.

It is not possible to take up much horizontal space for the new gates since there are adjacent culverts to culvert number 2. For this reason the following gates are excluded: sector gate (vertically hinged), vane gate, sliding gate and rolling gate.

The foundation of the Elshoutsluice is chosen to remain unaffected. Including a gate type which will sink into the sill of the culvert results in changes in the bottom slab. This is not preferred and therefore the sector gate (horizontally hinged), drum gate and vertical sink gate are excluded. The flap gate is an option when the rotary axis is at the top of the culvert instead of the sill. This reduces the list of possible gates to:

- Flap gate (rotary axis at top).
- Rotary segment gate.
- Single-leaf gate.
- Mitre gate.
- Lift-and-turn gate.
- Inflatable gate.
- Unfolding (horizontally/vertically).

The last option is to close off the culvert 2 completely in case of a pedestrian tunnel above culvert 2 and increase the pumping capacity of the pumps in culvert 3 and 4.

A second evaluation is made to compare the remaining gate alternatives. The evaluation is based on the number of movable parts, manual closure and the narrowing of the culvert. If a gate type consists of many elements which need to move, there is a higher probability of failure for this gate type. The possibility of manual closing of a gate has a positive influence on the flood risk safety of a gate type. This aspect is taken into account with the non-closure evaluation in the score-tables as well Rijkswaterstaat (2017b). The results of the evaluation of the gate type alternatives is given in Table 6.5.

Table 6.5: Comparison of the gate type alternatives

Gate type	Movable parts	Manual closure	Narrowing culvert	Result
Flap	1 part (+)	Yes (+)	No (+)	+ + +
Segment	1 part (+)	No (-)	Yes (-)	-
Single-leaf	1 part (+)	Yes (+)	Yes (-)	+
Mitre	2 parts (0)	Yes (+)	Yes (-)	0
Lift-turn	2 parts (0)	No (-)	No (+)	0
Inflatable	1 part (+)	No (-)	No (+)	+
Unfolding (h)	Many (-)	No (-)	Minimal (0)	- -
Unfolding (v)	Many (-)	Yes (+)	No (+)	+

From Table 6.5 can be concluded that the best alternatives are the flap gate, single-leaf gate, inflatable and the vertical unfolding gate.

Pedestrian tunnel

New gates are needed for the pedestrian tunnel to protect the hinterland against flooding. These gates can be used to close the pedestrian tunnel outside visiting hours as a secondary function. Waterschap Rivierenland has a preference for three closing mechanisms for the new pedestrian tunnel.

For the pedestrian tunnel, different closing mechanisms are considered than for the culverts. The decision is made to select only the gates with horizontal movements which take up minimal space in the Elshoutsluice. There is available space above culvert 1 and 3 for gate storage. The selection out of the inventory of section 5.3 is:

- Sliding/rolling gate
- Single-leaf gate
- Mitre gate

6.3. Selection of alternatives

A preference selection is made of all the best alternatives to perform the flood risk and the structural verification. Figure 6.11 shows the preference selection of the alternatives. The gates are numbered from hinterlands to the river side. The alternatives marked in grey are excluded based on the evaluations in section 6.2. Each selection is explained below:

- Location: the alternative above culvert 2 is chosen. The reason for this decision is the inclusion of the structure of the Elshoutsluice which has a preferable visual integration in the surrounding area
- Slope floor: a slope of 1:20 is selected for the floor of the pedestrian tunnel since it has no platforms which has a positive effect on the pedestrian flow.
- Gate type pedestrian tunnel: a sliding/rolling gate is chosen for all three gates since the gate can be concealed in open position above the adjacent culverts. This has a positive effect on visual integration.
- Gate type culvert: the location of gates will remain approximately the same to keep the self weight of the new gates at the same location. For gate location 1, a flap gate is selected which is located at the top of the culvert (very similar to a recoil valve) because of the high evaluation score in Table 6.5. At gate location 2 a vertical unfolding gate is selected. This gate can be placed exactly at the same location as the current lift gate. Currently, the radial gate (main

gate) is sometimes partly opened at 10% in dry periods according to Waterschap Rivierenland (2020). It is easier for the unfolding gate to be opened partly than the flap gate. Therefore, the unfolding gate is considered as the main gate and the flap gate as an emergency gate.

The selected preferred alternatives are combined. A 3D view of the Elshoutsluice is given in Figure 6.10. Figure 6.12 and Figure 6.13 show sketches of the selected design for culverts 2 and 3.

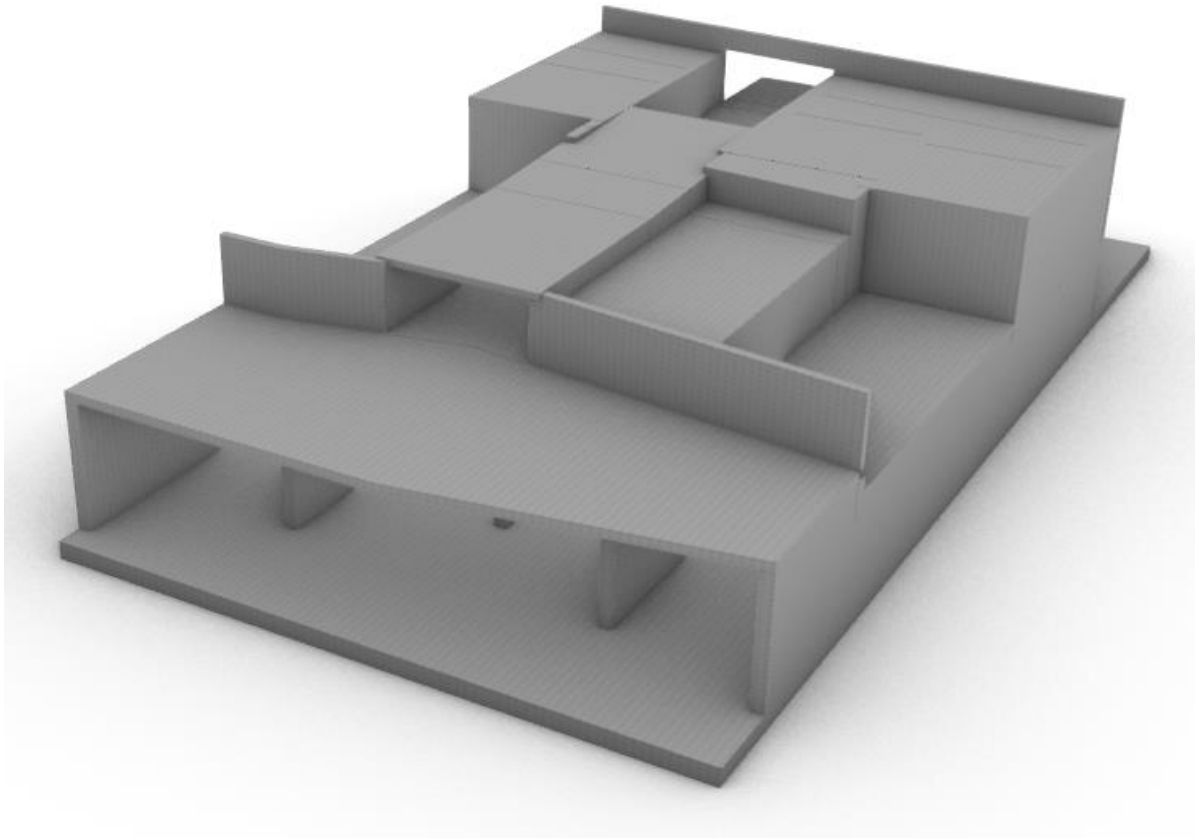

Figure 6.10: A 3D view of the concrete structure for selected preferred alternative. The river is at the top side of the figure.

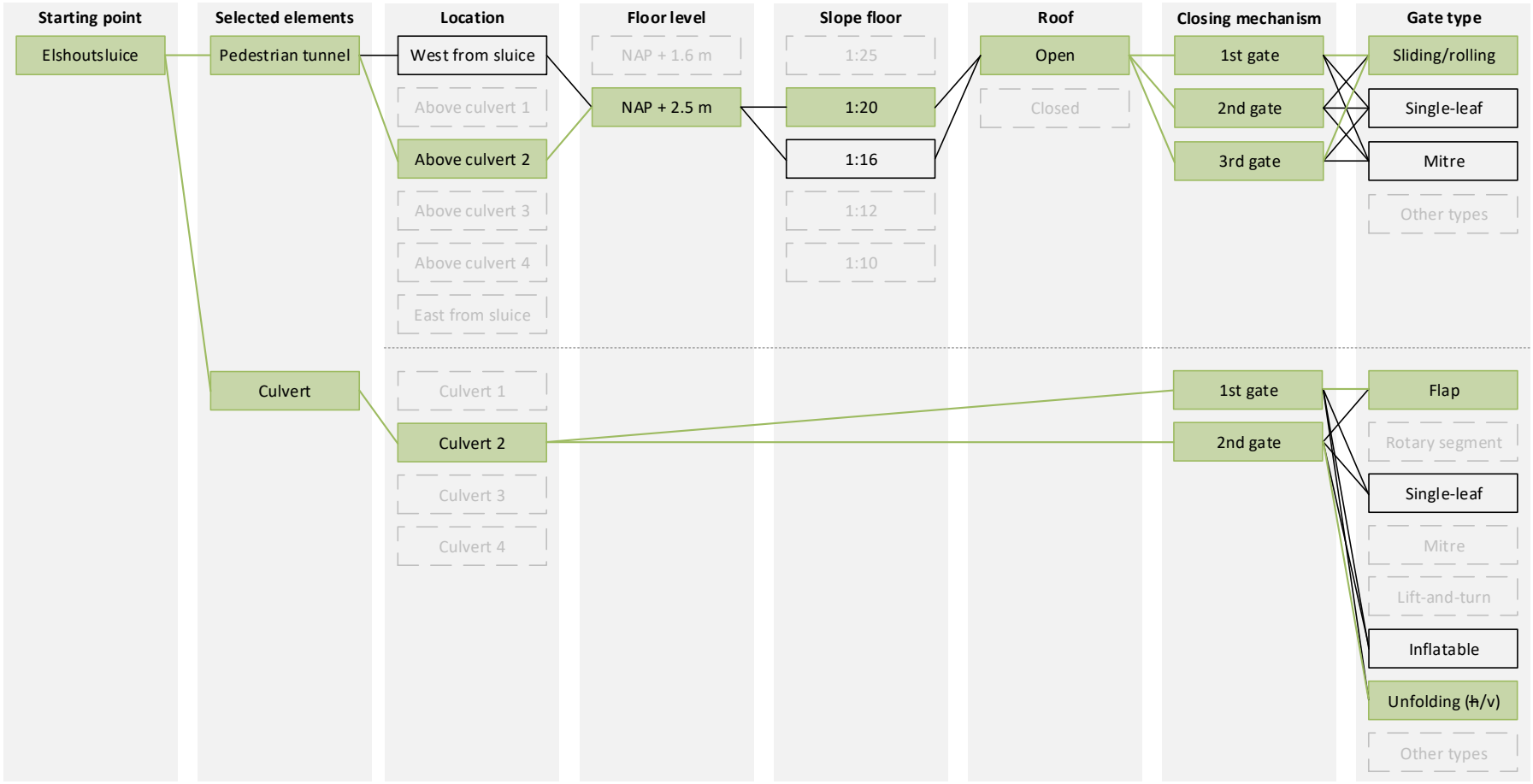

Figure 6.11: The design tree with the selection of the preferred alternatives.

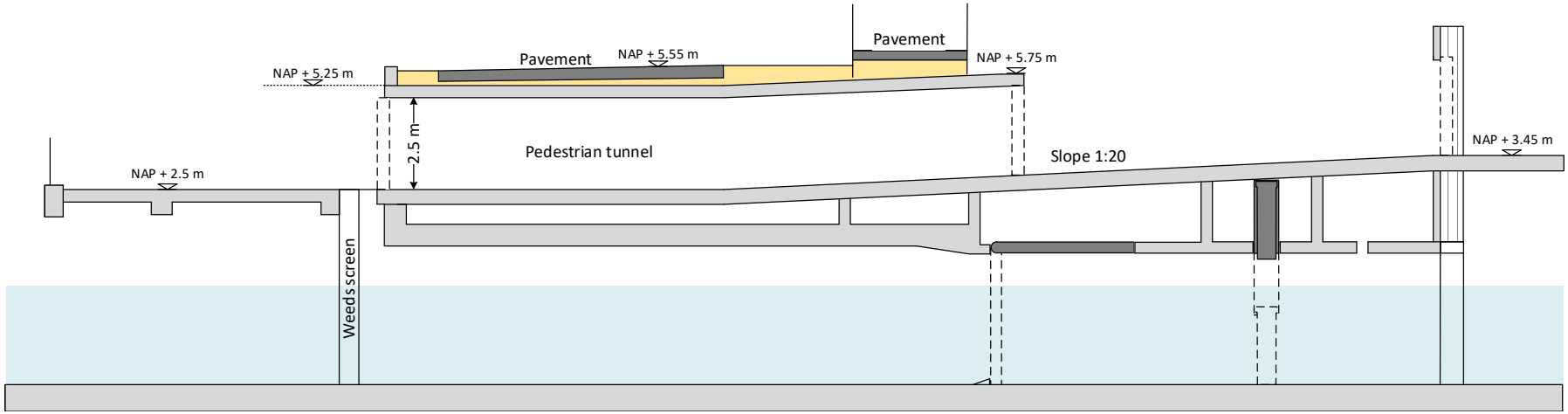

Figure 6.12: Side view sketch of the selected design for culvert number 2. The river side is at the right side of figure.

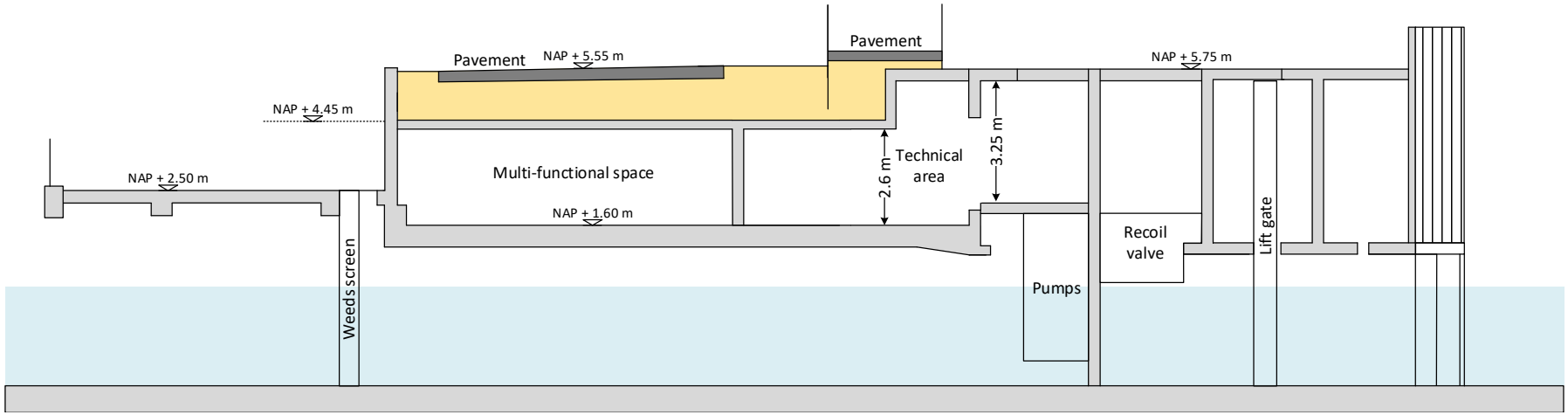

Figure 6.13: Side view sketch of the selected design for culvert number 3. The river side is at the right side of figure.

7

Construction sequence

In this chapter the construction sequence is given. The description of the construction sequence is necessary since it leads to governing load situations. The construction sequence consists of 10 phases. At last, a maintenance case is described in the use phase since this can lead to a governing load situation as well. In the following figures, the orange marked elements are the parts that will be removed and the green marked elements are the parts that will be added.

Phase 1

The first step of the construction sequence is to divert the traffic on the motorised vehicle road to the bicycle path. The bicycle path provides space for only one traffic lane. Temporary expansion of the bicycle path could be a solution if the capacity of 1 traffic lane is not enough. Removal of the pavement and the excavation of the soil above culvert 2 and 3 will be done in this phase. A temporary wall will be placed before excavation to keep the soil underneath the bicycle road in place. The outer concrete wall at the platform side will be removed. All the steps of phase 1 are marked in Figure 7.1.

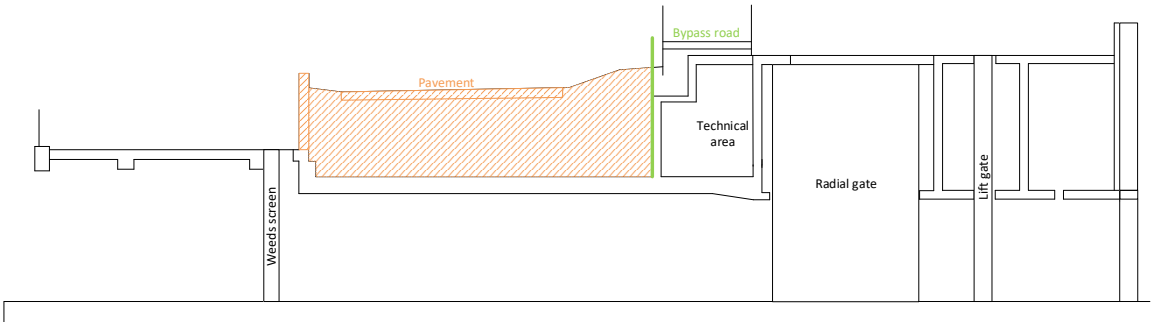

Figure 7.1: Side view of culvert 2 for construction phase 1

Phase 2

The second phase consists of the construction of the floor of the pedestrian tunnel up to the temporary wall. After the construction of the floor a new gate is placed at the end of the tunnel. The expansion of the technical area and construction of the multi-functional area above culvert 3 is included in construction phase 2 as well. Phase 2 above culvert 2 is shown in Figure 7.2.

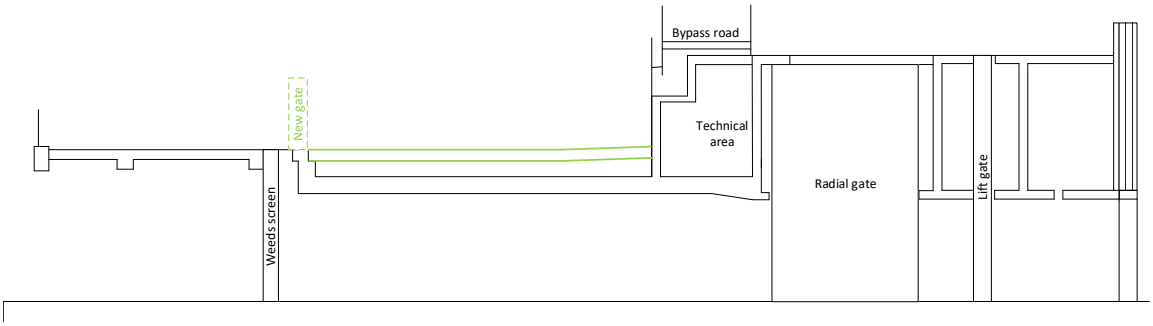

Figure 7.2: Side view of culvert 2 for construction phase 2

Phase 3

The new pedestrian tunnel roof is placed up to the temporary wall. A layer of soil is placed on top of the roof of the multi-functional area and above culverts 1 and 4 to provide a slope for the motorised vehicle road. The pavement is placed on top of the soil. Phase 3 above culvert 2 is given in Figure 7.3

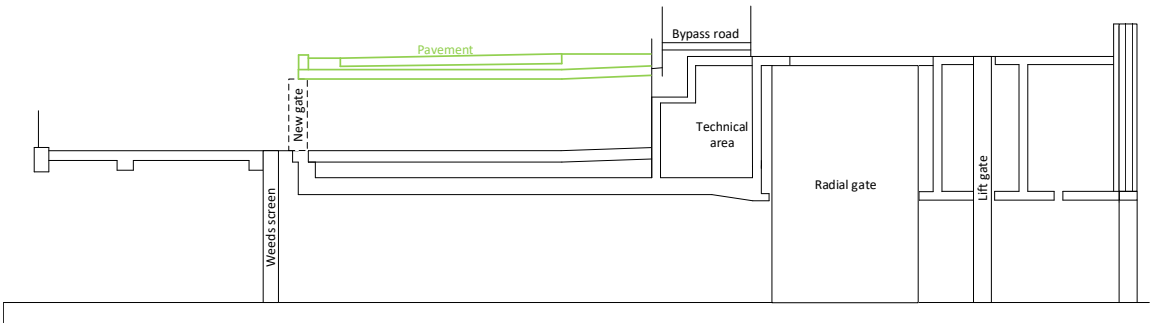

Figure 7.3: Side view of culvert 2 for construction phase 3

Phase 4

Culvert number 2 will be closed off by two temporary gates (stoplogs). One gate is placed at the river side and the other gate replaces the weeds screen. This is shown in Figure 7.4.

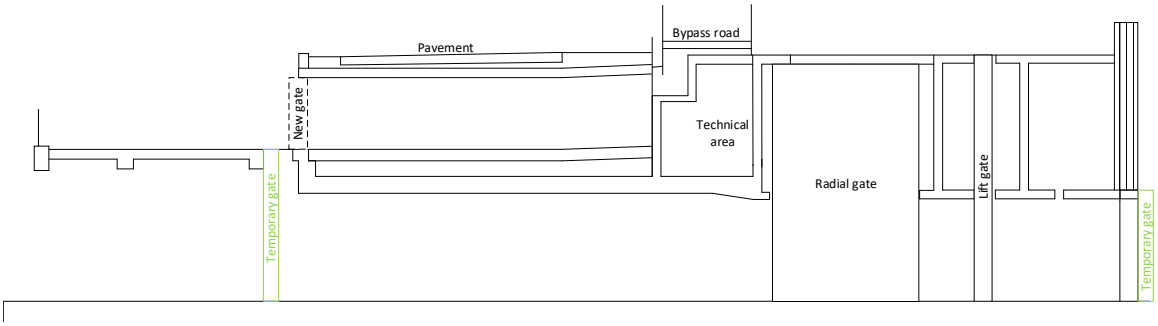

Figure 7.4: Side view of culvert 2 for construction phase 4

Phase 5

The traffic flow goes back to the motorised vehicle road. The bicycle path and roof of the Elshout-sluice is removed. Soil above the technical room is excavated. Parts of the technical room above culvert 2 are demolished. All the steps are marked in Figure 7.5.

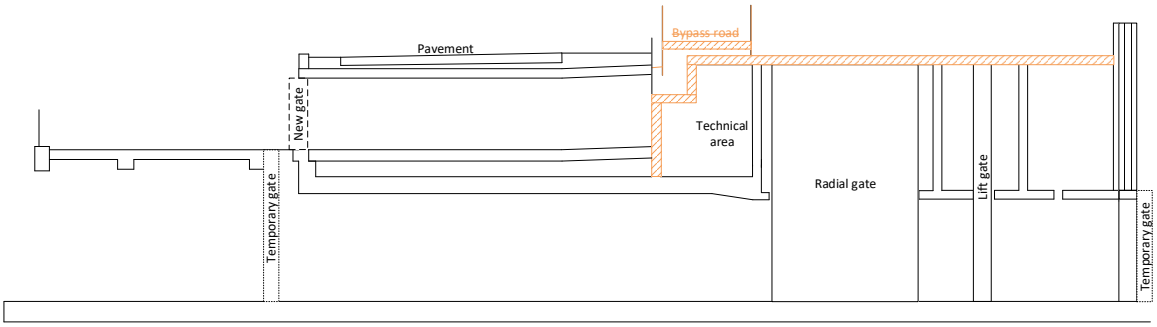

Figure 7.5: Side view of culvert 2 for construction phase 5

Phase 6

This phase consists of the removal of the current closing mechanisms and the walls which will block the new pedestrian tunnel. The parts which will be removed are indicated in Figure 7.6.

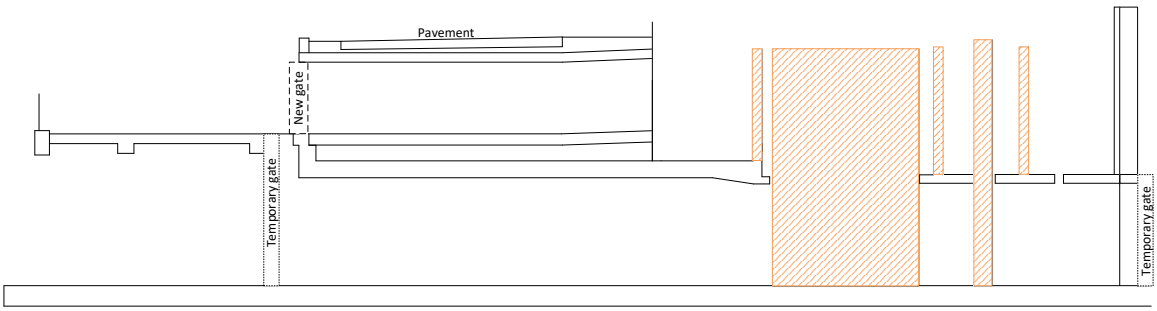

Figure 7.6: Side view of culvert 2 for construction phase 6

Phase 7

New gates will be placed on the location of the old closing mechanisms in this phase. Figure 7.7 shows construction phase 7.

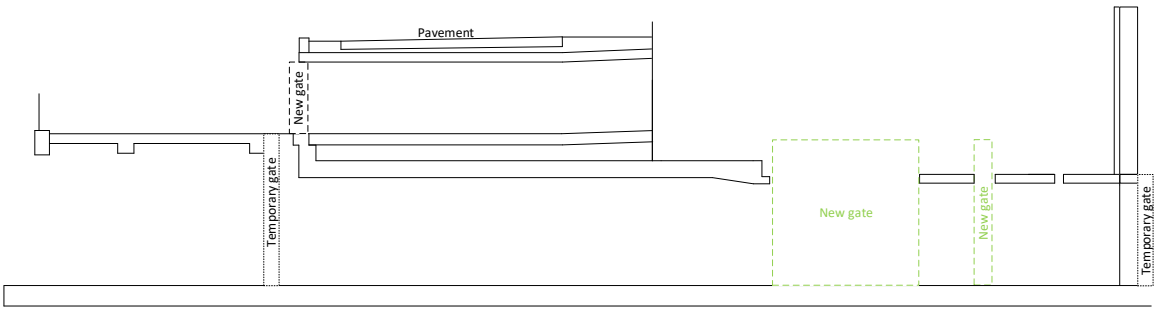

Figure 7.7: Side view of culvert 2 for construction phase 7

Phase 8

In phase 8, the remaining part of the floor of the pedestrian tunnel is made. An opening in the outer wall of the Elshoutsluice at the river side is realised. Two new gates are placed in the pedestrian tunnel. These steps are shown in Figure 7.8.

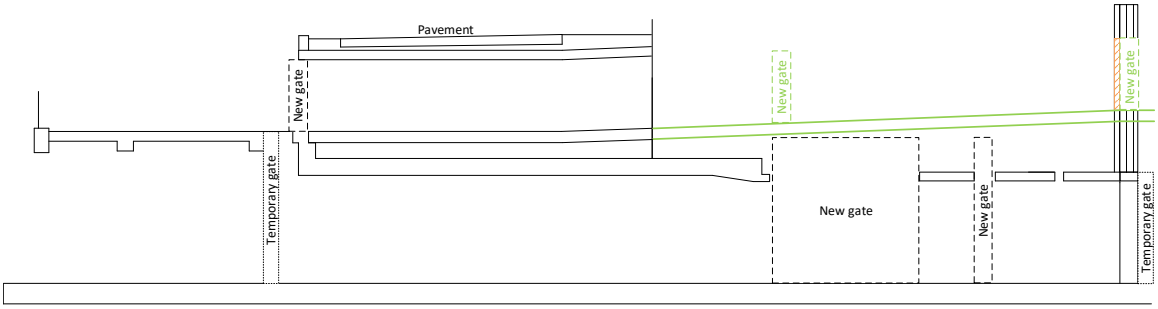

Figure 7.8: Side view of culvert 2 for construction phase 8

Phase 9

A roof on top of the Elshoutsluice is made. On top of this roof soil is placed before placing the bicycle road. This road is situated at the exact location as it was before. Figure 7.9 shows the steps of phase 9.

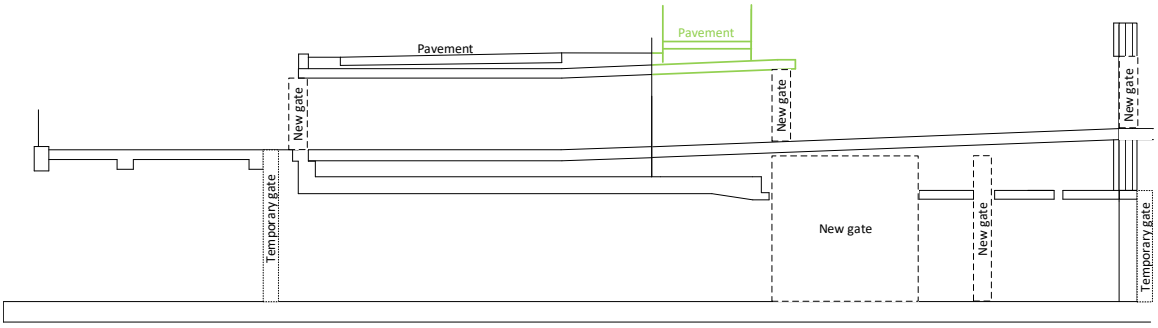

Figure 7.9: Side view of culvert 2 for construction phase 9

Phase 10

The last phase consists of the removal of the temporary gates, see Figure 7.10. The weeds screen is placed back on its former location in this phase. This results in the end of the construction sequence.

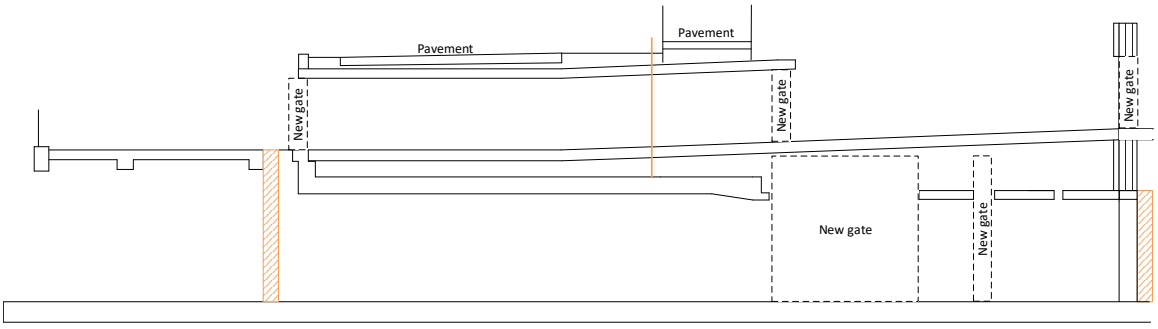

Figure 7.10: Side view of culvert 2 for construction phase 10

Maintenance

After the construction, the Elshoutsluice will be in use. Situations after the construction sequence can lead to governing load situations as well. A considered case is the maintenance and/or inspection of one of the culverts. The culvert will be closed off and the water will be pumped out of the culvert.

8

Flood risk verification

This chapter consists of the flood risk verification. The preliminary design of the Elshoutsluice must be checked for the flood risk. First, the failure modes specific for hydraulic structures and the required failure probability per failure mode are given. Second, the Elshoutsluice is checked for each failure mode. Third, the flood risk is checked for the construction phase of the discharge sluice.

8.1. Requirements per failure mode

Failure of a flood defence can be caused by different failure modes. An elaborate explanation is given in Appendix A. The contribution of a failure mode to the total failure probability depends on the failure probability factor ω given in Table 8.1 and the length-effect factor.

Table 8.1: The standard values for the failure probability factor ω (Rijkswaterstaat, 2017a)

Type of flood defence	**Failure mode**	**Segment type**	
		Sand coasts	**Other (levees)**
Levee	Overflow and overtopping	0	0.24
	Uplift and piping	0	0.24
	Macro instability inner slope	0	0.04
	Damage revetment and erosion	0	0.10
Engineering work	Non-closure	0	0.04
	Piping	0	0.02
	Structural failure	0	0.02
Dune	Dune erosion	0.70	0 / 0.10
Other		0.30	0.30 / 0.20
Total		**1**	**1**

Four failure modes are considered for hydraulic structures according to the work guide for the design of hydraulic structures which are part of a flood defence (Rijkswaterstaat, 2018b). These failure modes are given below and shown in Figure 8.1.

- Failure due to overflow or overtopping of structure.
- Failure due to non-closure of gates.
- Failure due to piping.
- Failure due to strength and stability.

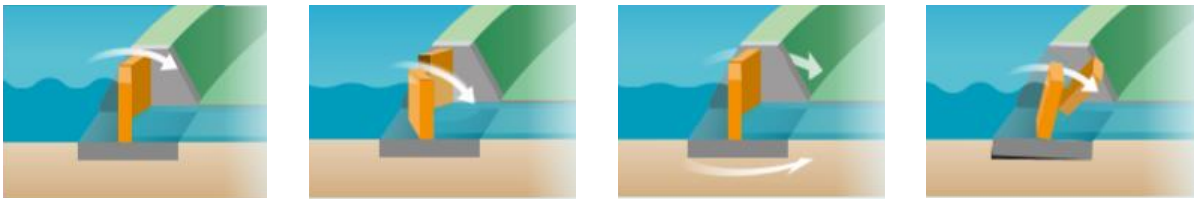

Figure 8.1: The failure modes for hydraulic structures (source: VNK (2014)).

The failure probability factor and length-effect factor for each failure mode is given in Table 8.2. An elaborate explanation of the failure modes specific for hydraulic structures and the determination of the required failure probabilities are given in Appendix C. The required failure probabilities per failure mode based on the alert value of 1/30,000 per year and lower threshold of 1/10,000 per year are shown in Table 8.3.

Table 8.2: The failure probability factor and length-effect factor for each failure mode based on Waterschap Rivierenland (2020).

Failure mode	Failure probability factor	Length-effect factor
Overflow/overtopping	0.24	2
Non-closure gates	0.04	1
Piping	0.02	1
Strength/stability	0.02	3

The conceptual design of the Elshoutsluice is checked for the selected failure modes in this chapter. Each failure probability must be at least lower than the lower threshold and preferably lower than the alert value. The starting point for the flood risk verification is the assessment of the current situation of the discharge sluice according to Waterschap Rivierenland (2020). The results of this flood risk assessment are given in Table 8.3.

Table 8.3: The required failure probabilities for the failure modes for the Elshoutsluice and the flood risk assessment according to Waterschap Rivierenland (2020) given in 1/year.

Failure mode	Alert value	Lower threshold	Waterschap Rivierenland
Overflow/overtopping	1/250,000	1/83,333	1/6,090,983
Non-closure gates	1/750,000	1/250,000	1/2,575,000
Piping	1/1,500,000	1/500,000	Suffice
Strength/stability	1/1,500,000	1/500,000	1/11,073,317

8.2. Overflow or overtopping of structure

The highest point of the hydraulic structure does not change. Even with the road level rise, the height of the Elshoutsluice is still NAP + 5.75 m. According to Waterschap Rivierenland (2020), the failure probability for overflow or overtopping is 1/6,090,983 per year. This value is lower than the alert value of 1/250,000. The Elshoutsluice does not exceeds the alert value more than sufficient.

The flood risk assessment of Waterschap Rivierenland (2020) is executed for reference year 2023. An additional check for reference year 2100 with climate scenario W^+ is included. This additional check is performed with HydraNL instead of Riskeer, since the calculated results with Riskeer are not in

line with the expectations of these results. Appendix I shows the HydraNL calculation. [1]

A grass cover on top of the discharge sluice is assumed for the critical discharge. According to EurOtop (2018), the critical discharge is 10 l/s/m'. A vertical wall profile is selected. The result of the calculation is a hydraulic load of NAP + 5.228 m for the lower threshold (1/83,333) and NAP + 5.574 m for the alert value (1/250,000). Both calculated hydraulic loads are below the current height of NAP + 5.75 m. The height of the Elshoutsluice is sufficient for 2100 W^+ as well.

8.3. Non-closure of gates

The Elshoutsluice changes from a situation with four openings to five openings. Culvert number 2 will include new gates which results in changes of the failure probability of this culvert for non-closure of gates. Figure 8.2 shows the failure tree of the new situation of the discharge sluice. There are no identical openings in the structure which results in a standard failure tree given in Figure 8.3 for each opening.

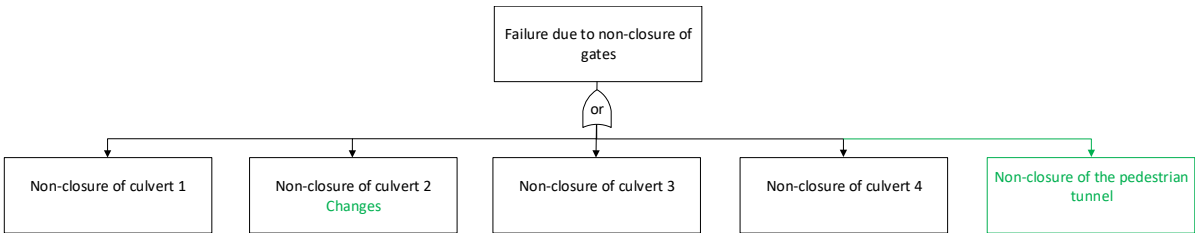

Figure 8.2: The failure tree for the failure mode non-closure of gates for the Elshoutsluice with the changes compared to the current situation marked in green.

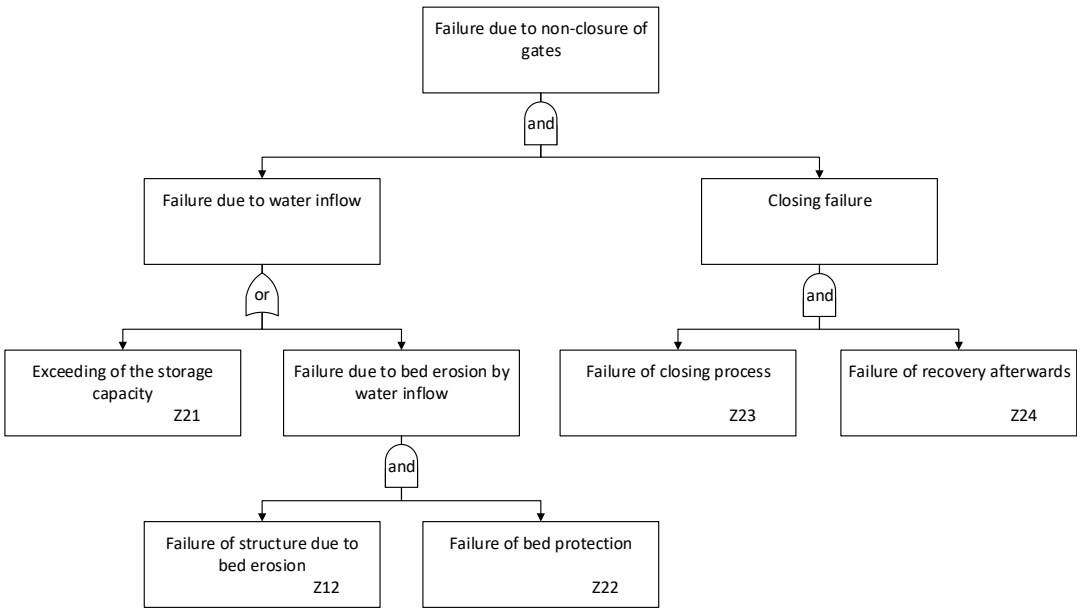

Figure 8.3: Standard failure tree of non-closure according to Rijkswaterstaat (2017a) for each opening in a hydraulic structure. The limit state functions Z are given and explained in Appendix J.

[1] Higher water levels are included for the reference years 2050 and 2100, but the resulting failure probabilities are lower than for the reference year of 2023. The illogical results can be explained due to the different calculations methods used by Riskeer and the rounding errors in combination with very low failure probabilities. The effect of the sea level rise at Kinderdijk is limited and model characteristics can influence the results according to Helpdesk Water. These findings are specific for the selected location at Kinderdijk.

Culverts

Culverts 1, 3 and 4 of the Elshoutsluice remain unchanged. The failure probabilities for these culverts according to Waterschap Rivierenland (2020) are described in section J.2. Table 8.4 shows the results of the failure probability for non-closure of gates per culvert based on the following failure probabilities for closing when asked per gate type:

- The radial gate: 1/10,000 per demand based on a standard value according to TAW (2003).
- The recoil valve: 1/100,000 per demand based on the standard value (TAW, 2003).
- The lift gate: 1/5052 per demand according to Waterschap Rivierenland (2020) based on the filled in score tables from Rijkswaterstaat (2017b).

Table 8.4: The failure probability per culvert of the Elshoutsluice for failure mode non-closure gates according to Waterschap Rivierenland (2020)

Culvert	Failure probability [1/year]
1	1/1,778,300,000
3	Negligibly small
4 (Radial gate)	1/5,150,000
4 (Recoil valves)	Negligibly small

The failure probability due to non-closure of gates for culvert 2 and the pedestrian tunnel is determined with Riskeer. Riskeer calculates the probability of failure for non-closure of an opening according to the standard failure tree given in Figure 8.3 using a first-order reliability method (FORM). Directional sampling is used when the FORM calculation does not converge. The probability of a limit state function Z being below zero is calculated for the limit state functions given and explained in Appendix J. The input for Riskeer are the mean value and standard deviation or variation coefficient of the parameters for the limit state functions.

Table 8.5 shows the input parameters for Riskeer for culvert number 2. An elaborate explanation for the determination of the Riskeer input is given in Appendix J. The failure probability of closing of the gates when asked and the probability of an open gate when high water occurs are input for limit state function Z23. Limit state function Z24 consist of the failure probability of recovery after failure of the gates. The inflow model type, the water level directly hinterlands of the structure, the inflow area of the opening in open situation and the discharge coefficient are input for both Z21 and Z22. For limit state function Z21, the storm duration and the factor for high water during the storm input are used. The storage area of the hinterland and the maximum allowable water level increase hinterlands are necessary for limit state function Z21 as well. The critical inflow of the bed protection and the width of this bed protection is necessary for function Z22. Limit state function Z12 is the parameter failure probability of bed erosion.

With the new closing mechanisms the probability of failure will change for culvert number 2. Two new gates will be placed instead of the old gates. The main gate will be the unfolding gate at the location of the old lift gate. This gate is chosen as the main gate, because of the possibility to open this gate partly in dry periods. Failure processes as alarm, mobilisation and control are not directly applicable to closing mechanisms which are opened and closed regularly according to Rijkswaterstaat (2018b). Only technical failure is applicable for this gate. The main gate will be considered as a sluice gate with a standard failure probability of 1/10,000 per demand.

The function of the flap gate will be similar to the old lift gate. The filled in score tables from Rijkswaterstaat (2017b) for the lift gate according to Waterschap Rivierenland (2020) are checked and will not differ largely for the new flap gate. Therefore the same failure probability of 1/5052 per demand is assumed for the flap gate. The total failure probability for non-closure when asked is 1/50,520,000

Table 8.5: Input parameters Riskeer for culvert 2.

Parameter	Value	Variation/st. deviation
Number of identical openings [-]	1	-
Failure probability of closing [-]	1/50,520,000	-
Probability of open gate [-]	1/4	-
Failure probability of recovery after failure [-]	1	-
Inflow model	Drowned opening	-
Water level hinterlands [m + NAP]	1.50	0.10
Inflow area [m^2]	21.00	0.01
Discharge coefficient [-]	1.00	0.20
Storm duration [hour]	6.00	0.25
Factor for high water storm duration [-]	1	-
Critical inflow discharge [$m^3/s/m$]	0.10	1.20
Width of bed protection [m]	15.00	0.05
Failure probability bed erosion [-]	1	-
Storage area [m^2]	2900000.00	0.10
Maximum allowable water level increase [m]	0.35	0.10

per demand, see explanation in Appendix J.

The assessment is done for reference year 2023, since it is not possible to perform a correct Riskeer calculations for a different reference year at this specific location. The result of the Riskeer calculation is a failure probability of 1/51,500,147 per year for culvert 2.

Pedestrian tunnel

The input parameters for the pedestrian tunnel are given in Table 8.6. Some input parameters differ from the situation for culvert number 2 due to a different inflow model type. In this case, the threshold level of the opening and the width of the opening are needed for limit state functions Z21 and Z22. The determination of the values of the input parameters are given in Appendix J.

Table 8.6: Input parameters Riskeer for the pedestrian tunnel with two gates.

Parameter	Value	Variation/st. deviation
Number of identical openings [-]	1	-
Failure probability of closing [-]	1/100,000,000	-
Probability of open gate [-]	1/1	-
Failure probability of recovery after failure [-]	1	-
Inflow model	Low threshold	-
Water level hinterlands [m + NAP]	1.50	0.10
Threshold level [m + NAP]	3.45	0.10
Width of inflow opening [m]	5.50	0.05
Storm duration [hour]	6.00	0.25
Factor for high water storm duration [-]	1	-
Critical inflow discharge [$m^3/s/m$]	0.10	1.20
Width of bed protection [m]	15.00	0.05
Failure probability bed erosion [-]	1	-
Storage area [m^2]	2900000.00	0.10
Maximum allowable water level increase [m]	0.35	0.10

Three new gates will be included in the pedestrian tunnel due to the requirement from Waterschap Rivierenland. At first, only two gates are considered for failure due to non-closure. The new gates will be opened and closed regularly for closing off the pedestrian tunnel outside visitor hours. Therefore, only technical failure is assumed with a standard failure probability of 1/10,000 per demand according to Rijkswaterstaat (2019). This failure probability is applicable to both gates which results in a total failure probability of 1/100,000,000 per demand for the pedestrian tunnel. This results in a failure probability of 1/514,972,218,999 per year for the pedestrian tunnel.

An additional assessment with three gates in the pedestrian tunnel is not necessary, since the failure probability for two gates is very low. The low value is due to a low probability of gate failure and a low probability of the river water level exceeding the threshold level of the tunnel opening. In addition, a calculation was performed for a situation with only 1 gate in the pedestrian tunnel. The failure probability of closing is 1/10,000 and results in a failure probability of 1/68.957.957 per year for the pedestrian tunnel.

Conclusion
The total failure probability for the failure mode non-closure of gates for the Elshoutsluice is approximately the summation of the failure probabilities per opening, see Appendix J. All the failure probabilities combined for a pedestrian tunnel with two gates results in a total failure probability of 1/4,669,484 per year for non-closure of the gates. This value is lower than the alert value of 1/250,000. The Elshoutsluice does not exceed the alert value more than sufficient. The calculated failure probability is lower than the value of 1/2,575,000 per year in the assessment of Waterschap Rivierenland (2020) as well. A pedestrian tunnel with three gates fulfils the requirements since a tunnel with two gates is already sufficient.

8.4. Piping
The Elshoutsluice fulfils the requirement for piping according to Waterschap Rivierenland (2020) due to the presence of sheet pile walls under the structure. The sheet pile wall at river side reaches a depth of NAP - 15.65 m and the other sheet pile walls reach a depth of NAP - 19.5 m. The foundation and the concrete bottom slab of the Elshoutsluice remains unchanged. Therefore, the assessment for failure due to piping does not change.

8.5. Strength and stability
According to the assessment of Waterschap Rivierenland (2020), the failure probability for strength and stability is 1/11,073,317 per year. The strength assessment is based on the steel closing mechanisms and the stability assessment is based on the concrete structure. A strength and stability calculation for the new situation according to the WBI2017 will not be performed. Strength and stability are discussed in more detail in the structural verification, since the construction phase can lead to critical situations.

8.6. Construction phase
At last the flood risk is checked for the construction phase. The governing phases are selected from the construction sequence.

The first check is for the failure mode overflow or overtopping of structure. Construction phase 8 lead to the governing situation. An opening is made in the outer wall at river side. The road at a level of NAP + 5.55 m is the highest point above culvert 2 for phase 8. The temporary lower height of the structure is checked with the use of HydraNL. Appendix I shows the calculation for reference year 2023 with climate scenario W^+. The result of the calculation is a hydraulic load of NAP + 4.824 m for

the lower threshold (1/83,333) and NAP + 5.111 m for the alert value (1/250,000). Both calculated hydraulic loads are below the height of NAP + 5.55 m. The height of the Elshoutsluice is sufficient for the construction phase.

The second check is for the failure mode non-closure of gates. Construction phase 4 is the governing case. Culvert 2 will be closed off by two temporary gates. The probability of the temporary gates being open when high water occurs P_{open} is approximately 0 since the gates will be permanently closed during the construction phases 4 to 10. This results in a negligible failure probability of the closing process and therefore a negligible failure probability for the failure mode non-closure.

9

Structural verification

This chapter consists of the structural verification of the selected preliminary design. First, a selection of stability checks are given. Second, the difference in force distribution on the Elshoutsluice is analysed.

9.1. Stability check

A selection of the stability checks is made and performed in this section.

9.1.1. Selection of stability checks

The following checks are suggested during critical load situations to provide stability for temporary and permanent structures (Molenaar & Voorendt, 2020):

- Piping
- **Uplift**
- **Lateral shear**
- **Bearing capacity and settlement**
- **Rotational stability**
- Embedded depth of retaining walls
- Potential support of walls
- Ensure dimensional stability
- Scour
- Earthquake impact
- Human and animal actions

Not all stability checks need to be performed. No changes are made in the foundation of the discharge sluice. This result in no differences for piping, embedded depth retaining walls and scour. These checks will not be performed. Earthquakes are not present at Kinderdijk (Figure B.3), which result in excluding the stability check for earthquake impact. The selected stability check are marked in bold in the list above.

The stability checks for the construction phase are performed with the hydraulic load for reference year 2023. In section 4.2 is given that the water level for the alert value is NAP +3.66 m and for the lower threshold NAP +3.48. For stability checks after the construction phase, the water levels for reference year 2100 W^+ are selected. A water level of NAP + 4.22 m corresponds with the alert value [1]. This results in the highest loads on the Elshoutsluice. In case of high water, the water level

[1] Normally, the lower threshold value is used for the design verification according to Rijkswaterstaat (2018b). The alert

hinterlands of NAP + 1.50 m is used for the stability calculations.

Multiple cases can be selected per stability check, since it is not always immediately clear what the governing situation will be. Different hydraulic loads are used based on the life cycle of the Elshoutsluice. Therefore, a governing case from the construction sequence is selected and a governing case in the use phase of the Elshoutsluice for some of the stability checks.

9.1.2. Uplift

The first stability check is the uplift check. A hydraulic structure can float due to the upward pressure of water. To perform this check, a permeable soil layer is assumed since this leads to the most unfavourable case. The buoyancy force F_b is depends on the water levels on both sides of Elshoutsluice, see Figure 9.1. The uplift check is given by:

$$\frac{S}{R} = \frac{F_b}{F_{self} + F_{t,piles}} < 1 \tag{9.1}$$

Where:

F_{self} = the self weight of the hydraulic structure in kN.
$F_{t,piles}$ = the tension resistance of the foundation piles in kN.
F_b = the buoyancy force due to the upwards water pressure under the hydraulic structure in kN.

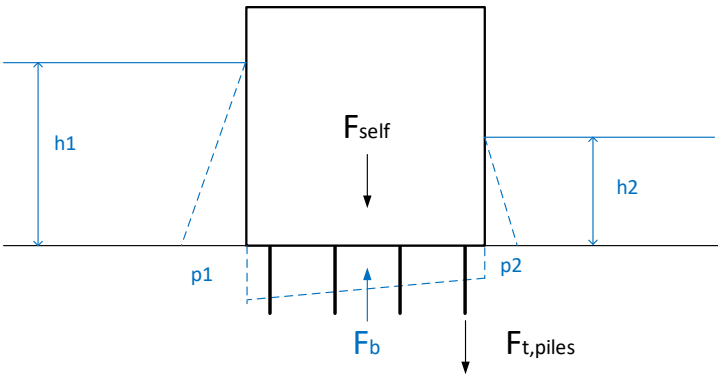

Figure 9.1: Sketch for uplifting for a structure founded on piles

The Elshoutsluice is founded on piles. First, it is checked if tension in the foundation piles will occur due to the buoyancy force. Tension in the piles $F_{t,piles}$ will occur when:

$$\frac{F_b}{F_{self}} < 1 \tag{9.2}$$

If the structure fulfils the unity check of Equation 9.2, this automatically leads to fulfilment of the unity check of Equation 9.1.

The most unfavourable case for uplift is when the self weight of the Elshoutsluice is small and the water levels are high. Two situations are chosen for which the uplift check is performed. The first is the construction phase 1. The self weight will be at a minimum in this case since approximately half of the volume of the soil on top of the structure will be excavated. Construction phase 1 will be checked for a high water level situation of NAP + 3.66 m. The second case for which the uplift check

value is selected because this case partly consists of the assessment of the remaining elements of the current structure.

is performed is for maintenance after the construction phase. Specifically when one of the culverts is set dry for inspections. This situation is combined with a high water level of NAP + 4.22 m at the Lek river. The calculation of the self weight for both cases is given in Appendix K. The results of the calculations is displayed in Table 9.1.

Table 9.1: The self-weight of the governing situations.

Situation	F_{self} **[kN]**
Construction phase 1	96208.93
Maintenance	99751.87

In Appendix K, the buoyancy forces are determined for both water level cases. Table 9.2 shows the results of the calculation for the high water levels at the river and a water level of NAP + 1.50 m hinterlands.

Table 9.2: The buoyancy force for different water levels at the Lek river.

Situation	**Water level**	F_b **[kN]**
Construction phase 1	NAP + 3.66 m	69061.00
Maintenance	NAP + 4.22 m	72434.82

The result of the uplift check for the selected cases is given in Table 9.3. In both situations no tensile forces in the foundation piles will occur. The foundation piles do not have to function as tensile piles. The structure is stable for uplifting.

Table 9.3: The result of the unity check for uplifting by filling in Equation 9.2

Situation	**Equation 9.2**	**Unity Check Uplifting**	
Construction phase 1	0.72	<1	OK
Maintenance	0.73	<1	OK

9.1.3. Lateral shear

For lateral shear the horizontal stability is checked. The Elshoutsluice is founded on 190 piles, therefore the horizontal forces on the discharge sluice will be transferred to the foundation piles. The friction force of the soil will not be taken into account, only the shear capacity of the foundation piles will be checked.

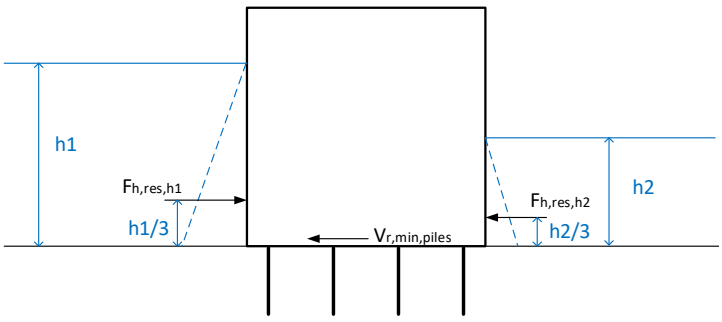

Figure 9.2: Sketch of the lateral shear.

For the horizontal stability the following check must be performed:

$$\frac{S}{R} = \frac{\sum F_h}{V_{r,min,piles}} < 1 \tag{9.3}$$

Where:

$\sum F_h$ = the sum of horizontal forces acting on the structure in kN.
$V_{r,min,piles}$ = the shear force capacity of the foundation piles in kN.

The sum of horizontal forces depends on the soil pressure and water pressure on the structure. Since the soil level is the same at both sides of the hydraulic structure, these horizontal forces cancel each other out. Therefore, the force due to soil is not included in the calculation. The sum of horizontal forces depends only on the water pressure sketched in Figure 9.2:

$$\sum F_h = F_{h,res,h1} - F_{h,res,h2} \tag{9.4}$$

The highest horizontal force results from the situation of the Elshoutsluice in finished state with a high water level of NAP + 4.22 m for reference year 2100. This is equal to the situation described for maintenance. The shear force capacity of reinforcement is neglected for the determination of the shear force capacity of the foundation piles since there is no information on the reinforcement. Table 9.4 shows the results from the calculation for the sum of horizontal forces and the shear capacity executed in Appendix K.

Table 9.4: The results from the calculation in Appendix K for lateral shear.

Situation	$\sum F_h$ **[kN]**	$V_{r,min,piles}$ **[kN]**
Maintenance	4158.76	10169.17

The unity check for the horizontal stability results in:

$$\frac{\sum F_h}{V_{r,min,piles}} = \frac{4158.76}{10169.17} = 0.41 < 1, \text{ OK} \tag{9.5}$$

The Elshoutsluice is stable for lateral shear.

9.1.4. Bearing capacity and settlement

The Elshoutsluice is founded on 190 piles. With the Koppejan method, the maximum bearing capacity of a foundation pile is determined. Figure 9.3 shows the slip planes of the soil around a foundation pile and a sketch of the forces for the bearing capacity check. The unity check for bearing capacity is given by:

$$\frac{S}{R} = \frac{\sum V}{F_{r,total}} < 1 \tag{9.6}$$

With:

$$\sum V = F_{self} - F_b \tag{9.7}$$

Where:

$F_{r,total}$ = the total bearing capacity of the foundation of a structure in kN.
F_{self} = the self weight of the hydraulic structure in kN.
F_b = the buoyancy force due to the upwards water pressure under the hydraulic structure in kN.

A high sum of vertical forces leads to a high acting stress on the soil. In Appendix K an analysis is made of which situation leads to the highest sum of vertical forces. The comparison is made between the case of the discharge sluice after the construction phase with a high water level of NAP

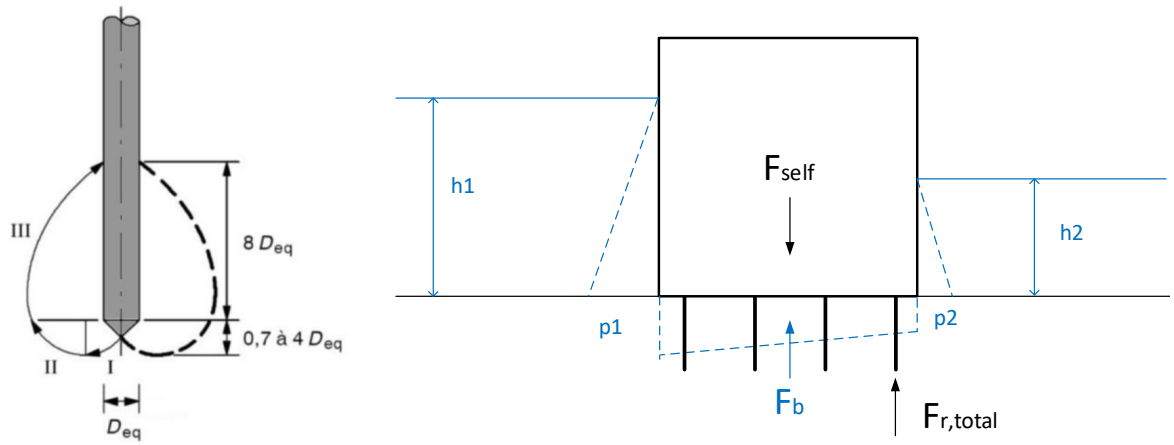

(a) The slip planes according to Koppejan (Voorendt & Molenaar, 2020).

(b) Sketch of the bearing capacity.

Figure 9.3: Bearing capacity.

+ 4.22 m and the case of the end result of the Elshoutsluice with a low water level at the river. The result was a highest sum of vertical forces of 64253.10 kN.

The stability check for the bearing capacity is given by:

$$\frac{\sum V}{F_{r,total}} = \frac{64253.10}{395697.80} = 0.16 < 1, \text{ OK} \tag{9.8}$$

The Elshoutsluice is stable for the vertical stability check. The existing foundation pile plan seems oversized even for the existing case. There is no information available on the exact placement of the piles, inclined or vertical. In case of inclined piles, the vertical bearing capacity could be lower than the determined value for this stability check. However, due to the large calculated bearing capacity it is assumed that the inclination of the piles will not result in instability.

The pile tip settlement of a prefab concrete foundation pile for a preliminary design can roughly be estimated with (Voorendt & Molenaar, 2020):

$$w_{tip} \approx 2\% \text{ to } 3\% \cdot D_{eq} \tag{9.9}$$

With an equivalent pile tip diameter D_{eq} of 0.474 m, this results in a rough settlement estimation between 9.5 and 14.2 mm. For the Elshoutsluice is assumed that the settlement of the prefab piles has (partly) been taken place since the structure exists for 35 years.

9.1.5. Rotational stability

In this section, it is checked if the Elshoutsluice structure does not start to rotate. The moments on the hydraulic structure will be transferred in a compression and tension force in the foundation piles. This is sketched in Figure 9.4a. In the previous subsection is determined that the piles of the Elshoutsluice have a high vertical bearing capacity left. First, a check is performed if tensile stresses will occur in the foundation piles. The assumption is made that there will be no tensile stresses in the foundation piles if the resulting action force intersects with the core of the hydraulic structure, see Figure 9.4b. The defined core is an area of 1/3 of the length (b) in the middle of the structure. No tension will occur when the structure fulfils:

$$\frac{S}{R} = \frac{\sum M / \sum V}{1/6b} < 1 \tag{9.10}$$

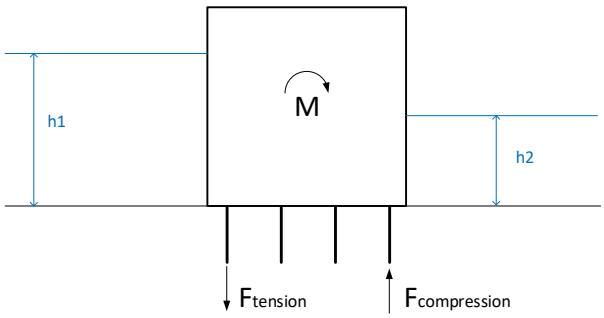

(a) Sketch of the rotational stability

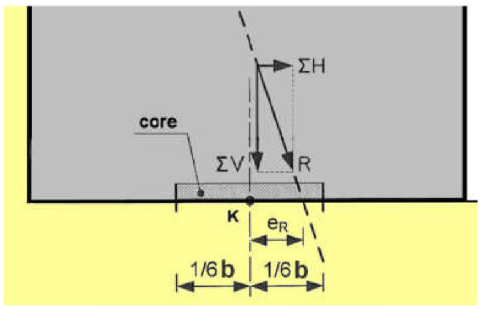

(b) Rotational stability (Voorendt & Molenaar, 2020)

Figure 9.4: Rotational stability

The sum of moments is caused by the horizontal loading forces on the Elshoutsluice multiplied with the distance to the bottom of the hydraulic structure and the buoyancy force under the structure. The vertical load due to the self weight is assumed to be in the centre of the structure as a simplification. Figure 9.5 shows the loads translated to the bottom slab of the structure. The most unfavourable situation is when the sum of the vertical forces is low and the horizontal forces is high. Therefore, the same two cases for the uplift check and lateral shear check are selected. The sum of vertical forces is given in Table 9.3. In Appendix K the sum of acting moments is determined. Table 9.5 shows the result of the calculations.

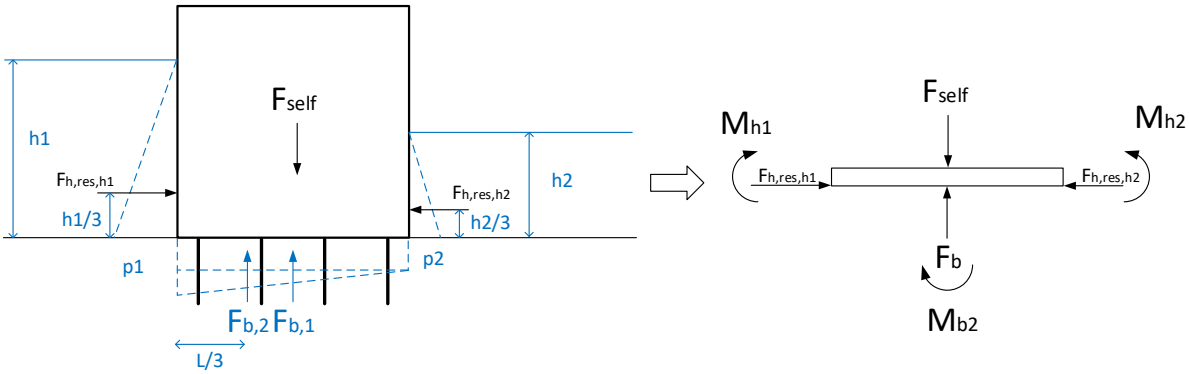

Figure 9.5: The translation of the forces on the structure to the bottom of the structure.

Table 9.5: The sum of acting moments for the selected cases.

Situation	$\sum M$ **[kNm/m']**
Construction phase 1	2315.33
Maintenance	2964.74

The length of the Elshoutsluice (b) is 46.73 m. The results of the performed check for tension in the foundation piles is given in Table 9.6. There is no tension in the foundation piles for both situations. Therefore, no additional check for the tension strength of the foundation piles is needed.

The moments on the structure lead to an additional compression force on the foundation piles near the hinterland, see Figure 9.4a. As a simplification, the largest moment is translated to one compression force at the outer end of the structure:

Table 9.6: The result of the unity check.

Situation	Equation 9.10	Unity Check Tension in Piles	
Construction phase 1	0.26	<1	OK
Maintenance	0.33	<1	OK

$$F_{M,comp,end} = \frac{M}{L/2} = \frac{2964.74 \cdot 24.7}{46.73/2} = 3134.20 \text{ kN} \tag{9.11}$$

Only two foundation piles with a bearing capacity of 2082.62 kN per pile are needed for this compression force. There are more than two foundation piles present near the hinterland site and the translation of the moment to a single force is a conservative approach. Therefore, it can be assumed that the foundation piles can resist the additional compression forces due to rotational moments on the Elshoutsluice.

9.2. Strength analysis

The loading on the Elshoutsluice will change due to the additional pedestrian tunnel. Besides the change in the structure, the regulations for designing concrete structures has altered over the years. The initial design situation for the discharge sluice will be assumed based on the VB 1974. This will be compared to the new situation in combination with the current design regulations according to the NEN 8700 series for existing structures and the NEN-EN 1991 series for new structures. The calculations are performed with the use of Matrixframe [2]. The analysis is performed for the use phase of the Elshoutsluice.

9.2.1. Input Matrixframe

A cross-section of 1 m width is selected from the Elshoutsluice to perform the structural 2D analysis. The location with the most changes in structure and loads is right underneath the motorised vehicle road is selected to perform the analysis, see Figure K.18. This cross-section has the highest loads due to the motorised traffic on top of the structure. The performed calculations are not governing over the entire length of the Elshoutsluice due to loading and geometry differences.

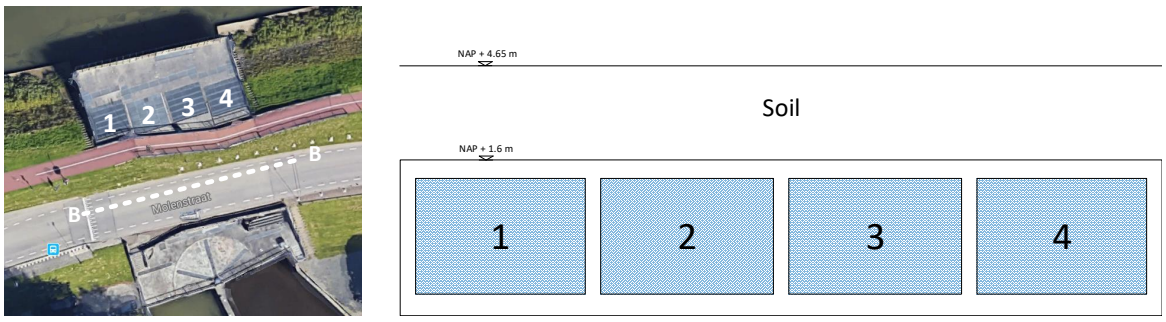

(a) Top view of the Elshoutsluice (source: Google Maps).

(b) Sketch of the front view of the cross-section B-B with the road level and the slab top level.

Figure 9.6: Selected cross-section for the load transfer analysis.

The structure in Figure 9.6b is modelled as a simplified 2D-frame model in Matrixframe, see Figure 9.7. The foundation piles are mostly located directly underneath or nearby a lateral wall and are

[2]The initial idea was to perform the calculations with the 3D model in SCIA Engineer. Unfortunately, the SCIA analysis provided no results. It is assumed that the high computational capacity could be the reason. However, due to limited time this is not further investigated. Therefore, Matrixframe is selected to perform the structural analysis.

included as vertical and horizontal constraints directly under the lateral walls. The Elshoutsluice is made with concrete of strength class B 22.5 (Haskoning B.V., 1984a). For the model, the modulus of elasticity of cracked concrete is assumed as input for the existing elements of the structure. The existing reinforcement is not taken into account because the reinforcement in the the selected cross-section is unknown. The modulus of elasticity for cracked concrete is assumed to be approximately 1/3 of E_{cm} which results in value of 9667 N/mm^2, see Appendix K. In reality this value is higher due to the presence of reinforcement.

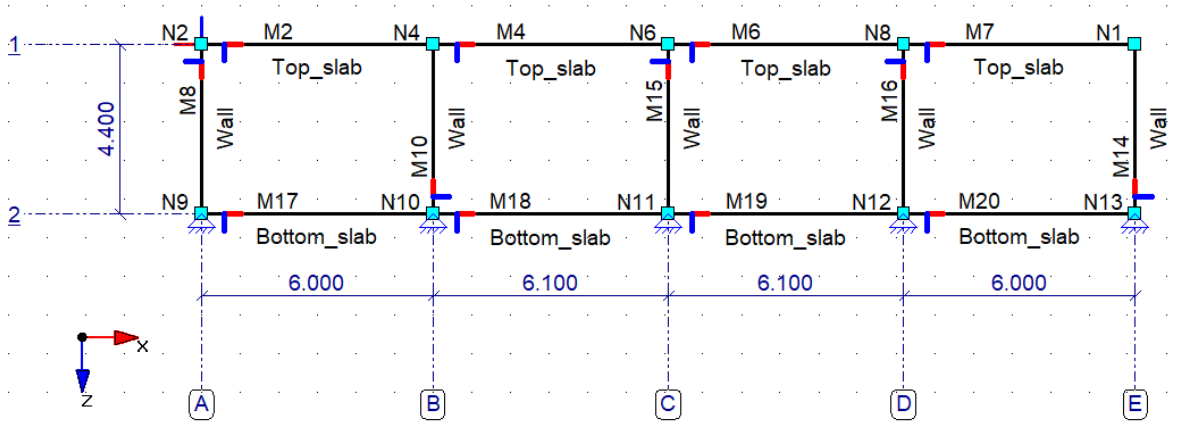

Figure 9.7: The geometry in Matrixframe for the current situation.

The applied characteristic loads are given in Table 9.7. Only the load differences are analysed. The loads due to water pressure in the culverts and under the structure are not taken into account because this remains the same. The loads are multiplied by a safety factor according to VB 1974 and different load cases on the structure are analysed in Appendix K.

Table 9.7: The initial loads on the old Elshoutsluice structure.

Characteristic loads	Value	Unit
Traffic	4.00	kN/m^2
Soil above culverts	47.87	kN/m^2
Self weight top slab	14.72	kN/m^2
Self weight walls	12.26	kN/m^2
Single axle load	100.00	kN

A pedestrian tunnel and a multi-functional area is placed on top of the existing structure for the new situation of the Elshoutsluice. Figure 9.8 shows the front view of the selected cross-section and Figure 9.7 shows the cross-section translated to a 2D frame in Matrixframe.

The characteristic loads for the Elshoutsluice in the new situation are given in Table 9.8. The loads are combined with load factors for two different load combination effects for existing structures according to NEN 8700. Various load combinations are inserted in Matrixframe, see Appendix K.

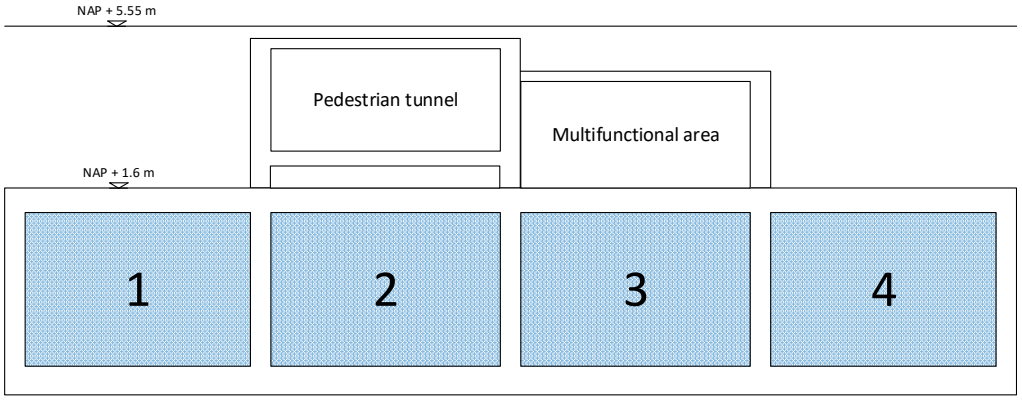

Figure 9.8: A front view sketch of the cross-section B-B of the Elshoutsluice including the pedestrian tunnel and multi-functional area.

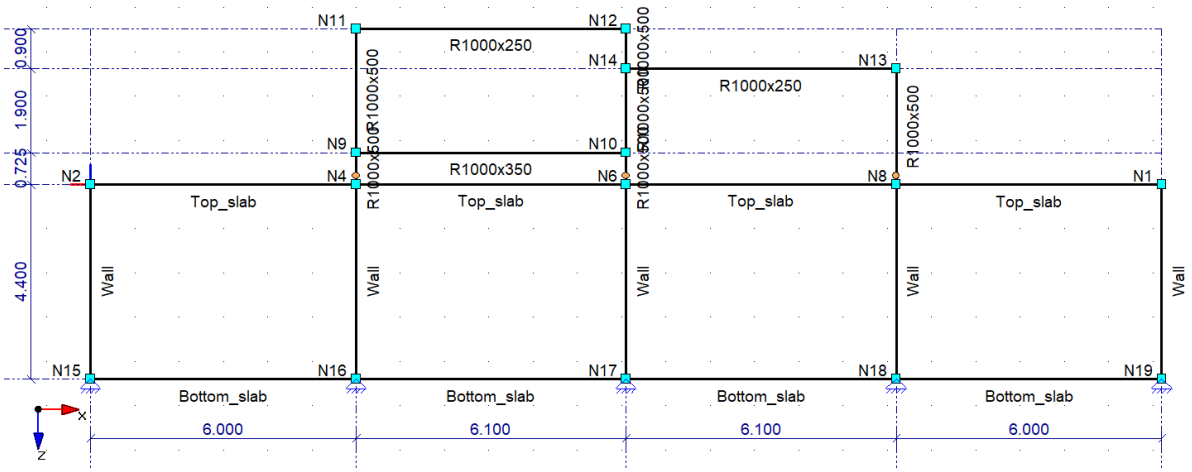

Figure 9.9: The geometry in Matrixframe for the new situation.

Table 9.8: The loads on the new situation of the Elshoutsluice.

Characteristic loads	Value	Unit
Pedestrian/bicycle	5.00	kN/m^2
Traffic, 1st lane	9.00	kN/m^2
Soil above culvert 2	4.71	kN/m^2
Soil above culvert 3	17.27	kN/m^2
Soil above culvert 1 & 4	62.00	kN/m^2
Self weight top slab	14.72	kN/m^2
Self weight walls	12.26	kN/m^2
Self weight roof	6.13	kN/m^2
Self weight pedestrian floor	8.58	kN/m^2
Single axle load	150.00	kN

9.2.2. Results

The linear analysis and the comparison of the forces on the Elshoutsluice structure for the old and new situation are performed in Appendix K. The following figures show the difference in normal forces, shear forces and bending moments of the first span of the existing top slab of the Elshoutsluice. This part is selected due to the largest difference in loading.

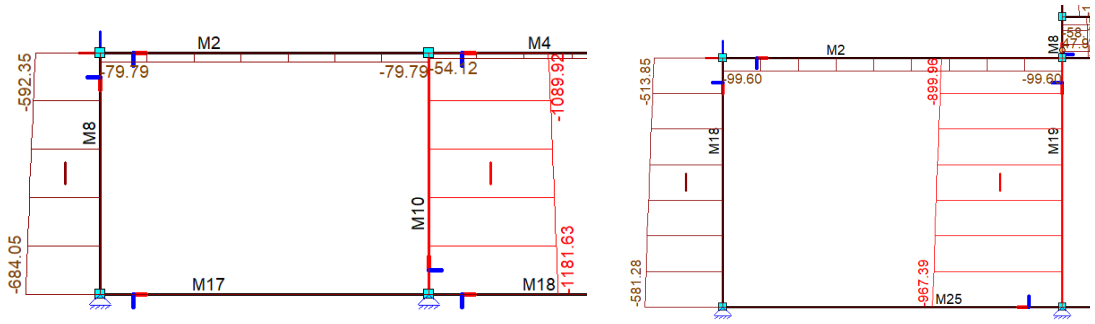

(a) The normal forces in the structure for the old situation.

(b) The normal forces in the structure for the new situation.

Figure 9.10: The comparison of the normal forces on the first span of the top slab and the first two lateral walls of the Elshoutsluice structure.

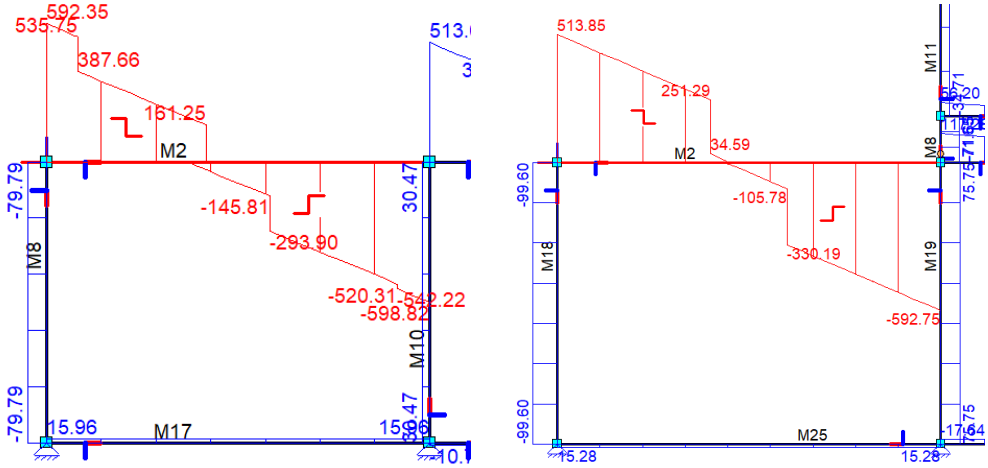

(a) The shear forces in the structure for the old situation.

(b) The shear forces in the structure for the new situation.

Figure 9.11: The comparison of the shear forces on the first span of the top slab and the first two lateral walls of the Elshoutsluice structure.

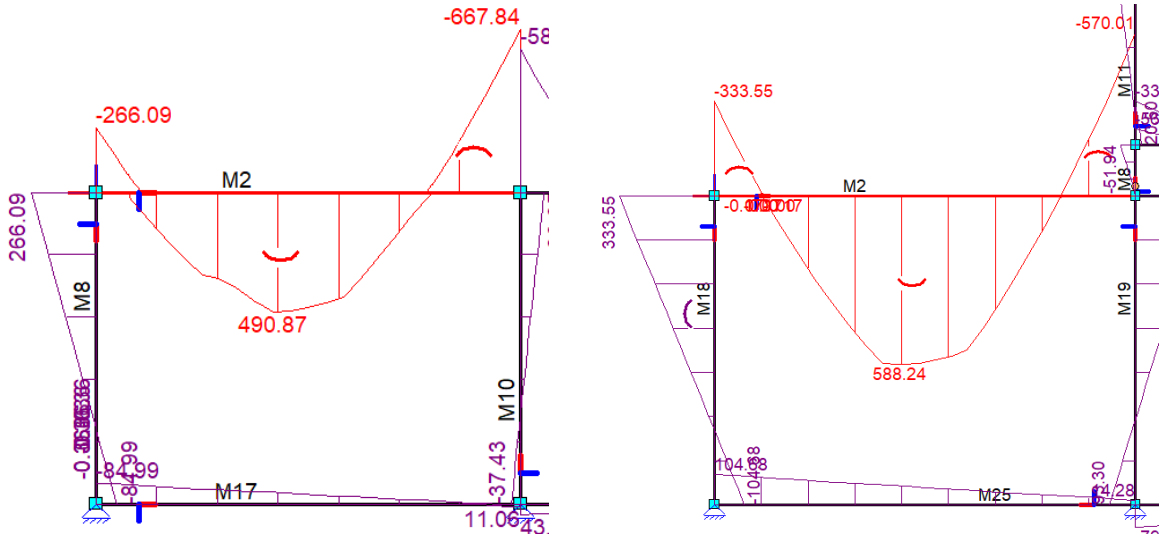

(a) The bending moments in the structure for the old situation.

(b) The bending moments in the structure for the new situation.

Figure 9.12: The comparison of the bending moments on the first span of the top slab and the first two lateral walls of the Elshoutsluice structure.

The maximum bending capacity of the slab without reinforcement is:

$$M_{Rd} = f_{ctd} \cdot W = 961.56 \cdot \frac{1}{6} \cdot 1 \cdot 0.6^2 = 57.69 \text{ kNm} \tag{9.12}$$

There must be reinforcement present in the slab, since the bending moments determined for the initial design situation exceed the calculated bending capacity.

The results of the comparison of the normal forces, shear forces and bending moments is given below:

- Normal forces: the normal forces in the lateral walls for the new case of the Elshoutsluice will not exceed the initial design situation. No additional check is needed and it is assumed that the walls will resist the normal forces.
- Shear forces: in the outer two spans of the selected cross-section the shear force in the new situation exceeds the old situation for parts of the span. The shear force in all five walls are larger in the new situation as well. These elements need an additional assessment of the existing reinforcement to determine the shear resistance.
- Bending moments: the sagging bending moments are larger in the two outer spans of the top slab for the new situation. The hogging bending moments in the top slab increase only nearby the connection to the outer walls. For the new situation, the bending moment in all 5 walls increase as well. Therefore, these elements need further investigation of the existing reinforcement to determine the bending moment capacity.

When the amount of current reinforcement in the structure is not sufficient for the increased loads, strengthening of an element is needed. There are different solutions for strengthening of an existing concrete element. Examples of strengthening are:

- Increasing the cross-sectional area.
- Adding of (prestressed) reinforcement internally or externally.
- Adding steel plates to a concrete cross-section externally.
- Applying Fibre-Reinforced Polymers (FRP) to the concrete elements.

Due to the high humidity of an hydraulic structure, the addition of external steel elements is not preferred because uncovered steel is prone to corrosion.

Due to the hogging moments in the top, strengthening could be needed at the top part of the slab near the walls. For the increase in sagging moments, possible strengthening must be applied to the bottom of the top slab in the middle of the outer spans.

10

General approach for modifying hydraulic structures

In this chapter a general approach is described for the modification of existing hydraulic structures which is derived from the Elshoutsluice case. Adapting an existing hydraulic structure is different than making a completely new design. The approach for this problem differs since it requires the inclusion of assessing the current structure. Modifying existing structure can bring difficulties which are described in this chapter with possible solutions.

The first step is collecting available information of the hydraulic structure and its location. The possibility of missing information is likely to occur for older structures. In the list below, difficulties are given with a possible solution.

- Difficulty: no design report available.
- Solution: determine with which regulations the structure was designed based on the construction year. An assumption of how the structure was designed can be deducted from these regulations.

- Difficulty: no drawings available.
- Solution: on site measurements can be made to determine the dimensions of the structure.

The second step is to determine the current functional requirements and specify the additional requirement(s). The requirements have an influence on different elements in a hydraulic structure. New requirements can lead to new elements. Figure 10.1 gives an example of the collection of functions and elements and the influences between them based on the Elshoutsluice case.

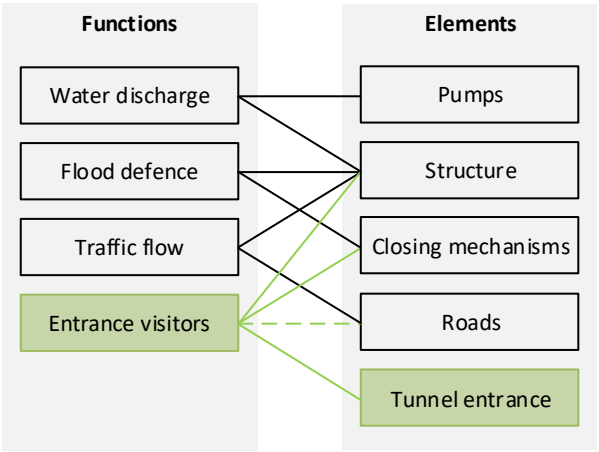

Figure 10.1: The functional requirements linked with the connected elements for the Elshoutsluice case. The new function and element are marked in green.

The third step is the development of concepts based on the outline of the existing structure and the required functions. The concepts must be realistic to fit into or around the current hydraulic structure. Preferably, the concepts will have a limited impact on the surroundings and the structure.

The fourth step is to analyse the geometrical and functional impact of the developed concepts. An analysis must be made to determine the function, capacity and dimensions of the new element(s). The impact of each concept on the existing structure is analysed. Concepts which do not fulfil the functional requirements and boundary conditions will be excluded during this design step.

The fifth step is the description of the construction sequence for each concept. It must be possible to construct a concept otherwise it will be excluded. The construction phases of the concepts are needed for the flood risk and structural verification.

The sixth step is the assessment of the flood safety of the existing structure and the new design concepts. A flood risk assessment according to the WBI2017 needs to be performed for the existing structure. For the new elements the OI2014 is used. The failure modes specific for hydraulic structures must be analysed. The difference in flood safety for the existing and new situations can be analysed with the use of failure trees per failure mode. Riskeer can be used to determine the failure probabilities for the failure modes when a customary test track is necessary. The use of the climate scenarios in Riskeer depends on the specific location of an hydraulic structure. It must be checked beforehand if the calculated probabilities for different reference years with climate scenarios are in line with the expectations. Calculations for the necessary height of a structure can be performed with the use of HydraNL for the different reference years and climate scenarios.

The seventh step is the structural safety verification. The assessment of the structural safety consist of an inspection of the current state of the hydraulic structure. The structure needs to be checked for cracks, erosion, displacements, etc. Old elements must be verified according to the NEN8700 series and new elements according to the NEN-EN 1990 series. Stability checks and strength calculations must be performed for the different concepts. The remaining concepts after the functional, constructability, flood risk and structural verification (step four, five, six and seven) are named alternatives. The difficulty for this design step and the possible solutions are given below:

- Difficulty: determining the remaining strength of elements in the existing structure.
- Solution: extract samples of the existing structure to perform (tensile/compression) tests.
- Solution: set an extra requirement of not exceeding the initial design load on the selected elements in the structure.
- Solution: strengthening of elements for which the loading will exceed the initial design load.

After these steps, the design process is similar to the design of a completely new structure. The design process includes the evaluation of alternatives and selection, the integration of subsystems and the validation of the result. Designing is a cyclical process which means that the different design steps are repeated until the finished product is complete.

11

Conclusion

This chapter consists of the conclusion, discussion and recommendations. The conclusion of this report is the resulting design.

11.1. The resulting design

The objective of this thesis is to provide a conceptual structural design for the multi-functional use of the discharge sluice at Kinderdijk including the functions for water discharge, flood defence, passage for (motorised) vehicles and pedestrians, which fulfils standards for flood safety and buildings in the Netherlands. The conclusion is a conceptual design for the Elshoutsluice for which it seems possible to fulfil the old and new requirements with possible strengthening or replacement of a number of existing elements. A 3D view of the design is given in Figure 11.1.

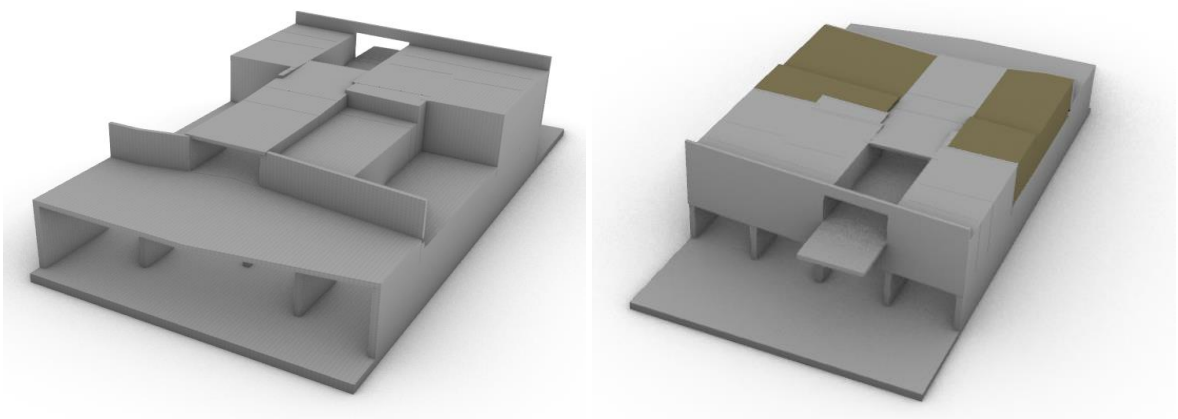

(a) The 3D view of the concrete elements of the design. The river side is at the top of the figure.

(b) The 3D view of the design including the soil on top of the structure. The river side is at the bottom of the figure.

Figure 11.1: The design for the Elshoutsluice.

Sketches of the side view for culvert number 2 and 3 are shown in Figure 11.2 and Figure 11.3.

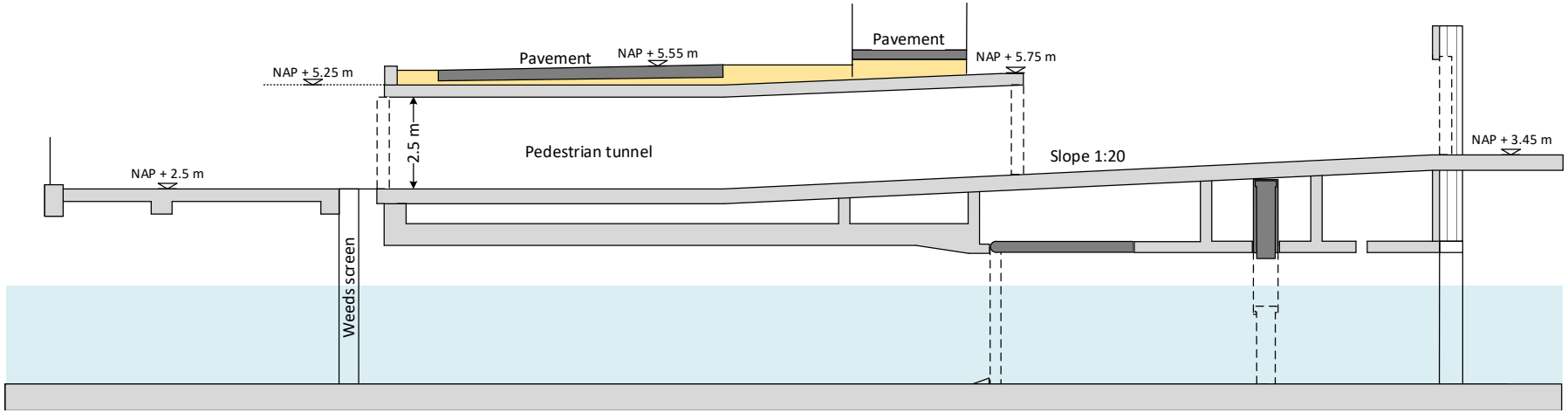

Figure 11.2: Side view sketch of the design for culvert number 2 with a new flap gate and vertical unfolding gate and the locations of the rolling/siding gates in the pedestrian tunnel. The river side is at the right side of figure.

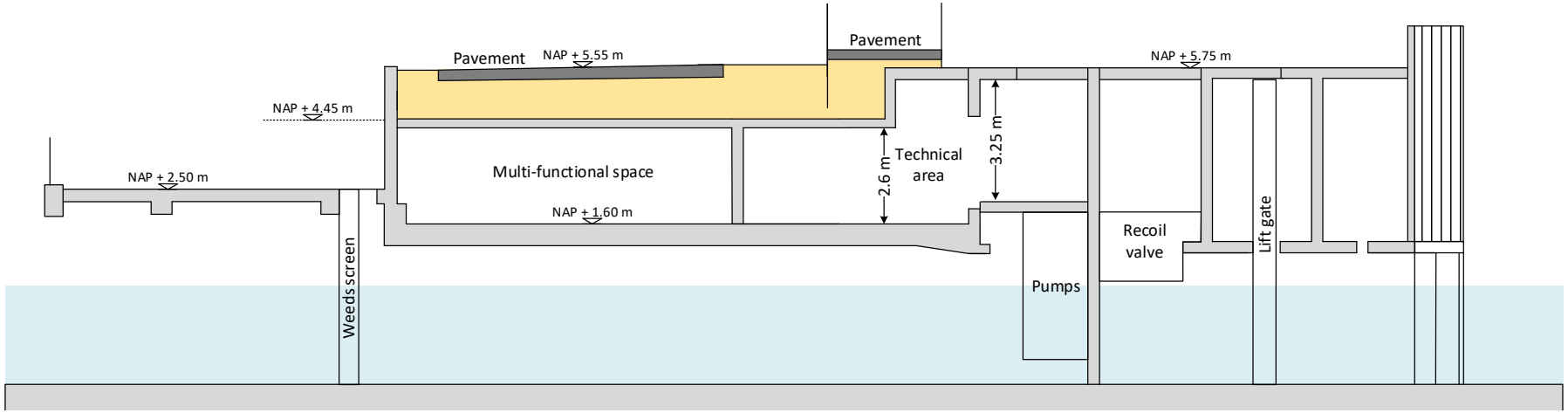

Figure 11.3: Side view sketch of the design for culvert number 3. The river side is at the right side of figure.

The largest difference between this design and the 'Derde Trap' design according to Tijhuis et al. (2019) is the floor configuration of the pedestrian tunnel and the selection of closing mechanisms.

The design fulfils the functional requirements for water discharge, flood defence and passage for (motorised) vehicles and pedestrians.

The Elshoutsluice fulfils the function as a flood defence by closing the gates at high water levels. In Table 11.1 is shown that the end result of the discharge sluice meets the requirements for the flood safety regarding flood defences. The structure fulfils the flood risk requirements during the construction phase as well.

Table 11.1: The required failure probabilities and the failure probabilities of the Elshoutsluice in the new situation.

Failure mechanism	**Alert value**	**Lower threshold**	**Elshoutsluice**
Requirement for the trajectory	1/30,000	1/10,000	
Overflow/overtopping	1/250,000	1/83,333	1/6,090,983
Non-closure gates	1/750,000	1/250,000	1/4,669,484
Piping	1/1,500,000	1/500,000	Suffice
Strength and stability	1/1,500,000	1/500,000	1/11,073,317

The flood risk safety is determined for a situation with two gates in the pedestrian tunnel. A situation with three gates, which is a requirement according to Waterschap Rivierenland, is safer against flooding than a situation with two gates. The probability of flooding of the pedestrian tunnel is very low. An additional calculation was performed with a pedestrian tunnel with one gate. This situation fulfils the requirements for the flood risk safety as well. It is not necessary to place three gates in the pedestrian tunnel since only 1 gate is already sufficient.

Stability checks are performed for the structural safety. The Elshoutsluice is stable during the construction phase, in the finished state and during maintenance. The result of the loading difference analysis is an increase in loads in the slab above culvert number 1 and 4 and the lateral walls of the culverts. An additional analysis is needed to determine if these elements need an increase in strength. Strengthening could be provided by increasing the cross-section area, adding reinforcement (internally) or adding FRP to the concrete elements.

11.2. Discussion

The list below gives the discussion points for certain design choices and assumptions made in this report.

1. A decision was made for the pedestrian tunnel to have a slope of 1:20. This decision resulted in a floor level of NAP + 2.45 m at he river side. The top of the tunnel will be at NAP + 5.95 m for a clearance of 2.50 m. Figure 11.4 shows that there are letters written on the outer wall of the Elshoutsluice. The bottom of these letters end at NAP + 5.75 m. The new pedestrian tunnel will run through the word Alblasserwaard. It must be considered if the letters will be preserved. With a slope of 1:25 the top of the pedestrian tunnel will be at exactly NAP + 3.75 m. The letters can be preserved for this situation, but the probability of needing to close of the tunnel due to high water levels increases. A water retaining parapet could be the solution if the closing frequency is to high for a pedestrian floor at NAP + 3.25 m.
2. There is a single emergency gate present in the Elshoutsluice which hangs on a rail. This gate can be lowered to close one of the four culverts. The rail and the emergency gate will be removed, since it will obstruct the new pedestrian tunnel. The effect of the removal of this gate is not addressed in the flood safety verification due to the fact that this additional emergency gate is not included in the safety assessment according to Waterschap Rivierenland (2020).

3. The floor of the multi-functional area and technical room are chosen at a level of NAP + 1.60 m. Another option is to increase the floor level of these areas to NAP + 2.50 m. This option will be profitable if an expansion of the pedestrian passage is needed in the future.

Figure 11.4: Letters on the outer wall of the Elshoutsluice saying Spuisluis Alblasserwaard (translated: discharge sluice Alblasserwaard). The outline of the letters is marked. Source: https://beeldbank.cultureelerfgoed.nl/.

11.3. Recommendations

The enumeration below gives advice on further research subject and procedures to obtain a more detailed design for the modifications for the Elshoutsluice.

1. The dimensions of the Elshoutsluice were determined via three available drawings of the discharge sluice. There were unknown values and many differences in these drawings. The calculations in this report are based on own interpretations of the drawings. Measurements on site will be needed for more accurate structural verification calculations
2. Inspection is needed to get a better insight in the current state of the Elshoutsluice. The structure needs to be checked for displacements/settlements, cracking, loose elements, corrosion and bleeding. If one of these symptoms is present in the structure, this needs to be included in the structural analysis.
3. The calculations including the foundation piles of the Elshoutsluice are performed for vertical foundation piles. In reality the piles are inclined in various angles. With the made assumptions, the calculated bearing capacity is very high. Additional investigation and calculation is needed to get a better insight in the bearing capacity of inclined foundation piles for the Elshoutsluice.
4. As a continuation of this design process, the strength calculations must be performed for the new elements in the Elshoutsluice. The dimensions must be checked and the necessary reinforcement must be determined according to NEN-EN 1992. The existing structural elements for which the loading will increase need an additional verification. Assumptions of the reinforcement can be made based on the concrete regulations according to the VB 1974.
5. Culvert number 2 will include two new gates in the conceptual design. Completely closing off culvert number 2 could be an option as well. This solution is only possible if the pump capacity increases to fulfil the water discharge function. The options for pumps and with

how much the capacity can be increased needs investigation. Completely closing off culvert number 2 increase the safety for the failure mode non-closure of gates.

6. The design process can be continued for the connection of the pedestrian tunnel at river side to the piers for the waterbus and river cruise. A link between the pedestrian tunnel hinterlands and the entrance of the World Heritage Site Kinderdijk must be made as a complete solution for the infrastructure problem in Kinderdijk.

Appendices

A

Background information on safety

This appendix describes the background information for the general safety principles, flood risk safety assessment and the existing structural safety assessment.

A.1. Structural safety principles

For structural elements it is necessary to know the expected loads and material characteristics. A structure fails permanently when it collapses. Descriptions are given in which way a structure is not able to fulfil its function with failure mechanisms. The conditions right before failure are limit states. Two different limit states are considered. The Serviceability Limit State (SLS) indicates when the normal use is disrupted and the Ultimate Limit State (ULS) indicates the collapse of (a part of) a structure. The different types of failure are (Molenaar & Voorendt, 2019):

- EQO: loss of static equilibrium of (a part of) a structure considered as a rigid body.
- STR: failure of structural elements or internal failure of the structure.
- GEO: failure or excessive deformation of the ground providing resistance.
- FAT: failure of structural elements or structure due to fatigue.
- UPL: loss of equilibrium due to uplift by vertical actions like water pressure.
- HYD: piping, hydraulic heave and internal erosion caused by hydraulic gradients.

The relation between the load and the resistance to failure can be described with the limit state function:

$$Z = R - S \tag{A.1}$$

Where S is the load (solicitation) and R is the strength (resistance). If the limit state function has a negative value (Z<0), the structure will fail according to the given failure mode. In the Eurocodes safety is often expressed with a dimensionless unity-check:

$$S/R < 1 \tag{A.2}$$

Uncertainties must be taken into account with an engineering design. The main categories for these uncertainties are (Molenaar & Voorendt, 2019):

- Physical uncertainties, which are caused by a lack of data of strength or loading.
- Statistical uncertainties, which are caused if distribution functions of strength or loading are not exactly known.
- Modelling uncertainties, which consists of imperfectness of models, describing phenomena and failure modes.

- Human error, which forms a big thread to the reliability.

To take into account these uncertainties, safety margins between strength and loading are introduced. Various techniques are classified to incorporate the safety margins in a structural design (Molenaar & Voorendt, 2019):

- Level 0: deterministic design
- Level I: semi-probabilistic design
- Level II: simplified probabilistic design
- Level III: full probabilistic design

A.1.1. Deterministic design (level 0)

For the deterministic design overall safety factors (γ) are applied to create a margin between strength and loading. These safety factors are based on experience or engineering judgement. A structure is considered safe, where $\gamma > 1.0$, if:

$$S \cdot \gamma < R \tag{A.3}$$

A.1.2. Semi-probabilistic design (level I)

For the semi-probabilistic design, strength and load variables are distributed around a mean value (μ). Figure A.1 shows the characteristic value of the load (S_k) which is exceeded by only 5% of the samples and the characteristic value of the strength (R_k) which is exceeded by 95%. The functions of the characteristic values can be expressed as:

$$S_k = \mu_S - k \cdot \sigma_S \text{ and } R_k = \mu_R - k \cdot \sigma_R \tag{A.4}$$

Where σ is the standard deviation and k is the multiplication constant for the standard deviation to determine the 5% and 95% value. For a normal distribution the multiplication factor is constant ($k = 1.64$).

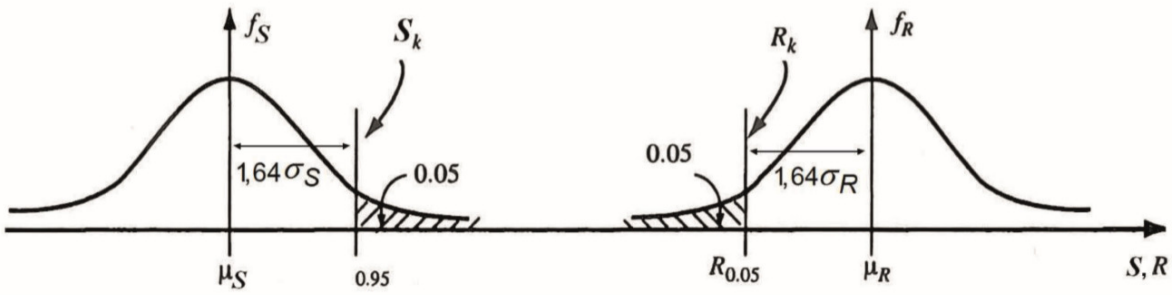

Figure A.1: The characteristic values for load and strength (Molenaar & Voorendt, 2019)

According to the Eurocode, the characteristic value for loading can be multiplied with the combination factor (ψ_0), the frequent factor (ψ_1) or the quasi-permanent factor (ψ_2) to obtain the representative load value (S_{rep}). The representative value for the strength (R_{rep}) is mostly the same as the characteristic value. With partial safety factors (γ_R, γ_S) the design values can be determined. A design has to have a larger design value for the strength (R_d) than the design value for the load (S_d). The design values are determined with:

$$R_d = \frac{R_{rep}}{\gamma_R} \text{ and } S_d = \gamma_S \cdot S_{rep} \tag{A.5}$$

To determine the design value of the load, different load types must be combined to obtain the most critical circumstances. Loads are categorised in permanent, variable or accidental loads. In

the Eurocode the main variable load is considered apart from the remaining variable loads and the load from pre-stressing is considered as a separate permanent load. The combined characteristic values of the load and the partial factors result in the calculation of the design value of the load effect:

$$E_d = E\left\{\sum_{j\geq 1}^{n} \gamma_{G,j}\cdot G_{k,j} + \gamma_p \cdot P + \gamma_{Q,1}\cdot Q_{k,1} + \sum_{i>1}^{n} \gamma_{Q,i}\cdot \psi_{0,i}\cdot Q_{k,i}\right\} \tag{A.6}$$

Where:

$E\{..\}$	=	combination of permanent an variable loads
$\gamma_{G,j}$	=	partial factor for the permanent load j
γ_p	=	partial factor for the pre-stressing load
$\gamma_{Q,1}$	=	partial factor for the main variable load
$\gamma_{Q,i}$	=	partial factor for the variable load i
$G_{k,j}$	=	characteristic value of the permanent load j
P	=	representative value for the pre-stressing load
$Q_{k,1}$	=	characteristic value of the main variable load
$Q_{k,i}$	=	characteristic value of the variable load i
$\psi_{0,i}$	=	combination reduction factor for the variable load i

The most unfavourable of the two following equations should be used in the limit states GEO and STR. In the following equations the combination reduction factor for the main variable load ($\psi_{0,1}$) and the reduction factor for unfavourable permanent load j (ξ_j) are introduced. Tables for the reduction factors γ, ψ and ξ are given in tables according to Eurocode 0.

$$\begin{aligned} E_d &= E\left\{\sum_{j\geq 1}^{n} \gamma_{G,j}\cdot G_{k,j} + \gamma_p \cdot P + \gamma_{Q,1}\cdot \psi_{0,1}\cdot Q_{k,1} + \sum_{i>1}^{n} \gamma_{Q,i}\cdot \psi_{0,i}\cdot Q_{k,i}\right\} \\ E_d &= E\left\{\sum_{j\geq 1}^{n} \xi_j\cdot\gamma_{G,j}\cdot G_{k,j} + \gamma_p \cdot P + \gamma_{Q,1}\cdot Q_{k,1} + \sum_{i>1}^{n} \gamma_{Q,i}\cdot \psi_{0,i}\cdot Q_{k,i}\right\} \end{aligned} \tag{A.7}$$

For the load combination with accidental loads, like fire or impact, the choice between the reduction factor $\psi_{1,1}$ and $\psi_{2,1}$ depends on the relevant accidental design situation. A design value of the accidental action (A_d) is included which results in the following design value of the load effect:

$$E_d = E\left\{\sum_{j\geq 1} G_{k,j} + P + A_d + (\psi_{1,1} \text{ or } \psi_{2,1})\cdot Q_{k,1} + \sum_{i>1} \psi_{2,i}\cdot Q_{k,i}\right\} \tag{A.8}$$

A.1.3. Probabilistic design (levels II and III)

The design levels II and III are both probabilistic. The level II is the simplification of level III. Level III is explained first and then the simplification level II.

Full probabilistic design (level III)

In the full probabilistic design level the probability density distributions of all the stochastic variables are described. Figure A.2 shows the probability density distributions of the loading, the strength and the resulting distribution of the limit state. The area where $Z < 0$ is the failure probability (p_f). For a probability density function a 'compact' distribution around the mean value implies a high certainty while a 'wide' distribution implies a large uncertainty. An impression of the reliability can be made based on the width of a probability density function. The reliability of a structure can be expressed with the reliability index (β), which depends on the mean value of the limit state (μ_z) and

the standard deviation of the limit state (σ_z):

$$\beta = \frac{\mu_z}{\sigma_z} \tag{A.9}$$

With:

$$\mu_z = \mu_R - \mu_S \text{ and } \sigma_z = \sqrt{\sigma_R^2 + \sigma_S^2} \tag{A.10}$$

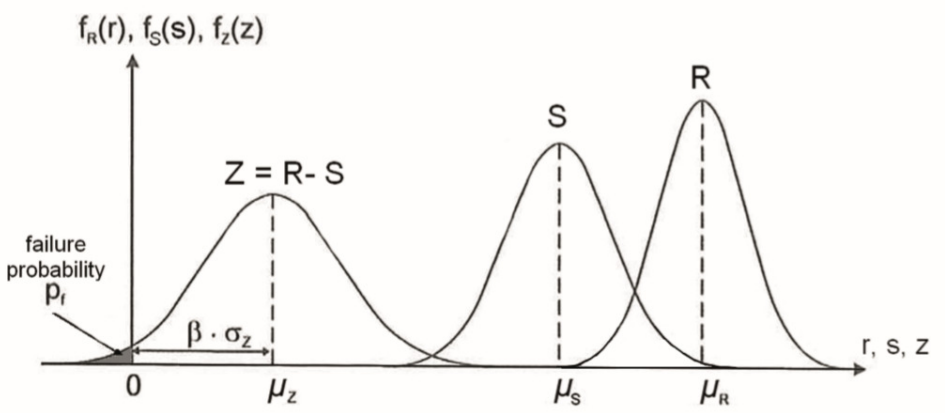

Figure A.2: The probability density distribution of the limit state function, the loading and the strength (Molenaar & Voorendt, 2019).

The influence of the strength and load on the probability density function of the limit state function can be expressed by influence coefficients (α_R, α_S), which depends on the standard deviations of the strength, load and limit state function ($\sigma_R, \sigma_S, \sigma_Z$):

$$\alpha_R = \frac{\sigma_R}{\sigma_Z} \text{ and } \alpha_S = -\frac{\sigma_S}{\sigma_Z} \tag{A.11}$$

If the reliability index and influence coefficient are known, the partial factors for level I calculations can be derived with level II and III calculations. The equations for the partial safety factors are:

$$\gamma_R = \gamma_M = \frac{1 - k_R \cdot V_R}{1 - \alpha_R \cdot \beta \cdot V_R} \text{ and } \gamma_S = \frac{1 - \alpha_S \cdot \beta \cdot V_S}{1 - k_S \cdot V_S} \tag{A.12}$$

Where k_R and k_S indicates the limit factor of the representative value of the strength or load. V is the coefficient of variation for the strength ($V_R = \sigma_R/\mu_R$) or the load ($V_S = \sigma_S/\mu_S$).

The probability of the loading exceeding the strength is called the probability of failure (p_f). Probability of failure can be described as the exceeding of the limit state function as well:

$$p_f = P(R < S) = P(Z < 0) \tag{A.13}$$

When strength and loading are independent, the failure probability can be expressed as the following equation:

$$p_f = \iint_{R<S} f_R(r)\, f_S(s)\, dr\, ds \tag{A.14}$$

The probability density function of strength ($f_R(R)$) and the probability density function of the load ($f_S(S)$) can be multiplied which results in the joint probability function:

$$f_R(r)\, f_S(s) = f_{R,S}(r, s) \tag{A.15}$$

The joint density function including the limit state ($Z = 0$) is shown in Figure A.3. With the joint density function the failure probability can be formulated as:

$$p_f = \int_{-\infty}^{r} \int_{-\infty}^{s} f_{R,S}(r,s)\, dr\, ds \tag{A.16}$$

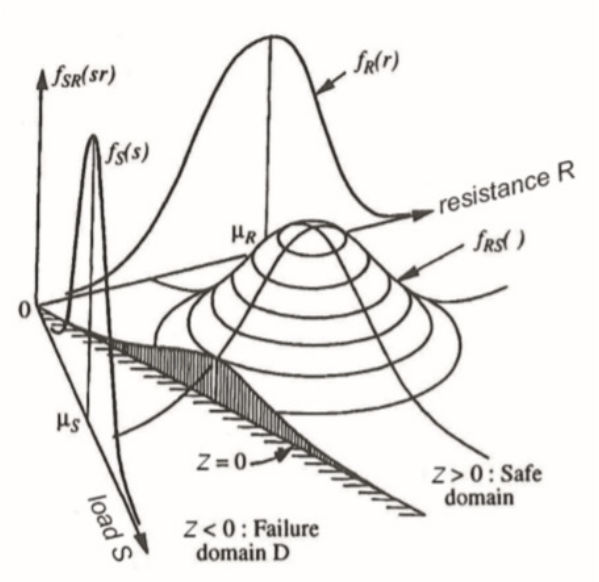

Figure A.3: The joint density function (Molenaar & Voorendt, 2019).

When more than one structural element or more than one failure mode is considered, the failure probability can be expressed with independent variables x_i as the following integral:

$$p_f = \iint_{Z(x)<0} \dots \int \prod_{i=1}^{n} f_{x_i}(x_i)\, dx_i \tag{A.17}$$

This integral can be solved with a Monte Carlo simulation in the case with not too low failure probabilities. Applying probabilistic techniques can be difficult due to the required detailed knowledge of each variable and its relationship to other variables.

Simplified probabilistic design (level II)

Since the full deterministic design level has drawbacks, a simplified method is developed to approximate the distribution of the strength and the load. In this simplification all parameters are considered to be independent for most methods. The probability density functions for the strength and load are described with normal distributions instead:

$$f(x) = \frac{1}{\sigma_x \sqrt{2\pi}} \cdot e^{-\frac{(x-\mu_x)^2}{2\sigma_x^2}} \tag{A.18}$$

A firs-order risk method (FORM) or second-order risk method (SORM) can be used depending on the order of the approximation (Molenaar & Voorendt, 2019).

A.2. Flood risk safety assessment

Managers of primary flood defence must assess at least once every twelve years whether their defence meets the legal safety requirements. This is according to the water act (Waterwet). The requirements for criticising the primary flood defences is described by legal assessment instruments (Wettelijk Beoordelingsinstrumentarium, WBI). Rijkswaterstaat updates the WBI for each round. The current assessment round runs from 2017 to 2023, which resulted in the name WBI 2017. The update for this round is more drastic than previous times because of the new safety standards which were introduced in 2017 (see subsection 1.3.2). The flood risk assessment is needed in this study to analyse the current state of the Elshoutsluice.

With the new standardisation of primary flood defence, the alert values and the lower thresholds are introduced. Exceeding of the alert value means an early signal that a flood defence needs strengthening in time. This signal goes to the ministry of infrastructure and the environment. There is still sufficient time for measures. The goal is to finish the strengthening measures before the lower threshold is reached. When the lower threshold is exceeded, the flood defence does not satisfy the maximum allowable flooding probability. This is stated in the water act.

The assessment starts with a filter at segment level and at a section level. Segment references to a dike segment and a section to a part of this segment, for example a part of a levee, an engineering structure or a dam. If a section or segment fulfils the criteria of the general filter, a customary test can be carried out. When the criteria aren't met, a judgement will be carried out according to the test procedure for hydraulic loads and strength and safety regulations. An assessment procedure consists of four tests going from global to detailed. First and secondly is the simple test and the detailed test per section which are both executed per section and per test track. Third is the assessment per segment which is done for the whole dike segment where sections or test tracks are combined. Finally is customary test which can either be executed per section and test track as the entire dike segment.

The safety assessment of a flood defence is based on the strength at the end of the assessment period. For the current round this is 31 December 2022, which is called the reference date. It is necessary to determine what the expected state of the flood will be at the reference date. This could be obtained by results of (visual) inspection or monitoring and/or by programming of the expected maintenance measures.

In the simple test a test track is checked by simple decision rules. These rules are based on safe dimensions of flood defence (parts), general rules of excluding failure mechanisms and simple calculation rules. Different failure mechanisms are shown in Figure A.4. If a failure mechanism meet the criteria of the decision rules it can be neglected since the probability of failure is extremely small. When the criteria isn't met, the assessment needs to be continued with a detailed test per section.

With the detailed test per section the requirements for a section are derived from the legal probability of flooding of a dike segment. This probability will be divided to failure mechanisms, which are assessed in different test tracks, with a different ratio and thereafter divided over the sections. In this way the maximum allowable failure probability is determined for each section. The test consist of determining if the calculated failure probability meets the required probability. Executing the detailed test could be an iterative process.

For the detailed test per segment a probabilistic approach is used where the fixed length-effect and fixed failure probability distribution between test tracks aren't used. The results of this test gives an insight in which parts and characteristics of the flood defence have the most influence on the flooding probability of a segment.

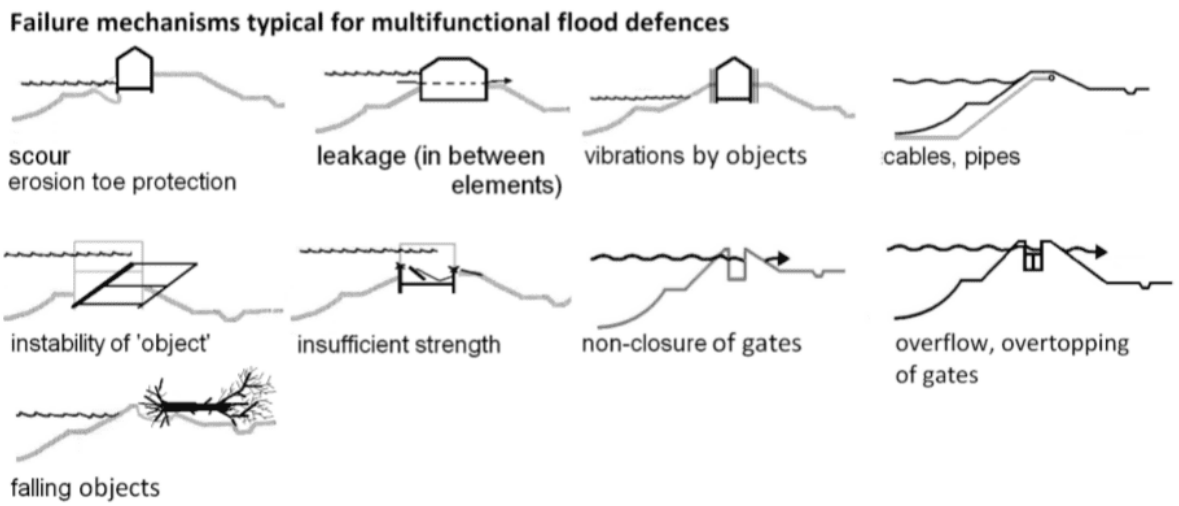

Figure A.4: Different failure mechanisms for multi-functional flood defences described by Voorendt (2017)

The custom test gives the possibility to analyse specific locations, to make a more advanced analysis or to make a judgement based on the knowledge of the manager of a flood defence. The analyses can vary between simple or advanced and deterministic or probabilistic per section or segment.

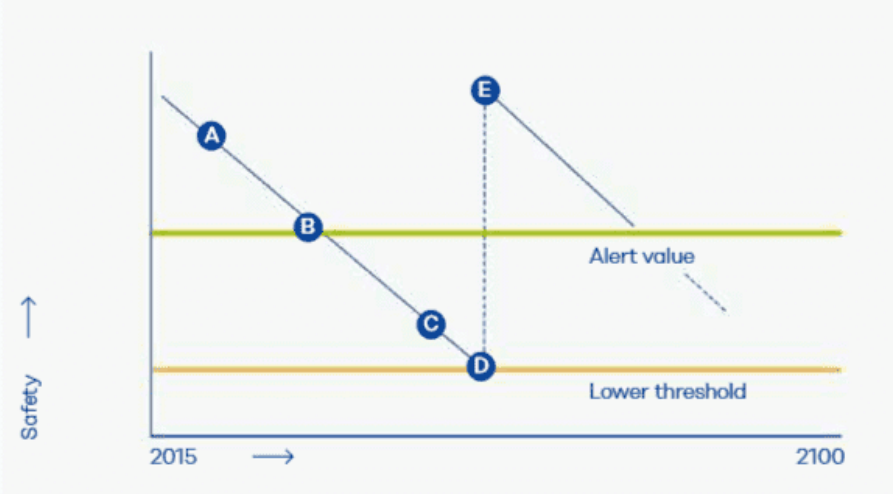

Figure A.5: The function of the lower threshold and alert value (TAW-ENW, 2016).
A: Safety declines due to increasing load as result of climate change and declining levee strength due to ageing.
B: Preparations for measures can commence as soon as the alert value is reached
C: Work on levee reinforcement commences
D: Lower threshold
E: Safety level immediately after reinforcements

After the whole test procedure a decision is made about the safety. The decision is determined by assembling of uneven test assessments per section and segment. With the assembly it is possible to determine a globally alert value (P_{alert}) and lower threshold for a dike segment (P_{max}). The safety assessment is divided in different categories (Rijkswaterstaat, 2017a):

- A+: Dike segment does not exceeds the alert value more than sufficient:

  $$P_{segment} < 1/30 * P_{alert}$$

- A : Dike segment does not exceeds the alert value more than sufficient:

$$1/30 * P_{alert} < P_{segment} < P_{alert}$$

- B : Dike segment does not exceeds the lower threshold, but does exceed the alert value:

$$P_{alert} < P_{segment} < P_{max}$$

- C : Dike segment does exceed the lower threshold:

$$P_{max} < P_{segment} < 30 * P_{max}$$

- D : Dike segment does exceed the lower threshold by a lot:

$$P_{segment} > 30 * P_{max}$$

Failure mechanisms

Failure is caused by a failure mechanisms. All considered failure mechanisms for the detailed test on segment level are failure due to (Rijkswaterstaat, 2017a):

- Insufficient height of a structure or erosion of the grass cover on the crest and inner slope.
- Piping.
- Macro instability of the inner slope.
- Erosion of the grass cover on the outer slope.
- Other covers of the outer slope.
- Non-closure of a structure.
- Piping by a structure.
- Insufficient strength and instability of a point structure.
- Dune erosion.
- Remaining failure mechanisms.

For a dike segment a maximum failure probability is determined by the water act. With this value the failure probability requirement per failure mechanism can be determined:

$$P_{max;i} = \frac{\omega_i P_{max}}{N_i} \tag{A.19}$$

With:

$P_{max;i}$	=	Required failure probability per cross-section or structure per failure mechanism i [1/year].
P_{max}	=	Standard for the dike segment [1/year].
ω_i	=	Failure probability factor for a failure mechanism i determined with Table A.1 [-].
N_i	=	Length-effect factor for a cross-section or structure for failure mechanism i [-].

Table A.1 gives an indication for the failure probability factor distribution. It is possible to deviate from this given distribution. The sum of all failure mechanism factors is equal to 1.

To determine the failure probability requirement per section, the length-effect factor N_i must be taken into account. This factor can be calculated with:

$$N_i = 1 + \frac{a_i \cdot l_{seg}}{b_i} \tag{A.20}$$

Where:

a_i	=	Failure mechanisms sensitive fraction of the dike segment [-].

Table A.1: The failure probability factor ω (Rijkswaterstaat, 2017a)

Type of flood defence	**Failure mechanism**	**Segment type**	
		Sand coasts	**Other (levees)**
Levee	Overflow and overtopping	0	0.24
	Uplift and piping	0	0.24
	Macro instability inner slope	0	0.04
	Damage revetment and erosion	0	0.10
Engineering work	Non-closure	0	0.04
	Piping	0	0.02
	Structural failure	0	0.02
Dune	Dune erosion	0.70	0 / 0.10
Other		0.30	0.30 / 0.20
Total		**1**	**1**

b_i = The reference length for the intensity of the length-effect within a failure mechanism sensitive length of a dike segment [m].

l_{seg} = The length of the dike segment stated in the water act [m].

A.3. Existing structural safety assessment

Failure probabilities and reliability indices are related (Jongejan & Steenbergen, 2015):

$$P_f = \Phi(-\beta) \tag{A.21}$$

Where $\Phi(..)$ is the standard normal distribution. For the reliability indices for new structures, the NEN-EN 1990 series are used. The assessment of existing structures is described in te NEN 8700 series. There can be different motivations for the assessment of a structure:

- Periodic assessment
- End of design- or remaining lifespan
- Fatigue and/or detected damage
- Change in functionality
- Redesign
- Change in design standards

Normcommissie (2011) makes a distinction between renewal and disapproval of structural safety. Only renovation is discussed, since this is applicable to the Elshoutsluice case. The structure needs to fulfil the current safety standards for new structures.

A new structure is designed for a period in which the structure must fulfil the standards. This is called the lifespan of a structure. The residual lifespan is the estimated period for which an existing structure or structural element is serviceable for its function. This is different from the reference period which is used for determination of the variable loading and is the time unit of a required failure probability (Normcommissie, 2011) and (Jongejan & Steenbergen, 2015).

Structures are categorised in consequence classes (CC) Normcommissie (2011):

- CC1: Low consequences with respect to casualties and/or small or negligible economical or social effects on the surrounding area.
- CC2: Moderate consequences with respect to casualties and/or considerable economical or social effects on the surrounding area.
- CC3: Large consequences with respect to casualties and/or substantial economical or social effects on the surrounding area.

In general, CC3 is chosen for primary flood defences by Rijkswaterstaat. However (Jongejan & Steenbergen, 2015) suggests that the consequence classes should depend on the lower threshold given by the water act for hydraulic structures. Structures with a standard of 1/300 per year are categorised in CC1, with a standard of 1/1,000 or 1/3,000 per year in CC2 and with a standard of 1/10,000 or 1/30,000 per year in CC3. Per consequence class a minimum reference period and minimum reliability index is given for renewal in Table A.2.

Table A.2: The minimum values for the reliability index β with a minimum reference period (ULS) (Normcommissie, 2011)

Minimum reliability indices for renewal			
Consequence Class	**Minimum reference period**	β	
		wind is not dominant	wind is dominant
CC3	15 years [b]	3.8 (3.6)	3.3 [a] (2.6)
CC2	15 years [b]	3.3 (3.1)	2.5 [a]
CC1	15 years	2.8	1.8
[a] The lower threshold for individual safety is governing. [b] In general, a residual lifespan is recommended and therefore a reference period of 30 years. The value between brackets is only applicable to structures with a permit according to 'Het Bouwbesluit 2003' and earlier regulations.			

Since a different value is used for the residual lifespan than the design lifespan, the reference period can differ from the situation with a new structure. The approach used in NEN-EN 1991 for situations with a reference period other than 50 years can be used. For the cases where NEN-EN 1991 doesn't have applicable rules, the following equation can be used (Normcommissie, 2011):

$$F_t = F_{t_0}\left\{1 + \frac{1-\psi_0}{9}\ln\left(\frac{t}{t_0}\right)\right\} \tag{A.22}$$

Where:

- F_t = The modified extreme value of a variable distributed load with the reference period which belongs to the chosen residual lifespan.
- F_{t_0} = The extreme value of a variable distributed load with the basis reference period.
- ψ_0 = The combination reduction factor.
- t = The reference period which belongs to the chosen residual lifespan.
- t_0 = The basis reference period in case of a new structure (50 years in general).

An existing structure can have the following visible or invisible symptoms due to current and previous loading (Normcommissie, 2011):

- Displacements or settlements
- Cracking
- Loose elements
- Corrosion
- Bleeding

These events can be accounted for to define the occurrence in ULS and to include the conditions in a failure probability analysis. In case of a level I approach, the changed situation needs to be included in modelling. In addition, it needs to be checked if the symptoms can be a reason to change the representative values of the loads, geometry or material characteristics (Normcommissie, 2011).

Table A.3: (Normcommissie, 2018)

Regulation	Quality Class	f_{ck} [MPa]
GBV 1912	-	8
GBV 1918	-	8
GBV 1930	-	8
GBV 1940	K 150	8
	K 200	11
	K 250	13.5
GBV 1950	K 150	8
	K 200	11
	K 250	13.5
GBV 1962	K 160	9
	K 225	13
	K 300	19
	K 400	28
	K 450	32
RVB 1962 and RVB 1967	K 500	33
	K 600	40

Regulation	Strength Class	f_{ck} [MPa]
VB 1974 and VB 1974/1984	B 12.5	10
	B 17.5	14
	B 22.5	18
	B 30	25
	B 37.5	30
	B 45	35
	B 52.5	42.5
	B 60	50
NEN 6720, VBC	B 15	12
	B 25	20
	B 35	28
	B 45	35
	B 55	45
	B 65	53

For remarks, see Table 1 from Normcommissie (2018)

A.4. Climate scenarios

The Royal Netherlands Meteorological Institute (Koninklijk Nederlands Meteorologisch Instituut in Dutch) developed scenarios for the future climate changes in the Netherlands for 2050 and 2085. This is named the KNMI'14 climate scenarios. There are four different scenarios based on the amount of global warming or possible changes in the air circulation pattern relative to the climate from 1981 to 2010, see Figure A.6. Global warming is categorised as moderate or warm and the changes in air circulation patterns are categorised as low or high. A climate scenario provides a picture of changes in 12 climate variables. This includes the sea level, precipitation and the temperature. Figure A.7 shows the key figures of the climate scenarios for 2050 and 2085. The climate scenarios are relevant for this project since it includes the water level rise in the Netherlands.

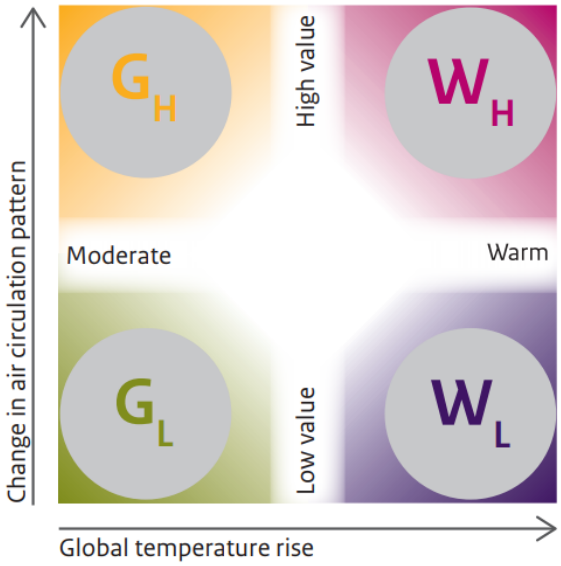

Figure A.6: The four climate scenarios according to the KNMI (2015).

Variabele	Indicator	Climate 1981-2010	Scenario changes for the climate around 2050				Scenario changes for the climate around 2085				Natural variations averaged over 30 years
			G_L	G_H	W_L	W_H	G_L	G_H	W_L	W_H	
Global temperature rise:			+1 °C	+1 °C	+2 °C	+2 °C	+1.5 °C	+1.5 °C	+3.5 °C	+3.5 °C	
Change in air circulation pattern:			low value	high value	low value	high value	low value	high value	low value	high value	
Sea level at North Sea coast	absolute level	3 cm above NAP	+15 to +30 cm	+15 to +30 cm	+20 to +40 cm	+20 to +40 cm	+25 to +60 cm	+25 to +60 cm	+45 to +80 cm	+45 to +80 cm	±1.4 cm
	rate of change	2.0 mm/yr.	+1 to +5.5 mm/yr.	+1 to +5.5 mm/yr.	+3.5 to +7.5 mm/yr.	+3.5 to +7.5 mm/yr.	+1 to +7.5 mm/yr.	+1 to +7.5 mm/yr.	+4 to +10.5 mm/yr.	+4 to +10.5 mm/yr.	±1.4 mm/yr.
Temperature	mean	10.1 °C	+1.0 °C	+1.4 °C	+2.0 °C	+2.3 °C	+1.3 °C	+1.7 °C	+3.3 °C	+3.7 °C	±0.16 °C
Precipitation	mean amount	851 mm	+4 %	+2.5 %	+5.5 %	+5 %	+5 %	+5 %	+7 %	+7 %	±4.2 %
Solar radiation	solar radiation	354 kJ/cm²	+0.6 %	+1.6 %	-0.8 %	+1.2 %	-0.5 %	+1.1 %	-0.9 %	+1.4 %	±1.6 %

Figure A.7: The key figures for the climate change scenarios KNMI'14.

The KNMI'14 climate scenarios is a follow up of the KNMI'06 climate scenarios for 2050 and 2100. These climate scenarios are relative to the climate in the time period 1976 - 2005. The G_H and W_H are expressed as G^+ and W^+ in the KMNI'06 scenarios. G_L and W_L are expressed as G and W. Table A.4 shows these scenarios. Some computational programs still use the KNMI'06 climate scenarios.

Table A.4: The KMNI'06 climate scenarios

2050	**G**	**G^+**	**W**	**W^+**
Increase in global temperature	+1°C	+1°C	+2°C	+2°C
Changes in air circulation	No	Yes	No	Yes
2100	**G**	**G^+**	**W**	W^+
Increase in global temperature	+2°C	+2°C	+4°C	+4°C
Changes in air circulation	No	Yes	No	Yes

B

Information Elshoutsluice

This appendix describes the geological, hydraulic, meteorological and geo-technical conditions. Furthermore the current design of the Elshoutsluice is explained.

B.1. Geological conditions

The Elshoutsluice is located next to the river named the Lek and is part of the flood defence of dike ring 16, see Figure B.1.

Figure B.1: Dike ring 16 divided in sections with the location of the Elshoutsluice (VNK2, 2014)

Kinderdijk is located in the western part of the Netherlands, which is adjacent to the sea. Therefore the salinity of the water at the Lek river is checked. According to Rijkswaterstaat (n.d.) the water in the lek river is fresh water, see Figure B.2.

Figure B.2: The salinity of the Lek river water. Souce: https://waterinfo.rws.nl/.

From Figure B.3 can be concluded that there is no earthquake risk at Kinderdijk.

Figure B.3: The areas in the Netherlands where there may be an earthquake risk (orange areas). Source:https://www.risicokaart.nl/

B.2. Hydraulic conditions

The section hydraulic conditions consists of the water levels, the waves, the storage capacity and the critical discharge. This information is necessary for the flood risk and structural calculations.

Water levels

There is a hydraulic database available of the water levels at the Lek river, which is WBI2017_Benedenrijn_16-2_v04. The nearest point of the hydraulic database to the Elshoutsluice is determined with Riskeer. This is the location 016-02_0081_9_LE_km0988 which is shown in Figure B.4.

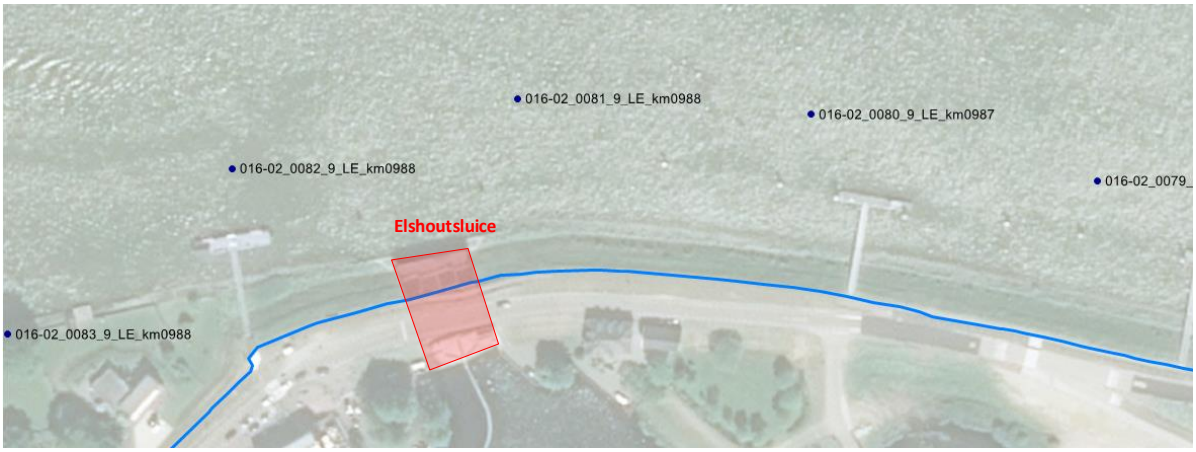

Figure B.4: The hydraulic database locations near the Elshoutsluice.

The water levels at the Lek river for the alert value (1/30,000 per year) and lower threshold (1/10,000 per year) are determined for different scenarios with Riskeer. For the assessment the reference year 2023 is used. The water levels are determined for the KNMI'06 G and W^+ climate scenarios, which are explained in section A.4. All these water levels are given in Table B.1.

Table B.1: The water levels corresponding with the alert value and lower threshold determined with Riskeer.

Probability	**2023**	**2050**		**2100**	
[1/year]	**-**	**G**	**W^+**	**G**	**W^+**
1/30,000	NAP + 3.66 m	NAP + 3.72 m	NAP + 3.88 m	NAP + 3.86 m	NAP + 4.22 m
1/10,000	NAP + 3.48 m	NAP + 3.55 m	NAP + 3.69 m	NAP + 3.67 m	NAP + 4.05 m

Waves

The waves at the Lek river are determined with the hydraulic database and Riskeer. For the lower threshold a value of 1.42 m and for the alert value 1.32 m. These values are the same for the reference years 2023, 2050 and 2100 for each climate scenario. For the discharge reservoirs minimal waves are assumed since there is no navigation and the area of the reservoirs are relatively small.

Storage capacity

The water from the Lek going through or over the Elshoutsluice ends up in the discharge reservoirs at first. The storage capacity of these discharge reservoirs are limited, so the water will discharge to the high storage basins of the Overwaard and Nederwaard. The high storage basin of the Overwaard will not be used as storage capacity from 2023. Therefore, the low storage basin is used for the storage capacity for the Overwaard (Waterschap Rivierenland, 2020).

The capacity of the Nederwaard according to Waterschap Rivierenland (2020) is:

- The acceptable water level increase is 0.50 m.
- The storage area is 632,000 m^2 (= 0.8 · 789,895 m^2 high basin area).
- The storage volume is 316,000 m^3.

The capacity of the Overwaard according to Waterschap Rivierenland (2020) is:

- The acceptable water level increase is 0.35 m.
- The storage area is 2,900,000 m^2 (= 0.8 · 3,622,838 m^2 low basin area).
- The storage volume is 1,015,000 m^3.

Critical discharge

The bed protection hinterlands is a concrete floor with a length of approximately 18 m (Waterschap Rivierenland, 2020). The discharge reservoir of the Nederwaard is surrounded by a vertical concrete wall. The discharge reservoir of the Overwaard is partly surrounded by a concrete wall and mainly by a grass covered levee, see Figure B.5.

Figure B.5: Picture of the discharge reservoirs Overwaard (left) and Nederwaard (right) from February 2020.

The discharge reservoirs will flood when they are completely full with water. The water discharge over the levee surrounding the discharge reservoir of the Overwaard is governing (Waterschap Rivierenland, 2020). The values for the critical discharge for grass covers is given in Table B.2. Waves in the discharge reservoir will be minimal and are categorised in 0 - 1 m. An open sod is assumed, which results in a mean critical discharge of 0.10 $m^3/s/m$' and a standard deviation of 0.12 $m^3/s/m$'.

Table B.2: The parameters μ and σ for the log-normal distribution of the critical overflow discharge for grass covers (Rijkswaterstaat, 2018a).

Wave height	**Closed sod**		**Open sod**	
	μ **[m^3/s/m']**	σ **[m^3/s/m']**	μ **[m^3/s/m']**	σ **[m^3/s/m']**
0 - 1 m	0.225	0.250	0.100	0.120
1 - 2 m	0.100	0.120	0.070	0.080
2 - 3 m	0.070	0.080	0.040	0.050

B.3. Meteorological conditions

The governing wind direction which influences the water levels is the direction W. For the waves, the governing wind direction is WNW. This is determined with the help of Riskeer.

B.4. Geo-technical conditions

The soil layers at the location of the Elshoutsluice consists predominantly of clay and peat. The sand layer starts at approximately NAP -14 m,(Waterschap Rivierenland, 2020).

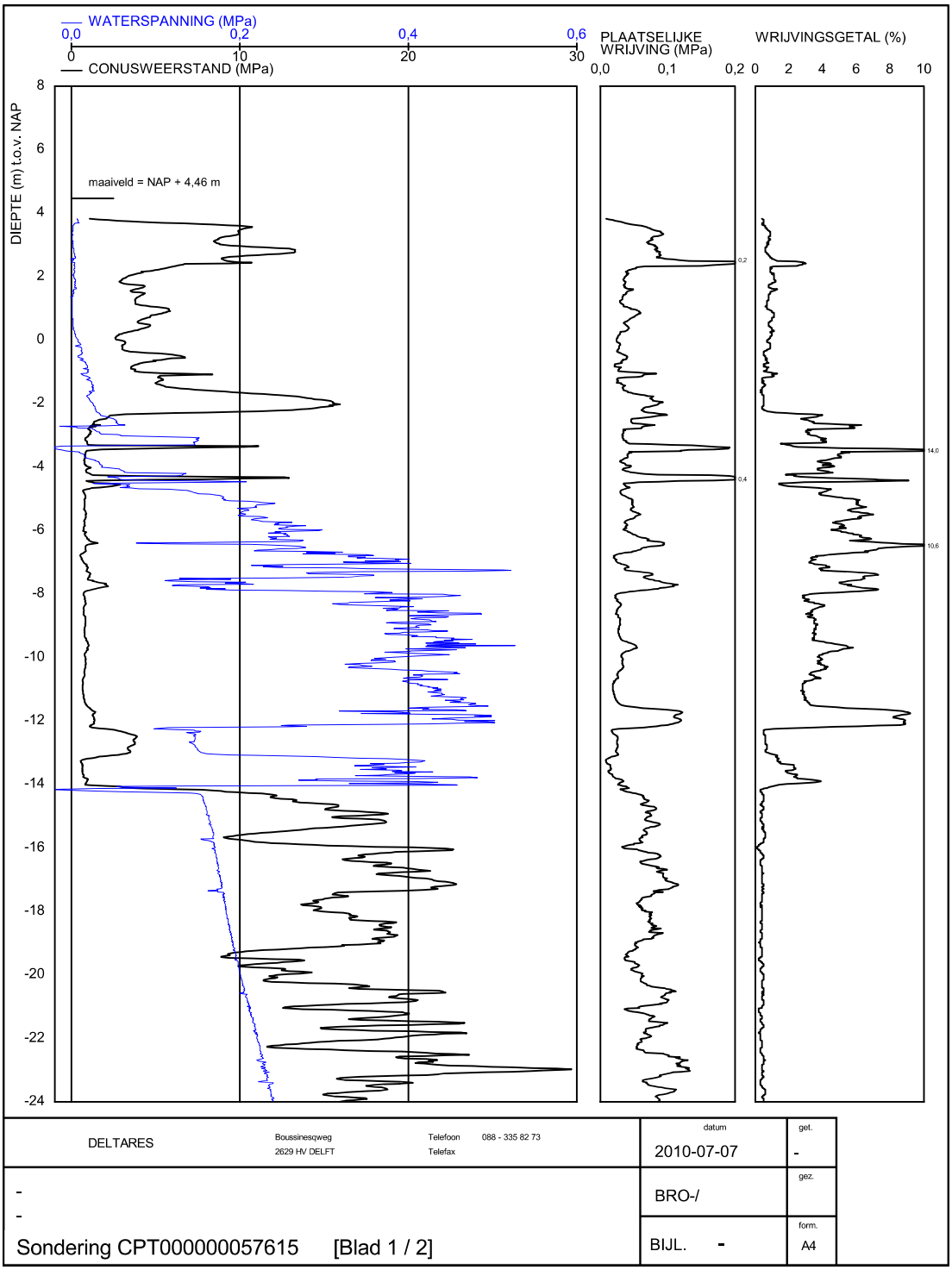

Figure B.6: Cone penetration test. Source: Waterschap Rivierenland (2020)

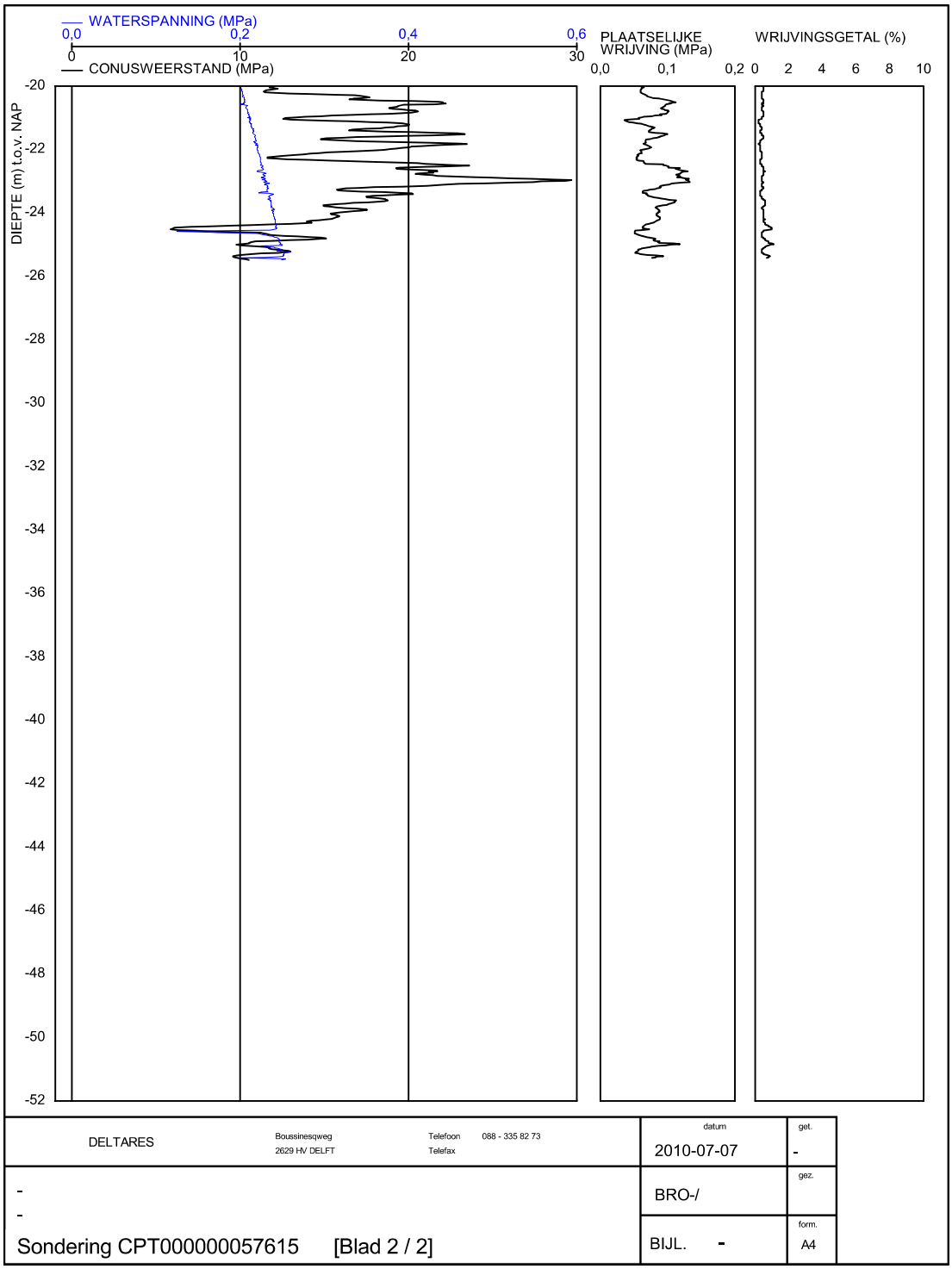

Figure B.7: Cone penetration test. Source: Waterschap Rivierenland (2020)

B.5. Elshoutsluice structure

For the Elshoutsluice, the design rapport is not available. There are drawings of the structure, but they do not include the reinforcement. Most information is derived from the flood risk safety assessment of the Elshoutsluice according to Waterschap Rivierenland (2020). The orientation of the normal axis of the discharge sluice relative to the north is 343°. The height of the structure is at NAP +5.75 m. The design water level is NAP +3.80 m for the lek river and NAP +0.90 m hinterlands.

The situation for the culverts in the Elshoutsluice is recently adjusted. New pumps are placed in culvert number 3. A sketch is made of the Elshoutsluice with the new pumps in culvert number three, see Figure B.9. The position of the distribution flap is moved to the position given in Figure B.9. This results in the situation of a water discharge from the Nederwaard through culvert 1 and a water discharge from the Overwaard through culverts 2, 3 and 4. An overview of this situation according to (Waterschap Rivierenland, 2020) is given in Figure B.8:

- Culvert number 1:
  - Discharge from the low storage basin Nederwaard.
  - Maximum water level for closing the radial gate is NAP +2.00 m.
  - No pumping system.
  - Maximum water level for closing lift gate is NAP +2.50 m.
- Culvert number 2:
  - Discharge from the low storage basin Overwaard.
  - Maximum water level for closing the radial gate is NAP +1.50 m.
  - No pumping system.
  - Maximum water level for closing lift gate is NAP +2.50 m.
- Culvert number 3:
  - Discharge from the low storage basin Overwaard.
  - Radial gate will be removed.
  - Three pumps with a recoil valve.
  - Maximum water level for closing the recoil valve is NAP +3.00 m. The pumping system will stop.
  - Maximum water level for closing lift gate is NAP +3.00 m.
- Culvert number 4:
  - Discharge from the low storage basin Overwaard.
  - Maximum water level for closing the radial gate is NAP +1.50 m.
  - Three pumps with a recoil valve.
  - Maximum water level for closing the recoil valve is NAP +3.00 m. The pumping system will stop.
  - Maximum water level for closing lift gate is NAP +3.00 m.

Besides the closing mechanisms listed above, Figure B.9 indicates one maintenance/emergency gate which can be placed in one of the four culverts via a gate frame. The locations of the bicycle path and the road on top of the Elshoutsluice are given in the sketch in grey. There is a technical area levelled between the bicycle path and culverts number 2 and 3. This area can be reached via a tunnel starting at the plateau hinterlands of the discharge sluice. The locations of the weed screens in front of the culverts are indicated as well in the sketch. Figure B.10 and Figure B.11 shows the sketches of the cross-sections of culvert number 2 and 3.

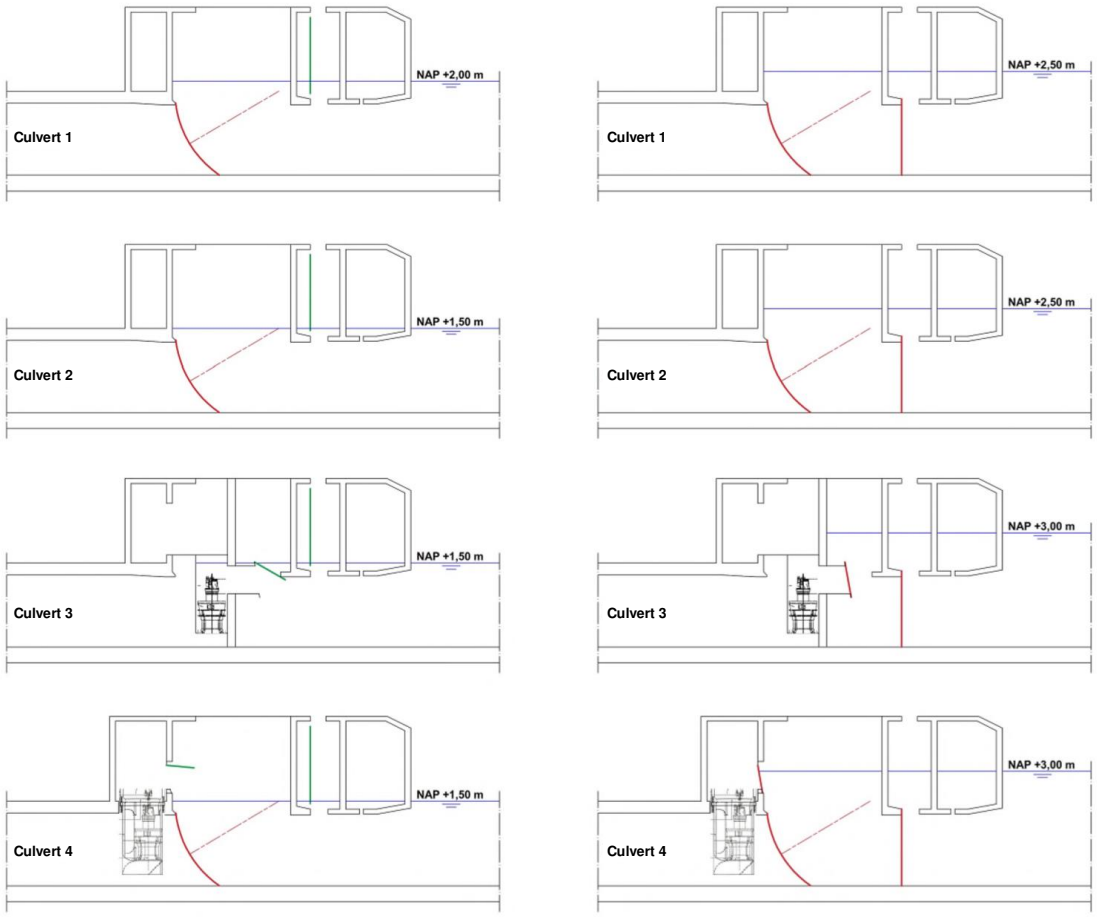

Figure B.8: Schematic overview of gate positions per culvert (Waterschap Rivierenland, 2020).

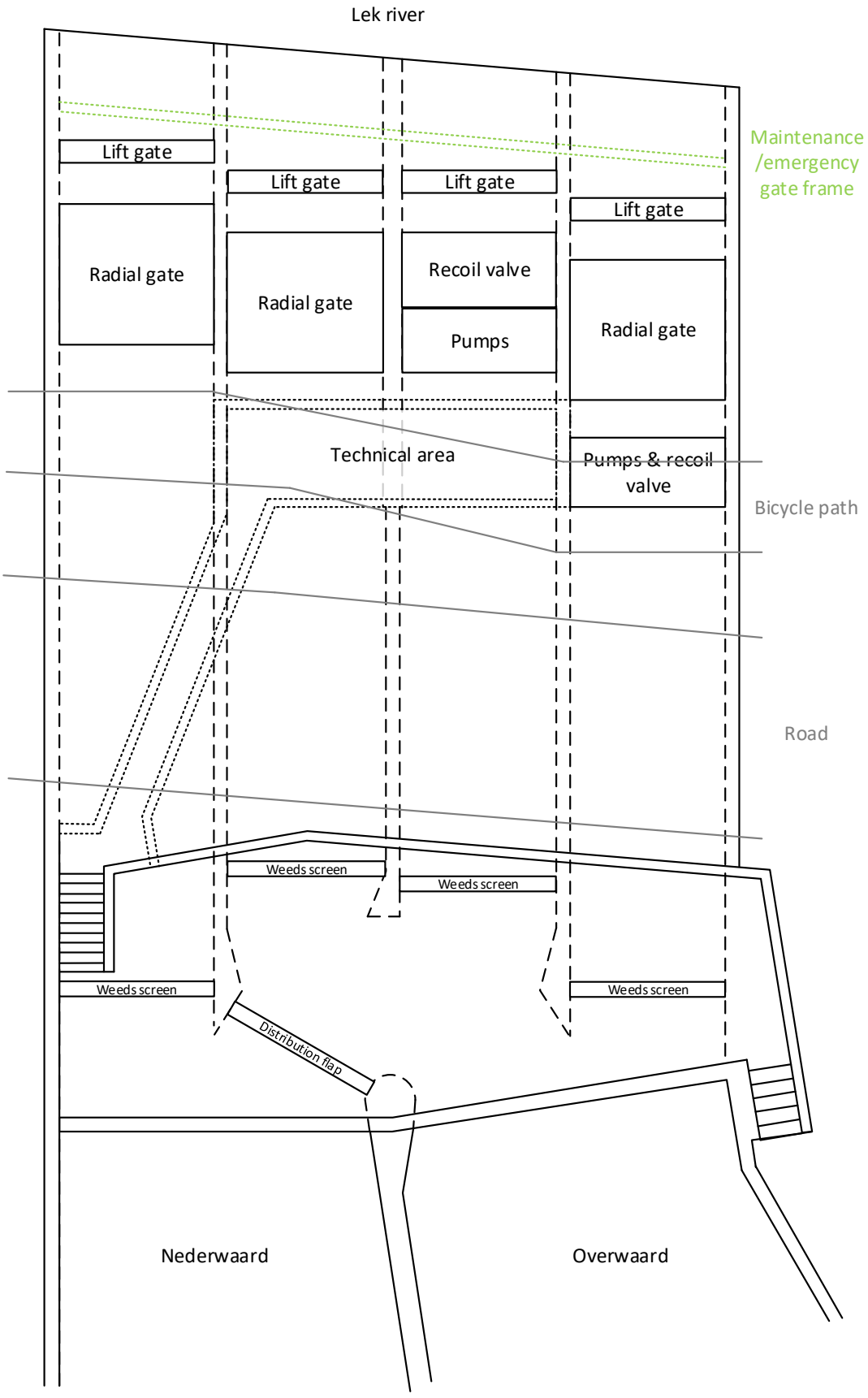

Figure B.9: Sketch of the layout of the Elshoutsluice including the bicycle path and motorised vehicle road.

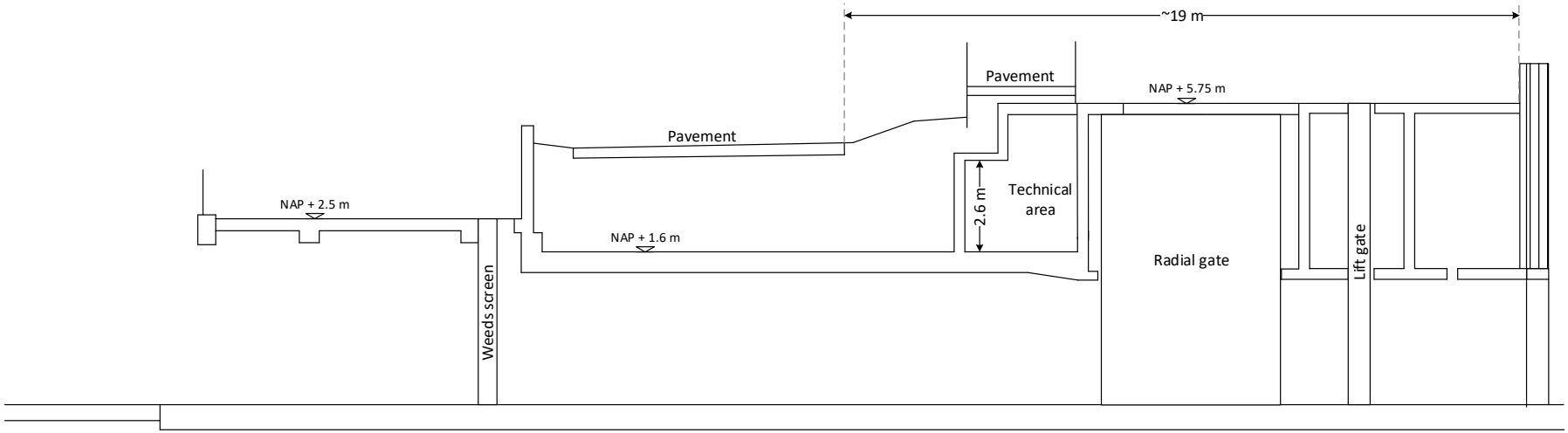

Figure B.10: Sketch of culvert number 2

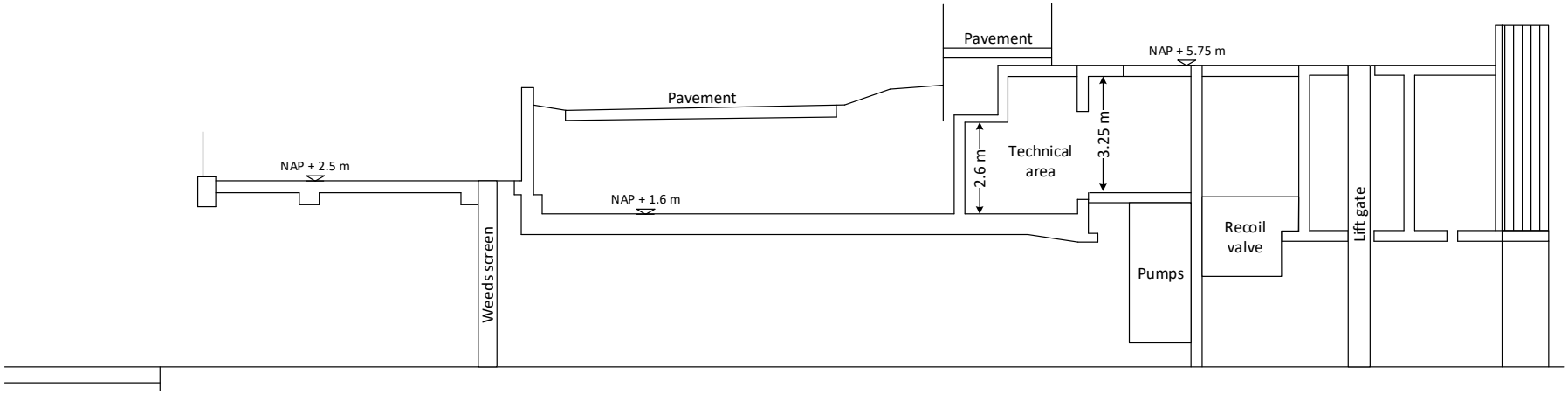

Figure B.11: Sketch of culvert number 3

The lower threshold standard of the Elshoutsluice is 1/10,000 per year which results in a consequence class 3 (CC3), see section A.3. The strength class of the used concrete is B 22.5 according to Haskoning B.V. (1984a). This results in a compression strength of f_{ck} = 18 MPa according to Table A.3. For the discharge sluice reinforcement steel of the class FeB 400 HW is used (Haskoning B.V., 1984a). This results in f_{yk} = 400 MPa and f_{yd} = 348 MPa according to Normcommissie (2018).

C

Determination (allowable) flood probability

This appendix describes the different failure modes specific for hydraulic structures. The standard failure tree is given for these specific failure modes. The calculation of the required failure probabilities for each failure mode are given in this appendix as well.

C.1. Failure modes

The considered failure modes for a hydraulic structure are (Rijkswaterstaat, 2017a):

- Failure due to overflow or over topping of Structure.
- Failure due to non-closure of gates.
- Failure due to piping.
- Failure due to strength and stability.

With the use of fault trees the required failure probabilities can be determined per failure mode. A fault tree consists of two type of gates: The AND gate which indicates a parallel system and the OR gate which describes a series system. The standard failure tree for a hydraulic structure as a part of a flood defence is given by Figure C.1. Table C.2 shows the standard values for the failure probability factor.

Table C.1: Values for the system failure probability with different dependencies where n is the number of components, source:(lecture by T. Schweckendiek)

System	**Gate**	**Components**		
		Mutually exclusive	**Independent**	**Fully dependent**
Series	OR	$\sum_{i=1}^{n} P_i$	$1 - \prod_{i=1}^{n} (1 - P_i)$	$max\{P_i\}$
Parallel	AND	0	$\prod_{i=1}^{n} P_i$	$min\{Pi\}$

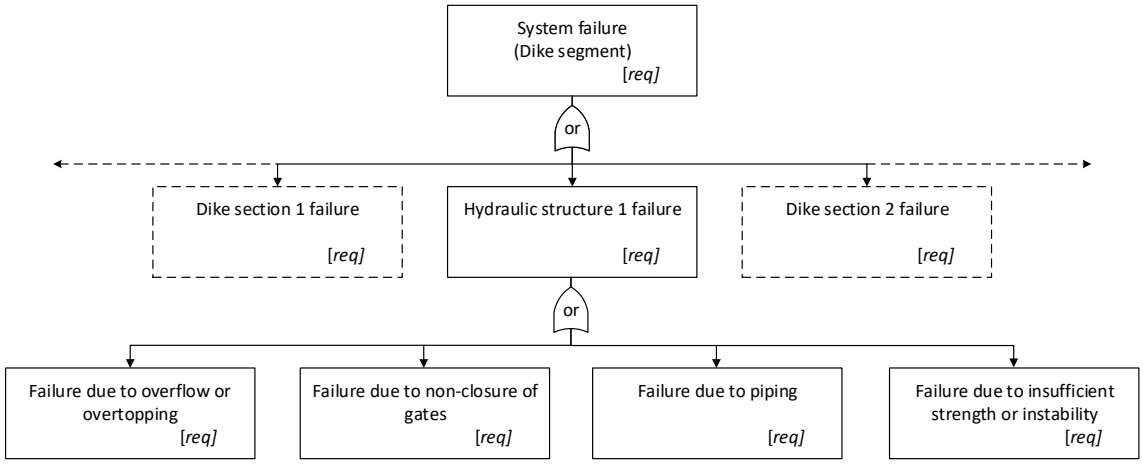

Figure C.1: Standard failure tree of the system failure according to Rijkswaterstaat (2017a).

Table C.2: The standard values for the failure probability factor ω (Rijkswaterstaat, 2017a)

Type of flood defence	**Failure mechanism**	**Segment type**	
		Sand coasts	**Other (levees)**
Levee	Overflow and overtopping	0	0.24
	Uplift and piping	0	0.24
	Macro instability inner slope	0	0.04
	Damage revetment and erosion	0	0.10
Engineering work	Non-closure	0	0.04
	Piping	0	0.02
	Structural failure	0	0.02
Dune	Dune erosion	0.70	0 / 0.10
Other		0.30	0.30 / 0.20
Total		**1**	**1**

Failure due to overflow or overtopping of structure

Failure due to overtopping or overflow of the structure depends on the height of the structure or adjacent levee, the storage capacity and erosion. Figure C.2 shows the standard fault tree for this failure mode.

The limit state function for failure of the bed protection is given by (Rijkswaterstaat, 2017a):

$$Z_{11} = Q_c - Q_{of/ot} \tag{C.1}$$

Where Q_c is the critical discharge determined by the critical discharge per unit width q_c and the width of the bed protection B_{sv}. In equation form (Rijkswaterstaat, 2017a):

$$Q_c = q_c \cdot B_{sv} \tag{C.2}$$

$Q_{of/ot}$ is the water discharge for overflow or overtopping determined by the discharge per unit width $q_{of/ot}$ and the width of the structure B. In equation form (Rijkswaterstaat, 2017a):

$$Q_{of/ot} = q_{of/ot} \cdot B \tag{C.3}$$

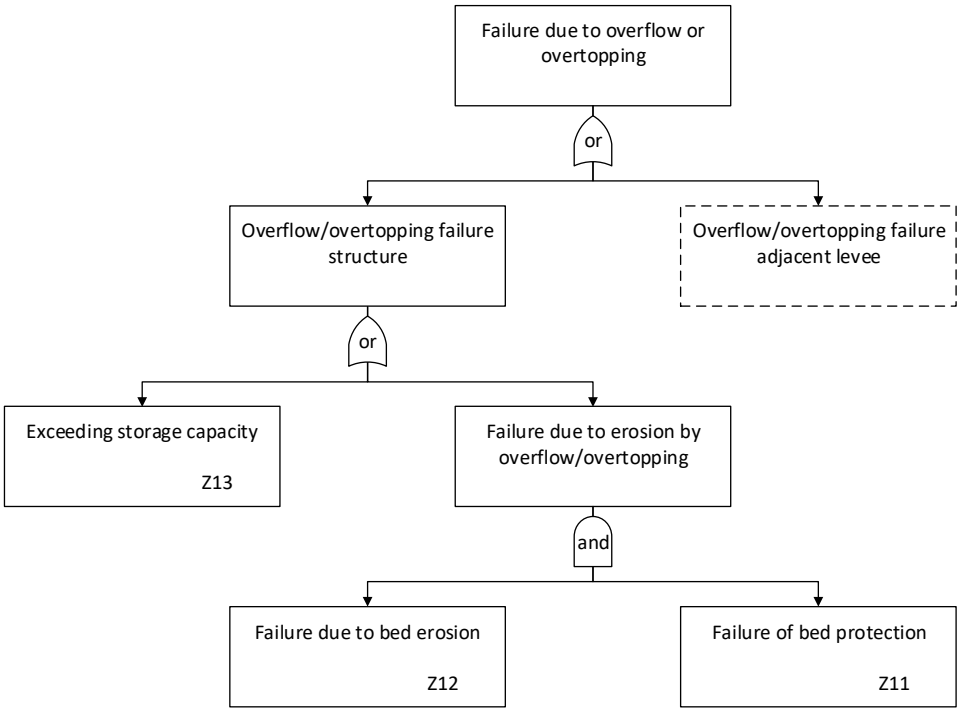

Figure C.2: Standard failure tree of overflow/overtopping according to Rijkswaterstaat (2017a)

The limit state function for failure due to bed erosion is (Rijkswaterstaat, 2017a):

$$Z_{12} = -\Phi^{-1}(P_{f,kw:erosion}) - u \tag{C.4}$$

The standard value for this parameter is 1.0 which is a conservative value indicating that there is no residual strength according to the WBI 2017.

The limit state function for exceeding the storage capacity in equation form is (Rijkswaterstaat, 2017a):

$$Z_{13} = V_c - V_{req;of/ol} \tag{C.5}$$

With:

$$V_c = m_{kom} \cdot A_{kom} \cdot \Delta h_{kom} \tag{C.6}$$

$$V_{req;of/ol} = m_{in} \cdot t_s \cdot q_{of/ot} \cdot B \tag{C.7}$$

Where:

m_{kom} = the model factor for storage capacity which has a standard mean value of 1 and a standard deviation of 0.20 [-] according to Rijkswaterstaat (2017a)
A_{kom} = the storage area in m^2.
h_{kom} = the maximum allowable water level increase in m.
m_{in} = the model factor for the inflow volume and has an expected value of 1 [-] according to Rijkswaterstaat (2017a).

The required failure probability for the failure mode overflow and overtopping is calculated with:

$$P_{max;htkw} = \frac{P_{max} \cdot \omega_{htkw}}{N_{htkw}} \tag{C.8}$$

With:

$P_{max;htkw}$ = The required failure probability per cross-section for the height of the structure [1/year]
P_{max} = The required failure probability for a dike segment (=1/10,000 for segment 16-2) [1/year]
ω_{htkw} = The failure probability factor for overflow and overtopping (=0.24 see Table C.2) [-]
N_{htkw} = Length-effect factor for the height of the structure (=2 for segment 16-2 according to Rijkswaterstaat (2017a)) [-]

This results in the required failure probabilities of:

$$P_{max;htkw} = \frac{1/10,000 \cdot 0.24}{2} = 1/83,333 \text{ per year} \tag{C.9}$$

$$P_{alert;htkw} = \frac{1/30,000 \cdot 0.24}{2} = 1/250,000 \text{ per year} \tag{C.10}$$

Failure due to non-closure of gates

The failure mode non-closure of gates depends on the storage capacity, erosion and gate failure.Figure C.3 shows the standard failure tree for this failure mode. The explanation of the limit state functions is given in Appendix J. Gate failure can occur due to (Rijkswaterstaat, 2017a):

- Gate structural failure
- Gate drive failure
- Gate operational system failure
- Human error
- Power shutdown
- Other

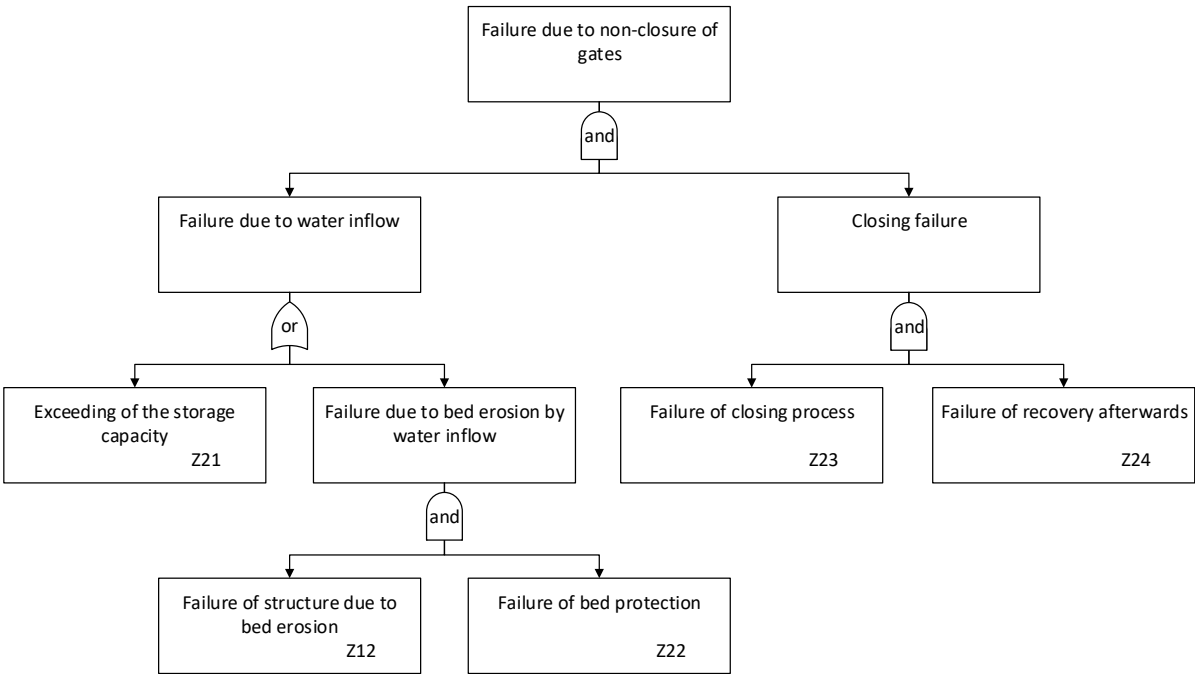

Figure C.3: Standard failure tree of non-closure according to Rijkswaterstaat (2017a)

The required failure probabilities are determined with:

$$P_{max;bskw} = \frac{P_{max} \cdot \omega_{bskw}}{N_{bskw}} \tag{C.11}$$

The length-effect factor for failure due to non-closure of gates per dike section is calculated with (Rijkswaterstaat, 2017a):

$$N_{bskw} = max(1; c \cdot n_{2a}) \tag{C.12}$$

With:

c = A reduction factor to indicate the differences of the failure probabilities per hydraulic structure (=0.5) [-].

n_{2a} = The number of hydraulic structures for which the failure probability is not negligible according to the simplified test (=2 according to Waterschap Rivierenland (2020)).

This results in a length-effect factor of:

$$N_{bskw} = max(1; 0.5 \cdot 2) = 1 \tag{C.13}$$

From Table C.2 is concluded that ω_{bskw} is 0.04. The required failure probability of the lower threshold and the alert value are:

The calculated required failure probabilities are:

$$P_{max;bskw} = \frac{1/10,000 \cdot 0.04}{1} = 1/250,000 \text{ per year} \tag{C.14}$$

$$P_{alert;bskw} = \frac{1/30,000 \cdot 0.04}{1} = 1/750,000 \text{ per year} \tag{C.15}$$

Failure due to piping

The failure mode due to piping has the standard failure tree given in Figure C.4. This failure mode depends on the water flow under the hydraulic structure.

The required failure probability is determined with:

$$P_{max;pkw} = \frac{P_{max} \cdot \omega_{pkw}}{N_{pkw}} \tag{C.16}$$

With a length effect factor of 1 and the failure probability factor from Table C.2, this results in:

$$P_{max;pkw} = \frac{1/10,000 \cdot 0.02}{1} = 1/500,000 \text{ per year} \tag{C.17}$$

$$P_{alert;pkw} = \frac{1/30,000 \cdot 0.02}{1} = 1/1,500,000 \text{ per year} \tag{C.18}$$

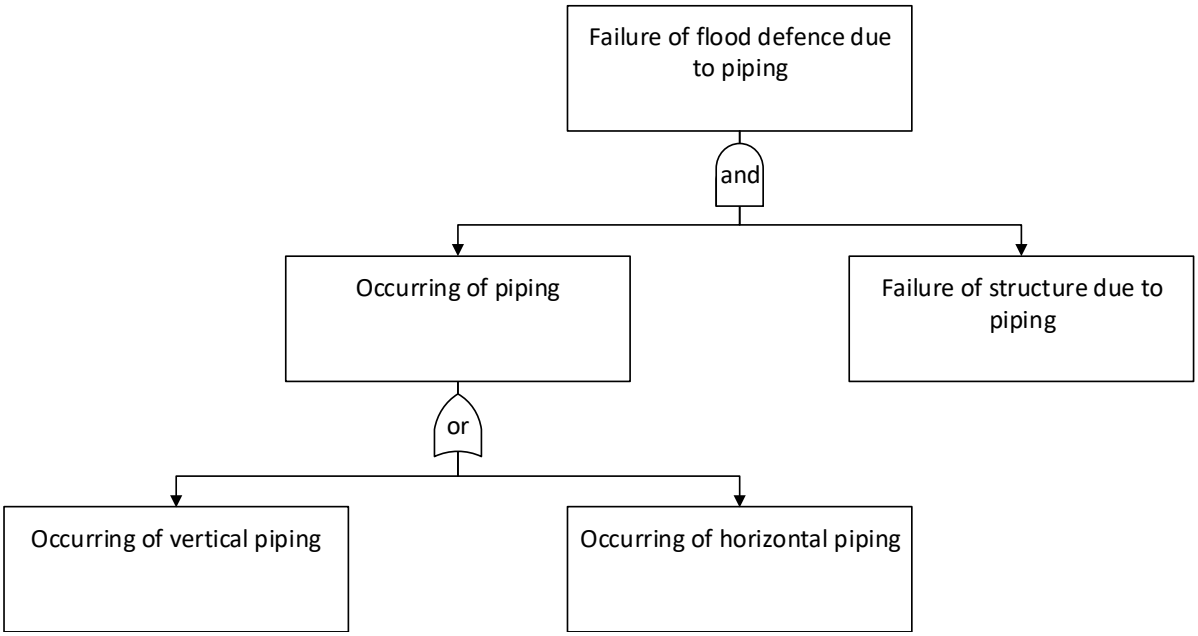

Figure C.4: Standard failure tree of piping according to Rijkswaterstaat (2017a)

Failure due to strength and stability

The standard failure tree of the failure mode strength and stability is given in Figure C.5.

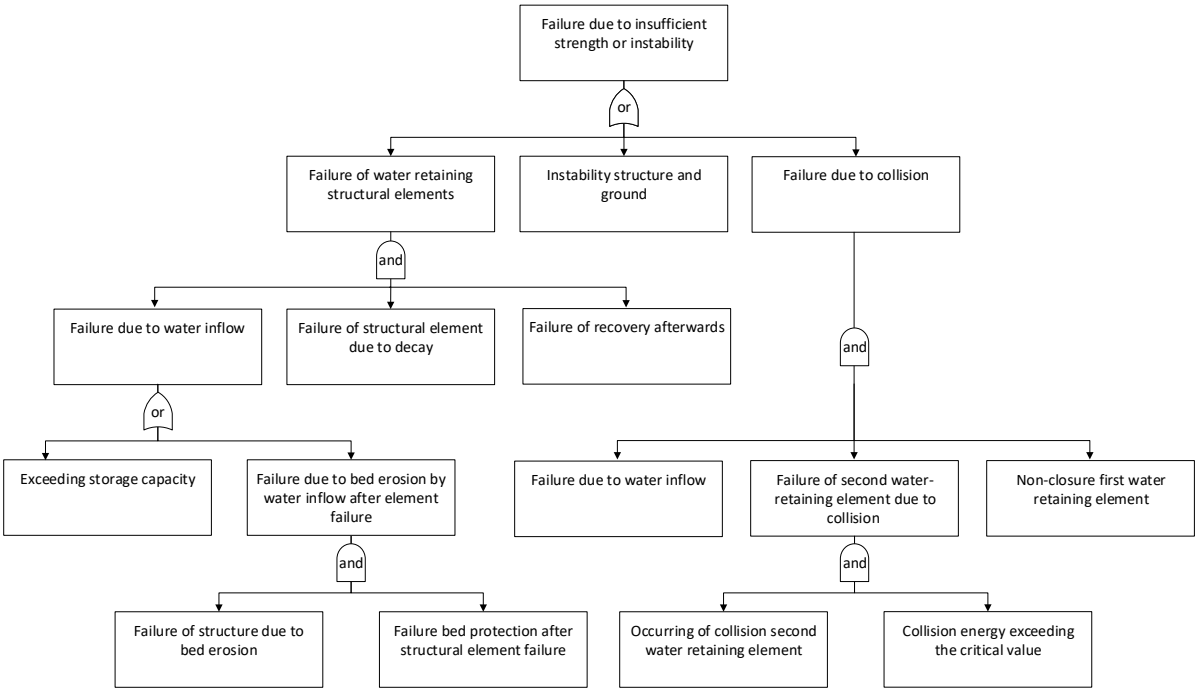

Figure C.5: Standard failure tree of strength and stability according to Rijkswaterstaat (2017a)

The required failure probability for the failure mode strength and stability is given by (Rijkswaterstaat, 2018b):

$$P_{max;stkw} = \frac{P_{req} \cdot \omega_{stkw} \cdot c}{N_{stkw}} \tag{C.19}$$

Correction factor c is taken into account for designing a hydraulic structure. This correction factor is not taken into account for the flood safety assessment according to the WBI 2017.

The parameters for the Elshoutsluice are:

$P_{max;stkw}$= Required failure probability for structural failure of an individual hydraulic structure with a reference period of t_{ref} = 1 year [-].
ω_{stkw} = The failure probability factor for structural failure (= 0.02) [-], see Table C.2.
c = Correction factor for the correlation between structural failure and failure due to overtopping/overflow (=3 according to Rijkswaterstaat (2018b)) [-].
N_{stkw} = Length-effect factor for structural failure (= 3 according to Rijkswaterstaat (2017a)) [-].

This results in the required failure probabilities of:

$$P_{max;stkw} = \frac{1/10,000 \cdot 0.02 \cdot 3}{3} = 1/500,000 \text{ per year} \tag{C.20}$$

$$P_{alert;stkw} = \frac{1/30,000 \cdot 0.02 \cdot 3}{3} = 1/1,500,000 \text{ per year} \tag{C.21}$$

Table C.3: The correction factor c for the correlation between failure due to overtopping/overflow and structural failure Rijkswaterstaat (2018b).

P_{max} **[1/year]**	1/100	1/300	1/1,000	1/3,000	1/10,000	1/30,000
c **[-]**	7	5	4	3	3	3

C.2. Conclusion

All the required failure probabilities for each failure mechanism are summarised in Table C.4. The current and new design of the Elshoutsluice need to fulfil these requirements for the flood risk.

Table C.4: The required failure probabilities for the failure modes for the Elshoutsluice.

Failure mechanism	**Alert value [1/year]**	**Lower threshold [1/year]**
Overflow/overtopping	1/250,000	1/83,333
Non-closure gates	1/750,000	1/250,000
Piping	1/1,500,000	1/500,000
Strength/stability	1/1,500,000	1/500,000

D

Drawings of concepts

This appendix includes all the drawings for the top and side view of the concepts for Chapter 5.

D.1. Top view of concepts

This section shows the top view drawings for the concepts 1, 2, 3 and 4 given in subsection 5.2.1. For each concept an indication is given which gates will need replacement. Changes for the technical are and a possible multi-functional area is included in the drawings as well.

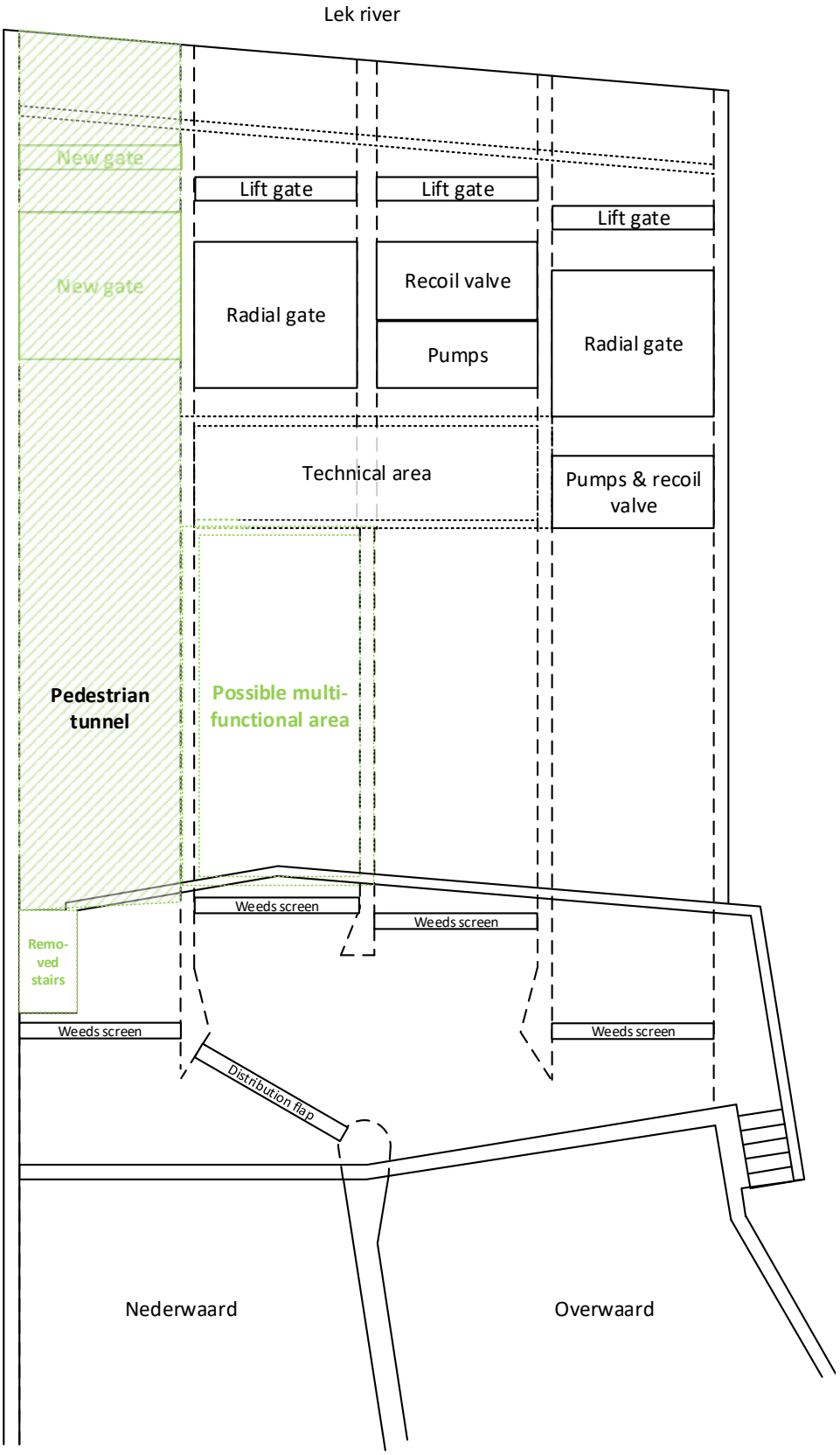

Figure D.1: Sketch of the top view of concept number 1

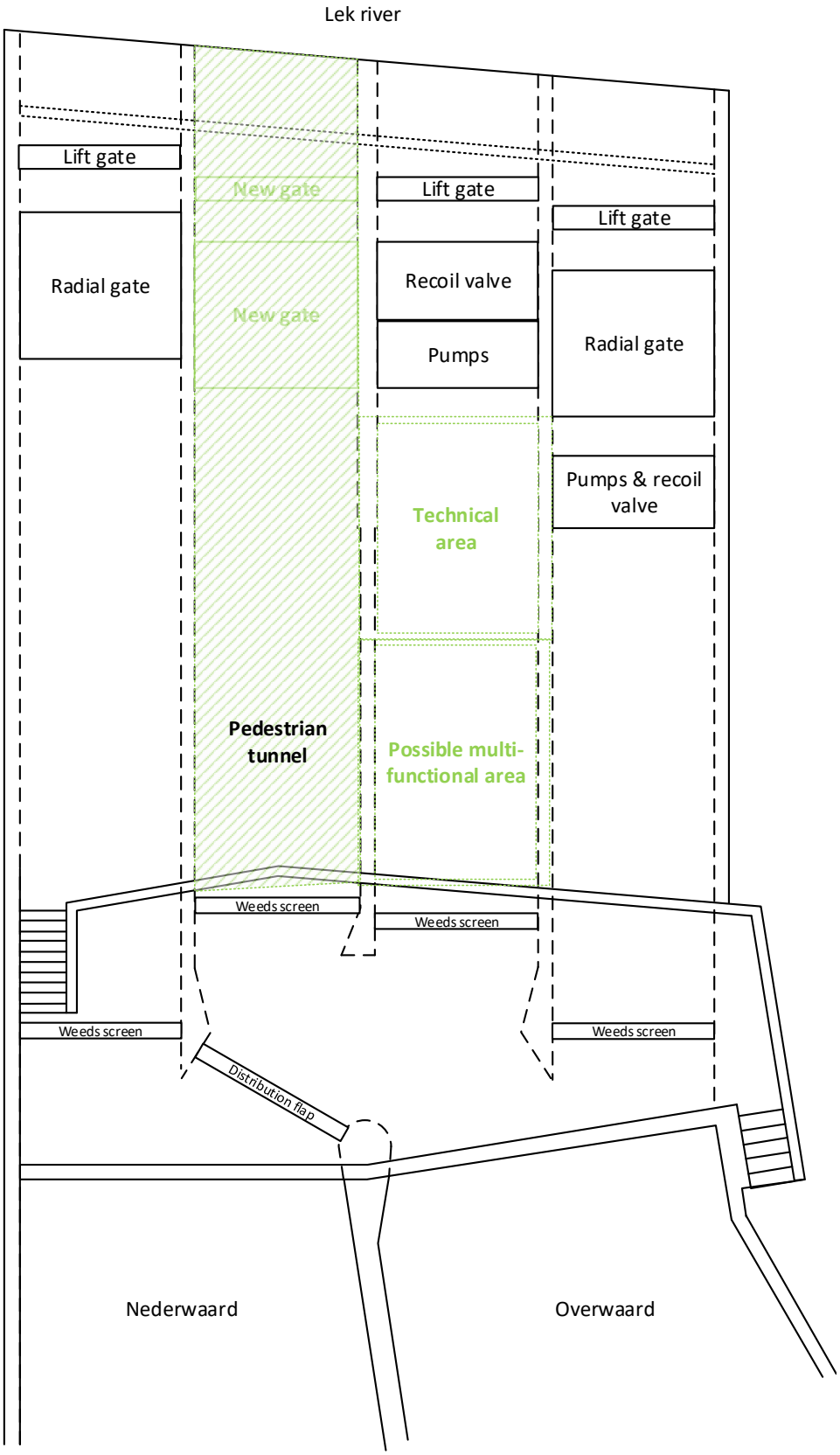

Figure D.2: Sketch of the top view of concept number 2

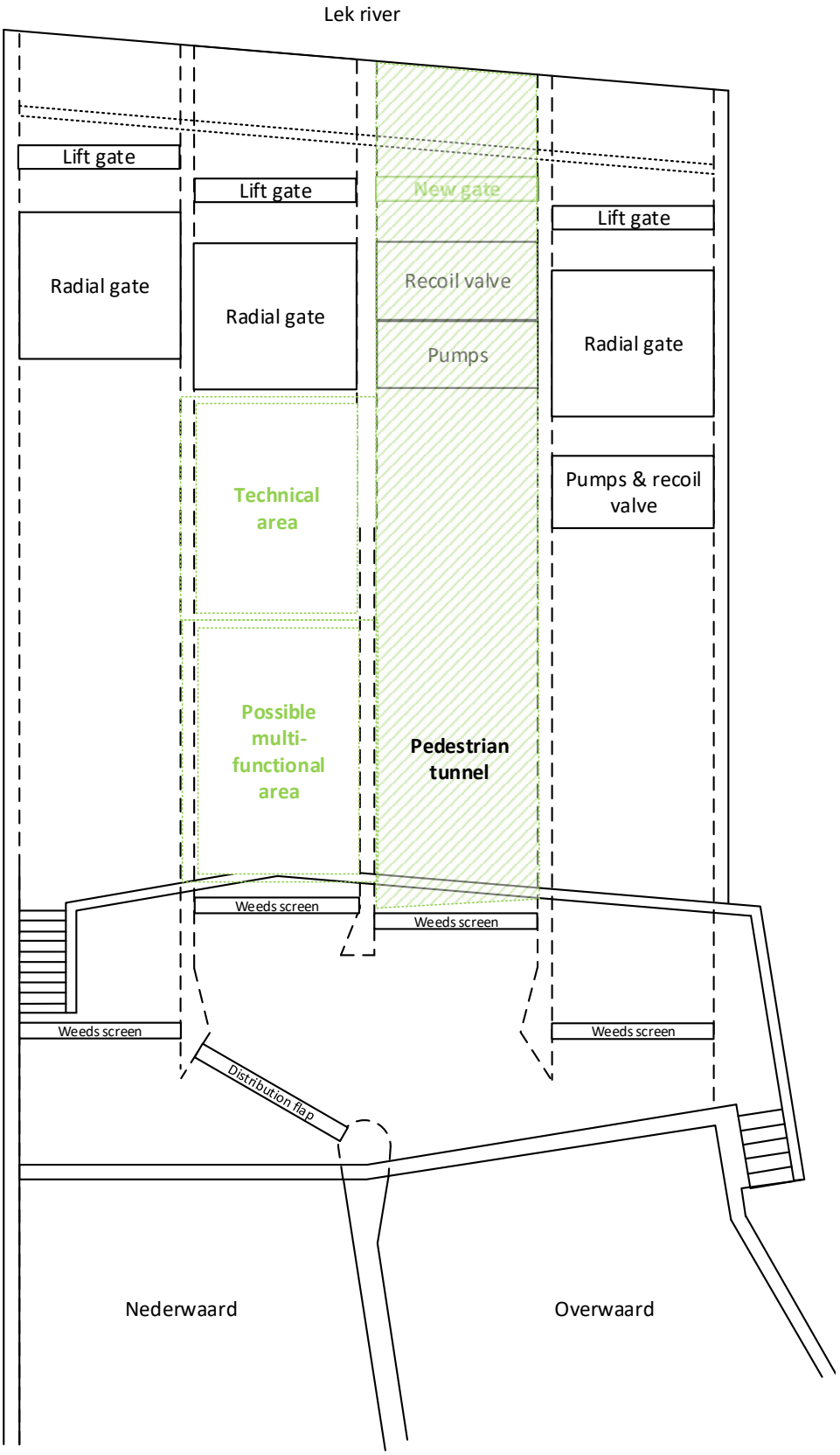

Figure D.3: Sketch of the top view of concept number 3

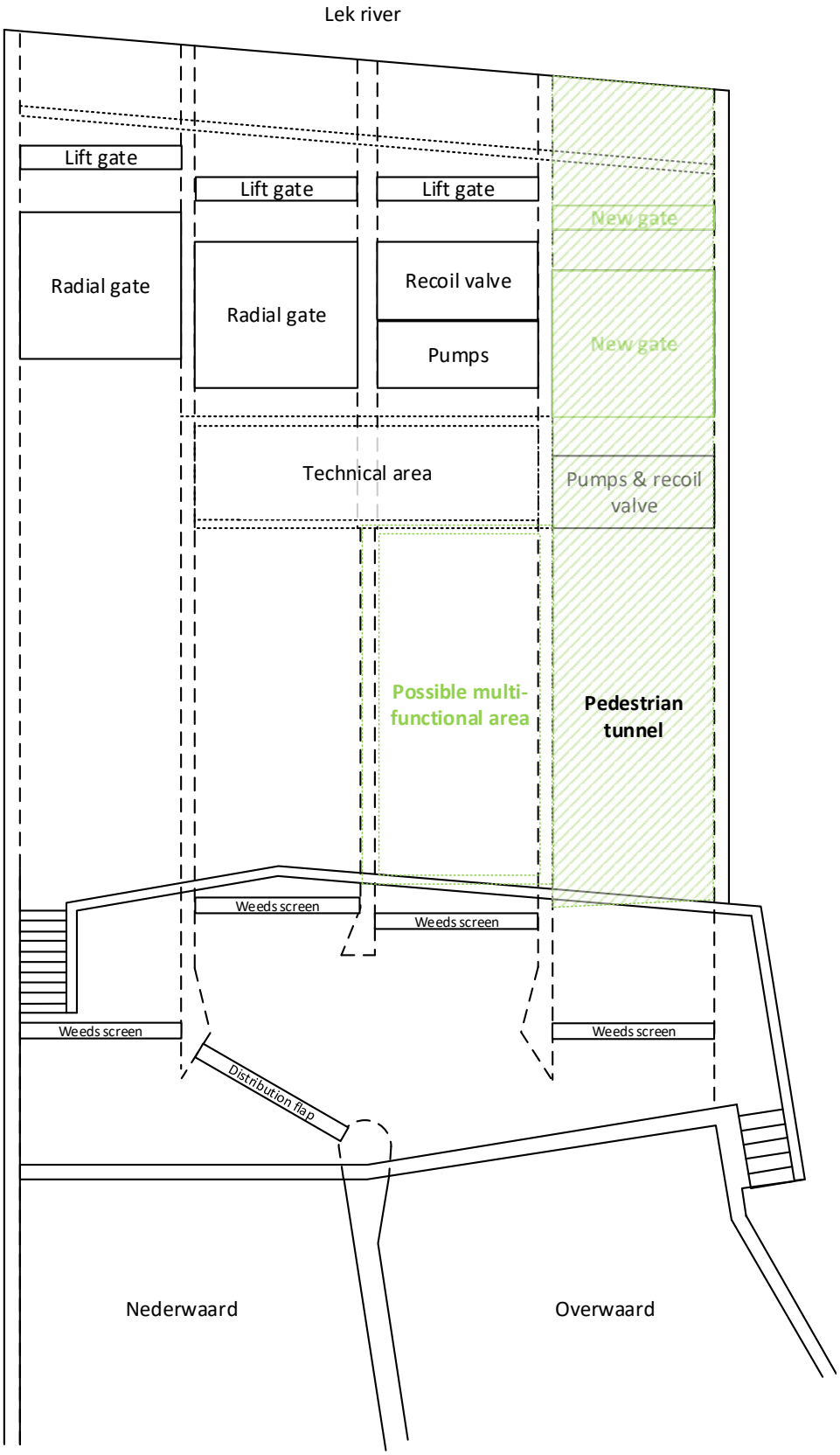

Figure D.4: Sketch of the top view of concept number 4

D.2. Side view of concepts

This section consist of drawings of culvert number 2 and 3 for different concepts

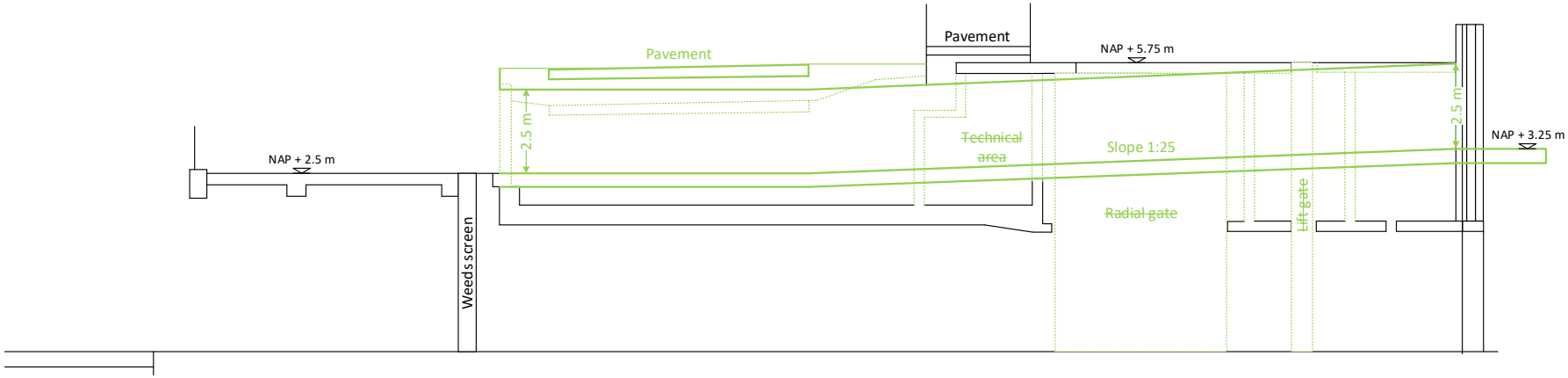

Figure D.5: Sketch of the side view of culvert 2 with a sloped pedestrian tunnel for the option with a higher floor. The river side is at the right side of figure.

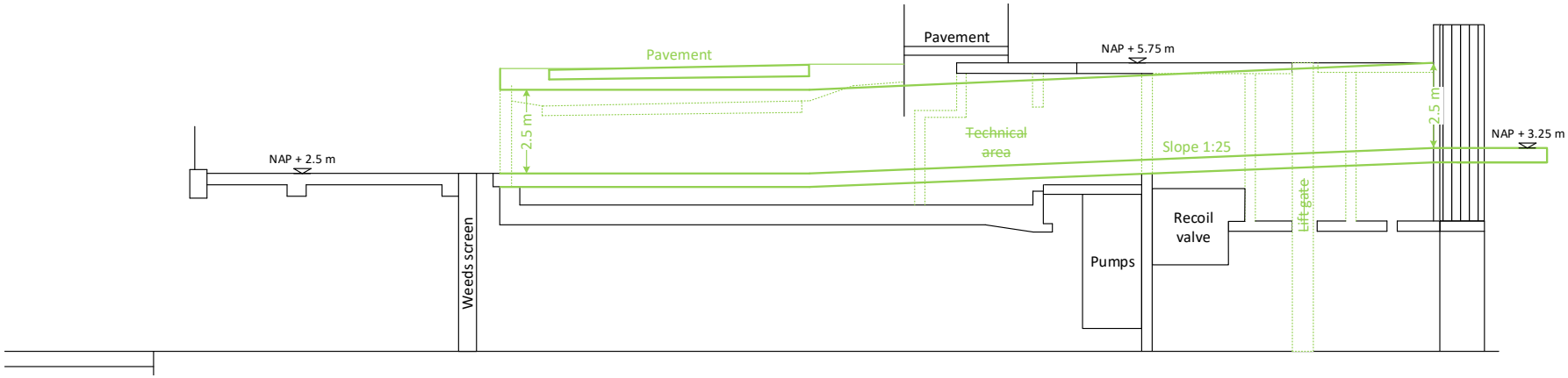

Figure D.6: Sketch of the side view of culvert 3 with a sloped pedestrian tunnel for the option with a higher floor.The river side is at the right side of figure.

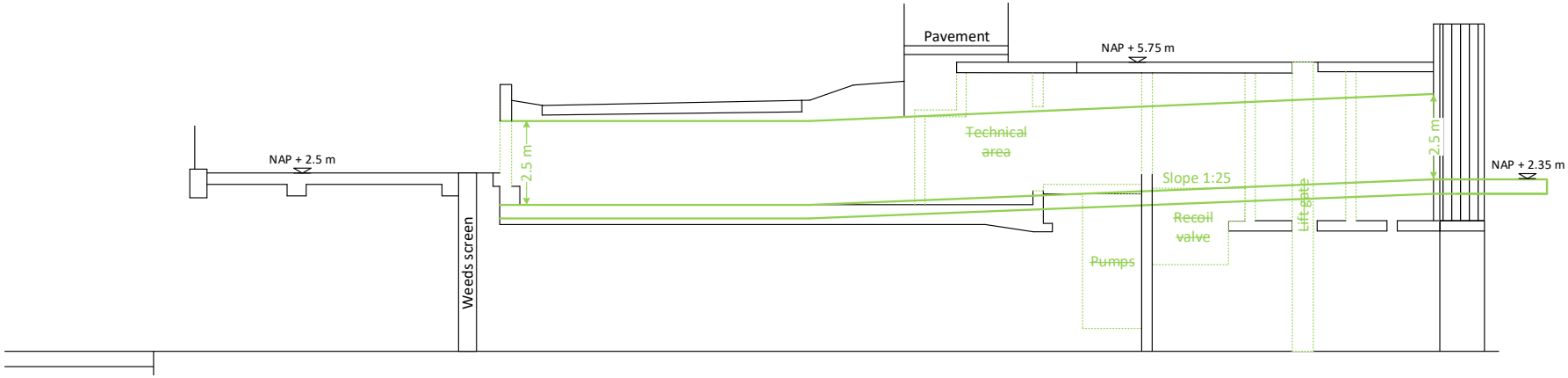

Figure D.7: Sketch of the side view of culvert 3 with a sloped pedestrian tunnel for the option with a lower floor. The river side is at the right side of figure.

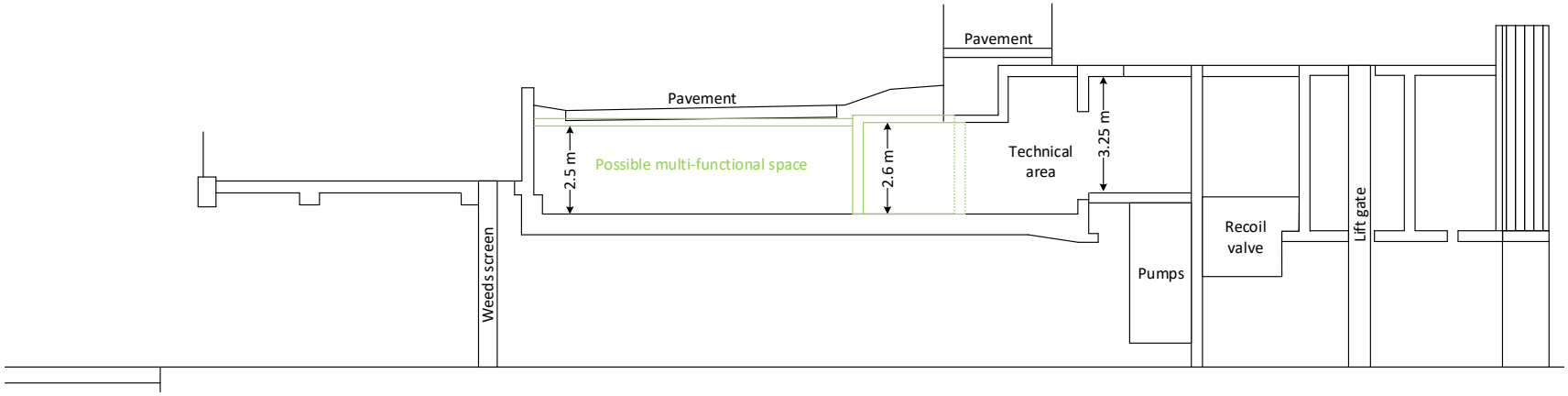

Figure D.8: Sketch of the side view of culvert 3 for the expansion of the technical area and a possible multi-functional area. The river side is at the right side of figure.

E

Number of visitors

This appendix gives an estimation of the expected number of visitors which will use the new pedestrian tunnel. An analysis is made for a pedestrian tunnel with a width of 5.5 m based on these expectations.

E.1. Expected number of visitors

The world heritage site Kinderdijk receives many tourists which is expected to increase each year. The busiest period of visitors in Kinderdijk is in April up to and including June. The least amount of tourist are from January until April. Visitors stay approximately two hours at the world heritage site (Land-ID & Cultuurhistory Projecten, 2016).

The amount of paying visitors of the world heritage site Kinderdijk is 308,000 according to Defacto Stedenbouw (2019). Only the paying visitors are counted, but it is possible to enter the site without paying. Based on samples, it is estimated that the amount of paying visitors is approximately 50% which gives a total amount of 600,000 visitors. The province South-Holland expects an increase in tourism of 4% per year. The growth in tourism of Kinderdijk was 7% in 2018. It is expected that the amount of paying visitors will increase to 60% in 2022 and 80% in 2030 due to improvements for the entrance of the world heritage site. Based on this the predicted number of visitors for 2022 is given in Table E.1.

Table E.1: The number paying and non-paying visitors in Kinderdijk and the expected visitors based on an increase of 4% - 7% per year (Defacto Stedenbouw, 2019).

Number of visitors in 2018	**600,000**
Paying (50%)	300,000
Non-paying	300,000

Expected visitors 2022	**700,000 - 800,000**
Paying (60%)	420,000 - 480,000
Non-paying	280,000 - 320,000

Defacto Stedenbouw (2019) made an estimation of the number of visitors based on three different possible scenarios for 2030:

- The zero variant: a stabilisation of the amount of visitors from 2022.
- The moderate variant: a growth of number of visitors 4% per year based on the province tourism prosperity.
- The stimulated variant: an increase of visitors by 7% per year based on the current growth in Kinderdijk.

The estimated number of visitors based on all the scenarios for 2022 up to 2030 are given in Table E.2.

Table E.2: The expected number of visitors in 2030 based on different growth scenarios (Defacto Stedenbouw, 2019).

Expectations of 2022 - 2030	**0%**	**4%**	**7%**
Number of visitors 2030	**700,000 - 800,000**	**960,000 - 1,100,000**	**1,200,000 - 1,375,000**
Paying (80%)	560,000 - 640,000	770,000 - 880,000	960,000 - 1,100,000
Non-paying (20%)	140,000 - 160,000	190,000 - 220,000	240,000 - 275,000

Defacto Stedenbouw (2019) did an investigation of the visitors of Kinderdijk with a sampling of two days in July, which is just after the peak season. One of the two days was at a Thursday, the other day was on a Sunday. The average amount of visitors per day is 3,746, based on these two days. Figure E.1a shows the distribution of how these visitors arrived at Kinderdijk. The highest number of visitors was 4,307 on the Sunday. The busiest hour had a visitors peak of 749 people arriving at the world heritage site, see Figure E.1b. The largest amount of visitors arriving at once is due to the river cruise with an average of 166 people on board.

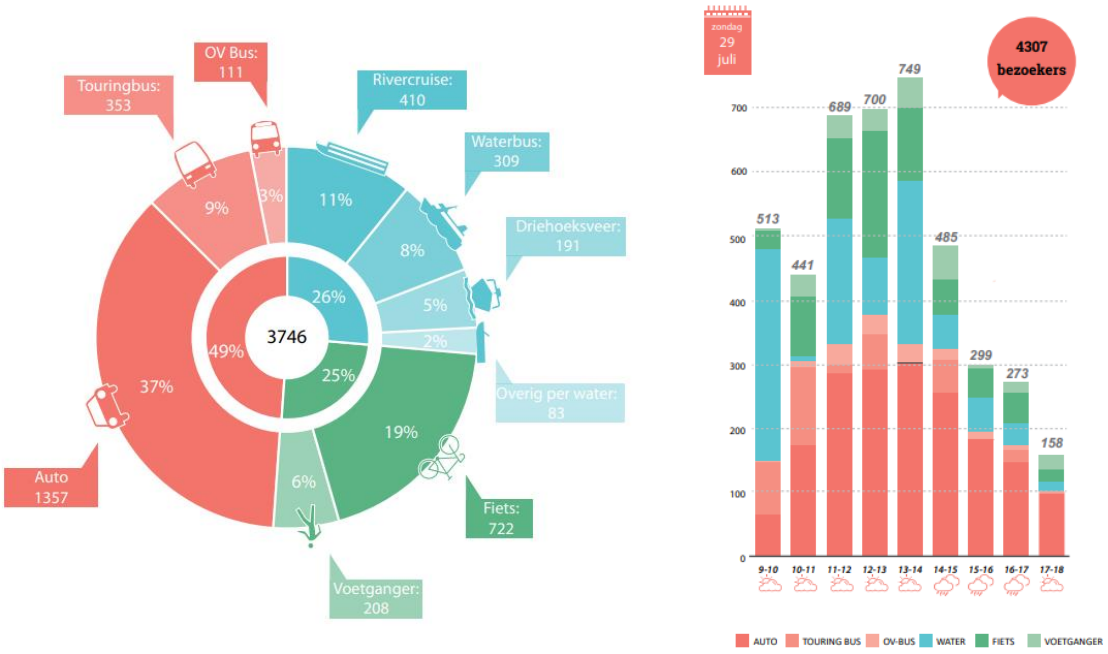

(a) The average amount of visitors per day, based on two days in July, and how they arrived.

(b) Visitors per hour on the 29th of July.

Figure E.1: Visitors information of the world heritage site Kinderdijk obtained by Defacto Stedenbouw (2019).

Based on the peak information of Figure E.1b an estimation is made for the average amount of visitors that will have to go through the pedestrian tunnel. With 749 people entering the world heritage site in one hour, the average rate is around 13 visitors per minute. People who arrived approximately two hours earlier at Kinderdijk will leave through the same pedestrian tunnel. From Figure E.1b can be concluded that 689 visitors entered two hours before the peak hour. This results in an average outflow of 12 persons per minute during the peak hour.

Table E.3: The expected peak inflow and outflow in the pedestrian based on a 4% and 7% visitors increase per year for 2022 and 2030.

	Peak flow 2022		**Peak flow 2030**	
	4%	**7%**	**4%**	**7%**
Entering	15 visitors/min	17 visitors/min	20 visitors/min	29 visitors/min
Leaving	14 visitors/min	16 visitors/min	19 visitors/min	26 visitors/min

E.2. Pedestrian capacity

The dimension of the new pedestrian tunnel depends on the expected amount of visitors which will go through it. A pedestrian walkway can be classified in a level of service (LOS) according to TRB (2000). Figure E.2 shows these different levels:

- LOS A: pedestrians can move without conflicts between other pedestrians and without altering their movements due to other pedestrians. The walking speed can be freely selected.
- LOS B: pedestrians begin to respond to other pedestrians by selecting a walking path. The walking speed can be chosen freely. There is sufficient area to bypass other pedestrians.
- LOS C: pedestrians still have sufficient space for bypassing in unidirectional streams for normal walking speeds. A stream in reverse direction can cause minor conflicts.
- LOS D: pedestrians are restricted to choose an individual walking speed or to bypass other pedestrians. A reverse flow has a high probability to cause conflicts.
- LOS E: pedestrians have insufficient space for passing slower pedestrians. All pedestrians restrict their walking speed. A reverse flow is only possible with extreme difficulties.
- LOS F: pedestrians are forced to shuffling. There is unavoidable contact with other pedestrians. A reverse flow is impossible.

The categories A and B are considered as comfortable. These are the levels of service the pedestrian tunnel has to fulfil.

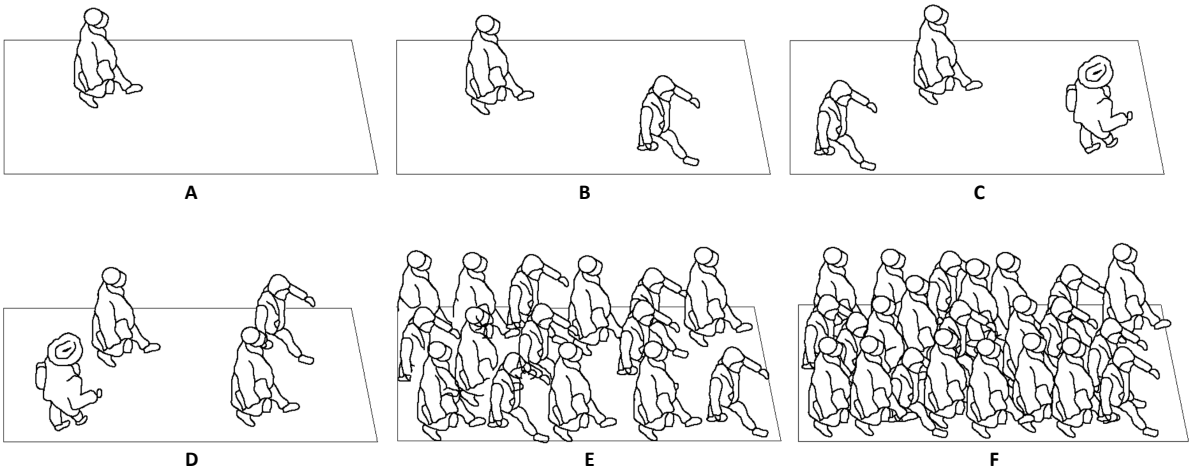

Figure E.2: The different levels of service for pedestrian walkways (TRB, 2000)

Pedestrians don't use the whole available width of a walkway. It is not possible to walk all the way up to the wall of the tunnel. People leave space if there is an oncoming pedestrian. These spaces are

Table E.4: Average flow level of service criteria for walkways and sidewalks according to TRB (2000).

Level of service	Space [m^2/p]	Flow rate [p/min/m]	Speed [m/s]
A	> 5.6	≤ 16	> 1.30
B	> 3.7 - 5.6	> 16 - 23	> 1.27 - 1.30
C	> 2.2 - 3.7	> 23 - 33	> 1.22 - 1.27
D	> 1.4 - 2.2	> 33 - 49	> 1.14 - 1.22
E	> 0.75 - 1.4	> 49 - 75	> 0.75 - 1.14
F	≤ 0.75	variable	≤ 0.75

named the shy distances. The effective width is determined with (TRB, 2000):

$$W_E = W_T - W_O \tag{E.1}$$

W_E = the effective walkway width [m].
W_T = the total walkway width [m]
W_O = the sum of shy distances and the widths from obstructions on the walkway [m]

The smallest pedestrian tunnel width considered is a width of 5.5 m. The shy width consist of 0.5 m for each wall in the pedestrian tunnel and 0.5 m for the space between the two opposite pedestrian flows (TRB, 2000). The effective width for this pedestrian tunnel is:

$$W_E = 5.5 - 3 \cdot 0.5 = 4.0m \tag{E.2}$$

It is assumed that the number of visitors are equally distributed over one hour for the peak flow. This assumption is not entirely true in reality. Visitors can arrive in big groups all together due to the river cruise, water bus and touring cars. An assumption is made to multiply the average peak flow per minute by a factor 1.5 to include the effect of visitors entering in big groups. The average number of visitors is the summation of the in- and outflow of people. The level of service is determined for the situation in 2018 and the expected amount of visitors in 2030 with a growth rate of 4% and 7%. Table E.5 shows that for all the cases the level of service is A or B. A tunnel of 5.5 m has a sufficient width for the pedestrians.

Table E.5: The determination of the level of service for a pedestrian tunnel of 5.5 m wide.

Year	Average number of people	Estimated peak	People over W_E	LOS
2018	25 p/min	38 p/min	10 p/min/m	A
2030 with 4% increase	39 p/min	59 p/min	15 p/min/m	A
2030 with 7% increase	55 p/min	83 p/min	21 p/min/m	B

In the future the number of visitors can still increase. The pedestrian tunnel could be categorised in a lower level of service. This problem can be decreased by introducing different time spans in which a certain amount of people can arrive at Kinderdijk.

F

Slope of the pedestrian tunnel

In this appendix different concepts of the slope layout for the pedestrian tunnel are discussed. First, the requirements are given for slopes for wheelchair users. A selection is made of the slope options to use as concepts for subsection 5.2.2.

F.1. Requirements wheelchair users

A slope is needed for wheelchair users to travel over an height difference. The effort needed to ascend a slope depends on the steepness of a slope in relation to the length. This effort is limited by making a less steep slope when there is a higher height difference, see Table F.1. Horizontal resting platforms are needed in case of a longer slope which is shown in Figure F.1. The minimum required length of such a platform (a2 in Figure F.1) is 1.5 meter.

Table F.1: Slope requirements for accessibility of wheelchair users (CROW, 2014).

Height difference (h in Figure F.1)	Maximum slope
0.00 - 0.10 m	1:10
0.10 - 0.25 m	1:12
0.25 - 0.50 m	1:16
0.50 - 1.00 m	1:20
All	1:25

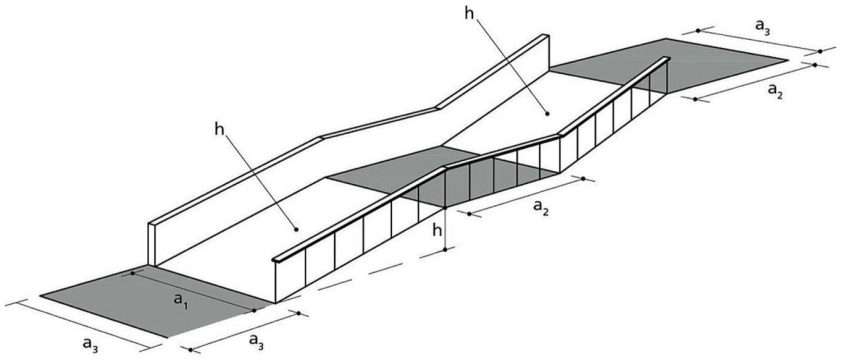

Figure F.1: Slope requirements for wheelchair users (CROW, 2014).

F.2. Concepts

The available length for the slope inside the Elshoutsluice is approximately 19 meter, see Figure B.10. This is due to the choice to maintain the same passage height underneath the road on top of the discharge sluice. The slope can start where the road ends. The horizontal part of the tunnel differ from NAP + 1.6 m to NAP + 2.5 m. Different options for the slope of the pedestrian tunnel are considered based on the different slopes given in Table F.1:

- Option 1: a slope of 1:25.
- Option 2: a slope of 1:20.
- Option 3: a slope of 1:16.
- Option 4: a slope of 1:12.
- Option 5: a slope of 1:10.

The horizontal platforms are set to a fixed length of 1.5 meter to obtain the highest possible height difference. Figure F.2 shows the height difference possible over a length of 19 meters with a maximum height difference of 1 meter.

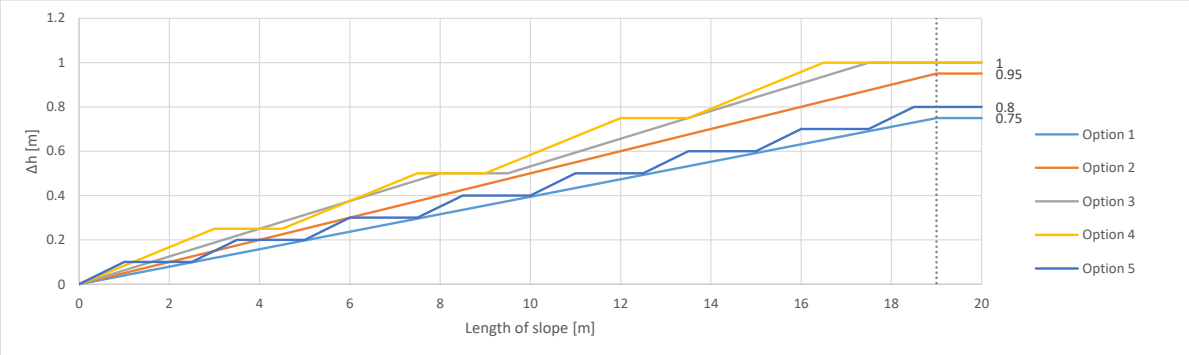

Figure F.2: All the different slope configurations over a length of 19 meter

Option 1

A slope of 1:25 or less steep is considered as a really small slope and does not have a maximum height requirement. For option 1, the height difference over 19 meters is 0.75 meter which gives a slightly less steeper slope than 1:25. No horizontal platforms are needed in this case. The floor layout of the pedestrian tunnel for the upper and lower option are given in Figure F.3. This results in a floor level of NAP + 2.35 m and NAP + 3.25 m at the Lek river.

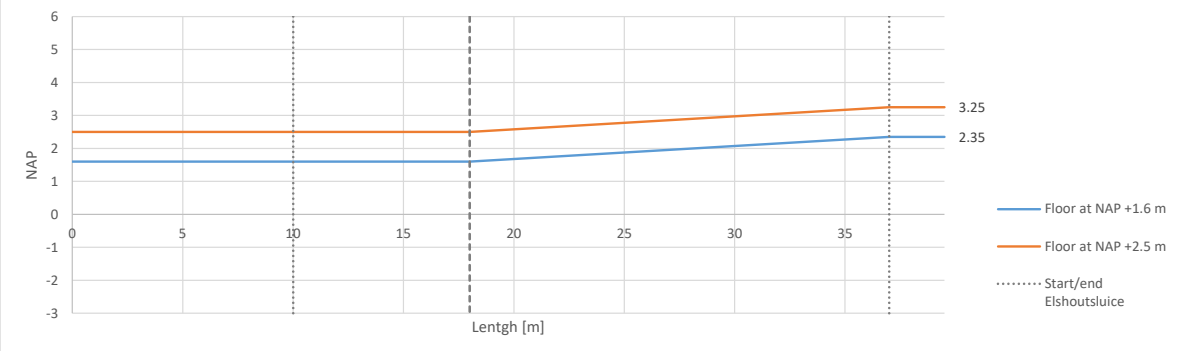

Figure F.3: Option 1: a slope of approximately 1:25 for different floor levels

Option 2

No horizontal platform is needed for a slope of 1:20 since the total available length is 19 meters. This results in a minimum floor level of NAP + 2.55 m and a maximum floor level of NAP + 3.45 m at the river side, see Figure F.4.

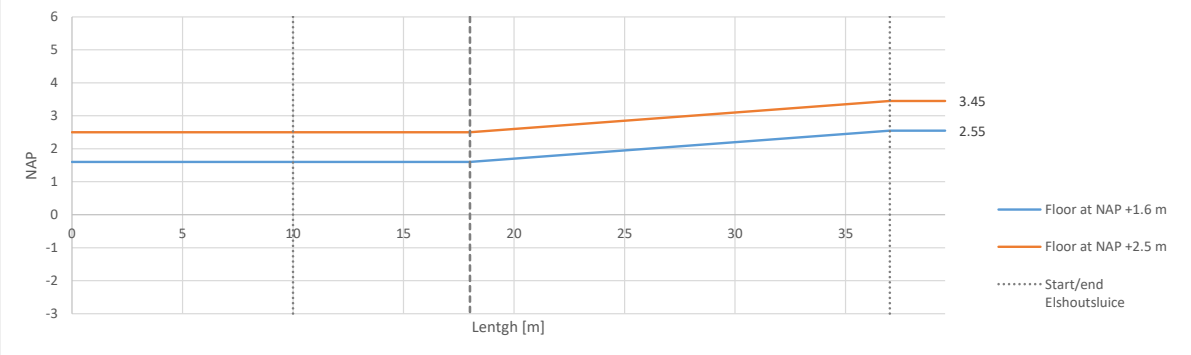

Figure F.4: Option 2: a slope of 1:20 for different floor levels

Option 3

Option 3 has two mandatory horizontal platforms. One around the middle of the slope and the other at the end, see Figure F.5. An advantage of a horizontal platform is an easier placement of a gate at this position than at a sloped position. The maximum and minimum of the floor level outside the Elshoutsluice are NAP + 3.5 m and NAP + 2.6 m.

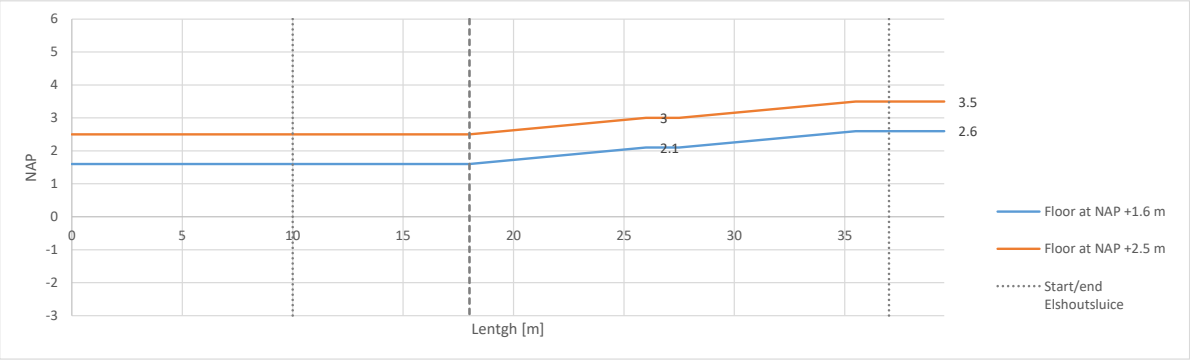

Figure F.5: Option 3: a slope of 1:16 for different floor levels

Option 4

Four horizontal platforms are needed for a slope of 1:12. Figure F.6 shows the locations of these platforms for the maximum and minimum situation. This results in a height of the floor at NAP + 3.5 m and NAP + 2.4 m.

There can be an option to add a slope of 1 m long and 0.1 m high (slope 1:10) at the end of the pedestrian tunnel, since there is still 1 m available for a slope. This option is not considered because a more uniform slope design is preferred.

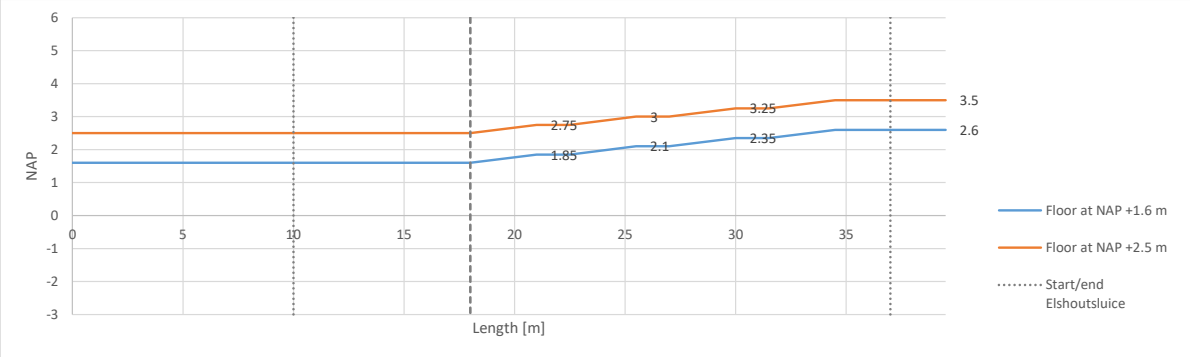

Figure F.6: Option 4: a slope of 1:12 for different floor levels

Option 5

The last option of a slope of 1:10 must include 8 horizontal platforms, see Figure F.7. The floor levels at the river side are NAP + 3.3 m and NAP + 2.4 m for option 5.

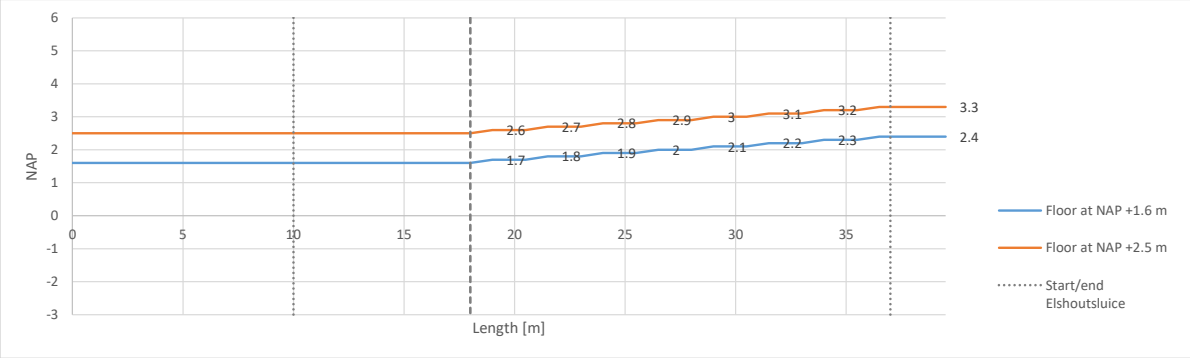

Figure F.7: Option 5: a slope of 1:10 for different floor levels

F.3. Conclusion

The analysis in this appendix results in five different slope configurations combined with two different floor level heights. For each option the floor level at the outer wall of the Elshoutsluice at the river side is determined. The results are summarised in Table F.2.

Table F.2: The floor level at the river side of the Elshoutsluice for all slope configurations.

Slope	Floor level at NAP + 1.6 m	Floor level at NAP + 2.5 m
1:25	NAP + 2.35 m	NAP + 3.25 m
1:20	NAP + 2.55 m	NAP + 3.45 m
1:16	NAP + 2.60 m	NAP + 3.50 m
1:12	NAP + 2.60 m	NAP + 3.50 m
1:10	NAP + 2.40 m	NAP + 3.30 m

G

Inventory and preliminary selection of hydraulic gate types

For the decision of the new closing mechanism an inventory of the available gate types is given in this appendix. The terminology for the closing mechanisms differs per report and country. For this report a mixed terminology of Daniel and Paulus (2019) and Mooyaart and Jonkman (2017) is used. An elaborate list of gate types can be categorised according to Daniel and Paulus (2019)[1]:

- Horizontal axis of rotation:
  - Flap gate
  - Radial gate
  - Sector gate
  - Segment gate
  - Drum gate
  - Roller gate
  - Visor gate
- Vertical axis of rotation:
  - Single-leaf gate
  - Vane gate
  - Mitre gate
  - Sector gate
- Horizontal sliding track:
  - Sliding gate
  - Rolling gate
- Vertical sliding track:
  - Vertical lift gate
  - Vertical sink gate
  - Stoney
  - Stoplog
- Combined motion directions:
  - Lift gate with flap
  - Lift-and-turn gate
  - Ball-supported sector gate
  - Hinged barge gate
- Other:
  - Inflatable gate
  - Needle and stack-up closures
  - Parachute
  - Unfolding gate

A short description of each gate type is given in this appendix. In the end of this appendix a selection is made of the considered gate types for the Elshoutsluice in Kinderdijk.

G.1. Horizontal axis of rotation

Flap gate

The flap gate is a straight or curved retaining surface which rotates around an axis fixed at the sill, see Figure G.1a. In the fully lowered position, the flap gate forms a continuous flat surface with the bottom. When the gate is fully raised, the straight surface makes an angle from 60 to 70 degrees with

[1] Some adjustments are made regarding the list of Daniel and Paulus (2019)

the horizontal floor. For this type the water flows over the gate (Erbisti, 2014). According to (Dijk & Van der Ziel, 2010) the sensitivity to failure probability is high for this type of gates. The characteristics of the flap gate are a high maintenance, an average material usage and it is not possible to retain water from two sides of the gate.

If a gate is formed by two flap gates which forms an inverted V structure, it is called the bear-trap gate. One leaf will be pushed up by the rising of the other leaf (Erbisti, 2014).

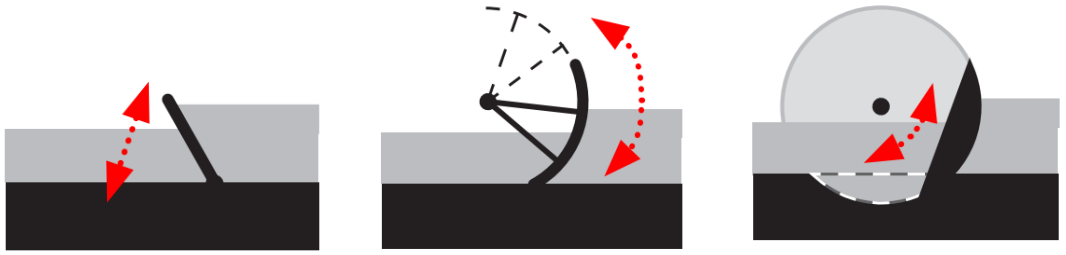

(a) Cross-section view of a flap gate

(b) Cross-section view of a radial gate

(c) Cross-section view of a rotary segment gate

Figure G.1: Horizontal axis rotation gate types (Dijk & Van der Ziel, 2010)

Radial gate

Figure G.1b shows an example of a radial gate. This gate type consists of a curved skin plate formed to a cylinder segment and is supported by radial compressed arms (Erbisti, 2014). A radial gate is typically considered the most suitable type of gate for controlled spillways. The application of the radial gate can be for underflow, overflow or both. A radial gate can be hinged both upstream and downstream (Daniel & Paulus, 2019).

Sector gate

A sector gate has a curved plate like the radial gate, but this gate is hinged at the bottom sill at downstream side (Erbisti, 2014). For this type of gate a gate chamber is build in the crest structure, which is shown in the example of the vertical axis sector gate as well in Figure G.3d.

Segment gate

The rotary segment gate, see Figure G.1c, is a cylindrical part which can be driven from both sides. Often only one side driving is applied. This type of gate has a wide range of applications as underflow, overflow or both options (Daniel & Paulus, 2019).

Drum gate

A drum gate leaf is a triangular shaped prism which is hinged at the bottom sill at the upstream side. The structure consists of a closed floating vessel as the gate. Due to water inflow in the gate chamber, the gate will close because of buoyancy forces (Erbisti, 2014).

Roller gate

Figure G.2b shows the roller gate type. The roller gate consists of a horizontal cylinder with toothed gears which connects the cylinder to the piers. This type of gates is often used when large amounts of floating ice is an issue for conventional gates (Erbisti, 2014). Roller gates are designed for overflow and underflow and primarily used for spillway control. Like the drum gate a roller gate uses buoyancy, but only to reduce the lift forces instead of driving the gate (Daniel & Paulus, 2019).

(a) Top view of a visor dam

(b) Cross-section view of a roller gate

Figure G.2: Horizontal axis rotation gate types (Dijk & Van der Ziel, 2010)

Visor gate

The visor structure has (semi-)cylindrical gates pivoted at the bottom. This is shown in Figure G.2a. Its application is mostly for weir gates, tidal, tsunami and storm surge barrier gates (Daniel & Paulus, 2019).

G.2. Vertical axis of rotation

Single-leaf gate

A Single-leaf structure is shown in Figure G.3a. This type of structure consists of a single leaf rotating rotating around the vertical axis at one side post of the gate (Daniel & Paulus, 2019). Another term for this type of gate is the swing gate.

Vane gate

The Figure G.3b shows the top view of a vertically hinged vane gate. This gate consist of two leaves fixed rigidly to each other. One leaf carries the water head and the other leaf drives the first leaf. No external drive is needed, since the gate is moved by water pressure differences (Daniel & Paulus, 2019).

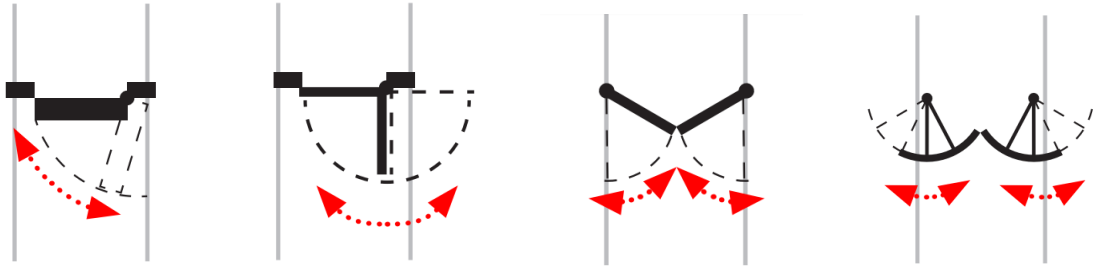

(a) Top view of a single-leaf gate

(b) Top view of a vane gate

(c) Top view of a mitre gate

(d) Top view of a double sector gate

Figure G.3: Vertical axis rotation gate types (Dijk & Van der Ziel, 2010)

Mitre gate

The mitre gate consists of two rotating leaves which meet at the centre in closed position, see Figure G.3c. If the mitre gate is opened, the leaves fit inside the side walls. This type of gate is often used for navigation locks. (Erbisti, 2014)

Sector gate

Figure G.3d gives a view of the vertically hinged sector gates which are used on navigation locks, hurricane protection sites or on storm surge (Daniel & Paulus, 2019). The structure consists of two

curved plate leaves which are linked to a point of rotation by a framed structure. A disadvantage of the vertically hinged sector gate is the requirement of hydraulic chambers at both side walls. This is inconvenient for the structure of a discharge sluice with multiple culverts.

G.3. Horizontal sliding track

Sliding and rolling systems are used for the horizontal translation of a gate shown in Figure G.4. The difference between rolling and sliding gates is the use of rolling supports for the first and sliding supports for the latter.

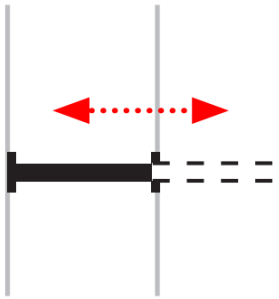

Figure G.4: Top view of a sliding/rolling gate (Dijk & Van der Ziel, 2010)

Sliding gate

A sliding gate utilises sliding pads, which produces more friction and wear than rolling. Sliding supports still have space to develop witch new contact materials and technologies (Daniel & Paulus, 2019).

Rolling gate

For the roller gate different configurations of the rolling support system are possible. The first option is the lower carriages and the second is the upper carriages. The third option is a combination of the two which is called the "wheelbarrow" (Daniel & Paulus, 2019).

G.4. Vertical sliding track

Vertical lift gate

Figure G.5a shows a closing mechanism where the gate is lifted vertically from the sill. In open stand the plane structure is located above the water. This type of gate stems from the stoplogs, but the difference is that stoplogs are rather replaceable than movable. Underflow is possible with the vertical lift gate. (Daniel & Paulus, 2019)

Vertical sink gate

A vertical sink gate refers to a gate which can move vertically from and into the bottom. Figure G.5b shows this type of gate. Only overflow is possible with a vertical sink gate.

Stoplog

The primary function of a stoplog is for maintenance of the main gates or equipment (Erbisti, 2014). In general stoplogs do not have rollers or wheels but a (gantry) crane.

Stoney

The stoney gate type consists of roller trains on each side of its frame held in position by vertical plates. This type of gates is not used often, since the great need of maintenance and high costs

(a) Front view of a vertical lift gate

(b) Cross-section view of a vertical sink gate

Figure G.5: Vertical sliding track gate types (Dijk & Van der Ziel, 2010)

(Erbisti, 2014). For the case of the discharge sluice this option is not convenient and is not included.

G.5. Combined motion directions

Lift gate with flap

A lift gate with flap is the combination of the vertical lift gate of Figure G.5a with a flap linked at the top of the lift gate. This provides for a vertical translation and a rotation with horizontal axis.

Lift and turn gate

The lift and turn gate is a vertical lift gate. However, in the open situation the gate is rotated with 90 degrees in a horizontal position.

Ball supported sector gate

This gate type is similar to the sector gate with the vertical axis of rotation. The difference is the hinge of this gate, which is a sphere. A spherical hinge ensures not only a rotation around the vertical axis, but also around the horizontal axis.

Hinged barge gate

A hinged barge gate is the combination of a swing gate with a buoyant hydraulic closure which can be floated or sunk by ballasting (Daniel & Paulus, 2019). Its application is for relative large structures. The barge gate is not suitable for weirs and is not discussed for the Elshoutsluice.

G.6. Other

Inflatable

Figure G.6a shows an inflatable closing type. In this case a rubber gate can be inflated with air or water to serve as a barrier. The rubber gate is deflated in open position. Another application of an inflatable closing mechanism is the steel-rubber gates where a tubular rubber bladder supports a pivoting steel panel. Inflatable structures contain more uncertainties due to the relative short experience with this type of gates (Daniel & Paulus, 2019).

Needle or stack up

Needle or stack-up is the group of closures where water retaining modules are added or removed. These modules can consist of vertical beams, horizontal planks, stiff panels, rolling/sliding curtains or other coupled elements. These elements are placed with the use of cranes (Daniel & Paulus, 2019). An example is given in Figure G.6b.

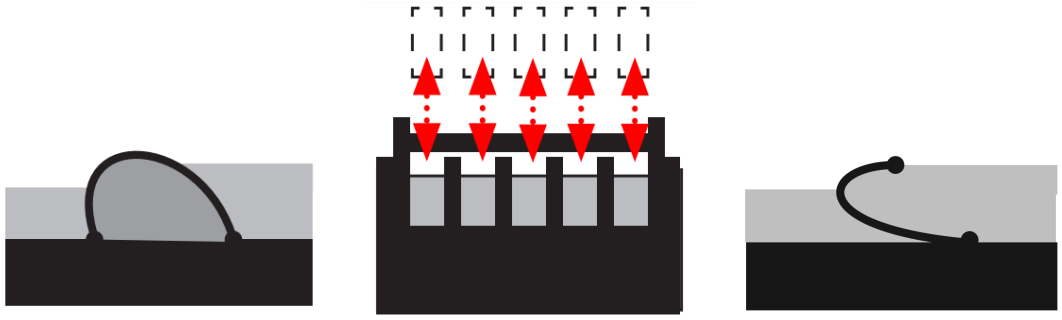

(a) Cross-section view of an inflatable dam

(b) Front view of a needle or stack up closure

(c) Cross-section view of a parachute gate

Figure G.6: Other gate types (Dijk & Van der Ziel, 2010)

Parachute

Figure G.6c shows the parachute dam which is an open fabric connected to the sill and a floating body. Due to cables, the floating body is kept in place. The parachute can be opened by the water flow and is kept open (partly) due to hydraulic pressure (Van der Ziel, 2009).

Unfolding

Unfolding effect is the term used for gates which consists of leaf parts which can slide/fold into a smaller gate to reduce the vertical or horizontal space in open situation. However, the total thickness of the gate increases. The leafs unfold in closed position.

G.7. Selection of closing mechanisms

Not all listed closing mechanisms are suitable for a discharge sluice. Large amounts of floating ice is not an issue for the Elshoutsluice. Therefore, a roller gate is excluded as an option for a closing mechanism. The visor gate is also not included, since it is used for large weirs. A stoplog is mainly for maintenance and is not considered as a primary or secondary closing mechanism. Stoney is excluded because it is not used very often due to high maintenance needs. The lift gate with a flap is not convenient for a culvert with small dimensions. The same is applicable to a ball supported sector gate and a hinged barge gate. All are mainly used in relatively large structures. A needle or stack up closure is mainly used as a dam and needs a crane for the placement of the elements. Therefore, the needle or stack up closure is excluded. The parachute dam is excluded as well since it is a solution for a large barrier and isn't applied yet. This results in the following options:

- Flap gate
- Radial gate
- Sector gate (horizontally/vertically hinged)
- Rotary segment gate
- Drum gate
- Single-leaf gate
- Vane gate
- Mitre gate
- Sliding gate
- Rolling gate
- Vertical lift gate
- Vertical sink gate
- Lift-and-turn gate
- Inflatable gate
- Unfolding gate (horizontally/vertically)

H

Slope of the road

A slope is needed for the motorised vehicle road to bridge a height difference. The minimal length of this slope is determined in this appendix since limited space is available around the Elshoutsluice. The maximum height difference is 1m, which is determined in subsection 5.2.2. Figure H.1 shows the parameters for the calculation of the minim length. This length consist of the slope length and the length due to the top and toe radius.

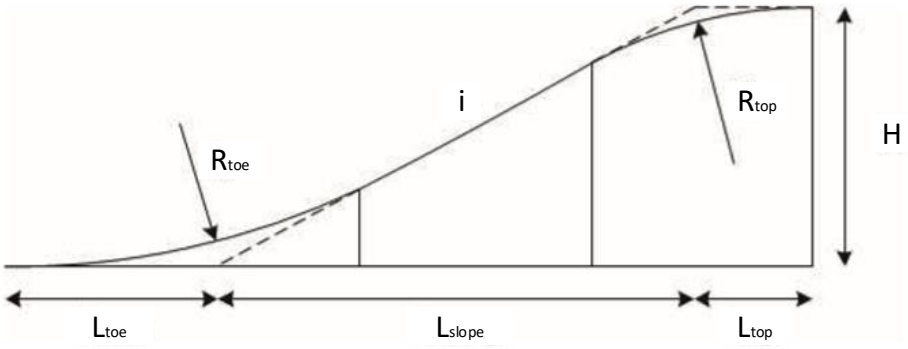

Figure H.1: The parameters for a slope (Van Nes, Wiggenraad, & Van Lint, 2018)

The formula to calculate the total length according to Van Nes et al. (2018) is:

$$L = \frac{p \cdot \sum R}{200} + \frac{100 \cdot H}{p} \tag{H.1}$$

L = The total horizontal length of the arches and slope together [m].
p = The slope percentage [%].
$\sum R$ = The summation of the top radius and the toe radius [m].
H = The total height difference [m].

The requirements for the slope and the radius depends on the design velocity. These requirement are given in Table H.1 and are for the situation of a large structure. This is the case for the Elshoutsluice.

The values for the toe radius from Table H.1 are based on comfort. The top radius is normally based on the sight distance and the object height. The driver eye level height is 1.1 m according to Rijkswaterstaat (2007) which is higher than the largest height difference of 0.9 m. There will be no sight

Table H.1: The requirements for a road based on design velocity for large structures (Rijkswaterstaat, 2007).

Design velocity	**Slope**	**Toe radius**
120 km/h	≤ 5 %	≥ 1200 m
100 km/h	≤ 5 %	≥ 850 m
80 km/h	≤ 6 %	≥ 500 m
50 km/h	≤ 7 %	≥ 200 m

obstacles due to a curvature. The toe radius based on comfort from Table H.1 will be used for the top radius as well in this case.

The maximum speed for the Molenweg is 50 km/h according to Van der Voet and Ligtermoet (2017). This results in a maximum slope p of 7 % and a minimum radius of 200 m. The values substituted in Equation H.1 gives a total minimum length of:

$$L = \frac{7 \cdot (200 + 200)}{200} + \frac{100 \cdot 0.9}{7} = 26.86\,m \tag{H.2}$$

Calculation HydraNL

This appendix contains calculation for the hydraulic load made with HydraNL. These calculation are used to check the height of the structure for flood risk verification.

I.1. Reference year 2100

The input for HydraNLis given by:

```
Invoerdatabase                                          = Copy_WBI2017_Benedenrijn_16-2_v04.sqlite
Locatie                                                 = 016-02_0081_9_LE_km0988
  X-coördinaat                                          =  103351 (m)
  Y-coördinaat                                          =  433783 (m)

De golfparameters uit de database zijn in de berekening gebruikt.

Profiel                                                 = Elshoutsluis.prfl
  Aanwezige kruinhoogte verticale wand                  =         0.00 (m+NAP)
  Verticale wand zonder neusconstructie
  Uitwendige dijknormaal                                =       343.00 (°N)

Berekeningstype                                         = Hydraulisch belastingniveau
Faalmechanisme                                          = Golfoverslag en overloop
  Kritiek overslagdebiet                                =        10.00 (l/s/m)
  De golfoverslag over de verticale wand is berekend zonder windinvloed

Berekening met statistische onzekerheid.
Berekening met onzekerheid in de waterstand, golfhoogte én golfperioden.
De parameterwaarden van de modelonzekerheid zijn uit de database afkomstig.
  Verwachtingswaarde onzekerheid waterstand             =         0.00 (m)
  Standaarddeviatie onzekerheid waterstand geopende EPK =         0.15 (m)
  Standaarddeviatie onzekerheid waterstand gesloten EPK =         0.25 (m)
  Aantal gebruikte waarden onzekerheid waterstand       =            7
  Verwachtingswaarde voor onzekerheid golfhoogte        =         0.96 (-)
  Standaarddeviatie voor onzekerheid golfhoogte         =         0.27 (-)
  Aantal gebruikte waarden onzekerheid golfhoogte       =            5
  Verwachtingswaarde onzekerheid spectrale golfperiode  =         1.03 (-)
  Standaarddeviatie onzekerheid spectrale golfperiode   =         0.13 (-)
  Verwachtingswaarde voor onzekerheid piekperiode       =         1.03 (-)
  Standaarddeviatie voor onzekerheid piekperiode        =         0.13 (-)
  Aantal gebruikte waarden onzekerheden golfperioden    =            5

Deze berekening is gemaakt voor het scenario W+ voor 2100
  en de afvoergolven worden afgetopt boven de afvoer 18000 m³/s.
Deze berekening is uitgevoerd met statistische gegevens van de Rijn
```

The resulting output is :

```
Berekeningsresultaten
    Frequentie:  Hydraulisch belastingniveau:
     1/  83333           5.228 (m+NAP)
     1/ 250000           5.574 (m+NAP)

  Terugkeertijd   Hydraulisch belastingniveau
     (jaren)             (m+NAP)
          10              3.492
          30              3.660
         100              3.835
         300              3.995
        1000              4.184
        3000              4.385
       10000              4.652
       30000              4.936
      100000              5.283
```

I.2. Reference year 2023

The input for HydraNLis given by:

```
Invoerdatabase                                          = Copy_WBI2017_Benedenrijn_16-2_v04.sqlite
Locatie                                                 = 016-02_0081_9_LE_km0988
  X-coördinaat                                          =  103351 (m)
  Y-coördinaat                                          =  433783 (m)

De golfparameters uit de database zijn in de berekening gebruikt.

Profiel                                                 = Elshoutsluis.prfl
  Aanwezige kruinhoogte verticale wand                  =         0.00 (m+NAP)
  Verticale wand zonder neusconstructie
  Uitwendige dijknormaal                                =       343.00 (°N)

Berekeningstype                                         = Hydraulisch belastingniveau
Faalmechanisme                                          = Golfoverslag en overloop
  Kritiek overslagdebiet                                =        10.00 (l/s/m)
  De golfoverslag over de verticale wand is berekend zonder windinvloed

Berekening met statistische onzekerheid.
Berekening met onzekerheid in de waterstand, golfhoogte én golfperioden.
De parameterwaarden van de modelonzekerheid zijn uit de database afkomstig.
  Verwachtingswaarde onzekerheid waterstand             =         0.00 (m)
  Standaarddeviatie onzekerheid waterstand geopende EPK =         0.15 (m)
  Standaarddeviatie onzekerheid waterstand gesloten EPK =         0.25 (m)
  Aantal gebruikte waarden onzekerheid waterstand       =            7
  Verwachtingswaarde voor onzekerheid golfhoogte        =         0.96 (-)
  Standaarddeviatie voor onzekerheid golfhoogte         =         0.27 (-)
  Aantal gebruikte waarden onzekerheid golfhoogte       =            5
  Verwachtingswaarde onzekerheid spectrale golfperiode  =         1.03 (-)
  Standaarddeviatie onzekerheid spectrale golfperiode   =         0.13 (-)
  Verwachtingswaarde voor onzekerheid piekperiode       =         1.03 (-)
  Standaarddeviatie voor onzekerheid piekperiode        =         0.13 (-)
  Aantal gebruikte waarden onzekerheden golfperioden    =            5

Deze berekening is gemaakt voor het scenario W+ voor 2023
  en de afvoergolven worden afgetopt boven de afvoer 18000 m³/s.
Deze berekening is uitgevoerd met statistische gegevens van de Rijn
```

The resulting output is :

```
Berekeningsresultaten
    Frequentie:  Hydraulisch belastingniveau:
     1/  83333           4.824 (m+NAP)
     1/ 250000           5.111 (m+NAP)

  Terugkeertijd   Hydraulisch belastingniveau
     (jaren)             (m+NAP)
          10              3.152
          30              3.406
         100              3.648
         300              3.846
        1000              4.047
        3000              4.223
       10000              4.417
       30000              4.611
      100000              4.867
```

J

Analysis non-closure of gates

This appendix analyses the situation for failure mechanism non-closure of gates for the current and new situations. The starting point is the assessment of the Elshoutsluice performed by Waterschap Rivierenland (2020)[1]. The standard failure tree of the failure mode non-closure of gates is given in Figure J.1.

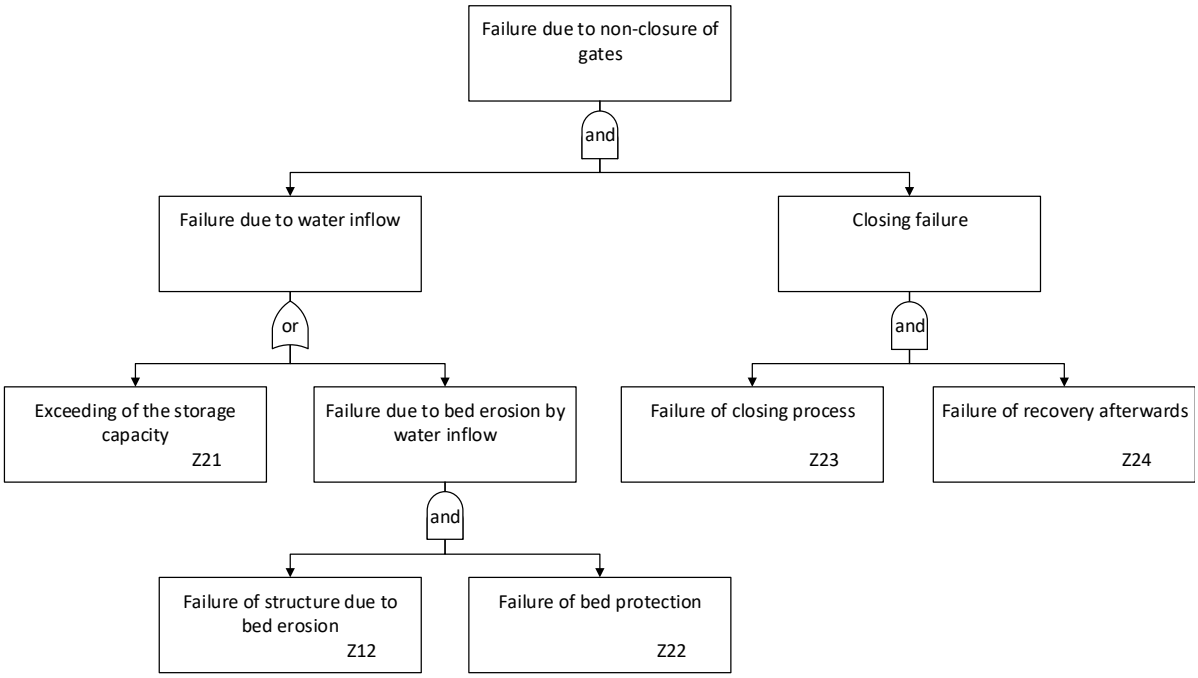

Figure J.1: Standard failure tree of non-closure according to Rijkswaterstaat (2017a)

J.1. Explanation failure mode

Riskeer determines the probability of failure for non-closure according to the standard failure tree given in Figure J.1. The probability of a limit state function Z being below zero is calculated for different limit state functions. The limit state functions for failure due to non-closure are explained in this section.

[1]The assessment of the Elshoutsluice was revised during the thesis process. The methodology with Riskeer is used for the non-closure analysis based on the first version of this document

The limit state function for failure due to erosion is:

$$Z_{12} = -\Phi^{-1}(P_{f,kw:erosion}) - u \tag{J.1}$$

Φ^{-1} is the inverse of the standard normal distribution. u is a stochastic help parameter which is automatically included in Riskeer for the failure due to erosion. The standard value for $P_{f,kw:erosion}$ is 1.0 which is a conservative value indicating that there is no residual strength according to Rijkswaterstaat (2019).

The limit state function for exceeding the storage capacity is given by (Rijkswaterstaat, 2017a):

$$Z_{21} = V_c - V_{in} \tag{J.2}$$

Where:

$$V_c = m_{kom} \cdot A_{kom} \cdot \Delta h_{kom} \tag{J.3}$$

$$V_{in} = m_{in} \cdot f_{ts;open} \cdot t_s \cdot Q_{in;open} \tag{J.4}$$

With:

V_c	=	storage capacity in m^3.
m_{kom}	=	model factor for the storage capacity.
A_{kom}	=	storage area in m^2.
Δh_{kom}	=	critical water level increase in m.
V_{in}	=	the inflow volume due to non-closure of gates in m^3.
m_{in}	=	model factor for inflow volume.
$f_{ts;open}$	=	factor for high water storm duration.
t_s	=	duration of the storm in hours.
$Q_{in;open}$	=	inflow discharge in m^3/hour.

The standard mean value for t_s is 6 hours with a variation coefficient of 0.25. Standard factor for m_{kom} and m_{in} is 1.0. $f_{ts;open}$ has standard value of 1.0.

The inflow discharge $Q_{in;open}$ depends on the inflow model. The inflow models are a vertical wall, a low threshold an a drowned opening. The equations for the inflow discharge per inflow model are given below.

For a vertical wall:

$$Q_{in;open} = B \cdot m_{OL} \cdot 0.55 \cdot \sqrt{-g \cdot (h_{kr;ns} - h_{bu})^3} + B \cdot m_{OS} \cdot \sqrt{g \cdot (H_s)^3} \tag{J.5}$$

For a low threshold:

$$Q_{in;open} = B \cdot m_{vl} \cdot (h_{bi} - h_{dr}) \cdot \sqrt{2 \cdot g \cdot (h_{bu} - h_{bi})} \qquad h_{bu} < 3/2 \cdot h_{bi} - 1/2 \cdot h_{dr} \tag{J.6}$$

$$Q_{in;open} = B \cdot m_{vl} \cdot 0.55 \cdot \sqrt{g \cdot (h_{bu} - h_{dr})^3} \qquad h_{bu} \geq 3/2 \cdot h_{bi} - 1/2 \cdot h_{dr} \tag{J.7}$$

For a drowned opening:

$$Q_{in;open} = \mu \cdot A \cdot \sqrt{2 \cdot g \cdot (h_{bu} - h_{bi})} \tag{J.8}$$

Where:

B	=	width of the inflow opening in m.
m_{OL}	=	model factor for the overflow discharge for a vertical wall.

$h_{kr;ns}$ = the height of the structure in an open situation in m + NAP.
h_{bu} = the river/sea side water level in m + NAP.
m_{OS} = model factor for the overtopping discharge for a vertical wall.
H_s = the significant wave height in m.
m_{vl} = model factor for long thresholds.
h_{bi} = the hinterlands water level in m + NAP.
h_{dr} = the height of the threshold in open situation in m + NAP.
μ = discharge coefficient for a drowned opening.
A = inflow area of a drowned opening in m^2.

m_{OL} has a standard mean value of 1.1 with a standard deviation of 0.03 and m_{OS} has a standard mean value of 0.09 with a standard deviation of 0.06. The threshold model factor m_{vl} has a standard mean value of 0.9 with a standard deviation of 0.05. μ has a mean value of 1.0 with a standard deviation of 0.2 (Rijkswaterstaat, 2019). It is not possible to change these values in Riskeer.

The limit state function for failure of the bed protection is:

$$Z_{22} = Q_c - Q_{in;open} \tag{J.9}$$

With:

$$Q_c = q_c \cdot B_{sv} \tag{J.10}$$

In which:

Q_c = the critical discharge in m^3.
$Q_{in;open}$ = inflow discharge in m^3/s.
q_c = the critical discharge per unit width m^2/s.
B_{sv} = flow width of the bed protection in m.

The limit state function for failure of the closing process is given by:

$$Z_{23} = -\Phi^{-1}(P_{f,closing}) - u \tag{J.11}$$

With:

$$P_{f,closing} = P_{ns,tot} \cdot P_{open} \tag{J.12}$$

$$P_{ns,tot} = n \cdot P_{ns} \tag{J.13}$$

Where:

$P_{f,closing}$ = the probability of failure of the closing process of the gates.
$P_{ns,tot}$ = the total probability of failure of the closing process per demand.
P_{open} = the probability of a gate to be open when high water occurs.
n = the number of identical openings in a structure.
P_{ns} = failure probability of closing an opening in the structure per demand.

There is a conservative estimation for the failure of closing per demand when gates are frequently used according to Rijkswaterstaat (2018b). For a recoil valve this is a failure probability of 10^{-5} per demand and for a sliding gate and for a sluice gate a failure probability of 10^{-4} per demand.

The limit state function of failure of recovery afterwards is:

$$Z_{24} = -\Phi^{-1}(P_{f,recovery}) - u \tag{J.14}$$

The standard value is 1.0 for $P_{f,recovery}$ according to Rijkswaterstaat (2019) which is a conservative approach. If P_{ns} is determined with the score-tables according to Rijkswaterstaat (2017b), the value for$P_{f,recovery}$ is 1.0 since the failure probability of recovery is already included in the score-table determination of P_{ns}.

J.2. Current situation

In the current situation of the Elshoutsluice there are four culverts in total. The structure fails if one of these four culverts doesn't close for the failure mechanism non-closure of gates. This is displayed in a fault tree in Figure J.2. The closing mechanism configuration and storage capacity differs for the culverts which results in a different standard failure tree, see Appendix C, for each culvert.

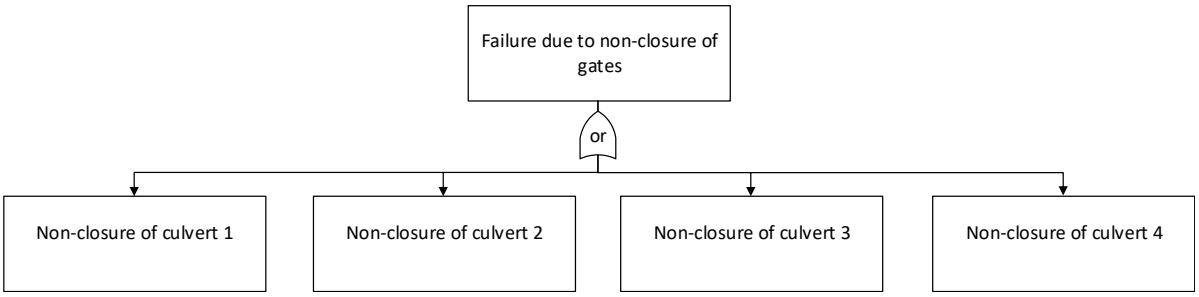

Figure J.2: The fault tree for the current state of the Elshoutsluice for the failure mechanism non-closure of gates

The probability of non-closure of gates when asked needs to be determined for each closing mechanism configuration. Currently there are three types of gates in the Elshoutsluice. The assessment of the Elshoutsluice according to Waterschap Rivierenland (2020) used the following values for the probability of non-closure when asked for each gate type:

- The radial gate: 1/10,000 per demand based on a standard value according to TAW (2003).
- The recoil valve: 1/100,000 per demand based on the standard value (TAW, 2003).
- The lift gate: 1/5052 per demand according to Waterschap Rivierenland (2020) based on the filled in score tables from Rijkswaterstaat (2017b).

Figure J.3: Flooding of the discharge reservoir of the Overwaard in 2015 (source: www.alblasserdamsnieuws.nl)

There is a standard failure tree for the failure mode non-closure of gates see Figure C.3. The probability of water inflow due to flooding of the discharge reservoirs is assumed to be much higher than failure of the bed protection. This assumption is based on the fact that both discharge basins are small, which results in water levels equal to the river level in case of open gates. The flood defences around the discharge reservoirs are relatively low, see Figure J.4a. In the assessment according to Waterschap Rivierenland (2020), the failure due to water inflow is based only on water levels exceeding the discharge reservoir flood defences. Flooding of the Overwaard has occurred before, see Figure J.3.

(a) The flood defences of the discharge reservoirs from the Overwaard and Nederwaard.

(b) The distribution flap in the current position.

Figure J.4: Photos of the Elshoutsluice in February 2020

J.2.1. Culvert 1

Culvert 1 has a radial gate and a lift gate. Failure will occur when both these gates fail, see the fault tree in Figure J.5. This results in a failure probability of 1/50,520,000 per demand.

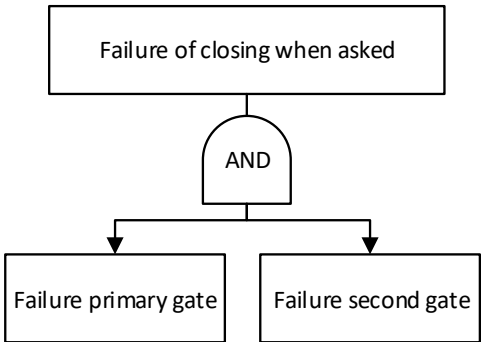

Figure J.5: The fault tree for the current situation for non-closure of gates when asked of culvert 1 and 2.

If the gates of culvert 1 fail, the water will flow into the discharge reservoir of the Nederwaard. This reservoir is surrounded by a concrete wall up to a height of NAP + 2.5 m, see Figure J.4a. From the analysis according to Waterschap Rivierenland (2020) the exceeding probability for NAP + 2.5 m is 1/7.5 per year. The probability of the radial gate to be open when high water levels occur is 0.213 per year which results in a calculated failure probability of 1/1,778,300,000 according to Waterschap Rivierenland (2020).

J.2.2. Culvert 2

The closing mechanism configuration of culvert 2 is exactly the same as culvert number 1. This results in the same failure probability of 1/50,520,000 per demand for the gates. The water will discharge to the discharge reservoir of the Overwaard in case of gate failure due to the distribution flap, see Figure J.4b. The flood defence around the discharge reservoir of the Overwaard has a lower part. Figure J.3 shows this part when the discharge reservoir flooded in 2015. According to Waterschap Rivierenland (2020) this lower part has a height of NAP + 1.5 m. This level has a exceeding probability of 46 per year. The probability of the radial gate to be open is 0.213 per year. The total failure probability for the failure mode non-closure is 1/5,150,000 per year for culvert 2 according to Waterschap Rivierenland (2020).

J.2.3. Culvert 3

Culvert number 3 has three recoil valves, because of the three pumps, and a lift gate. Figure J.6 shows the fault tree for failure of closing when asked. This results in a failure probability of 1/168,400,000 per demand. The water will discharge to the Overwaard when there is gate failure, which results in the same results for exceeding the water level of NAP + 1.5 m as culvert 2. The recoil valves are only open when the three pumps are used. This is only in case of emergency at high water levels (Waterschap Rivierenland, 2020). Therefore, it is assumed that the probability of the recoil valves to be open at high water levels is negligibly small. As a result, the total failure probability due to non-closure is negligibly small for culvert 3 according to Waterschap Rivierenland (2020).

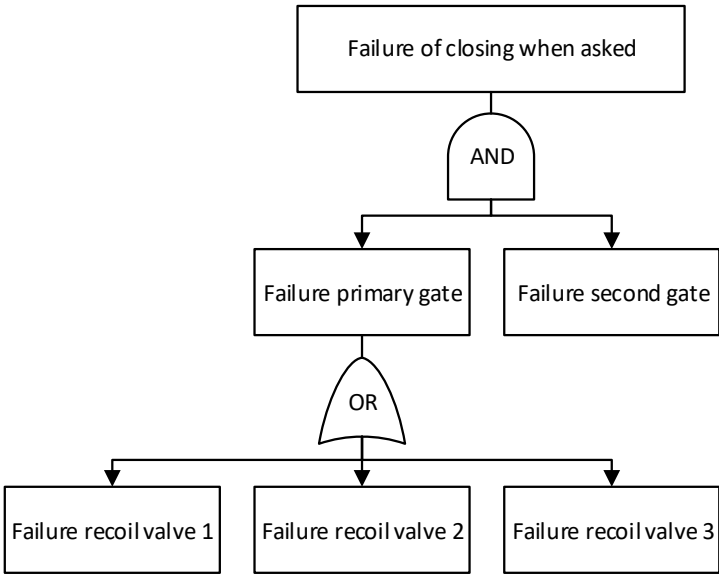

Figure J.6: The fault tree for the current situation for non-closure of gates when asked of culvert 3.

Culvert 4

In culvert 4 are three pumps with a recoil valve each. These recoil valves are located right above the radial gate, see Figure B.8. A lift gate is included in this culvert as well which results in a fault tree given in Figure J.7. Since the probability of the gates to be open at high water levels differs for the recoil valves and radial gate the assessment of culvert 4 is split in two different assessments according Waterschap Rivierenland (2020). The first assessment consists of the combination of the lift gate with the radial gate and the second consists of the lift gate with the recoil valves. If gate failure occurs, the water will discharge to the Overwaard. A maximum water level of NAP + 1.5 m is allowed.

For the first assessment, the probability of non-closure when asked results in a value of 1/50,520,000 per demand. This assessment is exactly the same as for culvert number 2, which results in a total failure probability of 1/5,150,000 per year according to Waterschap Rivierenland (2020).

In the second assessment the probability of the recoil valves to be open is negligibly small. This assessment is exactly the same as culvert number 3, which gives an negligibly small failure probability (Waterschap Rivierenland, 2020).

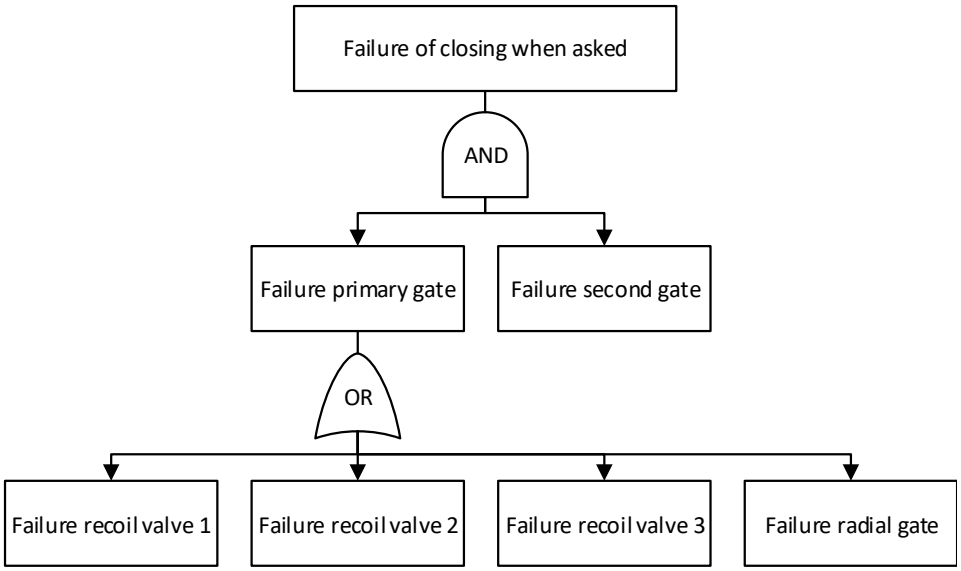

Figure J.7: The fault tree for the current situation for non-closure of gates when asked for culvert 4.

J.2.4. Conclusion

All the failure probabilities for failure due to non-closure of gates for each culvert are given in Table J.1.

Table J.1: The flood safety assessment results for the failure due to non-closure of gates for the Elshoutsluice according to Waterschap Rivierenland (2020).

Culvert	**Failure probability [1/year]**
1	1/1,778,300,000
2	1/5,150,000
3	Negligibly small
4 (Radial gate)	1/5,150,000
4 (Recoil valves)	Negligibly small
4 (Total)	1/5,150,000

An analysis is made to prove which situation is governing for failure due to non-closure. This analysis is given in Table J.2. The highest failure probability is for the situation where 1 culvert fails and has a value of 1/2,575,000 per year.

Table J.2: The probability analysis of non-closure for the current situation of the Elshoutsluice.

Failure of	**Failure probability [1/year]**	**Return period [year]**
Non-closure 1 culvert	*3.89E-07*	*2,571,277*
Culvert 1	5.62E-10	1,778,300,691
Culvert 2	1.94E-07	5,150,001
Culvert 3	0.00E+00	0
Culvert 4	1.94E-07	5,150,001
Non-closure 2 culverts	*3.79E-14*	*26,369,765,083,926*
Culvert 1&2	1.09E-16	9,158,246,778,300,340
Culvert 1&3	0.00E+00	0
Culvert 1&4	1.09E-16	9,158,246,778,300,340
Culvert 2&3	0.00E+00	0
Culvert 2&4	3.77E-14	26,522,500,014,915
Culvert 3&4	0.00E+00	0
Non-closure 3 culverts	*2.12E-23*	*47,164,961,750,000,000,000,000*
Culvert 1&2&3	0.00E+00	0
Culvert 1&2&4	2.12E-23	47,164,961,750,000,000,000,000
Culvert 2&3&4	0.00E+00	0
Non-closure 4 culverts	*0.00E+00*	*0*

J.3. The new situation

For the new situation a pedestrian tunnel with closing mechanisms is added. This pedestrian tunnel needs to be included in the determination of the failure probability for the failure mechanism non-closure of gates. There is need for a change in the closing mechanism arrangement for the culvert number 2. This results in the fault tree for the new situation given in Figure J.8. The calculation for the failure mode non-closure are performed with Riskeer according to a detailed test. The fist assessment according to Waterschap Rivierenland (2020) was performed with the detailed test for non-closure of gates as well, but for the revision the customary test is used for this failure mode.

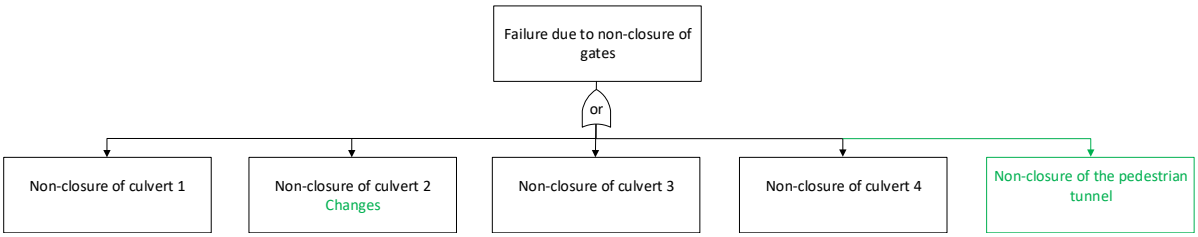

Figure J.8: The fault tree for the new possible situation of the Elshoutsluice.

J.3.1. Culverts

The culverts 1, 3 and 4 will remain exactly the same. With the new closing mechanisms the probability of failure will change for culvert number 2. Two new gates will be placed instead of the old gates.

The main gate will be the unfolding gate at the location of the old lift gate. This gate is chosen as the main gate, because of the possibility to open this gate partly in dry periods. Failure processes as alarm, mobilisation and control are not directly applicable to closing mechanisms which are opened and closed regularly according to Rijkswaterstaat (2018b). Only technical failure is applicable for

this gate. The main gate will be considered as a sluice gate with a standard failure probability of 1/10000 per demand.

The function of the flap gate will be similar to the old lift gate. The filled in score tables from Rijkswaterstaat (2017b) for the lift gate according to Waterschap Rivierenland (2020) are checked and will not differ largely for the new flap gate. Therefore the same failure probability of 1/5052 per demand is assumed for the flap gate.

The function of both new gates together will remain the same as the function of the old gates which results in the same fault tree as the current situation, see Figure J.5. Therefore, the total failure probability for non-closure when asked is 1/50,520,000 per demand.

According to Waterschap Rivierenland (2020), the probability of the current radial gate to be opened at high water levels is 0.213 per year. The function of the new closing mechanisms remains the same, so the probability of being open is still 0.213 per year. It is only possible to input this parameter as a round number fraction in Riskeer. Therefore, the input is set to 1/4 which is equal to 0.25 which is assumed higher than 0.213 per year. The decision is made to make assume the probability higher for a safer assessment.

For the failure probability of recovery after failure the conservative value of 1 is chosen. This means that it is assumed that there is no recovery possible after failure of the gates.

A drowned opening is selected as the water inflow model since the culvert will be drowned in a high water level situation. The water level in the discharge reservoir of the Overwaard will be at NAP + 1.5 m in this situation, which is the parameter water level hinterland. The width of the culvert is 5.6 m and the height is 3.75 m, which results in an inflow area of 21 m^2. A conservative standard value of 1 is chosen for the discharge coefficient according to Rijkswaterstaat (2019).

The storm duration value is set to the standard value of 6 hours according to Rijkswaterstaat (2019). This parameter describes the duration of the peak of a storm. With this parameter the volume of the inflow of river water can be determined. The factor for high water storm duration is set to the standard value 1 recommended according to Rijkswaterstaat (2019) as well. With this factor a part of the duration of a high water wave can be included.

For the critical inflow discharge, the assumption is made that the flood defence around the discharge basin will fail before the bed protection will fail based on Waterschap Rivierenland (2020). A concrete slab with a length of approximately 17 meters (Waterschap Rivierenland, 2020) is located at the bed hinterlands of the Elshoutsluice which serves as bed protection. The flood defence of the Overwaard has a lower part which starts to flood as first, see Figure J.3. According to Waterschap Rivierenland (2020) this lower part has a length of 15 m and a lowest height of NAP + 1.5 m and will reach the critical discharge before other parts will start to flood. The values for the critical discharge for grass covers is given in Table B.2 according to Rijkswaterstaat (2018a). Waves in the discharge reservoir will be minimal and are categorised in 0 - 1 m. An open sod is assumed, which results in a mean critical discharge of 0.10 $m^3/s/m$' and a standard deviation of 0.12 $m^3/s/m$'. The input for Riskeer is a mean value μ and the variation coefficient which is σ/μ = 0.12 / 0.10 = 1.20.

The failure probability due to bed erosion is set to 1, which means that if the bed protection (in this case the flood defence of the discharge reservoir) fails this directly results in failure.

The storage capacity of the Overwaard is given in Appendix B. This consists of a storage area of 2,900,000 m^2 with an acceptable water level increase of 0.35 m.

All the input parameters are summarised in Table J.3. The result of the Riskeer calculation is a failure probability of 1/51,500,147 per year for culvert 2 in the new situation.

Table J.3: Input parameters Riskeer for culvert 2.

Parameter	Value	Variation/st. deviation
Number of identical openings [-]	1	-
Failure probability of closing [-]	1/50,520,000	-
Probability of open gate [-]	1/4	-
Failure probability of recovery after failure [-]	1	-
Inflow model	Drowned opening	-
Water level hinterlands [m + NAP]	1.50	0.10
Inflow area [m^2]	21.00	0.01
Discharge coefficient [-]	1.00	0.20
Storm duration [hour]	6.00	0.25
Factor for high water storm duration [-]	1	-
Critical inflow discharge [$m^3/s/m$]	0.10	1.20
Width of bed protection [m]	15.00	0.05
Failure probability bed erosion [-]	1	-
Storage area [m^2]	2900000.00	0.10
Maximum allowable water level increase [m]	0.35	0.10

J.3.2. Pedestrian tunnel

Three new gates will be included in the pedestrian tunnel due to the requirement from Waterschap Rivierenland. At first, only two gates will be considered for failure due to non-closure. When the tunnel does not fulfil the requirement, the flood risk assessment will be performed for a tunnel with three gates. The new gates will be opened and closed regularly for closing off the pedestrian tunnel outside visitor hours. Therefore, only technical failure is assumed with a standard failure probability of 1/10,000 per demand according to Rijkswaterstaat (2019). This failure probability is applicable to both gates which results in a total failure probability of 1/100,000,000 per demand for the pedestrian tunnel.

The probability of an open gate is assumed at 1.0 as a conservative approach. The same conservative approach is chosen for the failure probability of recovery after failure.

(a) The platform hinterlands of the Elshoutsluice including the grating for the weed screen.

(b) Top view of maintenance entrance and part of the grating.

Figure J.9: Photos of the Elshoutsluice in February 2020

A low threshold inflow model is selected, since there is a very low probability of the pedestrian tunnel being drowned. If water flows through the new pedestrian tunnel, this will end up in the discharge reservoirs via the gratings in the platform hinterlands. These gratings are shown in Figure J.9a and Figure J.9b. Is is most likely the water will end up in culvert number 2 in case of flooding

of the pedestrian tunnel. Therefore, the water level hinterlands is equal to the maximum allowable water level of NAP + 1.5 m in the discharge reservoir of the Overwaard.

The top level of the floor of the pedestrian tunnel at river side is the threshold level, which is NAP + 3.45 m. The width of the inflow opening is the width of the pedestrian tunnel of 5.5 m.

The storm duration value is set to the standard value of 6 hours according to Rijkswaterstaat (2019). The factor for high water storm duration is set to the standard value 1 recommended according to Rijkswaterstaat (2019).

It is most likely for the water going through the pedestrian tunnel to end up in the discharge basin of the Overwaard. Therefore the same values for the critical inflow discharge, width of bed protection, failure probability of the bed erosion, the storage area and the maximum allowable water level increase are taken into account as for culvert number 2. All the input parameters are summarised in Table J.4.

Table J.4: Input parameters Riskeer for the pedestrian tunnel

Parameter	**Value**	**Variation/st. deviation**
Number of identical openings [-]	1	-
Failure probability of closing [-]	1/100,000,000	-
Probability of open gate [-]	1/1	-
Failure probability of recovery after failure [-]	1	-
Inflow model	Low threshold	-
Water level hinterlands [m + NAP]	1.50	0.10
Threshold level [m + NAP]	3.45	0.10
Width of inflow opening [m]	5.50	0.05
Storm duration [hour]	6.00	0.25
Factor for high water storm duration [-]	1	-
Critical inflow discharge [$m^3/s/m$]	0.10	1.20
Width of bed protection [m]	15.00	0.05
Failure probability bed erosion [-]	1	-
Storage area [m^2]	2900000.00	0.10
Maximum allowable water level increase [m]	0.35	0.10

The calculated failure probability for the new pedestrian tunnel is 1/514,972,218,999 per year. An additional assessment with three gates in the pedestrian tunnel is not necessary, since the failure probability is very low. In addition, a calculation is performed for a situation with only 1 gate in the pedestrian tunnel. The failure probability of closing is 1/10,000 and results in a failure probability of 1/68.957.957 per year for the pedestrian tunnel.

J.3.3. Conclusion

All the failure probabilities per passage of the Elshoutsluice are summarised in Table J.5. The result is a failure probability of 1/4,669,484 per year for the failure mode non-closure of gates for the Elshoutsluice including the pedestrian tunnel.

Table J.5: The flood safety assessment results for the failure probability due to non-closure of gates for the Elshoutsluice in the old and the new situation in [1/year].

Opening	Current situation	New situation
Culvert 1	1/1,778,300,000	1/1,778,300,000
Culvert 2	1/5,150,000	1/51,500,147
Culvert 3	Negligibly small	Negligibly small
Culvert 4 (Radial gate)	1/5,150,000	1/5,150,000
Culvert 4 (Recoil valves)	Negligibly small	Negligibly small
Pedestrian tunnel	-	1/514,972,218,999

In addition, the failure probability for the failure mode non-closure of gates for the pedestrian tunnel with only one gate is calculated. The determined failure probability is 1/68.957.957 per year which is below the alert value of 1/250,000.

K

Structural verification calculations

This appendix consists of the structural verification calculations for the selected alternative design in section 6.3. First, all the loads acting on the Elshoutsluice are determined. Second, the chosen stability checks of section 9.1 are performed. Finally, load distribution checks are performed for a selected cross-section of the discharge sluice in section 9.2.

K.1. Loads

For the structural verification, the loads on the Elshoutsluice are analysed. In this section, the loads are determined and summarised. The loads can be divided into permanent loads and variable loads.

K.1.1. Permanent load

The permanent loads consists of loads due to resting elements on the structure and the self weight of the structure. To determine the loads and the self weight of the discharge sluice, the specific weight of the present materials is necessary. The Lek river consists of fresh water, see Appendix B. A layer of soil is situation on top of the Elshoutsluice and the sluice itself is made of concrete. A selection of specific weights according to Soons, Van Raaij, and Wagemans (2014) is shown in Table K.1.

Table K.1: The specific weight of materials (Soons et al., 2014).

Material	**Weight [kg/m^3]**
Soil/clay dry	1600
Soil/clay wet	2000
Fresh water	1000
Reinforced concrete	2400 - 2550

Soil

The self weight of the soil on top of the discharge sluice is determined for three different situations. First, the load due to the soil is determined for current state of the Elshoutsluice. The soil is simplified into two floor plan areas with a constant height, see Table K.3.

The assumption is made that the soil on top of the Elshoutsluice is dry. This results in a specific weight of 1600 kg/m^3 according to Table K.1. From the determination of Table K.2 results a volume of 1081 m^3. Combined with the selected specific weight, this results in:

Table K.2: Determination of the volume of the soil on top of the Elshoutsluice.

Parameter	Value	Unit
A_top soil_1	330.70	m^2
A_top_soil_2	65.45	m^2
h_1	3.05	m
h_2	1.10	m
37 *V_total_soil*	*1080.64*	m^3

$$F_{v,soil,start} = V_{soil,start} \cdot \frac{g \cdot \gamma_{soil,dry}}{1000} = 1080.64 \cdot \frac{9.81 \cdot 1600}{1000} = 16961.74 \text{ kN} \tag{K.1}$$

Construction phase 1, see Chapter 7, is the second scenario for which the soil self weight is calculated. In this phase the amount of soil on top of the Elshoutsluice will be at a minimum. The soil above two of the four culverts will be excavated. Therefore, the assumption is made that the excavated soil is approximately the half of the initial volume. This results in a half of the load $F_{v,soil,start}$ which gives:

$$F_{v,soil,min} = F_{v,soil,start}/2 = 16961.74/2 = 8480.87 \text{ kN} \tag{K.2}$$

The last scenario considered is after the construction phase. A new layer of soil is added to provide a slope for the motorised vehicle road. This slope is simplified to the situation shown in Figure K.1 based on the evaluation of Equation H.1 and Figure H.1. Only the additional soil above the Elshoutsluice is included in the self weight calculation. The determination of the total volume of the soil on top of the discharge sluice is given in Table K.3.

Table K.3: Determination of the volume of the soil on top of the Elshoutsluice at the end of the construction phase.

Parameter	Value	Unit
V_min	540.32	m^3
A_add_culvert1	5.40	m^2
A_add_culvert2	1.905	m^2
A_add_culvert3	6.985	m^2
A_add_culvert4	5.40	m^2
Length_add	12.13	m
V_additional	238.84	m^2
V_total_soil_end	*779.16*	m^3

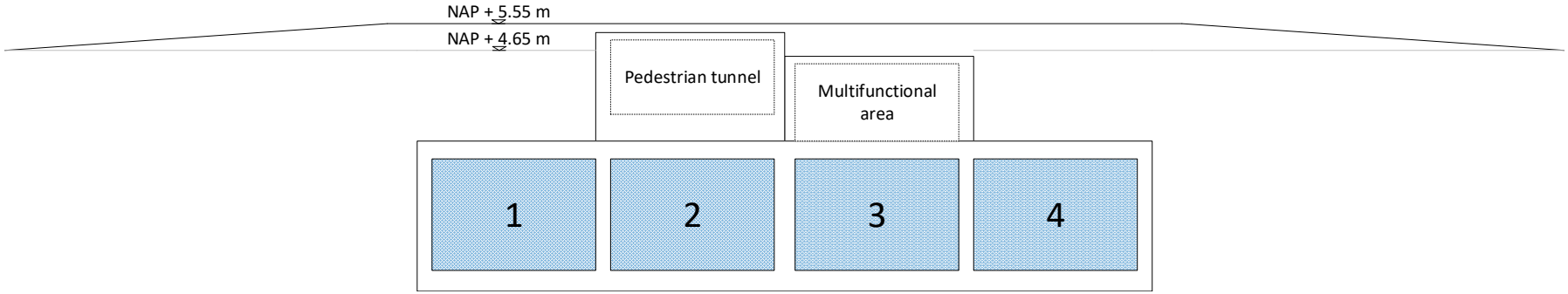

Figure K.1: Simplification of the soil layer in the new situation.

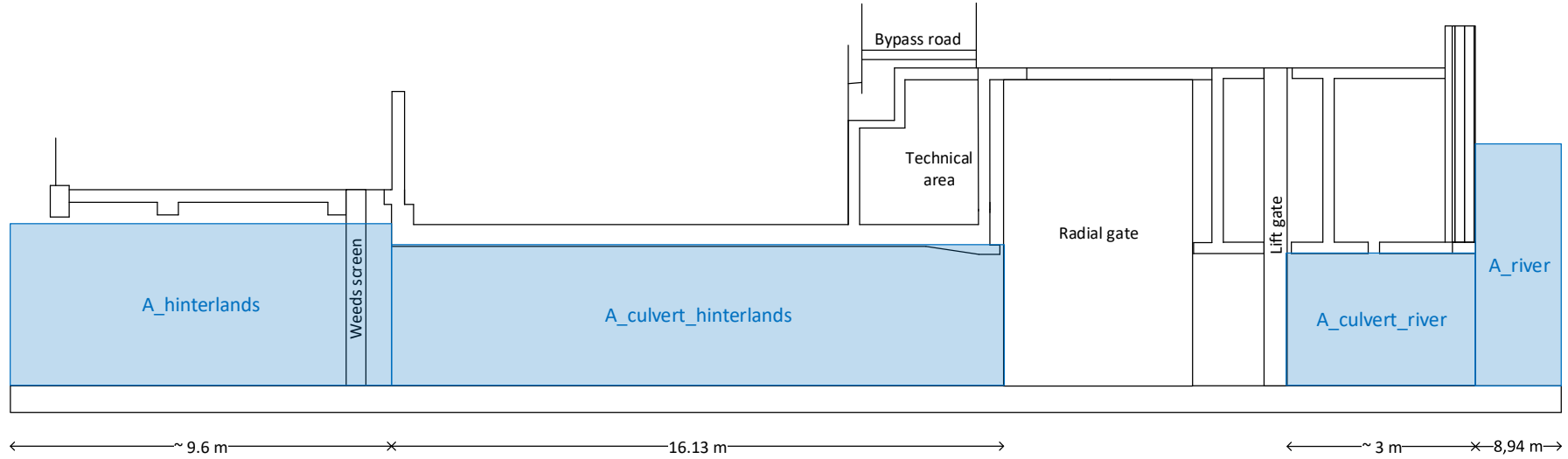

Figure K.2: Sketch of a culvert filled with water at high water levels at the river side.

The result of Table K.3 is a total soil volume of 779 m^3 on top of the Elshoutsluice. The volume converted to a vertical force gives:

$$F_{v,soil,start} = V_{soil,start} \cdot \frac{g \cdot \gamma_{soil,dry}}{1000} = 779.16 \cdot \frac{9.81 \cdot 1600}{1000} = 12229.70 \text{ kN} \quad \text{(K.3)}$$

A horizontal force is present due to the soil pressure on the bottom slab of the Elshoutsluice. Since the soil top level is exactly the same at the river side as hinterlands, the soil pressures cancel each other out. The horizontal load due to the soil pressure is not further included in the calculations.

Concrete

With the help of SCIA Engineer the self weight of the concrete elements of the Elshoutsluice are determined. The density of the concrete is set tot 2500 kg/m^3, which is within the boundaries given in Table K.1. Two situations are considered for the self weight of the concrete elements. First, the current state of the Elshoutsluice. Second, the Elshoutsluice after the construction phase.

Figure K.3 shows the modelled Elshoutsluice in SCIA Engineer, which resulted in a self weight of 4962089 kg. The self weight converted to a load gives $F_{v,concrete,start}$ = 48678.09 kN.

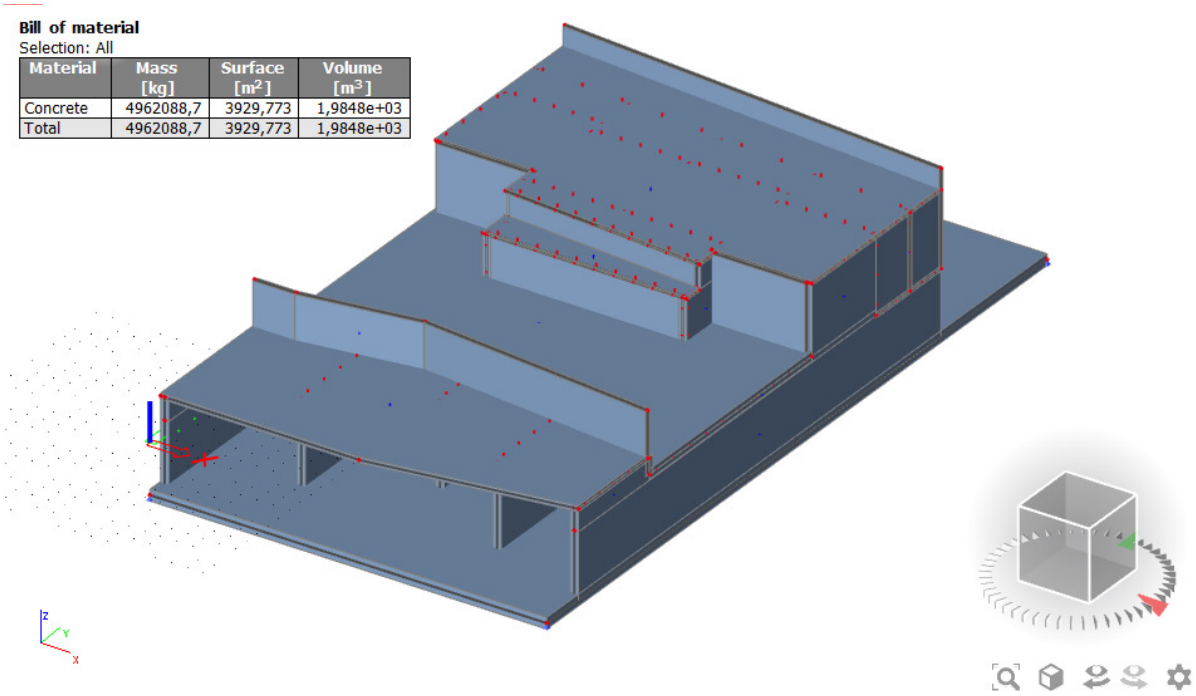

Figure K.3: The concrete elements of the current Elshoutsluice modelled in SCIA Engineer including the self weight at the start of the construction sequence. Top of the figure is the river side.

For the second situation, the new pedestrian tunnel above culvert 2 and the multi-functional area above culvert 3 is included in SCIA Engineer. Figure K.4 shows the modelled concrete elements of the Elshoutsluice in the finished condition. The total weight of the concrete elements is 5208699 kg. Converted to a load results in $F_{v,concrete,end}$ = 51097.34 kN.

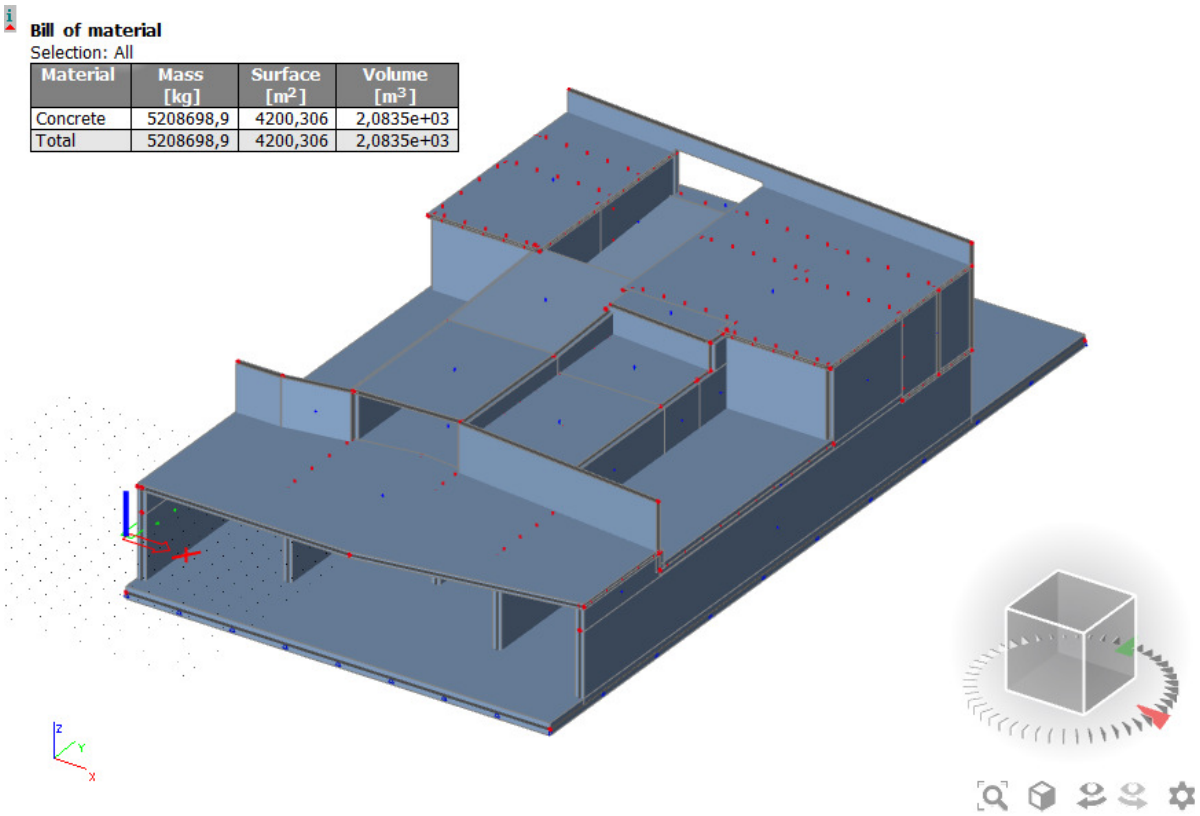

Figure K.4: The concrete elements of the current Elshoutsluice modelled in SCIA Engineer including the self weight at the end of the construction sequence.Top of the figure is the river side.

Other elements

The Elshoutsluice consists of more elements than soil, concrete and water. The remaining elements which increases the self weight are given in Table K.4.

Table K.4: The weight of single elements of the Elshoutsluice

Element	Weight [kN]	Reference
Radial gate	70	Jansen Venneboer BV (1986)
Lift gate	85	Jansen Venneboer BV (1986)
Distribution flap	70	Own assumption
Individual pump	51	Motralec (n.d.) and Waterschap Rivierenland (2018b)
Flap gate	70	Own assumption
Unfolding gate	85	Own assumption

K.1.2. Variable loads

The variable loads consists of the loads due to water and the loads due to traffic

Water

There is water present in the culverts of the Elshoutsluice. This volume of water increases the vertical downward force of the discharge sluice. A sketch is made of the water volume in culvert 2 when a high water level at the river occurs, see Figure K.2. As a simplification it is assumed that the volume of water in a culvert is approximately the same for each of the four culverts.

Three different load cases are considered for the self weight due to water. The fist situation is a high

water level of NAP + 3.66 m for reference year 2023 with a exceeding probability of 1/30,000 per year. This water level is used for the verification during the construction phase.

Table K.5: Determination of water load for situation 1.

Parameter	Value	Unit
A_hinterlands	40.80	m^2
A_culvert_hinterlands	60.49	m^2
A_culvert_river	10.65	m^2
A_river	57.31	m^2
V_water_culverts	1565.03	m^3
V_water_riverside	1415.44	m^3
V_water_hinterlands	905.76	m^3
F_v_water_1	*38123.90*	*kN*

The second load situation is similar to the first, but now culvert 2 is completely closed of due to the placement of the new gates. This situation corresponds to the construction phases 5 to 10, see Chapter 7.

Table K.6: Determination of water load for situation 2.

Parameter	Value	Unit
A_hinterlands	40.80	m^2
A_culvert_hinterlands	60.49	m^2
A_culvert_river	10.65	m^2
A_river	57.31	m^2
V_water_culverts	1173.77	m^3
V_water_riverside	1415.44	m^3
V_water_hinterlands	905.76	m^3
F_v_water_2	*34285.68*	*kN*

The last load situation is after the construction phase. A reference year of 2100 with climate scenario W^+ is considered. The water level corresponding to a exceeding probability of 1/30,000 per year is NAP + 4.22 m, see Table B.1 in Appendix B. A maintenance situation is considered where one culvert is completely dry due to inspection.

Table K.7: Determination of water load for situation 3.

Parameter	Value	Unit
A_hinterlands	40.80	m^2
A_culvert_hinterlands	60.49	m^2
A_culvert_river	10.65	m^2
A_river	62.31	m^2
V_water_culverts	1173.77	m^3
V_water_riverside	1539.10	m^3
V_water_hinterlands	905.76	m^3
F_v_water_3	*35498.76*	*kN*

Horizontal loads

The water pressure on both sides on the Elshoutsluice results in horizontal loads on the structure. Only horizontal loads due to water pressure is considered for two situations. The first is a high water

level of NAP + 3.66 m and the second a level of NAP + 4.22 m at the river. For both situation a hinterland water level of NAP + 1.50 m is considered. Table K.8 shows the determination of the sum of the horizontal forces for both high water level situations.

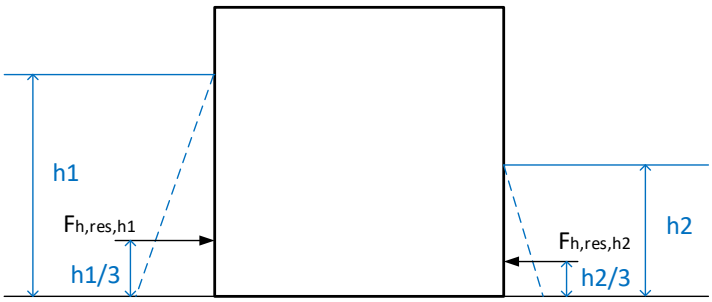

Figure K.5: The horizontal load due to the water pressure.

Table K.8: The calculation of the sum of the horizontal loads due to water pressure on the Elshoutsluice.

Parameter	NAP + 3.66 m	NAP + 4.22 m	Unit
h1	7.11	7.67	m
h2	4.95	4.95	m
$F_{h,res,h1}$	252.76	294.14	kN/m'
$F_{h,res,h2}$	-122.51	-122.51	kN/m'
$\sum F_h$	*130.25*	*171.63*	*kN/m'*

K.1.3. Infrastructure loads

The Elshoutsluice is designed according to the regulations VB 1974 (Stichting Commissie Voorschriften Beton, 1974). VB 1974 is the regulation for concrete structures. The current regulation is the NEN-EN 1991 series. The main difference between the design loads of the Elshoutsluice and the current design loads is the mobile load. The infrastructure loads according to the old and the current regulations are given in this subsection.

VOSB 1963

Design mobile loads were used according to the VOSB 1963. VOSB 1963 is the regulation for designing steel bridges. The mobile load includes traffic loads. These loads are divided into three load classes:

- Class 60: bridges in main traffic routes. Traffic diversion is not possible.
- Class 45: bridges in main traffic routes with a minimal use by heavy vehicles. Heavy vehicles are diverted via a different route.
- Class 30: bridges not intended for heavy vehicles.

It is assumed that the Elshoutsluice is categorised in load class 60. The characteristic distributed load for this class is 4 kN/m^2 with a maximum of 12 kN per m' lane. The concentrated load consists of three axle loads of 200 kN caused by one 2.5 m wide vehicle. Each axle load is distributed over four wheels. The spacing between the axle loads are given in Figure K.6.

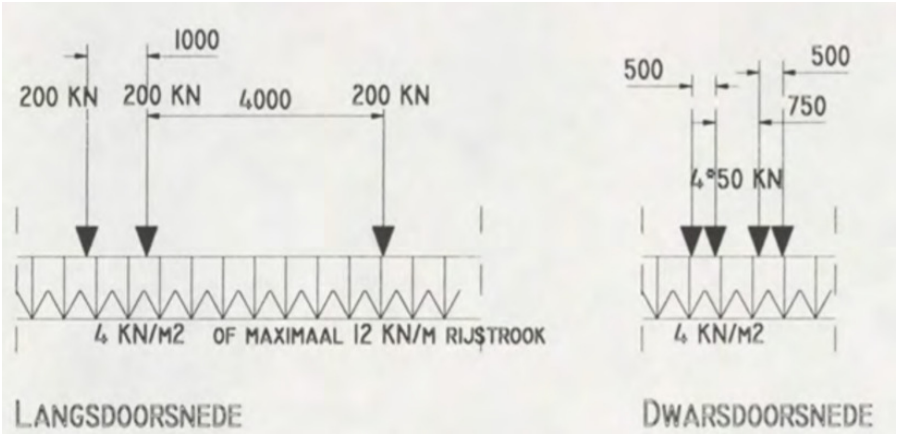

Figure K.6: The mobile load according to the VOSB 1963.

NEN-EN 1991

The infrastructure loads consists of loads due to pedestrians and the motorised vehicles. Table K.9 shows the loads according to NEN-EN 1991. For the traffic loads, the load situation number 1 for loads on bridges is considered according to Normcommissie (2015).

Table K.9: The used characteristic loads for buildings according to Normcommissie (2019a) and Normcommissie (2015)

Type of load	q_k **[kN/m^2]**	Q_k^a **[kN]**
People walking without obstacles	5	7
A large crowd	5	7
Traffic lane number 1	9	300
Traffic lane number 2	2.5	200

Figure K.7 shows the loading of the traffic on different traffic lanes. The spacing between the axle forces is 1.2 m. The most unfavourable situation of heavy traffic is assumed which results in a factor of α_{Qi} of 1.0 (Normcommissie, 2015).

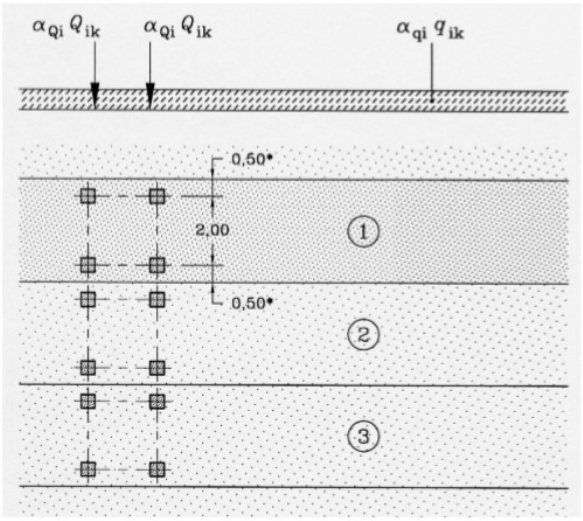

Figure K.7: The traffic load situation 1 according to NEN-EN 1991-2.

K.1.4. Summary vertical forces concrete, water and soil.

All the calculated loads due to self weight for different scenarios are summarised in Table K.10. These loads can be used for the stability checks.

Table K.10: Weight of the concrete, water inside the discharge sluice and the soil on top of the structure in different construction phases.

Parameter	Weight [kN]
$F_{v,concrete,start}$	48678.09
$F_{v,concrete,end}$	51097.34
$F_{v,soil,start}$	16961.74
$F_{v,soil,min}$	8480.87
$F_{v,soil,end}$	12229.70
$F_{v,water,1}$	38123.90
$F_{v,water,2}$	34285.68
$F_{v,water,3}$	35498.76

K.2. Stability checks

In this section the stability checks selected in section 9.1 are performed. The uplift check will be performed first. After that the lateral shear, rotational stability and bearing capacity is checked.

K.2.1. Uplift

Uplift of the hydraulic structure can occur if the water pressure under the structure is higher than the self weight. A sketch for uplifting is given in Figure K.8. The requirement for the uplift in equation form is:

$$\frac{S}{R} = \frac{F_b}{F_{self} + F_{t,piles}} < 1 \tag{K.4}$$

Where:

F_{self} = the self weight of the hydraulic structure in kN.
$F_{t,piles}$= the tension resistance of the foundation piles in kN.
F_b = the buoyancy force due to the upwards water pressure under the hydraulic structure in kN.

For the Elshoutsluice the following check is performed first:

$$\frac{S}{R} = \frac{F_b}{F_{self}} < 1 \tag{K.5}$$

This equation shows if tension in the foundation piles will occur due to the buoyancy force. If the structure does not fulfil the unity check above, the unity check in Equation K.4 must be performed as well for uplifting.

The water pressure under the structure by the water levels on both sides of the hydraulic structure, see Figure K.8. A permeable soil layer is assumed for this calculation. The water pressure at the bottom of the structure is calculated with:

$$p = h \cdot g \cdot \rho_{water} \tag{K.6}$$

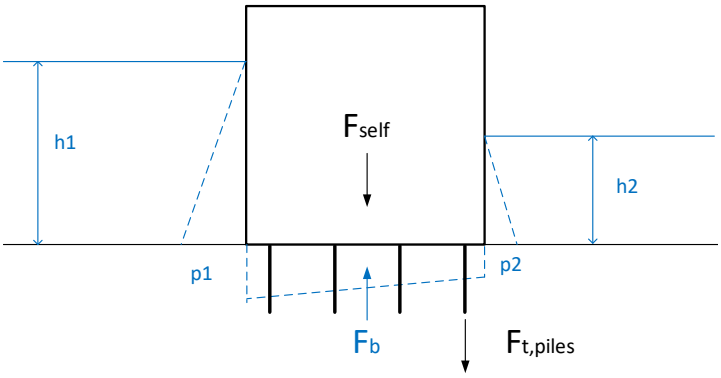

Figure K.8: Buoyancy force on a hydraulic structure.

There are sheet pile walls present under the Elshoutsluice structure. The first wall is located at the end of the bottom slab at river side and reaches a depth of NAP - 15.65 m. The second wall is located at the end of the bottom slab at the hinterland side and reaches a depth of NAP - 19.5 m. Figure K.9 shows the effect of the impermeable walls on the water pressure under the hydraulic structure.

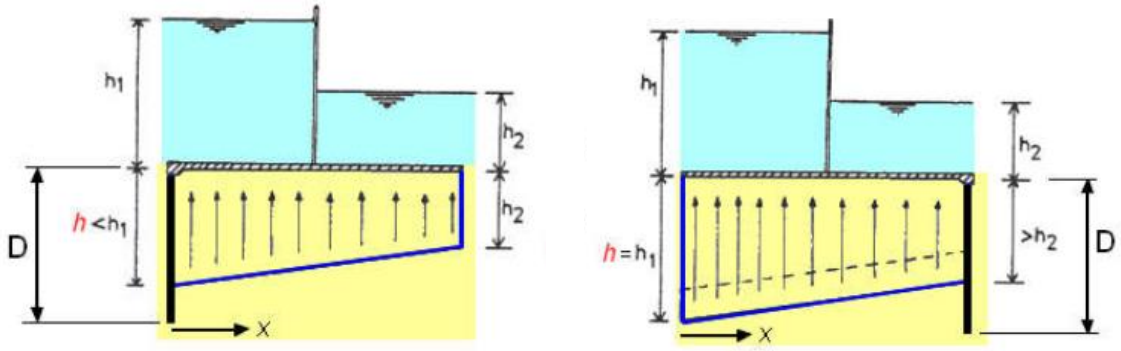

(a) A wall at the high water level side.

(b) A wall at the low water level side.

Figure K.9: The effect of an impermeable wall on the water pressure under a structure (source: Hydraulic Structures lecture-slides).

For Figure K.9a, the water pressure is calculated with:

$$p_x = \left[h - (h_1 - h_2) \cdot \frac{2D + x}{2D + L} \right] \tag{K.7}$$

The water pressure for Figure K.9b is determined with:

$$p_x = \left[h - (h_1 - h_2) \cdot \frac{x}{2D + L} \right] \tag{K.8}$$

The selected situations in section 9.1 for the check in uplift are performed. First the self weight for the Elshoutsluice in construction phase 1 is determined, see Table K.11.

Table K.11: The self weight of the Elshoutsluice for construction phase 1.

Parameter	Load [kN]
$F_{v,concrete,start}$	48678.09
$F_{v,soil,min}$	8480.87
$F_{v,water,1}$	38123.90
3 radial gates	210.00
4 lift gates	340.00
Distribution flap	70.00
6 pumps	306.07
$\sum V_1$	*96208.93*

The buoyancy force for construction phase 1 is calculated for a high water level of NAP + 3.66 m. The water level hinterlands is NAP + 1.50 m in this case. Table K.12 shows the determination of the water pressure.

Table K.12: Determination of the water pressure under the hydraulic structure with a high water level of NAP + 3.66 m at the Lek river.

(a) Determination of $p_{x,1}$.

Parameter	Value	Unit
h	7.11	m
h_1	7.11	m
h_2	4.95	m
D	12.2	m
x	0.00	m
L	46.73	m
ρ	1000	kg/m^3
g	9.81	m/s^2
$p_{x,1}$	*62.48*	*kN/m^2*

(b) Determination of $p_{x,2}$.

Parameter	Value	Unit
h	7.11	m
h_1	7.11	m
h_2	4.95	m
D	16.05	m
x	46.73	m
L	46.73	m
ρ	1000	kg/m^3
g	9.81	m/s^2
$p_{x,2}$	*57.19*	*kN/m^2*

$$F_b = \frac{p_{x,1} + p_{x,2}}{2} \cdot B \cdot L = \frac{62.48 + 57.19}{2} \cdot 24.7 \cdot 46.73 = 69061.00 \text{ kN} \tag{K.9}$$

The unity check for tension in the foundation piles for construction phase 1 is:

$$\frac{F_b}{F_{self}} = \frac{69061.00}{96208.93} = 0.72 < 1, \text{ OK} \tag{K.10}$$

There is no tension in the foundation piles. The Elshoutsluice will not float upwards due to the water pressure for construction phase 1.

The second situation in which the uplift check is performed is for the maintenance of one culvert in the use phase when high water occurs. The Elshoutsluice is finished in this situation. A calculation of the load due to self weight is made and given in Table K.13.

Table K.13: The self-weight of the Elshoutsluice in finished form during the maintenance of 1 culvert in the use phase.

Parameter	**Load [kN]**
$F_{v,concrete,end}$	51097.34
$F_{v,soil,end}$	12229.70
$F_{v,water,3}$	35498.76
2 radial gates	140.00
3 lift gates	255.00
Distribution flap	70.00
Unfolding gate	85.00
Flap gate	70.00
6 pumps	306.07
$\sum V_{maintenance}$	*99751.87*

A selection is made for an extreme water level of NAP + 4.22 m at the river. The water level hinterlands remains NAP + 1.50 m. With these values the water pressure is determined. The calculation and results are shown in Table K.14.

Table K.14: Determination of the water pressure under the hydraulic structure with a high water level of NAP + 4.22 m at the Lek river.

(a) Determination of $p_{x,1}$.

Parameter	**Value**	**Unit**
h	7.67	m
h_1	7.67	m
h_2	4.95	m
D	12.2	m
x	0.00	m
L	46.73	m
ρ	1000	kg/m^3
g	9.81	m/s^2
$p_{x,1}$	*66.09*	*kN/m^2*

(b) Determination of $p_{x,2}$.

Parameter	**Value**	**Unit**
h	7.67	m
h_1	7.67	m
h_2	4.95	m
D	16.05	m
x	46.73	m
L	46.73	m
ρ	1000	kg/m^3
g	9.81	m/s^2
$p_{x,2}$	*59.43*	*kN/m^2*

$$F_b = \frac{p_{x,1} + p_{x,2}}{2} \cdot B \cdot L = \frac{66.09 + 59.43}{2} \cdot 24.7 \cdot 46.73 = 72434.82 \text{ kN} \tag{K.11}$$

The unity check for tension in the foundation piles is performed for a maintenance situation in the use phase:

$$\frac{F_b}{F_{self}} = \frac{72434.82}{99751.87} = 0.73 < 1, \text{ OK} \tag{K.12}$$

The result is no tension in the foundation piles for the maintenance case. It can be concluded that the Elshoutsluice is stable for uplifting for both the construction phase 1 and the maintenance in use phase.

K.2.2. Lateral shear

The Elshoutsluice is founded on 190 piles, therefore the horizontal forces on the discharge sluice will be transferred to the foundation piles. The friction force of the soil will not be taken into account, only the shear capacity of the foundation piles will be checked. A sketch of the horizontal stability

is shown in Figure K.10. The check for the lateral shear is:

$$\frac{S}{R} = \frac{\sum F_h}{V_{r,min,piles}} < 1 \tag{K.13}$$

Where:

$\sum F_h$ = the sum of horizontal forces acting on the structure in kN.
$V_{r,min,piles}$ = the shear force capacity of the foundation piles in kN.

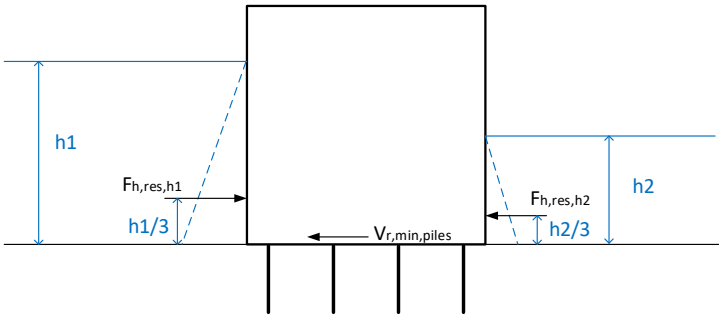

Figure K.10: Side view sketch of the horizontal stability.

The sum of horizontal forces depends on the soil pressure and water pressure on the structure. Since the soil level is the same at both sides of the hydraulic structure, these horizontal forces cancel each other out. Therefore, the force due to soil is not included in the calculation. The sum of horizontal forces depends only on the water pressure sketched in Figure K.10.

The horizontal force due to the water pressure is calculated with:

$$F_{h,res,h} = \frac{1}{2} \cdot g \cdot \rho_{water} \cdot h^2 \tag{K.14}$$

The determination of the sum of horizontal forces is given in Table K.8.

Table K.15: The determination of the total horizontal force due to water pressure for different water levels.

Parameter	**NAP + 3.66 m**	**NAP + 4.22 m**	**Unit**
h1	7.11	7.67	m
h2	4.95	4.95	m
$F_{h,res,h1}$	247.96	288.56	kN/m'
$F_{h,res,h2}$	-120.18	-120.18	kN/m'
$\sum F_h$	*127.77*	*168.37*	*kN/m'*

The maximum horizontal force is 168.37 times the width of 24.7 of the structure. This results in horizontal force of 4158.76 kN. The maximum horizontal force must not exceed the shear capacity of the foundation piles. The lowest value for the shear capacity for concrete without reinforcement is used according to NEN-EN 1992:

$$V_{r,min} = b \cdot d \cdot 0.035 \cdot k^{3/2} \cdot \sqrt{f_{ck}} \tag{K.15}$$

Where:

$$k = 1 + \sqrt{\frac{200}{d}} \leq 2 \tag{K.16}$$

With:

b = width of a cross-section in mm.
d = effective depth of a cross-section in mm.
f_{ck} = the characteristic compressive cylinder strength of concrete at 28 days in MPa.

The dimension of one foundation pile is assumed to be 420 mm x 420 mm. The selection of these dimensions is based on a drawing according to Haskoning B.V. (1984b) for which the square locating the foundation pile is slightly less than a culvert wall of 0.5 m thick. The assumption is made that d = 0.9 · h. The characteristic compressive cylinder strength is from the concrete class B22.5. Table K.16 shows the determination of the shear capacity of one foundation pile with the use of the equations Equation K.15 and Equation K.16.

Table K.16: The minimum shear capacity for one foundation pile.

Parameter	Value	Unit
b	420	mm
h	420	mm
d	378	mm
f_{ck}	18	MPa
k	1.73	-
$V_{r,min}$	*53521.97*	*N*

The calculated minimum shear resistance is for 1 singe pile. Shear resistance of the reinforcement is neglected since there is no information available on possible reinforcement in the foundation piles. There are 190 piles in total. The total shear resistance is:

$$V_{r,min,piles} = V_{r,min} \cdot n = 53.52 \cdot 190 = 10169.17 \text{ kN} \tag{K.17}$$

The horizontal stability check is performed:

$$\frac{\sum F_h}{V_{r,min,piles}} = \frac{4158.76}{10169.17} = 0.41 < 1, \text{ OK} \tag{K.18}$$

K.2.3. Pile bearing capacity

The Elshoutsluice is founded on piles. With the Koppejan method, the bearing capacity of the soil under the tip of the foundation pile and the shaft friction are determined. The soil bearing capacity check is given by:

$$\frac{S}{R} = \frac{\sum V}{F_{r,total}} < 1 \tag{K.19}$$

With:

$F_{r,total}$ = the total bearing capacity of the foundation of a structure in kN.
$\sum V$ = the sum of vertical forces in kN.

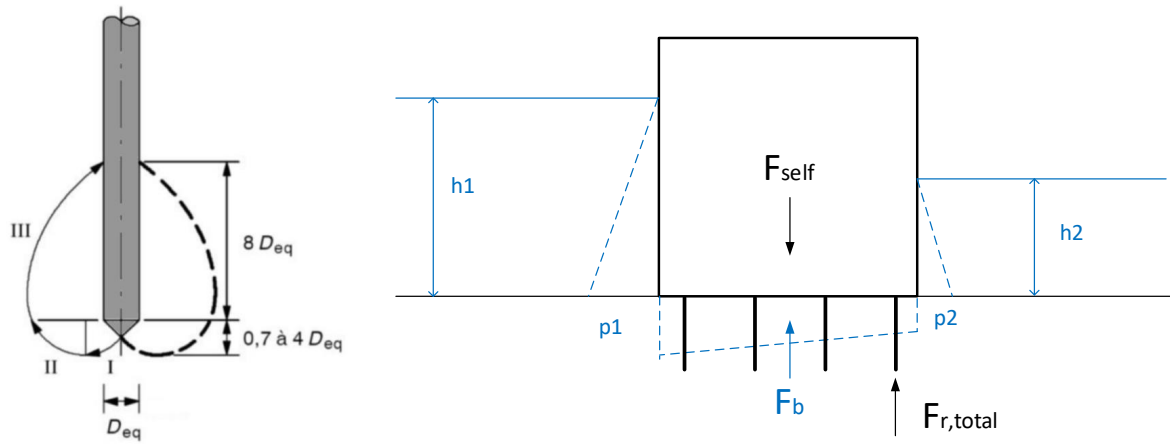

(a) The slip planes according to Koppejan (Voorendt & Molenaar, 2020).

(b) Sketch of the bearing capacity.

Figure K.11: Bearing capacity.

The bearing capacity of a compression pile consist of the shaft friction, the negative shaft friction and the tip resistance. In equation form (Voorendt & Molenaar, 2020):

$$F_{r,max} = F_{r,max,tip} + F_{r,max,shaft} - F_{s,nk} \tag{K.20}$$

$F_{r,max,tip}$ = the tip resistance in kN.
$F_{r,max,shaft}$ = pile shaft friction in kN.
$F_{s,nk}$ = negative shaft friction in kN, which is not included in the ULS.

The formulas in the list above are given by (Voorendt & Molenaar, 2020):

$$F_{r,max,tip} = A_{tip} \cdot p_{r,max,tip} \tag{K.21}$$

$$F_{r,max,shaft} = O_{p,avg} \int_0^{\Delta L} p_{r,max,shaft} dz \tag{K.22}$$

$$F_{s,nk} = O_s \sum h \cdot \sigma'_{v,avg} \cdot K_0 \cdot \tan\delta \tag{K.23}$$

Where:

A_{tip} = the tip surface area of the foundation pile in kN.
$p_{r,max,tip}$ = the maximum tip resistance in kN/m^2.
$O_{p,avg}$ = the circumference of the pile shaft in m^2.
ΔL = the length of the pile in m.
$p_{r,max,shaft}$ = the maximum shaft friction of a foundation pile in kN/m^2.
O_s = circumference of the pile in m.
h = height of the soil layer in m.
$\sigma'_{v,avg}$ = the average effective soil stress in a soil layer in kN/m^2.
K_0 = the neutral soil pressure coefficient.
$tan\delta$ = the friction between concrete and soil.

The maximum tip resistance is determined with the use of the Koppejan method:

$$p_{r,max,tip} = 1/2 \alpha_p \beta s \left(\frac{q_{c,I,avg} + q_{c,II,avg}}{2} + q_{c,III,avg} \right) \tag{K.24}$$

With:

α_p	=	pile class factor, determined with Figure K.12.
β	=	shape factor for the influence of the foot of the pile, which can be determined with Figure K.13a.
s	=	shape factor for the cross-section of the foot of the pile, which can be determined with Figure K.13b.
$q_{c,I,avg}$	=	the average value of the cone resistance along section I, see Figure K.11a.
$q_{c,II,avg}$	=	the average value of the cone resistance along section II, see Figure K.11a.
$q_{c,III,avg}$	=	the average value of the cone resistance along section III, see Figure K.11a.

pile class / type	α_p
• **soil displacing placement methods**	
- driven piles	0,70
- driven piles, formed in the soil	0,70
- screwed piles, formed in the ground	0,63
- prefabricated screwed piles	0,56
• **piles with little soil displacement, such as steel profiles and open steel tubes**	0,70
• **piles made with soil replacement**	
- auger piles	0,56
- drilled piles	0,35
- pulsated piles	0,35

Figure K.12: The values of α_p. Source: (Voorendt & Molenaar, 2020).

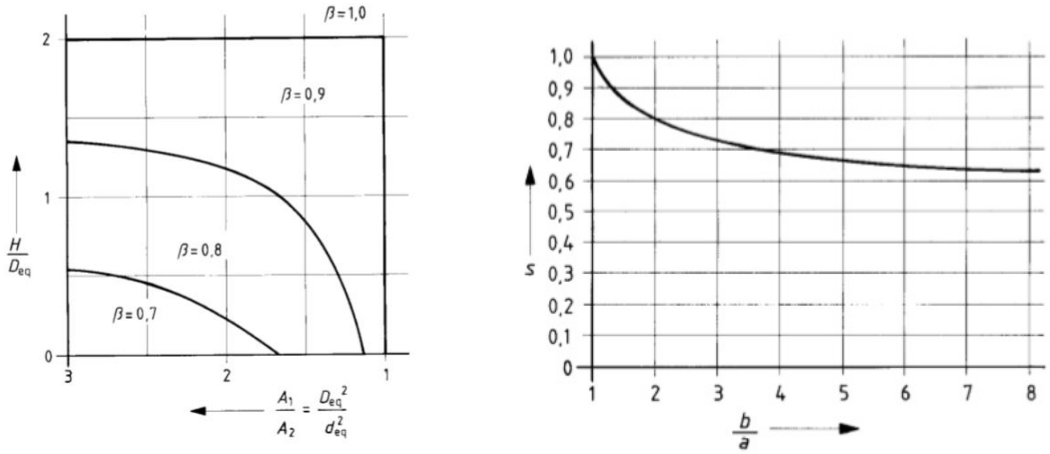

(a) Factor for the shape of the pile footing β.

(b) Factor for the shape of the pile footing s.

Figure K.13: Tables for determining the shape factors (Voorendt & Molenaar, 2020)

For the Koppejan method the equivalent pile tip diameter is needed. The equivalent pile tip diameter for a square or rectangular pile is:

$$D_{eq} = \sqrt{\frac{4}{\pi}} a\sqrt{b/a} = \sqrt{\frac{4}{\pi}} 420\sqrt{420/420} = 474 \text{ mm} \tag{K.25}$$

The average maximum shaft friction is calculated with (Voorendt & Molenaar, 2020):

$$p_{r,max,shaft} = \alpha_s q_{c,z,a} \tag{K.26}$$

With the average shaft friction, the calculation of the pile shaft friction is simplified to:

$$F_{r,max,shaft} = O_s \cdot L_s \cdot p_{r,max,shaft} \tag{K.27}$$

In which:

α_s = the influence factor of the method of the pile installation determined with Figure K.14.
$q_{c,z,a}$ = the average cone resistance over length L_s in kN/m^2.
L_s = the distance from the pile tip up to the point of a cone resistance of 2 MPa given in m.

Pile class / type	α_s
• **ground displacing placement methods**:	
- driven smooth prefab concrete pile and steel tube pile with closed tip	0,010
- pile made in the soil, whereby the concrete column presses directly onto the ground and the tube was driven back out of the ground	0,0014
- in the case of a tube removed by vibration	0,0012
- tapered wooden pile	0,0012
- screwed piles	
with grout injection or grout mix	0,009
without grout	0,006
• **piles with little ground displacement**	
- steel profiles	0,0075
• **piles made with ground replacement**	
- auger piles	0,006
- drilled piles	0,006
- pulsated piles	0,005

Figure K.14: The values of α_s. Source: (Voorendt & Molenaar, 2020).

The depth of most of the foundation piles is NAP - 17.5 m according to drawings of Haskoning (1984). Figure K.15 shows the determination of the average cone resistance values with the Koppejan method. The calculation of the tip resistance is given in Table K.17.

Table K.17: The tip resistance of one foundation pile.

Paramter	Value	Unit
α_p	0.7	-
β	1	-
s	1	-
$q_{c,I,avg}$	16.3	N/mm^2
$q_{c,II,avg}$	9.5	N/mm^2
$q_{c,II,avg}$	8.0	N/mm^2
$p_{r,max,tip}$	7.31	N/mm^2
$F_{r,max,tip}$	*1288.82*	*kN*

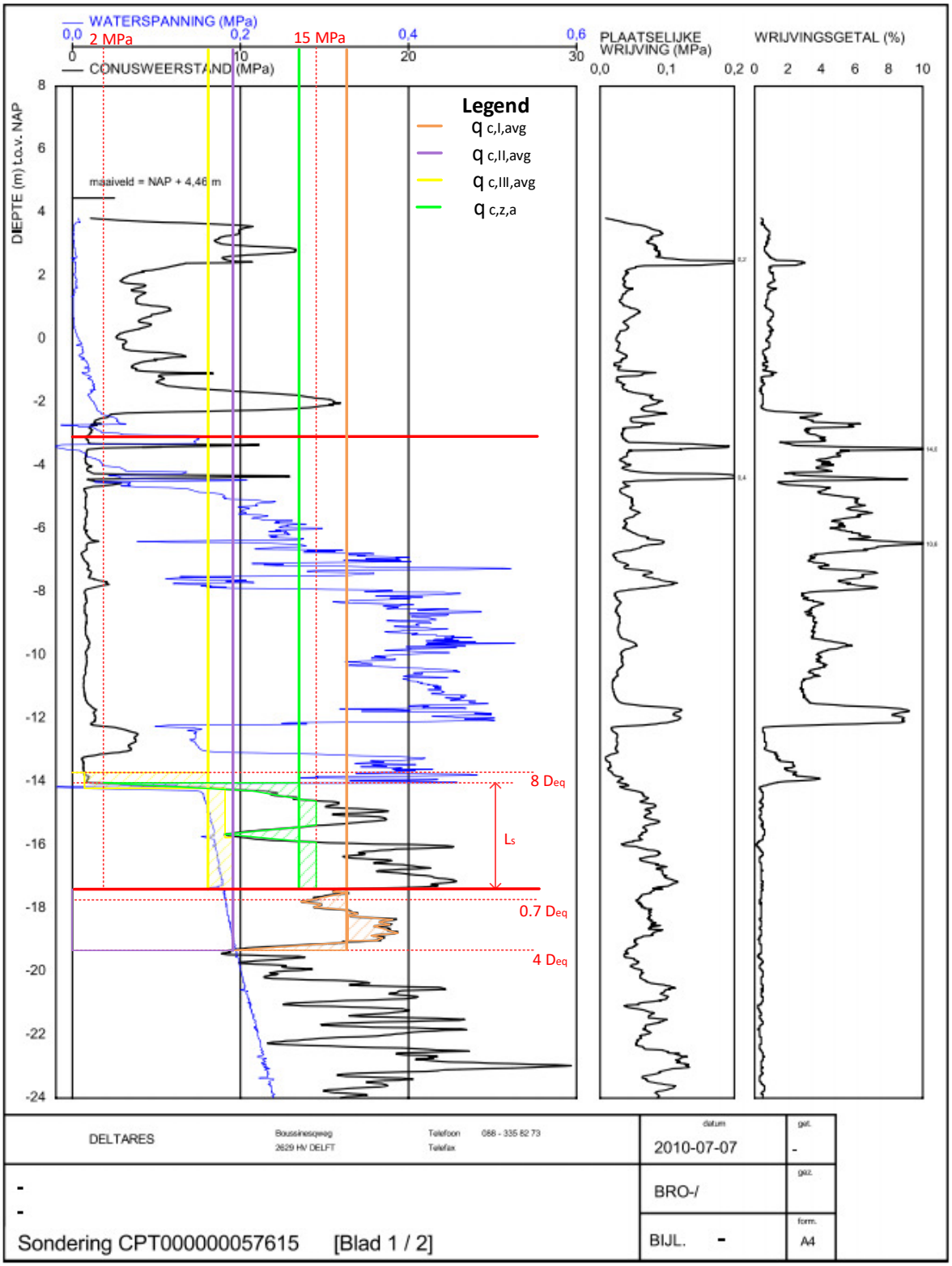

Figure K.15: Execution of the Koppejan method.

The circumference is determined as following:

$$O_s = 4 \cdot B_{pile} = 4 \cdot 0.42 = 1.68 \text{ m} \tag{K.28}$$

With this value the pile shaft friction is calculated, see Table K.18.

Table K.18: The pile shaft friction determination.

Paramter	Value	Unit
α_s	0.01	-
$q_{c,z,a}$	13.5	N/mm^2
L_s	3.5	m
O_s	1.68	m
$p_{r,max,shaft}$	0.135	N/mm^2
$F_{r,max,shaft}$	*793.80*	*kN*

For the pile shaft friction, only the clay layer is considered. The sand layer starts at approximately NAP - 14 m. The angle of internal friction φ' for clay is selected from Normcommissie (2019b). The angle of wall friction for clay is calculated with Voorendt and Molenaar (2020):

$$\delta = 1/3\varphi' \tag{K.29}$$

The average effective soil stress for the saturated clay layer is determined for a low water level of NAP - 0.40 m, which is determined according to Rijkswaterstaat (n.d.). Table K.19 gives the determination of the negative pile shaft friction. The bearing capacity of one foundation pile in ULS is:

Table K.19: The negative pile shaft friction calculation.

Paramter	Value	Unit
O_s	1.68	m
h_{clay}	10.55	m
$\sigma'_{v,avg}$	55.67	kN/m^2
K_0	0.658	-
φ'	20	°
δ	6.67	°
tan δ	0.117	-
$f_{s,nk}$	*115.33*	kN

$$F_{r,max} = F_{r,max,tip} + F_{r,max,shaft} = 1288.82 + 793.80 = 2082.62 \text{ kN} \tag{K.30}$$

There are 190 foundation piles underneath the Elshoutsluice structure, this results in a total bearing capacity of:

$$F_{r,tot} = F_{r,max} \cdot n = 2082.62 \cdot 190 = 395697.80 \text{ kN} \tag{K.31}$$

The sum of vertical forces for a high water level of NAP + 4.22 m and a low water level after the construction phases are calculated. Table K.20 shows the determination of the sum of vertical forces forces for the first case.

Table K.20: The sum of vertical forces for Elshoutsluice after the construction phase with a high water level of NAP + 4.22 m.

Element	**Vertical Force [kN]**	**Unit**
$F_{v,concrete,end}$	51097.34	m
$F_{v,soil,end}$	12229.70	m
$F_{v,water,4}$	39336.99	m
2 radial gates	140.00	m
3 lift gates	255.00	m
Distribution flap	70.00	m
Unfolding gate	85.00	kg/m^3
Flap gate	70.00	m/s^2
6 pumps	306.07	kN/m^2
F_b	-72434.82	kN
$\sum V$	*31155.27*	kN

The water level in the discharge sluice is equal to the water level in the Lek river for the low water level case. The buoyancy force is assumed to be approximately equal to the weight of the water inside the four culverts. Therefore, these forces cancel each other out and are not included in the sum of vertical forces for this situation. Table K.21 gives the sum vertical forces for the low water situation.

Table K.21: The self-weight of the Elshoutsluice in a finished state for low water levels.

Element	**Vertical Force [kN]**
$F_{v,concrete,end}$	51097.34
$F_{v,soil,end}$	12229.70
2 radial gates	140.00
3 lift gates	255.00
Distribution flap	70.00
Unfolding gate	85.00
Flap gate	70.00
6 pumps	306.07
$\sum V$	*64253.10*

From the analysis of both situations can be concluded that the highest sum of vertical forces is 64253.10 kN. The bearing capacity check is:

$$\frac{64253.10}{395697.80} = 0.16 < 1, \text{ OK} \tag{K.32}$$

K.2.4. Rotational stability

For the rotational stability the foundation piles are checked if tension occurs:

$$\frac{S}{R} = \frac{\sum M / \sum V}{1/6b} < 1 \tag{K.33}$$

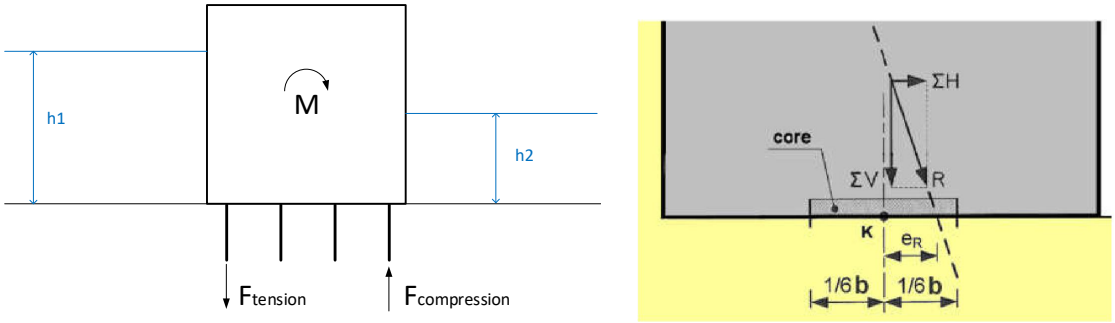

(a) Rotational stability

(b) Rotational stability

Figure K.16: Sketch of the rotational stability Voorendt and Molenaar (2020)

The selected cases from section 9.1 are the construction phase 1 with a high water level and a maintenance situation after the construction phases. The sum of vertical forces are calculated in subsection K.2.1 for the uplift check. The sum of moments consist of the horizontal forces due to the water pressure and the distance to the bottom of the structure, see Figure K.10. Table K.22 shows the determination of the sum of acting moments on the Elshoutsluice for the selected cases.

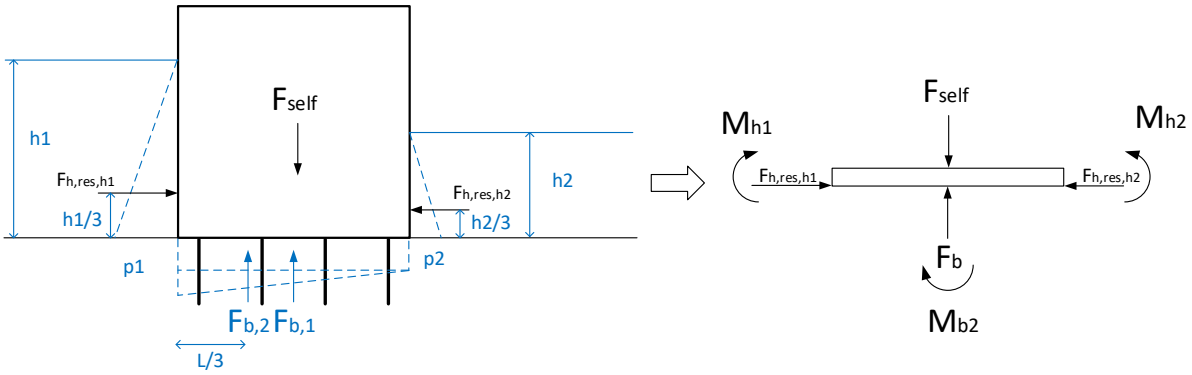

Figure K.17: The translation of the forces on the structure to the bottom of the structure.

Table K.22: The determination of the sum of acting moments on the Elshoutsluice.

Parameter	NAP + 3.66 m	NAP + 4.22 m	Unit
h1	7.11	7.67	m
h2	4.95	4.95	m
$F_{h,res,h1}$	247.96	288.56	kN/m'
$F_{h,res,h2}$	-120.18	-120.18	kN/m'
Distance_bottom_1	2.37	2.56	m
Distance_bottom_2	1.65	1.65	m
M_{h1}	587.66	737.74	kNm/m'
M_{h2}	-198.30	-198.30	kNm/m'
p_{x1}	61.12	64.38	kN/m^2
p_{x2}	55.83	57.71	kN/m^2
F_{b2}	123.65	155.70	kN/m'
Distance_centre	15.58	15.58	m
M_b	1925.98	2425.31	kNm/m'
$\sum M$	*2315.33*	*2964.74*	*kNm/m'*

The calculated values for the sum of moment in Table K.22 are multiplied by the width of the Elshoutsluice of 24.7 m. This results in the unity check for the construction phase 1:

$$\frac{\sum M/\sum V}{1/6b} = \frac{57188.74/27932.66}{1/6 \cdot 46.73} = 0.26 < 1, \text{ OK} \tag{K.34}$$

For the maintenance situation in the use phase, the unity check is given by:

$$\frac{\sum M/\sum V}{1/6b} = \frac{73229.11/28305.23}{1/6 \cdot 46.73} = 0.33 < 1, \text{ OK} \tag{K.35}$$

The result of the calculation is no tension in the foundation piles due to moments for both selected situations.

K.3. Strength analysis

The transfer of forces of the current situation of the Elshoutsluice is compared to the new situation for the Elshoutsluice. A cross-section of 1 m width is selected from the discharge sluice to perform the load transfer analysis. The location with the most changes in structure and loads is right underneath the motorised vehicle road, see Figure K.18. For this cross-section, the load transfer analysis is performed. The difference in loading on the existing lateral walls of the culverts and the slab on top of these walls is checked with the use of Matrixframe.

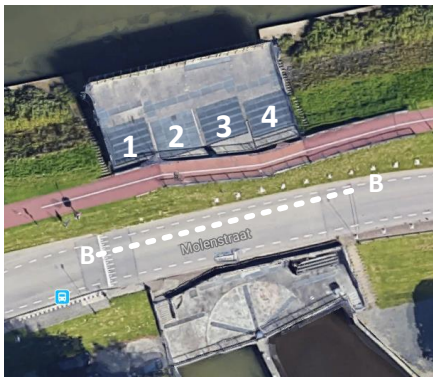

Figure K.18: The selected cross-section for the load distribution check. (source: google maps)

K.3.1. Matrixframe input

The cross-section of Figure K.18 is translated to a 2D beam geometry in Matrixframe, see Figure K.19. The connections of the concrete elements are assumed rigid. The foundation piles are mostly located directly underneath or nearby a lateral wall and are therefore included as vertical and horizontal constraints directly under the lateral walls.

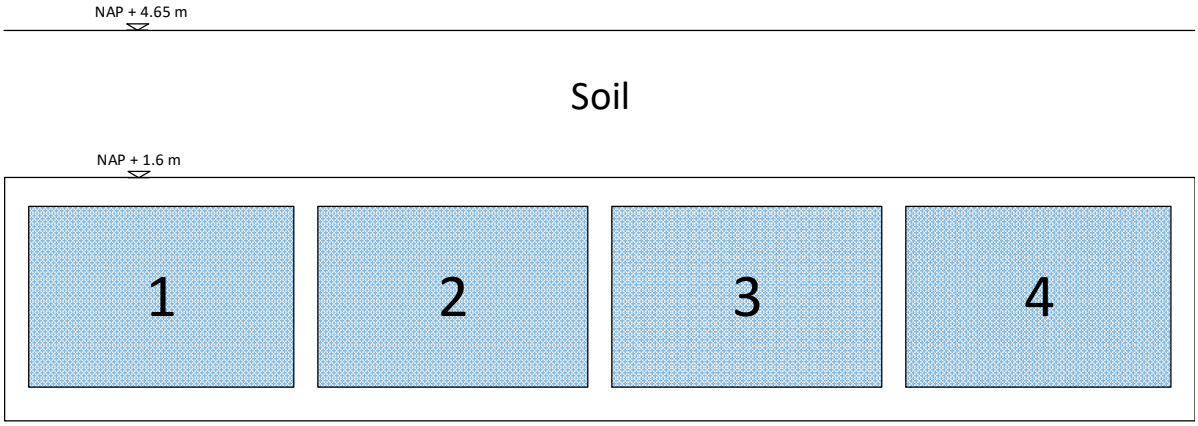

(a) A front view sketch of the cross-section B-B of the Elshoutsluice.

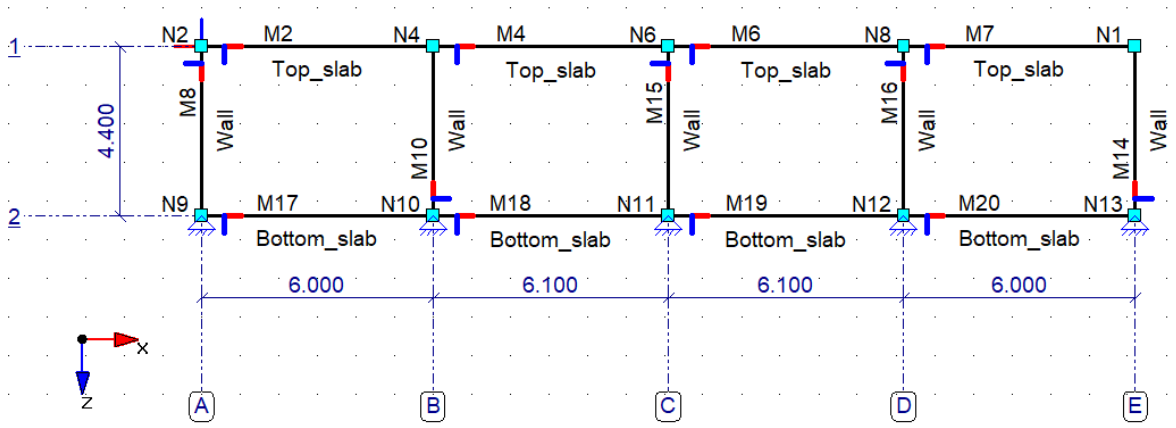

(b) The geometry in Matrixframe.

Figure K.19: The current situation of the Elshoutsluice.

The Elshoutsluice is made with concrete of strength class B 22.5 according to Haskoning B.V. (1984a). This results in a characteristic cylinder compression strength of f_{ck} = 18 MPa according to NEN 8700. For the discharge sluice reinforcement steel of the class FeB 400 HW is used (Haskoning B.V., 1984a). This results in f_{yk} = 400 MPa and f_{yd} = 348 MPa according to Normcommissie (2018).

The reinforcement in the lateral walls and the slab is unknown. The calculations are performed with the properties of concrete only, since this results in the most unfavourable resistance situation. For the input of Matrixframe, a modulus of elasticity for cracked concrete is used. The determination of the modulus of elasticity for concrete class B 22.5 is as following according to NEN-EN 1992:

$$f_{cm} = f_{ck} + 8 = 18 + 8 = 26 \text{ N/mm}^2 \tag{K.36}$$

$$E_{cm} = 22[f_{cm}/10]^{0.3} = 22[26/10]^{0.3} = 29 \text{ GPa} \tag{K.37}$$

The modulus of elasticity for cracked concrete is assumed to be approximately 1/3 of E_{cm} which

results in value of 9667 N/mm^2. The material input for the Matrixframe geometry is given in Table K.23.

Table K.23: The material input for Matrixframe for the current situation of the Elshoutsluice

Element	**h [m]**	**I [m^4]**	**E [kN/m^2]**
Top slab	0.6	0.018000	9666667
Bottom slab	0.7	0.028583	9666667
Walls	0.5	0.010417	9666667

The initial design loads on the Elshoutsluice are based on the VB 1974. The load due to the self weight of the soil on top of the structure is 47.87 kN/m^2 and is a permanent load. The characteristic load for traffic is 4 kN/m^2 and is a variable load, see subsection K.1.3. A variable load can be applied in various ways on the structure, see Figure K.20. Different load cases are made in Matrixframe to determine the highest loading on the structure elements. Only the top slab and walls are checked on the loading difference since the loads on the bottom slab will not differ much in the new situation. Therefore, only the self weight of the top slab (14.72 kN/m^2) and of the walls (12.26 kN/m^2) are included. The bottom slab is only included for the rotation stiffness of the connection between the wall and bottom slab. The safety factor for all the loads is 1.7 according to Stichting Commissie Voorschriften Beton (1974).

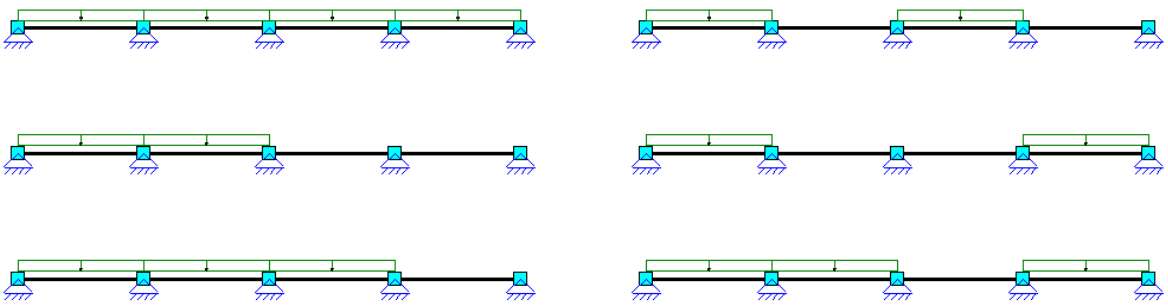

Figure K.20: The placement of the variable load on different spans of the structure.

For the new situation a pedestrian tunnel and a multi-functional area is added on top of the existing structure, see Figure K.21a. The new elements can only transfer horizontal and vertical loads to the existing structure as a simplification of the analysis.

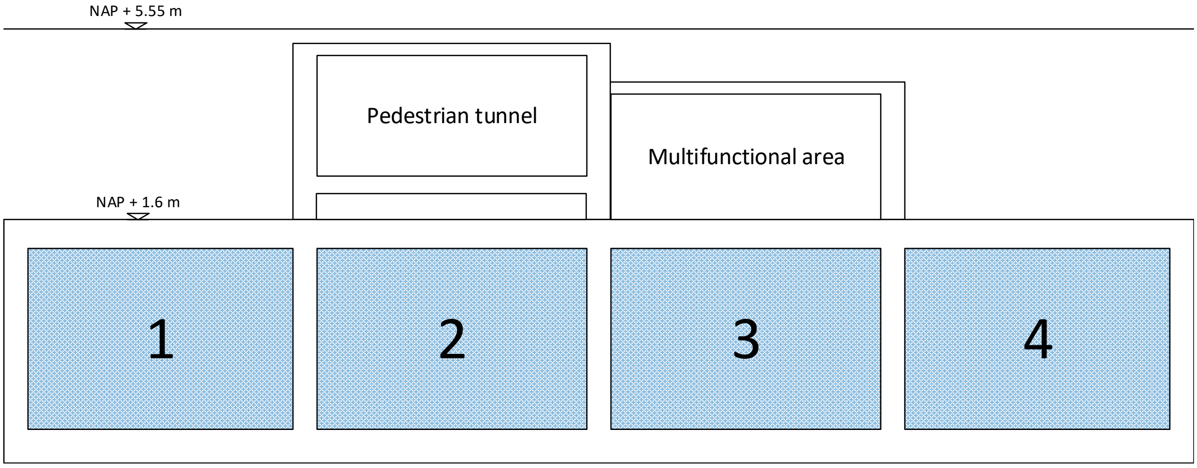

(a) A front view sketch of the cross-section B-B of the Elshoutsluice including the pedestrian tunnel and multi-functional area.

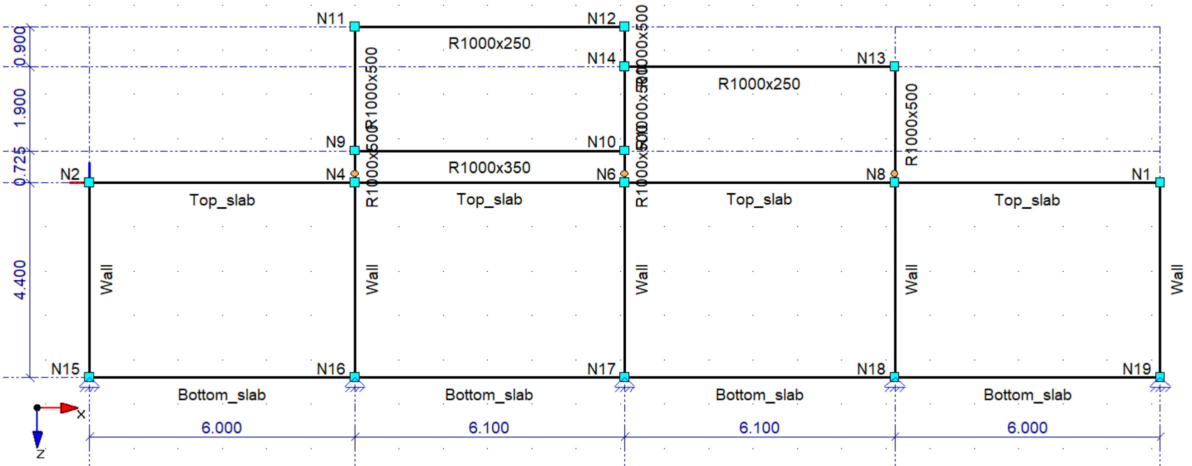

(b) The geometry in Matrixframe for the new situation.

Figure K.21: The new situation of the Elshoutsluice.

The loads on the new situation is determined according to Normcommissie (2019a). Two load combinations are considered for the limit state STR, see section A.1. The load effects are determined by:

$$E_{d,1} = E\left\{\sum_{j\geq 1}^{n} \gamma_{G,j}\cdot G_{k,j} + \gamma_p \cdot P + \gamma_{Q,1}\cdot \psi_{0,1}\cdot Q_{k,1} + \sum_{i>1}^{n} \gamma_{Q,i}\cdot \psi_{0,i}\cdot Q_{k,i}\right\}$$
$$E_{d,2} = E\left\{\sum_{j\geq 1}^{n} \xi_j \cdot \gamma_{G,j}\cdot G_{k,j} + \gamma_p \cdot P + \gamma_{Q,1}\cdot Q_{k,1} + \sum_{i>1}^{n} \gamma_{Q,i}\cdot \psi_{0,i}\cdot Q_{k,i}\right\} \quad \text{(K.38)}$$

The Elshoutsluice is part of a primary flood defence and therefore categorised in consequence class 3 (Rijkswaterstaat, 2018b). For the load combination 1 the following values are determined for the load factors and reduction factor for consequence class 3 for adjustments of an existing structure according to NEN 8700 (Normcommissie, 2018):

$\gamma_{G,unfavourable} = 1.4$
$\gamma_{G,favourable} = 0.9$
$\gamma_Q = 1.5$
$\psi_0 = 0.7$, which result from traffic areas.

$$\gamma_Q \cdot \psi_Q = 1.5 \cdot 0.7 = 1.05 \quad \text{(K.39)}$$

The following load factors are used for the second load effect combination according to NEN 8700 (Normcommissie, 2018):

$\xi \cdot \gamma_{G,unfavourable} = 1.25$
$\gamma_{G,favourable} = 0.9$
$\gamma_Q = 1.5$

Table K.24 shows the used characteristic loads and the load factors of both load combinations for the structural linear analysis performed with MatrixFrame. The pedestrian/bicycle load and traffic load is based on NEN-EN 1991. The level of the road on top of the sluice is heightened which results in an increase of soil on top of the structure.

Table K.24: The characteristic loads and the load factors as input for Matrixframe

Load type	**Characteristic load [kN/m^2]**	**Load factor for $E_{d,1}$**	**Load factor for $E_{d,2}$**
Pedestrian/bicycle	5.00	1.05	1.5
Traffic, 1st lane	9.00	1.05	1.5
Soil above culvert 2	4.71	1.4	1.25
Soil above culvert 3	17.27	1.4	1.25
Soil above culvert 1 & 4	62.00	1.4	1.25
Self weight top slab	14.72	1.4	1.25
Self weight walls	12.26	1.4	1.25
Self weight roof	6.13	1.4	1.25
Self weight ped. floor	8.58	1.4	1.25

K.3.2. Comparison of results

A linear analysis is performed with the use of Matrixframe. The highest normal forces, shear forces and bending moments are determined from all the load combinations for the current and new situations. A comparison is made between the new and current situation to determine if and where in the top slab and walls possible strengthening is needed.

First, the normal forces are compared. The normal forces in the current situation are given in Figure K.22. Figure K.23 shows the result of the normal forces for the new situation.

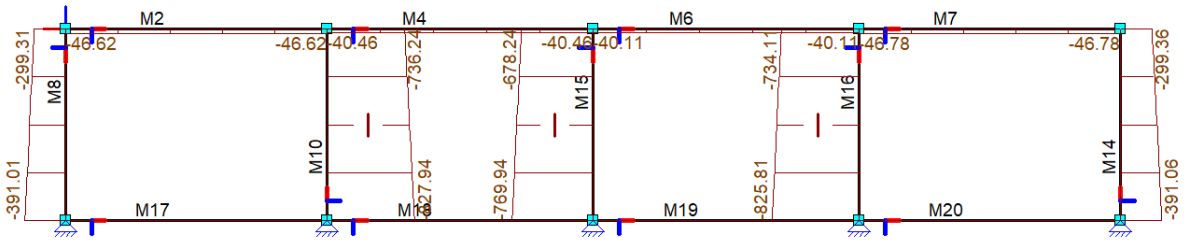

Figure K.22: The normal forces in the structure based on the initial design loads.

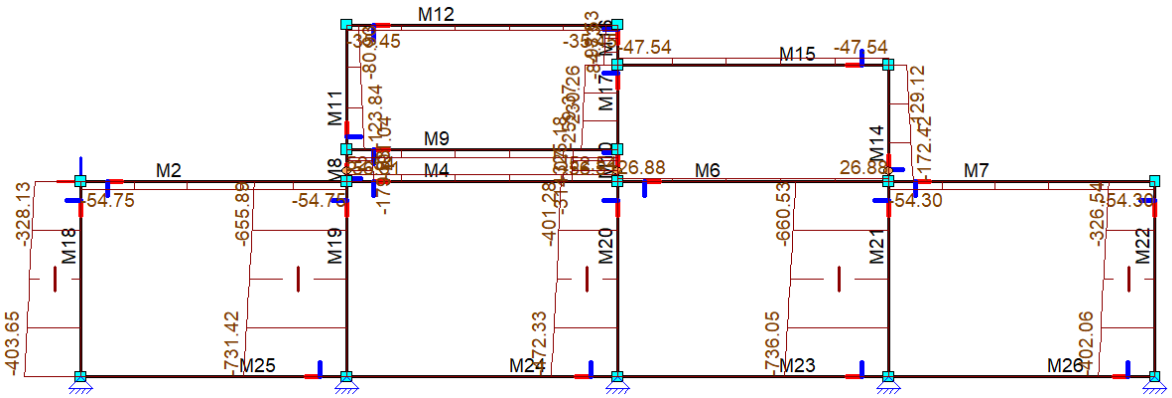

Figure K.23: The normal forces in the structure for the new situation.

The existing lateral walls in the structure are selected as the elements for the comparison of the normal forces. It can be concluded that the normal forces in the two outer walls will increase and in the three inner walls will decrease in the new situation.

The shear force distribution for the old and new situation is given in Figure K.24 and Figure K.25.

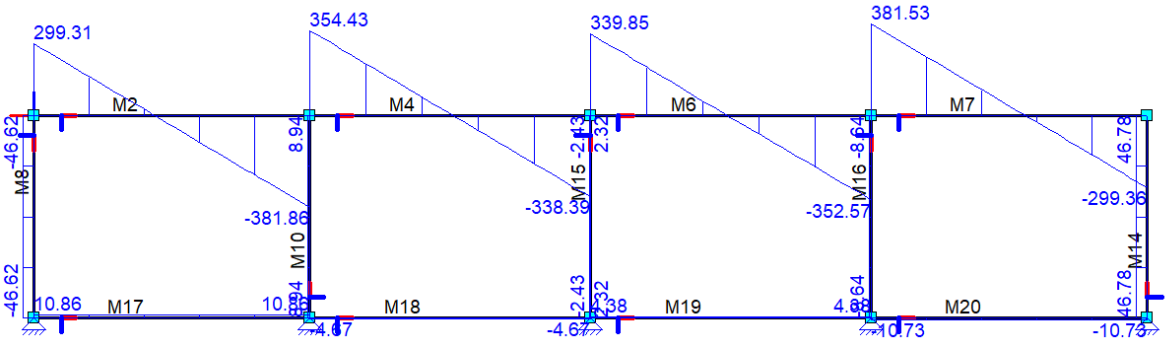

Figure K.24: The shear forces in the structure based on the initial design loads.

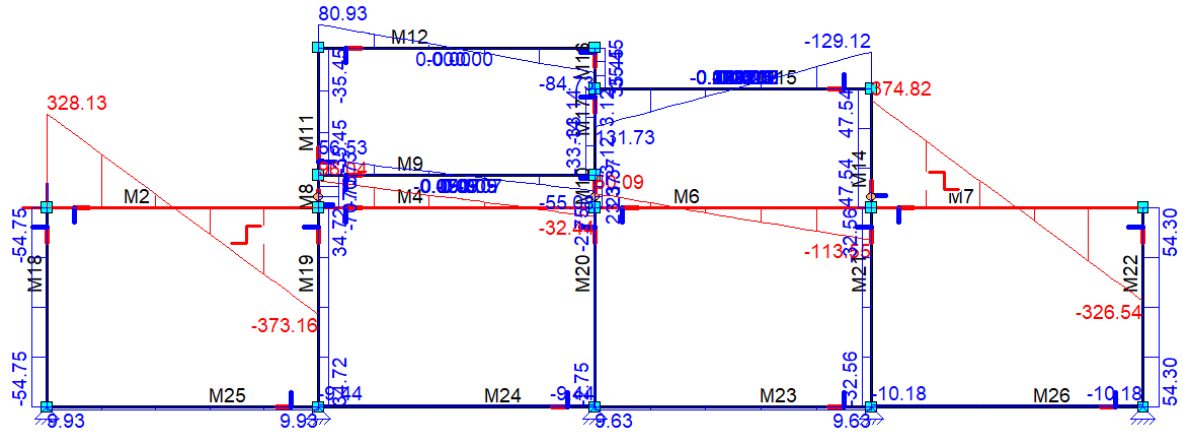

Figure K.25: The shear forces in the structure for the new situation.

From Figure K.25 the shear force distribution of the top slab is selected and shown separately in Figure K.26.

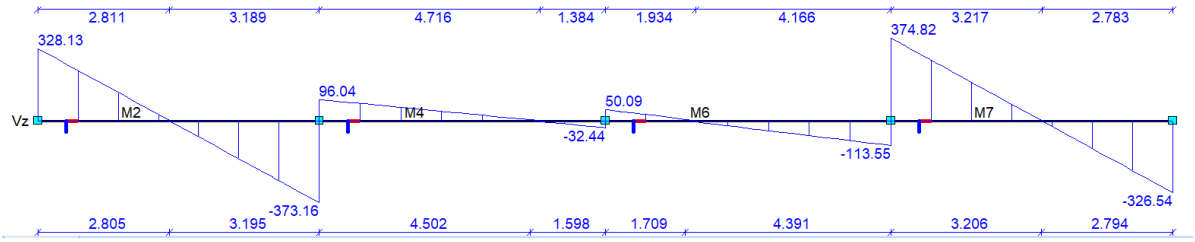

Figure K.26: The shear forces in the top slab for the new situation.

From the comparison can be concluded that the shear force in the top slab will increase near the outer walls. The shear force in the new situation does not exceed the old situation in the other parts of the top slab. Furthermore, the shear distribution increases for all the existing lateral walls.

Figure K.27 and Figure K.28 shows the bending moments in the structure for the old and new situation.

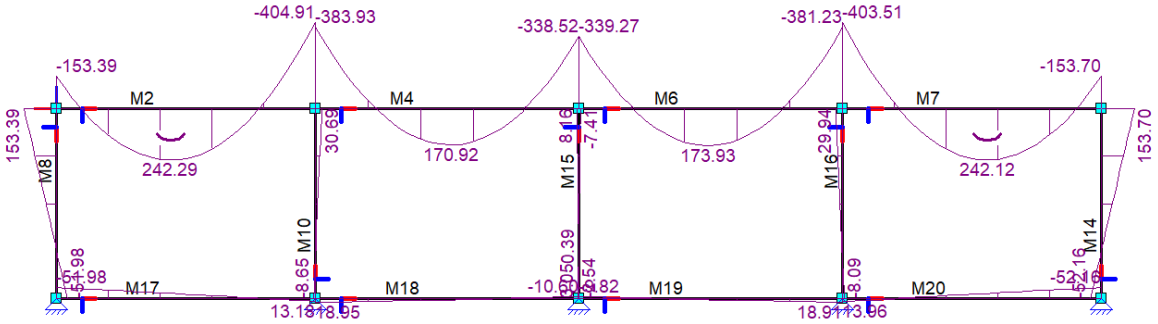

Figure K.27: The bending moments in the structure based on the initial design loads.

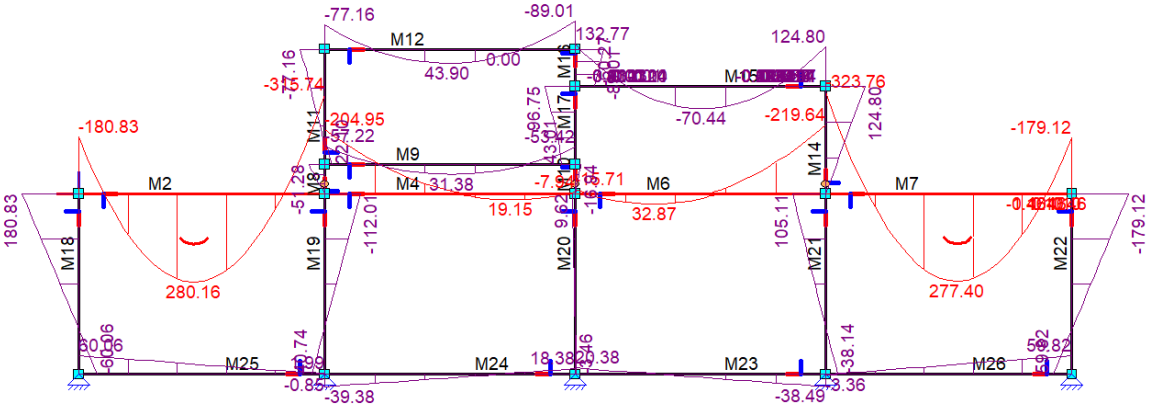

Figure K.28: The bending moment in the structure for the new situation.

The top slab is selected and shown separately in Figure K.29 for a better overview.

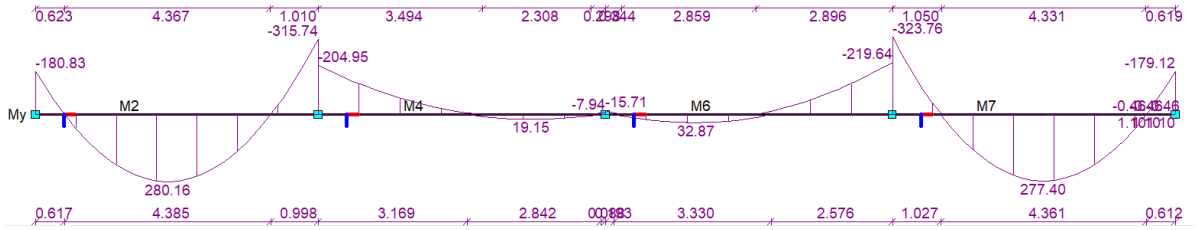

Figure K.29: The bending moments in the top slab for the new situation.

The conclusion of the comparison of the bending moment is an increase in sagging moments in the outer spans of the top slab. In the middle two spans, the sagging moment is lower in the new situation than the old situation. The hogging moments in the top slab increase only near the outer walls. An increase of bending moments near the connection of the top slab and bottom slab will occur in the new situation.

The largest increase in shear forces and bending moment occur in the first span of the top slab.

K.3.3. Analysis axle loads

For the first Matrixframe linear analysis the axle forces due to traffic loads are neglected. In this subsection the axle forces are included in the Matrixframe analysis and placed on the span of the top slab with the highest increase in bending moments and shear forces which is the first span. The distributed loads are applied on the structure as well. The placement of the loads are based on the most unfavourable situation for the bending moments.

The selected cross-section is 1 m wide. Not all the axle loads are placed on the structure since the spacing according the VOSB 1963 is 2.5 m and the spacing according to NEN-EN 1991 is 2 m. Therefore, 1/2 of the axle load is used for this analysis.

The axle load according to VOSB 1963 consists of 3 axle loads of 200 kN. This results in 200/2 = 100 kN per axle load. Two situations are analysed for the axle load on the top slab for the initial design situation. Figure K.30 shows both situations. These loading situations are selected to analyse the largest bending moments. The axle load is multiplied by the factor 1.7 for the load combination input.

(a) Situation 1 for placement of the axle load.

(b) Situation 2 for placement of the axle load.

Figure K.30: The placement of the axle load on the structure according to VOSB 1963.

The axle load according to NEN-EN 1991 consists of two loads of 300 kN. Divided by 2 results in axle loads of 150 kN. Figure K.31 shows the placement of the axle on the first span of the top slab for the highest bending moments. The axle load is a variable load and will be multiplied by the factor 1.05 or 1.5 depending on the load combination.

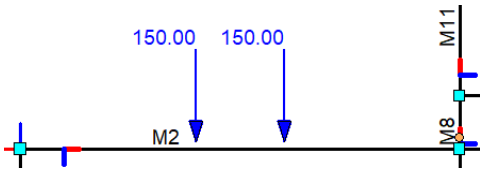

Figure K.31: The placement of the axle load on the structure according to NEN-EN 1991.

The normal forces in the walls are compared in Figure K.32. There are higher normal forces in the walls in the old situation compared to the new situation. It can be concluded that no additional check is needed for the compression force in the existing lateral walls of the Elshoutsluice.

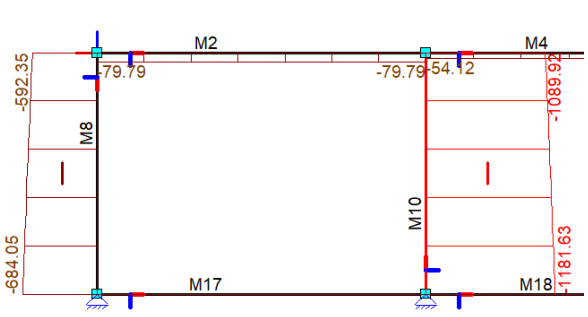

(a) The normal forces in the structure for the old situation.

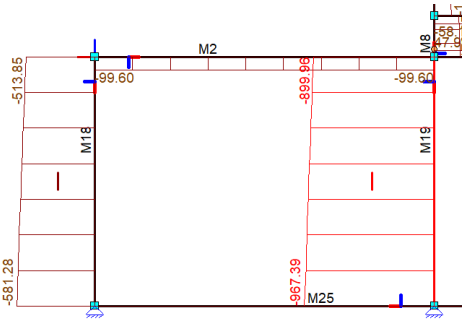

(b) The normal forces in the structure for the new situation.

Figure K.32: The comparison of the normal forces on the structure due to inclusion of the axle load.

Figure K.33 shows the comparison of the first span of the top slab for the shear force. The shear force directly above the walls is lower in the new situation compared to the old situation. However, the shear force in the old situation is not higher over the whole span compared to the new situation. The shear forces in the walls in the new situation are larger than the old situation. Therefore, additional shear checks must be performed for the walls and the top slab.

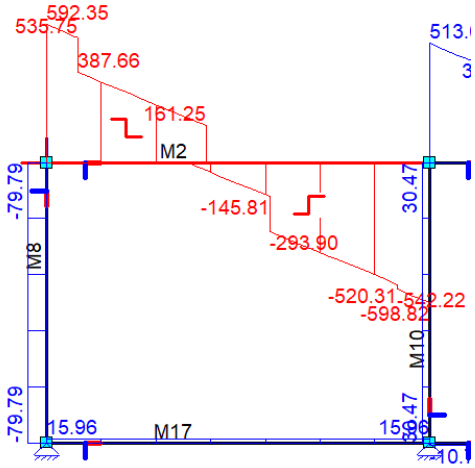

(a) The shear forces in the structure for the old situation.

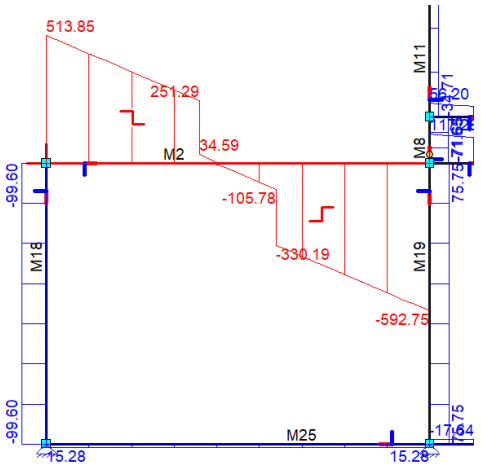

(b) The shear forces in the structure for the new situation.

Figure K.33: The comparison of the shear forces on the structure due to inclusion of the axle load.

The bending moments of the old and new situation are shown in Figure K.34. The sagging moment in the top slab, the hogging moment near the outer wall and the moments near the top connection of the walls increase compared to the old situation. Only the hogging moment near the second wall decreases. Therefore, additional checks must be performed for the bending capacity of the existing top slab and the walls of the Elshoutsluice.

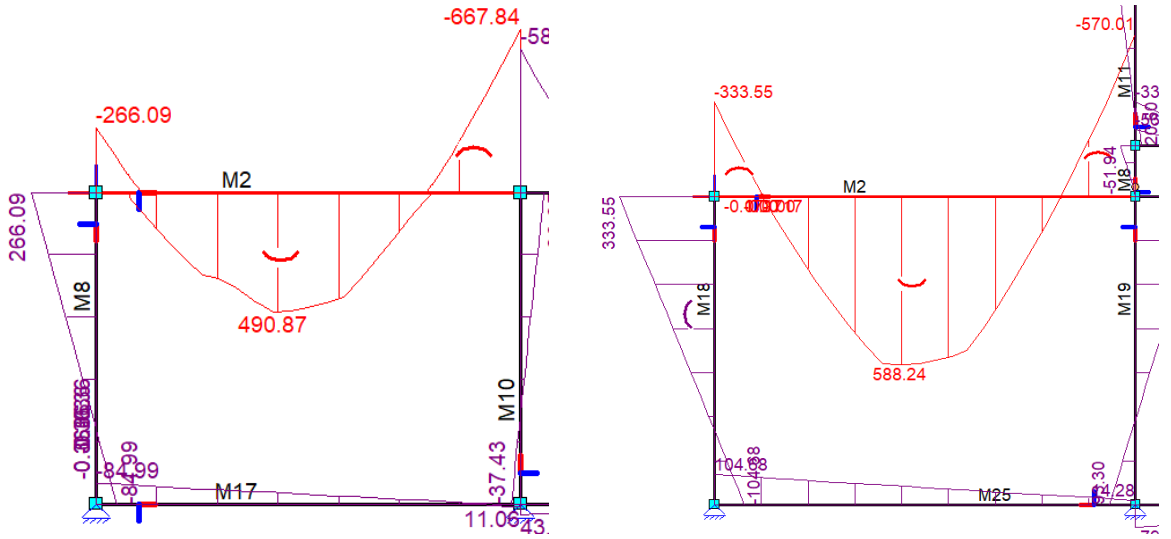

(a) The bending moments in the structure for the old situation.

(b) The bending moments in the structure for the new situation.

Figure K.34: The comparison of the bending moments in the structure due to inclusion of the axle load.

The strength of the concrete B22.5 is determined with the formulas according to EN1992-1-1. The characteristic compressive strength (f_{ck}) of B22.5 is 18 MPa according to NEN 8700.

First the design compressive strength is determined. With a value of 1.0 for the coefficient taking account of long term effects on the compressive strength (α_{cc}) and a material factor for concrete (γ_c) of 1.5:

$$f_{cd} = \alpha_{cc} \cdot \frac{f_{ck}}{\gamma_c} = 1.0 \cdot \frac{18}{1.5} = 12 \text{ N/mm}^2 \tag{K.40}$$

The characteristic mean tensile strength for concrete a concrete class ≤ C50/60 is:

$$f_{ctm} = 0.3 \cdot f_{ck}^{2/3} = 0.3 \cdot 18^{2/3} = 2.06 \text{ N/mm}^2 \tag{K.41}$$

With:

$$f_{ctk,0.05} = 0.7 \cdot f_{ctm} = 0.7 \cdot 2.06 = 1.44 \text{ N/mm}^2 \tag{K.42}$$

The coefficient taking account of long term effects on the tensile strength (α_{ct}) is 1.0. The design tensile strength of the concrete B22.5 without reinforcement is:

$$f_{ctd} = \alpha_{ct} \cdot \frac{f_{ctk,0.05}}{\gamma_c} = 1.0 \cdot \frac{1.44}{1.5} = 0.96 \text{ N/mm}^2 \tag{K.43}$$

The maximum bending capacity for the continuous slab of 0.6 m thickness without reinforcement is determined by:

$$M_{Rd} = f_{ctd} \cdot W = 961.56 \cdot \frac{1}{6} \cdot 1 \cdot 0.6^2 = 57.69 \text{ kNm} \tag{K.44}$$

The bending moments in the top slab determined with Matrixframe exceed the maximum bending capacity of concrete without reinforcement. It can be concluded that reinforcement must be present in the existing structure top slab. The same conclusion can be drawn for the existing walls in the Elshoutsluice structure.

K.3.4. Conclusion

It is assumed that the existing Elshoutsluice structure will resist the change in normal forces due to the loading difference. However, the existing structure needs a more detailed assessment of the reinforcement in the first and last span of the top slab and the walls due to the increase in shear forces and bending moments in these elements.

When the amount of current reinforcement in the structure is not sufficient for the increased loads, strengthening of an element is needed. There are different solutions for strengthening of an existing concrete element:

- Increasing the cross-section area.
- Adding of (prestressed) reinforcement internally or externally.
- Adding steel plates to a concrete cross-section externally.
- Applying Fibre-Reinforced Polymers (FRP) to the concrete elements.

Due to the high humidity of an hydraulic structure, the addition of external steel elements is not preferred because uncovered steel is prone to corrosion.

References

Architectuur Lokaal. (2019). *Team De derde trap wint prijsvraag Waterentree Werelderfgoed Kinderdijk - Architectuur Lokaal.* Retrieved 2019-09-12, from https://arch-lokaal.nl/team-de-derde-trap-wint-prijsvraag-waterentree-werelderfgoed-kinderdijk/

CROW. (2014). *Richtlijn toegankelijkheid.*

Daniel, R., & Paulus, T. (2019). *Lock Gates and Other Closures in Hydraulic Projects.* Matthew Deans. doi: https://doi.org/10.1016/C2015-0-05399-0

Defacto Stedenbouw. (2019). *Verkenning toekomstbeelden werelderfgoed - op weg naar een Gebiedsperspectief Kinderdijk.*

Dijk, A., & Van der Ziel, F. (2010). *Multifunctionele beweegbare waterkeringen [Multifunctional movable flood gates].* Delft.

Erbisti, P. C. F. (2014). *Design of Hydraulic Gates* (2nd ed.). London: CRC Press.

EurOtop. (2018). *Manual on Wave Overtopping of Sea Defences and Related Structures. An Overtopping Manual Largely Based on European Research, but for Worldwide Application* (2nd ed.). Retrieved from http://www.overtopping-manual.com/

Gemeente Molenwaard. (2018). *Prijsvraag Waterentree Werelderfgoed Kinderdijk.*

Haskoning B.V. (1984a). *Dijkversterkings- en aanpassingswerken aan de Elshout. Kunsterk I bodem wapening.*

Haskoning B.V. (1984b). *Dijkversterkings- en aanpassingswerken aan de Elshout - Kunstwerk I Bodem Matenplan.*

Haug, J. J. M., & Schuurman, F. (2019). *Voetpaden voor iedereen.*

Helpdesk Water. (n.d.). *Waterveiligheid - Helpdesk water.* Retrieved 2019-10-01, from https://www.helpdeskwater.nl/onderwerpen/waterveiligheid/

H+N+S Landschapsarchitecten, & Beek & Kooiman Cultuurhistory. (2013). *Gebiedsvisie Kinderdijk.*

Informatiehuis Water (IHW). (2017). *Waterveiligheidsportaal.* Retrieved 2019-10-01, from https://waterveiligheidsportaal.nl/{#}/nss/nss/norm

Jansen Venneboer BV. (1986). *Hijsgegevens mobiele kraan t.b.v segmentklep en rolschuif.*

Jongejan, R. B., & Steenbergen, R. D. J. M. (2015). *Beoordeling van de constructieve veiligheid van waterbouwkundige kunstwerken volgens het Bouwbesluit en de Waterwet.* Delft: InfraQuest.

Jonkman, S. N., Voortman, H. G., Klerk, W. J., & Van Vuren, S. (2018). Developments in the management of flood defences and hydraulic infrastructure in the Netherlands. *Structure and Infrastructure Engineering*, *14*(7), 895–910.

KNMI. (2015). *KNMI'14 - Climate scenarios for the Netherlands.*

Land-ID, & Cultuurhistory Projecten. (2016). *Werelderfgoed Kinderdijk-Elshout: Heritage Impact Assessment gebiedsontwikkelingen.*

Molenaar, W. F., & Voorendt, M. Z. (2019). *Manual Hydraulic Structures (Lecture notes).*

Molenaar, W. F., & Voorendt, M. Z. (2020). *Hydraulic structures - General Lecture Notes.*

Mooyaart, L. F., & Jonkman, S. N. (2017). Overview and Design Considerations of Storm Surge Barriers. *Journal of Waterway, Port, Coastal, and Ocean Engineering*(143(2)).

Motralec. (n.d.). *Flygt (Xylem) P 7121,pompe a helice,propeller pump submersible.* Retrieved 2020-05-11, from https://www.motralec.com/public/fichiers/docs/Flygt-P-7121-English

Normcommissie. (2011). *NEN 8700: Beoordeling van de constructieve veiligheid van een bestaand bouwwerk bij verbouw en afkeuren - Grondslagen.*

Normcommissie. (2015). *Eurocode 1: Actions on structures - Part 2: Traffic loads on bridges.*

Normcommissie. (2018). *NEN 8702: Beoordeling van de constructieve veiligheid van een bestaand bouwwerk bij verbouw en afkeur - Betonconstructies.*

Normcommissie. (2019a). *Eurocode 1 - Actions on structures - Part 1-1: General actions – Densities, self-weight, imposed loads for buildings.*

Normcommissie. (2019b). *Eurocode 7: Geotechnical design - Part 1: General rules.*

Rijkswaterstaat. (n.d.). *Waterinfo Versie: 1.6.12.0.* Retrieved from `https://waterinfo.rws.nl/`

Rijkswaterstaat. (2005). *Handreiking Functioneel Specificeren (The Guideline on Functional Specification).* ExpertiseCentrum Opdrachtgeverschap.

Rijkswaterstaat. (2007). *Nieuwe Ontwerprichtlijn Autosnelwegen.* Nijkerk: Drukkerij Van de Ridder bv.

Rijkswaterstaat. (2017a). *WBI-2017.*

Rijkswaterstaat. (2017b). *Werkwijzer bepalen kans op niet sluiten per sluitvraag met scoretabellen - Versie 1.2.* RWS-WVL.

Rijkswaterstaat. (2018a). *WBI 2017 - Schematiseringshandleiding grasbekleding - Versie 3.0.* Ministerie van Infrastructuur en Milieu.

Rijkswaterstaat. (2018b). *Werkwijzer Ontwerpen Waterkerende Kunstwerken - Ontwerpverificaties voor de hoogwatersituatie.*

Rijkswaterstaat. (2019). *WBI 2017 - Schematiseringshandleiding betrouwbaarheid sluiting kunstwerk - Versie 2.0.* Ministerie van Infrastructuur en Waterstaat.

Roozenburg, N. F. M., & Eekels, J. (1995). *Product Design: Fundamentals and Methods.* John Wiley & Sons Ltd.

Soons, F. A. M., Van Raaij, B. P. M., & Wagemans, L. A. G. (2014). *Quick reference - edition 2014.*

Stichting Commissie Voorschriften Beton. (1974). *Regulations for concrete 1974.*

TAW. (2003). *Leidraad Kunstwerken (Guideline Engineering Structures).*

TAW-ENW. (2016). *Grondslagen voor hoogwaterbescherming (Fundamentals of Flood Protection).*

Tijhuis, S., Buckers, M., Schrijver, R., Lodder, T., Kofmann, G., Franssen, M., & Gaydadjiev, A. (2019). *de derde trap.*

TRB. (2000). *Highway Capacity Manual: Metric Units.* Washington, D.C.: Transportation Research Board.

Van der Vlist, M., Barneveld, A., Breedeveld, J., Van Doorn, J., & Luyten, J. (2019). *Kennisprogramma Natte Kunstwerken - Kennisplan 2019.*

Van der Voet, M., & Ligtermoet, D. (2017). *Gemeentelijk Verkeer- en Vervoerplan Molenwaard.*

Van der Ziel, F. (2009). *Movable water barrier for the 21st century.*

Van Nes, R., Wiggenraad, P. B. L., & Van Lint, J. W. C. (2018). *Dictaat CTB1420-17: Transport & Planning.* Delft.

VNK. (2014). *Eindrapportage Veiligheid Nederland in Kaart* (No. November).

VNK2. (2014). *Overstromingsrisico Dijkring 16 Alblasserwaard en de Vijfheerenlanden.*

Voorendt, M. Z. (2017). *Design principles of multifunctional flood defences* (Doctoral dissertation, Delft University of Technology). doi: 10.4233/uuid:31ec6c27-2f53-4322-ac2f-2852d58dfa05

Voorendt, M. Z., & Molenaar, W. F. (2020). *Manual Hydraulic Structures.*

Waterschap Rivierenland. (2018a). *Hoge boezem Overwaard - Toelichting partiële herziening peilbesluit Alblasserwaard.*

Waterschap Rivierenland. (2018b). *Uitbreiding 3e trap Elshoutsluis.*

Waterschap Rivierenland. (2020). *Eerste Beoordeling Primaire Keringen Overstromingskans.*